Stellingen

1. De conclusie dat Arg42 in *para*-hydroxybenzoate hydroxylase essentieel is voor de binding van FAD wordt door studies, beschreven in hoofdstuk 4 van dit proefschrift, weerlegd.
   DiMarco, A.A., Averhoff, B.A., Kim, E.E. and Ornston, L.N. 1993. *Gene* **125**, 25-33

2. Mutagenese en modelling studies in dit proefschrift laten zien dat het gepostuleerde model voor het enzym/substraat/NADPH complex van *para*-hydroxybenzoate hydroxylase in Chaiyen et al., niet is gebaseerd op realistische gegevens.
   Chaiyen, P., Ballou, D.P. and Massey, V. 1997. *Proc. Natl. Acad. Sci. USA* **94**, 7233-7238.

3. Door de verschuiving van het laboratoriumwerk naar de computer is men minder praktisch ingesteld.

4. Voor biochemici blijft het zuiveren van een eiwit nog steeds een kunst.

5. Zonder een gedegen biochemische/biofysische kennis blijft eiwit homologie modelling een hachelijke onderneming.

6. Behalve aan studenten heeft de universiteit weinig te bieden aan jongeren.

7. De populariteit van een studierichting wordt vaak door de publieke opinie bepaald.

8. De controle van nieuwe eiwitstructuren in de "Protein Data Bank" wordt steeds strenger. Het wordt daarom ook tijd om oude eiwitstructuren nog eens goed onder de loep te nemen.

9. Menselijk ingrijpen in DNA/RNA is nog steeds kinderspel vergeleken met het genetisch geweld in de natuur.

10. Machtig op koers laat zien dat goed fundamenteel onderzoek steeds minder kans krijgt.

Coenzyme recognition

in

para-hydroxybenzoate hydroxylase

Promotor:	dr. N.C.M. Laane hoogleraar in de Biochemie
Co-promotoren:	dr. W.J.H. van Berkel Universitair docent, departement Biomoleculaire wetenschappen laboratorium voor Biochemie
	dr. H.A. Schreuder Groepsleider X-ray kristallografie Hoechst Marion Roussel Frankfurt, Duitsland

Coenzyme recognition in *para*-hydroxybenzoate hydroxylase

Michel Hendrikus Maria Eppink

Proefschrift
ter verkrijging van de graad van doctor
op gezag van de rector manificus
van de Landbouwuniversiteit Wageningen,
dr. C.M. Karssen,
in het openbaar te verdedigen
op vrijdag 11 juni 1999
des namiddags te half twee in de Aula

M.H.M. Eppink - Coenzyme recognition in *para*-hydroxybenzoate hydroxylase - 1999
Dutch: 'Co-enzym herkenning in *para*-hydroxybenzoaat hydroxylase'
Thesis Wageningen University - With summary in Dutch

ISBN 90-5808-065-X

Cover: Proposed binding mode of NADPH in *para*-hydroxybenzoate hydroxylase

Key words: aromatic hydroxylases / flavoprotein / *para*-hydroxybenzoate / site-specific mutagenesis / X-ray studies / coenzyme specificity / fingerprint region

Dankwoord

De wijze waarop dit proefschrift tot stand is gekomen geeft aan dat het mogelijk is om op een alternatieve manier het doel te bereiken. Het onderzoek zoals beschreven in dit proefschrift was niet eenvoudig omdat de werking van *para*-hydroxybenzoate hydroxylase al in detail was bestudeerd (meestal blijven de lastigste problemen over). Vooral door een multidisciplinaire aanpak bleek het mogelijk te zijn om nieuwe inzichten in dit enzym te verkrijgen.

Allereerst wil ik mijn promotor Colja Laane bedanken voor de gelegenheid die hij mij geboden heeft om te promoveren. Verder wil ik ook emeritus hoogleraar Prof. C. Veeger bedanken daar een deel van het onderzoek tijdens zijn leiding heeft plaatsgevonden.

Mijn meeste dank gaat uit naar mijn co-promotoren Willem van Berkel en Herman Schreuder die beiden ook gepromoveerd zijn op het enzym *para*-hydroxybenzoate hydroxylase. Door hun kennis en geduld en mijn "jeugdig" enthousiasme werkte deze onderzoekscombinatie uitstekend. Vanaf 1989, sinds hij mij oppikte uit het klinisch chemisch lab te Oss, is Willem mijn directe begeleider geweest. In het begin moest ik mij helemaal omturnen van de klinisch chemie naar de biochemie. Willem trad hierbij vooral op als sturende factor, en vanwege zijn zeer goede wetenschappelijke en kritische kijk op het onderzoek bleek hij van onschatbare waarde. Met Herman heb ik bijna alles op afstand gedaan, eerst vanuit Straatsburg (Marion Merrell Dow) waar ik de beginselen van röntgendiffractie heb geleerd en later vanuit Frankfurt (Hoechst Marion Roussel). Als expert op het gebied van eiwitkristallografie was ook jouw begeleiding onontbeerlijk. De ontelbare "hanging drops" met de belangrijke kristallen, hebben het in de auto bijna altijd overleefd zelfs bij 180 km/uur op de autobahn. Verder zijn er heel wat megabytes aan datasets via FTP heen en weer gestuurd, en voor de begeleiding op afstand was email vanaf het begin een uitstekend middel (de telefoonkosten zouden anders astronomisch hoog zijn geweest).

In de afgelopen jaren is met verschillende groepen samengewerkt in binnen- en buitenland, daarbij wil ik mijn dank uitspreken aan Prof. Dirk Roos van het CLB te Amsterdam, Dr. Ylva Lindqvist van het Karolinska Instituut te Stockholm, Dr. Mariët van de Werf, Dr. Wout Middelhoven en Dr. John van Oost van de Landbouwuniversiteit te Wageningen. I would like to thank Prof. Rudi Müller from the Technical University of Hamburg for the collaboration on *para*-hydroxybenzoate hydroxylase from *Pseudomonas* sp. CBS3. Furthermore, the help of Dr. Alex Tepliakov was indispensible for the collection of high resolution crystallographic data at the synchrotron facility (DESY) of the EMBL outstation in Hamburg.

Tijdens mijn onderzoek heb ik hulp gekregen van de afstudeerders Erica Fritse, Christine Bunthof, Yvonne Dortmans, Denise Jacobs, Karin Overkamp, Erwin Cammaert, Kees Ruiter, Bas Tomassen en Miew-Woen Sjauw-en-Wa. Graag wil ik ook jullie bedanken voor je inzet en gezelligheid.
Verder wil ik mijn lab 5 collega's van de afgelopen jaren Klaus, Frank, Marco, Elles, Robert, Marielle, Ulrike, Yves en Carlo bedanken voor de vele (niet) wetenschappelijke discussies. Ook alle medewerkers van de vakgroep Biochemie wil ik bedanken voor de prettige tijd die ik gehad heb in het Transitorium. Speciaal wil ik hierbij noemen Willy, Jan-Willem, Mark, Walter, Adrie, Aart, Hans, Huub, Ton, Jillert, Jacques, Sjef, Ans, Marelle en Ivonne. Ook de administratieve ondersteuning was belangrijk. Hiervoor ben ik Laura, Martin, Piet en Bery zeer erkentelijk. Verder heb ik vanaf 1989 vele studenten, promovendi en andere tijdelijke medewerkers zien komen en gaan. Teveel om op te noemen, maar allemaal bedankt voor de leuke tijd in Wageningen.
Fred van de Ent van Bioprocestechnologie bedank ik voor de hulp tijdens de vele 200 liter fermentor kweken. Van Moleculaire Fysica ben ik Frank Vergeldt zeer erkentelijk voor het oplossen van de computerproblemen tijdens het rekenen op diverse werkstations en Ruud Spruijt voor de moleculair biologische adviezen. Als er weer flink wat flessen met medium waren gevuld dan was Gerrit Nellestijn van Moleculaire Biologie altijd bereid om deze snel even te steriliseren. Verder deed ik in de eerste jaren zelf nog veel DNA sequencen, maar met de komst van Tony van Kampen bij Moleculaire Biologie nam het handmatig sequencen steeds verder af. Onze zeer actieve concierge Evert van de Pol is ook altijd een vertrouwd beeld geweest in het Transitorium waar ik zowel lopend als fietsend (ik was de enige die daar permissie voor had) naar binnen ging. Ook Jan Hontelez (hoofd BHV en tevens fervent fietser) en Marijke Hartog (naast mij de enige C3 deskundige) bedank ik voor de onderlinge samenwerking. Verder wens ik het "Bioinformatica" (BIT) team Sacco, Peter, Ton, Jacques en het "Probleem Gericht Onderwijs" (PGO) team Willem, John, Carlo, Thijs en Johan veel succes voor de komend jaren.
Als laatste wil ik Hanneke bedanken voor de niet wetenschappelijke kant van het leven. Een goede thuisbasis is essentieel geweest voor het werk van de afgelopen jaren, vanaf het begin heb je er achter gestaan wat totaal negen jaar heeft geduurd. Tijdens die jaren zijn Mike en Jim erbij gekomen. Zij zorgden ervoor dat ik niet altijd met mijn kop in de papieren zat. Jammer dat mijn ouders dit niet hebben mogen meemaken.

Ter nagedachtenis aan mijn ouders
Aan Hanneke, Mike en Jim

Abbreviations

Å	angstrom (0.1 nm)
ADP	adenosine 5'-diphosphate
AMP	adenosine 5'-monophosphate
ATP	adenosine 5'-triphosphate
B-value	displacement of an atom from thermal motion, conformational disorder, and static lattice disorder
dATP	deoxy-adenosine 5'-triphosphate
dNTP	deoxy-nucleoside 5'-triphosphate
ddNTP	dideoxy-nucleoside 5'-triphosphate
DNA	deoxyribonucleic acid
DOHB	dihydroxybenzoate
EDTA	ethylenediaminetetraacetic acid
EFl_{ox}	oxidized flavoenzyme
EFl_{red}	reduced flavoenzyme
Epps	4-(2-hydroxyethyl)-1-piperazinepropane sulfonic acid
ε	molar absorption coefficient
FAD	flavin adenine dinucleotide (oxidized)
FADH	flavin adenine dinucleotide (reduced)
FADHOH	flavin C(4a)-hydroxide
FADHOOH	flavin C(4a)-hydroperoxide
FMN	flavin mononucleotide
FPLC	fast protein liquid chromatography
F_c	calculated amplitude
F_o	observed amplitude
F_{obs}	fluorescence observed
Hepes	4-(2-hydroxyethyl)-1-piperazineethane sulfonic acid
Hepps	4-(2-hydroxyethyl)-1-piperazinepropane sulfonic acid
HPLC	high performance liquid chromatography
H_2O_2	hydrogen peroxide
I	ionic strength
k	rate constant
k_{cat}	turnover rate
K_d	dissociation constant
k_{red}	reduction rate
kDa	kilodalton
K_m	Michaelis constant

Mes	morpholineethane sulfonic acid
NAD	nicotinamide adenine dinucleotide
NAD^+	nicotinamide adenine dinucleotide (oxidized)
NADH	nicotinamide adenine dinucleotide (reduced)
NADP	nicotinamide adenine dinucleotide phosphate
$NADP^+$	nicotinamide adenine dinucleotide phosphate (oxidized)
NADPH	nicotinamide adenine dinucleotide phosphate (reduced)
nm	nanometer
O_2	molecular oxygen
P	product
PDB	Protein Data Bank
PHBH	*p*-hydroxybenzoate hydroxylase
pobA	gene encoding *p*-hydroxybenzoate hydroxylase
POHB, pOHB	*p*-hydroxybenzoate
R	correlation coefficient
R factor	crystallographic refinement factor (degree of correspondence of calculated and observed amplitudes)
R_{sym}	internal measure of the accuracy of a data set
S	substrate
SCOP	Structural Classification of Proteins
SDS	sodium dodecyl sulfate
Tris	2-amino-2-(hydroxymethyl)-1,3-propanediol
Q	fluorescence quantum yield
QAE	quaternary aminoethyl
UV	ultraviolet

Contents

CHAPTER 1

General Introduction

1.1. Nucleotides

This thesis deals with the way NADPH is bound and recognized by the FAD-containing enzyme *p*-hydroxybenzoate hydroxylase.

NADPH and FAD are dinucleotides, which are important compounds for the energy exchange in cellular metabolism (Fig.1). NADPH is a source of reducing equivalents and functions mostly as a coenzyme in different enzyme families, while FAD is an important prosthetic group in flavoenzymes.

In many enzymes, FAD and NAD(P)H are recognized by a common dinucleotide binding fold (Rossmann et al., 1974). However, other binding modes for FAD and NAD(P)H exist (Mathews, 1991; Lesk, 1995; Bellamacina, 1996; Enroth, 1998b).

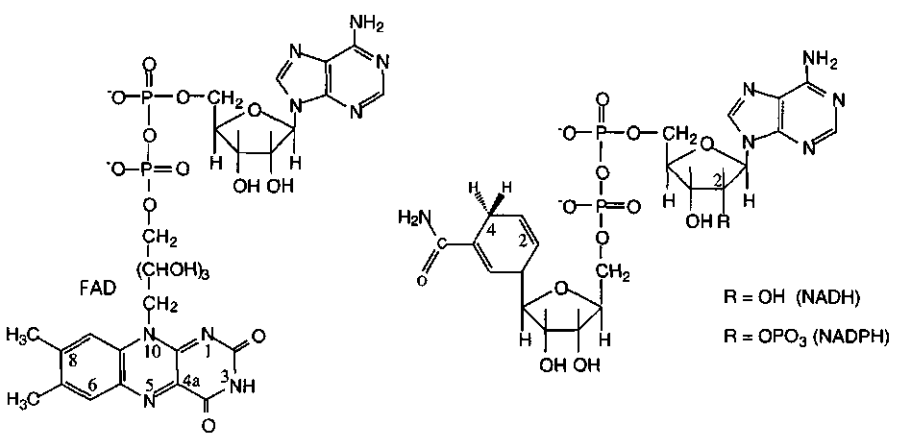

Fig. 1: Structures of FAD and NAD(P)H

The enzyme of interest in this PhD thesis, *p*-hydroxybenzoate hydroxylase from *Pseudomonas fluorescens*, has a unknown binding mode for NADPH. Before discussing the general properties of *p*-hydroxybenzoate hydroxylase, first an overview will be given of known NAD(P) binding folds.

1.2. NAD(P) binding proteins

1.2.1. Classification

NAD(P) binding proteins are ubiquitous. They are found in organisms as diverse as archaea, eubacteria, and higher organisms including yeasts, plants, animals, and humans. Enzymes that bind NAD(P) catalyze reactions that play a role in energy production, storage, and transfer. They do so by exploiting the ability of the nicotinamide group of the cofactor to transfer hydride ions or electrons and thereby couple a wide variety of reactions. These reactions are part of nearly all core metabolic pathways, such as glycolysis and photosynthesis. Dependent on the kind of reaction the *pro-R* (A specificity) or *pro-S* (B specificity) hydrogen of the C4 atom of the nicotinamide base is transferred (You, 1982). An exception are the ribosylating enzymes (Bell & Eisenberg, 1996), ribosome inactivating proteins (Xiong et al., 1994) and glycogen phosphorylase (Stura et al., 1983) which use NAD(P) as a substrate, substrate analog or inhibitor, respectively.

Up to now the atomic structures of more than 60 NAD(P) dependent enzymes in complex with NAD(P) have been determined by X-ray crystallography. These structures can be grouped into a relatively small number of subclasses, where members within the same subclass share many common properties. The structural database SCOP (Murzin et al., 1995) classifies the NAD(P) binding proteins with respect to biological relevance and domain folding, whereby they can be classified in $\alpha+\beta$, α/β and multidomain ($\alpha+\beta$) folds. Table 1 summarizes one representative of each of the fourteen known different domains, which can be extracted from the SCOP database.

Table 1. Crystal structures of proteins in complex with NAD(P).

Fold	Enzyme	PDB	Cofactor/ substrate	Source	Reference
Class: α+β multidomain					
Heme-linked catalases	Catalase	2cah	NADP	*P. mirabilis*	Gouet, 1995
Class: α+β domain					
Ferredoxin-like	HMG-CoA reductase	s094	NAD	*P. mevalonii*	Lawrence, 1995
ADP-ribosylation	Diphtheria toxin	1tox	NAD	*C. diphtheriae*	Bell, 1996
Ribosome inactivating proteins	Trichosanthin	1tcs	NADP	Mongolian snake gourd	Xiong, 1994
Class: α/β domain					
beta/alpha (TIM)-barrel	Aldose reductase	2acr	NADP	Human	Wilson, 1992
FAD/NAD(P)-binding domain	*Glutathione reductase	1gra	NADP	Human	Pai, 1988
Flavodoxin-like	*NAD(P)H:quinone reductase	1qrd	NADP	Rat	Li, 1995
Ferredoxin reductase-like	*Ferredoxin reductase	1fnb	NADP	Spinach	Serre, 1996
A nucleotide-binding domain	*Trimethylamine dehydrogenase	2tmd	ADP	*M. bacterium* W_3A_1	Lim, 1986
Aldehyde reductase (class III enzyme)	Aldehyde dehydrogenase	1ad3	NAD	Rat	Liu, 1997
NAD(P)-binding Rossman-fold	Lactate dehydrogenase	3ldh	NAD	Dogfish	White, 1976
Dihydrofolate reductases	Dihydrofolate reductase	3dfr	NADP	*L. casei*	Matthews, 1979
Isocitrate & isopropylmalate dehydrogenase	Isopropylmalate dehydrogenase	1hex	NAD	*T. thermophilus* HB8	Hurley, 1994
β–Glycosyltransferase & glycogen phophorylase	glycogen phosphorylase	1gpb	NAD	Rabbit	Stura, 1983

* flavoproteins

1.2.2. Rossmann fold

The most common fold among the different NAD(P) binding proteins with known structure (Table 1) is the NAD(P)-binding Rossmann-fold, containing a βαβαβ structural motif (Fig.2). Already in 1974, Rossmann showed that this substructure is a general nucleotide-binding motif present in several dehydrogenases, kinases and flavodoxins (Rossmann et al., 1974).

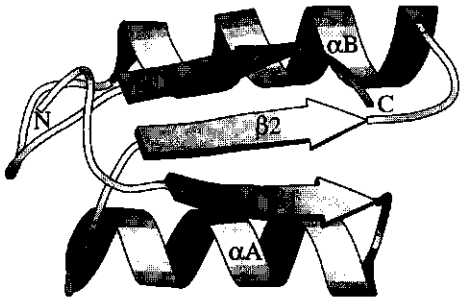

Fig. 2: NAD(P) binding motif (βαβαβ fold).

In dehydrogenases the NAD(P)-binding domain is mostly build from two identical βαβαβ-folds forming a six stranded parallel β-sheet with helices on both sides (Fig.3).

Fig. 3: Stereoview of lactate dehydrogenase + NADH (White et al., 1976).

The loop between the first β-sheet and the first α-helix of the Rossmann fold contains a common fingerprint sequence: GXGXXG (Fig.4), where X can be any amino

acid (Wierenga et al., 1986). This glycine-rich region is crucial for positioning the central part of the NAD molecule in its correct conformation close to the protein framework. The first two glycines are involved in binding the pyrophosphate moiety of the dinucleotide and the third, which is in the helix following the first strand, is involved in the packing of the helix against the β sheet. This last glycine residue is sometimes replaced by Ala, Ser or Pro in NADP-dependent enzymes. The negatively charged pyrophosphate group binds to the amino end of the first α-helix, because the dipole moment of an α-helix as well as the possibility to form hydrogen bonds to free NH groups at the end of the helix favors such binding (Hol et al., 1978). Furthermore, most enzymes with the GXGXXG fingerprint sequence contain a highly conserved Asp/Glu residue approximately 20 residues downstream from this motif. This acidic residue appears near the C terminus of the second β-strand and forms hydrogen bonds to the ribose of the adenosine moiety of the NAD. Formerly, it was stated that this acidic residue discriminates between NAD and NADP as a coenzyme. The Asp/Glu residue usually binds to the 2'-OH of the adenosine ribose of NAD. Most NADP-dependent enzymes have a Asn/Gln residue at this position, because the 2'-phosphate group prevents direct hydrogen bonding through repulsion with the Asp/Glu residue (Lesk, 1995; Bellamacina, 1996). However, other studies have implicated that this acidic residue also recognizes the 2'-phosphate group of NADP (Baker et al., 1992). Dependent on the ionization state of the 2'-phosphate of NADP this acidic residue interacts either by direct hydrogen-bonding or water-mediated (Baker et al., 1992).

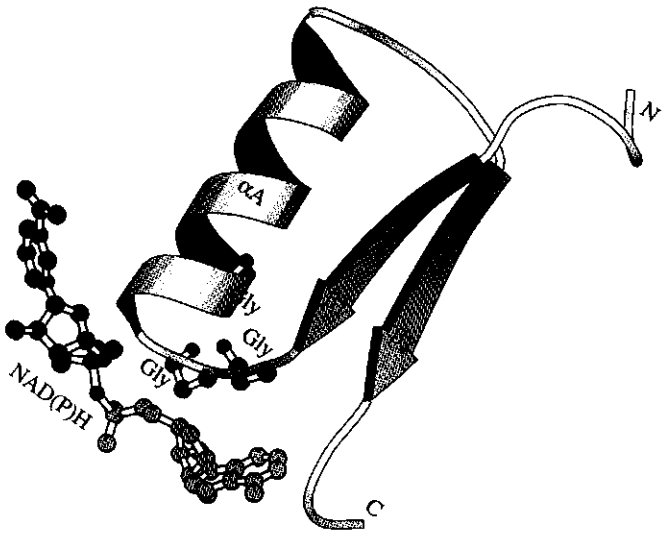

Fig. 4: Schematic diagram of the β1–αA–β2 moiety of the Rossmann fold with the GXGXXG fingerprint sequence.

1.2.3. Other NAD(P) binding folds

At least ten other types of folds have emerged for enzymes in which the cofactor NAD(P) plays the same function as in enzymes that contain the Rossmann fold (Table 1).

The folds or residues important for NAD(P) binding are indicated in dark in the different figures below.

1) TIM($\alpha_8\beta_8$)-barrel: In this fold the nicotinamide moiety is centered in the deep part of the active-site cavity, whereas the adenosine-2'-monophosphate is wedged in a shallow depression outside the β-barrel, between a couple of β-strands and α-helices. The presence of a large hydrophobic core in this type of structure allows the binding and reduction of a diverse and overlapping range of carbonyl substrates (e.g., monosaccharides, steroids, prostaglandin, aliphatic aldehydes, and xenobiotic compounds).

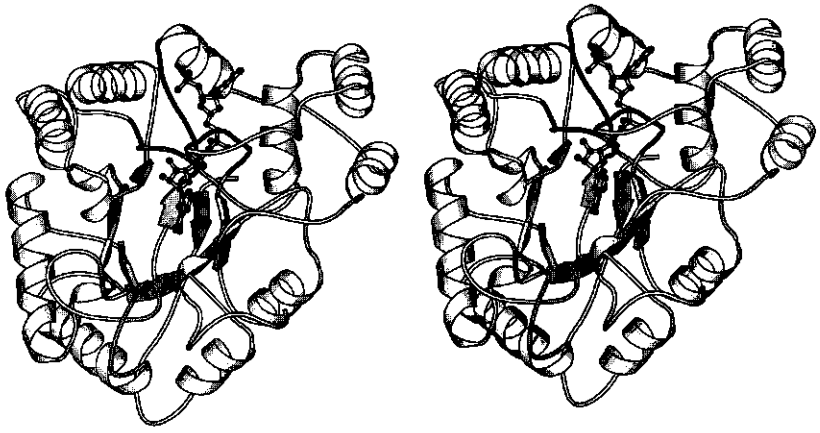

Fig. 5A: Stereoview of aldose reductase + NADPH (Rondeau et al., 1992; Wilson et al., 1992).

2) Flavodoxin-like: The binding site for NADP involves residues of the same subunit that binds FAD and residues from the other subunit of the dimer. Similar to other nucleotide binding proteins two glycines facilitate proximity of the main chain and cofactor. The only example with known structure, NAD(P)H:quinone reductase, involved in cancer chemoprotection and chemotherapy, catalyzes the reduction of different quinone derivatives. (Only structure with the NADP analog Cibacron blue is present in the PDB).

Fig. 5B: Stereoview of NAD(P)H:quinone reductase + FAD + Cibacron blue (Li et al., 1995).

3) Ferredoxin reductase-like, C-terminal NAD(P)-linked domain: The pyrophosphate part of NAD(P)H binds to a single βαβ unit, although the NAD(P)-binding domain differs from the Rossmann fold. The proteins containing this fold are electron transfer flavoproteins and mostly part of a multi-redox cofactor enzyme complex.

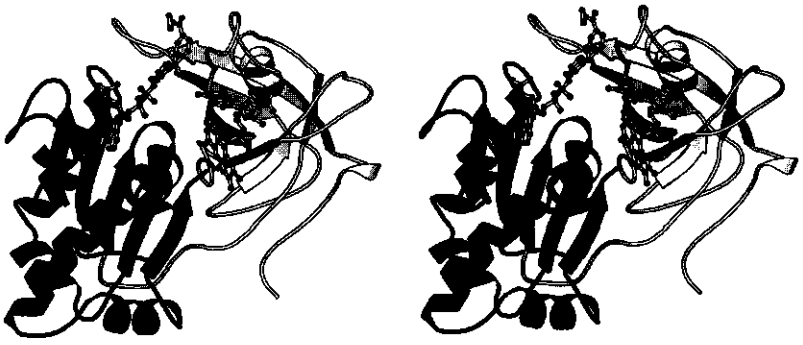

Fig. 5C: Stereoview of ferredoxin: $NADP^+$ oxidoreductase + FAD + $NADP^+$ (Karplus et al., 1991; Serre et al., 1996).

4) FAD/NAD(P)-binding domain: A central parallel β-sheet region of 5 strands is on one side covered by α-helices, almost similar to the Rossmann fold and the nucleotide binding domain fold. Enzymes of this class belong to the pyridine nucleotide-disulfide oxidoreductase family having similar folds for FAD and NAD(P) binding. Most of the enzymes catalyze the electron transfer between NAD(P)H and a disulfide/dithiol.

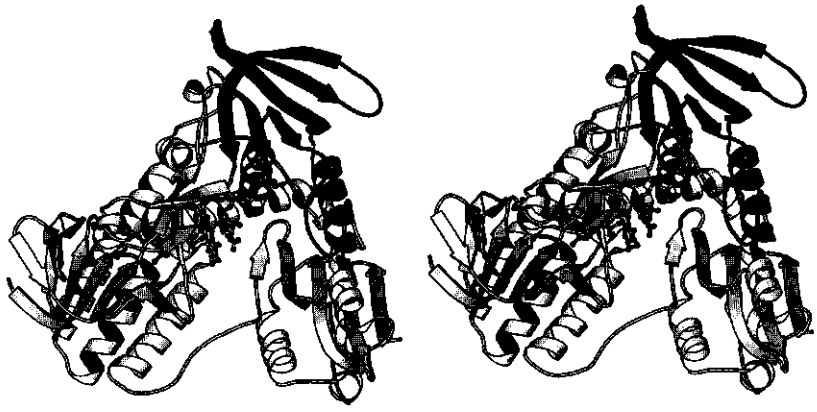

Fig. 5D: Stereoview of glutathione reductase + FAD + NADPH (Pai et al., 1988).

5) A nucleotide binding domain: Highly homologous to the Rossmann fold and the FAD/NAD(P)-binding fold, including the GXGXXG fingerprint. A parallel β-sheet region of five strands is surrounded on both sides by α-helices. The ADP molecule contacts the fingerprint region of the first βαβ-fold. The only example of this fold is trimethylamine dehydrogenase, an iron-sulfur containing flavoprotein, catalyzing the oxidative demethylation of trimethylamine to dimethylamine and formaldehyde, thereby transferring the reducing equivalents to an FAD-containing electron transfer flavoprotein.

Fig. 5E: Stereoview of trimethylamine dehydrogenase + FMN + ADP (Lim et al., 1988).

6) Aldehyde reductase (class III enzyme): This newly defined motif contains five β-strands connected by four α-helices and differs from the Rossmann fold by the absence of the

GXGXXG fingerprint sequence. Furthermore, the pyrophosphate moiety of NADH does not seem to interact specifically with a helix dipole. The only example with known structure is aldehyde dehydrogenase, which is a widely distributed enzyme important for the detoxification of aldehydes.

Fig. 5F: Stereoview of aldehyde dehydrogenase + NAD (Liu et al., 1997).

7) Dihydrofolate reductases: The NADP-binding site occupies a long shallow cleft that covers the C-terminal ends of five parallel β-sheets and the N-terminal positive ends of two α-helices, of which the helix dipoles are directed towards the pyrophosphate and adenosine moiety. Dihydrofolate reductase, the main target in antimicrobial and anticancer drugs, catalyzes the reduction of 7,8-dihydrofolate.

Fig. 5G: Stereoview of dihydrofolate reductase + NADPH (Matthews et al., 1979).

8) Isocitrate & isopropylmalate dehydrogenases: The NAD(P) is located at the entrance of a large cleft between the small and large domain. The adenosine-ribose moiety binds in the

interdomain cleft and is associated with two strands of the antiparallel β-sheet, which links both domains. Both enzymes belong to a unique class of metal-dependent decarboxylating dehydrogenases with varying substrate and cofactor specificities. The bifunctional enzymes catalyze two consecutive reactions, dehydrogenation and decarboxylation of 2-hydroxy acids.

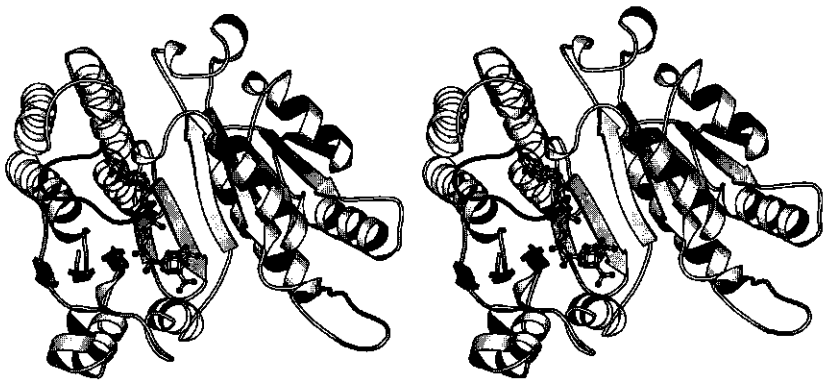

Fig. 5H: Stereoview of isopropylmalate dehydrogenase + NAD^+ (Hurley & Dean, 1994).

9) Heme-linked catalases: The NADPH molecule is situated in a shallow pocket at the junction of an α-helix- and an β-sheet-region. Interesting to note is that NADPH is folded into a right handed helix and that its function is still not clear. Heme-linked catalases are mostly homotetramers (Gouet et al., 1995) and decompose hydrogen peroxide into water and molecular oxygen.

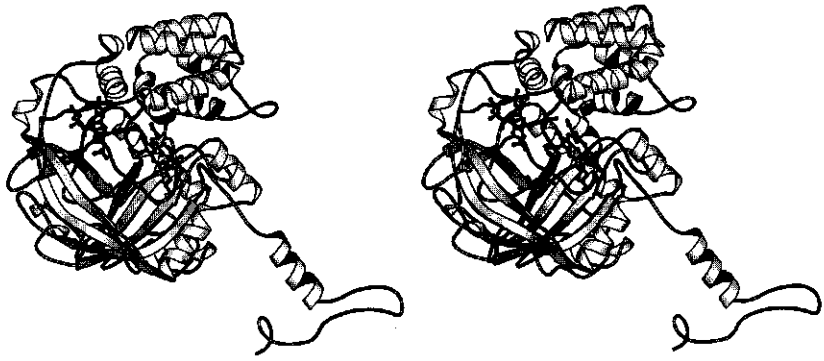

Fig. 5I: Stereoview of catalase + NADPH + heme (Gouet et al., 1995).

10) Ferredoxin-like: The NAD molecule binds in an extended conformation to an unusual type of dinucleotide-binding domain containing an interdigitated four-stranded antiparallel β-sheet with right-handed crossover helices on one side of the sheet. Like the Rossmann fold enzymes, the pyrophosphate of NAD is stabilized by a positive dipole at the N-terminus of an α-helix. The only example, HMGCoA-reductase, is involved in cholesterol biosynthesis, and requires two molecules of NADPH for the reduction of HMG-CoA to mevalonate (Lawrence et al., 1995; structure not submitted to PDB).

There are also three different protein folds known, which bind NAD(P), where the enzyme uses NAD(P) as a substrate (analog) or inhibitor:
1) ADP-ribosylation: The substrate NAD binds to a prominent cleft on the front face of the catalytic domain from diphtheria toxin. The conformation of the substrate differs substantially from the extended conformation found in most other NAD(P) binding proteins. Under physiological conditions diphtheria toxin catalyzes the transfer of an ADP-ribose group from NAD to a specific diphthamide (posttranslationally modified histidine) residue of elongation factor-2 to disrupt protein synthesis in mammalian cells resulting in cell death.

Fig. 5J: Stereoview of diphtheria toxin + NAD (Bell & Eisenberg, 1996).

2) Ribosome-inactivating proteins: The adenosine moiety of the substrate analog NADPH is located in an interdomain cleft, whereas the nicotinamide moiety extends into the solvent and interacts with the surface of an adjacent molecule. The crystal structure of trichosanthin with bound cofactor is the only known structure where the large NADPH molecule binds in the reversed mode. Ribosome-inactivating proteins are RNA N-glycosidases inactivating especially ribosomes.

Fig. 5K: Stereoview of trichosanthin + NADPH (Xiong et al., 1994).

3) β-Glucosyltransferase & glycogen phosphorylase: NAD acts as an inhibitor and binds to both the allosteric effector site (N), located at the subunit interface, and the nucleotide inhibitor site (I), situated at the entrance of the active site, in a highly folded conformation similarly as observed in catalase. NAD inhibits the AMP activation of glycogen phosphorylase b, which is the key enzyme in the first step of glycogen degradation. (Only structure with the NAD analog AMP available in the PDB)

Fig. 5L: Stereoview of phosphorylase b + AMP (Stura et al., 1983).

Finally, it should be mentioned that there are also enzymes that use NAD(P) as a prosthetic group (Ph.D. Thesis Hektor, 1998). In these enzymes, the NAD(P) molecule can only be released under denaturing conditions. For these so-called nicotinoproteins only the

structures of UDP-galactose-4-epimerase (Thoden et al., 1996) and glucose/fructose oxidoreductase (Kingston et al., 1997) are known. Both these enzymes belong to the α/β class containing a NAD(P)-binding Rossmann-fold (Table 1).

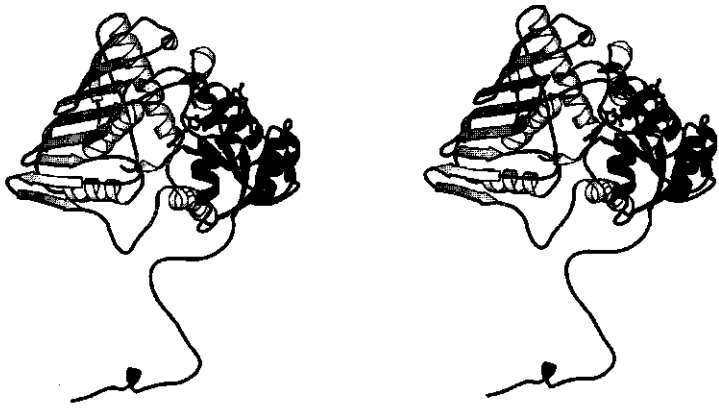

Fig. 5M: Stereoview of glucose/fructose oxidoreductase + NADP (Kingston et al., 1997).

1.3. Flavoenzymes

Flavoenzymes can be grouped into a relatively small number of classes, based on the type of reaction catalyzed, the ability to use molecular oxygen, and the nature of auxiliary redox centers (Massey, 1994).

The simple flavoproteins are classified in oxidases, electron transferases and flavoprotein monooxygenases, depending on the reactivity of the reduced enzyme with molecular oxygen. The more complex flavoproteins are divided in flavoprotein-disulfide oxidoreductases, *heme-containing flavoproteins* and *metal-containing flavoproteins*, depending on the type and use of auxiliary redox centers.

1.3.1. NAD(P) dependent flavoproteins

All flavoproteins with known NAD(P) binding site belong to the α/β class (Table 1). The enzymes of the disulfide oxidoreductase family (Williams, 1991) contain two $\beta\alpha\beta$-motifs for NAD(P) and FAD binding. The archetype of this class is glutathione reductase (Karplus & Schulz, 1991). Glutathione reductase contains four domains: a FAD- and a NADP-binding domain (both $\beta\alpha\beta$-topology), a central domain and an interface domain. The other flavoenzymes listed in Table 1 have different binding modes for the flavin cofactor (see also Mathews, 1991).

1.3.2. Flavoenzymes with unknown NAD(P) binding site

For some NAD(P)-binding flavoproteins of known structure, the mode of NAD(P) binding remains to be solved. For UDP-N-acetylenolpyruvylglucosamine reductase from *Escherichia coli* (Benson et al., 1996), NADH-oxidase from *Thermus thermophilus* (Hecht et al., 1996) and flavin reductase P from *Vibrio harveyi* (Tanner et al., 1996) the crystal structures without the pyridine nucleotide cofactor have recently been reported. However, for *p*-hydroxybenzoate hydroxylase from *Pseudomonas fluorescens*, the crystal structure without pyridine nucleotide cofactor is already known for almost 20 years (Wierenga et al., 1979; Schreuder et al., 1989).

UDP-N-acetylenolpyruvylglucosamine reductase (MurB) is a $\alpha+\beta$ protein composed of two domains (Benson et al., 1996). The N-terminal domain of MurB shares structural homology with the N-terminal domains of the flavoproteins *p*-cresol methylhydroxylase (PCMH) (Mathews et al., 1992) and vanillyl alcohol oxidase (VAO) (Mattevi et al., 1997). Recent sequence alignment studies have revealed that this domain is conserved and that many members of this novel class of structurally related flavoenzymes contain a covalently bound FAD (Fraaije et al., 1998). In contrast to MurB, both PCMH and VAO do not use dinucleotides as electron donor/acceptor (Fraaije & van Berkel, 1997).

NADH-oxidase and flavin reductase P are $\alpha+\beta$ proteins and belong to a novel structural NADH oxidase/flavine reductase family. Both proteins contain two domains, a sandwich domain and an excursion domain. The flavin cofactor binds in the interface between both subunits (Hecht et al., 1996; Tanner et al., 1996). Two isoforms of NADH oxidase are known which bind FAD and FMN, respectively (Hecht et al., 1996).

p-Hydroxybenzoate hydroxylase (PHBH) is the archetype of flavoprotein monooxygenases, and until recently the only enzyme from this class for which the crystal structure is known (Entsch & van Berkel, 1995). PHBH is an α/β protein which consists of 3 domains: a FAD binding domain, a substrate binding domain and an interface domain. The FAD binding domain contains a Rossmann fold with $\beta\alpha\beta$-topology for binding the ADP moiety of FAD (Wierenga et al., 1979; Schreuder et al., 1989). Structural relationships classify PHBH into two domains (Murzin et al., 1995; Mattevi, 1998), an FAD binding domain (including the interface domain) and a substrate binding domain. According to this structural classification, PHBH belongs to the same family as the NAD(P) independent flavoenzymes cholesterol oxidase (Vrielink et al., 1991), D-amino acid oxidase (Mattevi et al., 1996; Mizutani et al., 1996) and glucose oxidase (Hecht et al., 1993). Recently, the crystal structure of phenol hydroxylase, another flavoprotein monooxygenase was solved (Enroth, 1998a). However, as for PHBH, no binding site for NADPH was recognized in this enzyme sofar.

1.4. External flavoprotein monooxygenases

External flavoprotein monooxygenases catalyze the insertion of one atom of molecular oxygen into the substrate, using NAD(P) as external electron donor. Based on the reaction sequence these flavoenzymes can be divided in two subclasses:

1) Aromatic hydroxylases (e.g. *p*-hydroxybenzoate hydroxylase, phenol hydroxylase). Scheme 1A (Entsch et al., 1976, 1989; Maeda-Yorita & Massey, 1993).

2) Monooxygenases (e.g. mammalian (microsomal) flavin-containing monooxygenase, cyclohexanone monooxygenase). Scheme 1B (Beauty & Ballou, 1981; Ryerson et al., 1982).

The main difference in reaction sequence between both subclasses is that the aromatic hydroxylases release NAD(P) prior to oxygen attack.

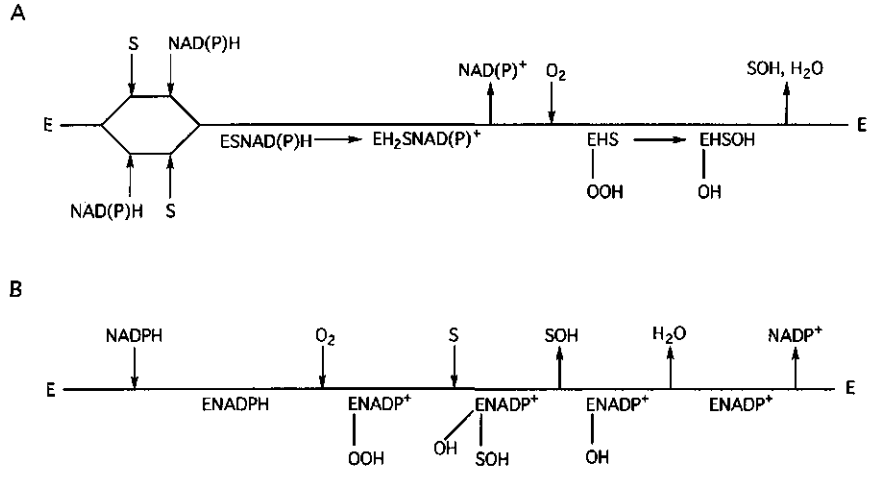

Scheme 1: Reaction pathways of external flavoprotein monooxygenases.

Two fingerprint motifs (βαβ-folds) are present in the monooxygenases both for FAD and NADP binding (Chen et al., 1988; Altenschmidt et al., 1992; Kubo et al., 1997; Stehr et al., 1998). In contrast, only one βαβ-fold for FAD binding is present in aromatic hydroxylases (Wierenga et al., 1983; 1986). The presence of two βαβ-folds in the monooxygenases could explain why in these enzymes the NADP remains bound during the entire reaction cycle (van Berkel, 1989).

1.5. *p*-Hydroxybenzoate hydroxylase

1.5.1. Biological function

p-Hydroxybenzoate hydroxylase (PHBH) catalyzes the conversion of *p*-hydroxybenzoate into 3,4-dihydroxybenzoate (protocatechuate) in the presence of NADPH and molecular oxygen (van Berkel & Müller, 1991; Entsch & van Berkel, 1995; van Berkel et al., 1997):

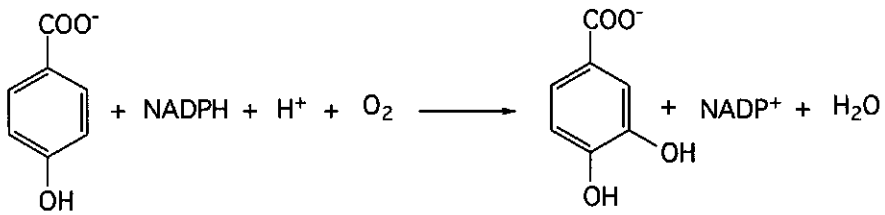

PHBH is responsible for channeling *p*-hydroxybenzoate via protocatechuate into the β-ketoadipate pathway of aromatic degradation (Ornston & Stanier, 1964; Stanier & Ornston, 1973; Harwood & Parales, 1996). *p*-Hydroxybenzoate is a common intermediate in the degradation of lignin and other plant compounds and this probably explains why PHBH is found extensively in soil organisms. Table 2 summarizes the purified *p*-hydroxybenzoate hydroxylases from different strains. The homodimeric enzymes of 88 kDa from *Pseudomonas fluorescens* and from *Pseudomonas aeruginosa* have been studied in detail (Entsch & van Berkel, 1995). Both enzymes can be treated interchangeably, because they differ in only two amino acids and do not have significant different catalytic properties.

Table 2. Characteristics of FAD-dependent 4-hydroxybenzoate hydroxylases. 3-PHBH: 4-hydroxybenzoate 3-hydroxylase; 1-PHBH: 4-hydroxybenzoate 1-hydroxylase.

Enzyme	Gene	Mass (kDa)	Source	Cofactor	Reference
3-PHBH	+	88 dimer	*P. fluorescens*	NADPH	(Weijer, 1983) (van Berkel, 1992)
	+	88 dimer	*P. aeruginosa*	NADPH	(Entsch, 1988)
		88 dimer	*P. putida*	NADPH	(Hosokawa, 1969)
		88 dimer	*P. desmolytica*	NADPH	(Yano, 1969)
		47 monomer	*C. cyclohexanicum*	NAD(P)H	(Fujii, 1985)
	+	88 dimer	*A. calcoaceticus*	NADPH	(Dimarco, 1993)
	+	88 dimer	*P. fluorescens* (isozyme)	NADPH	(Shuman, 1993)
	+	88 dimer	*R. leguminosarum* MNF300	NADPH	(Wong, 1994)
	+	88 dimer	*R. Legominosarum* B155	NADPH	(Wong, 1994)
	+	88 dimer	*Pseudomonas sp.* CBS3	NAD(P)H	(Seibold, 1996)
		88 dimer	*Moraxella sp.* GU_2	NAD(P)H	(Sterjiades, 1993)
		90 dimer	*R. erythropolis* S1	NADH	(Suemori, 1993; 1996)
1-PHBH		50 monomer	*C. parapsilosis*	NADH	(van Berkel, 1994a) (Eppink, 1997)

Recently, a novel *p*-hydroxybenzoate hydroxylase has been described, that catalyzes the FAD-dependent oxidative decarboxylation of *p*-hydroxybenzoate to 1,4-dihydroxybenzene (hydroquinone) in the yeast *Candida parapsilosis* (van Berkel, 1994a; Eppink, 1997). In yeast, catabolism of 4-hydroxybenzoate mostly proceeds through a modified β-ketoadipate pathway with 1,2,4-trihydroxybenzene (hydroxyhydroquinone) as ring-cleavage substrate (Anderson, 1980; Suzuki, 1986; Middelhoven, 1993; Wright, 1993; van Berkel, 1997).

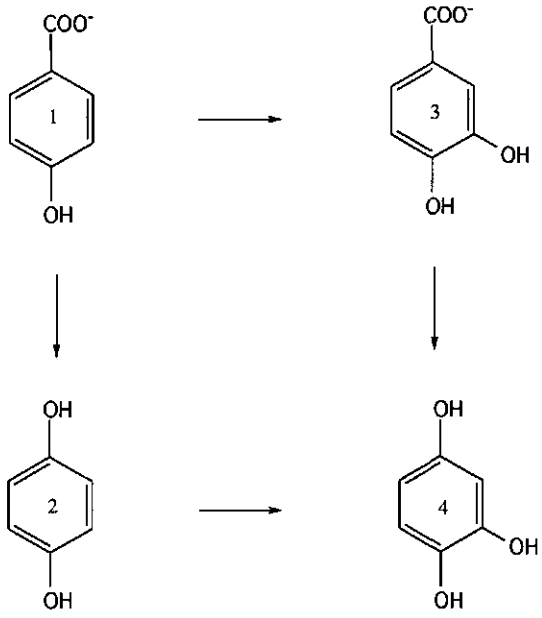

(1) *p*-hydroxybenzoate;

(2) hydroquinone;

(3) protocatechuate;

(4) hydroxyhydroquinone;

Scheme 2: Catabolism of 4-hydroxybenzoate in yeast.

1.5.2. Reaction mechanism

The reaction mechanism of PHBH has been studied with various spectroscopic techniques (Howell et al., 1972; Entsch et al., 1976; Entsch & Ballou, 1989; van Berkel & Müller, 1989; Vervoort, 1991). The catalytic cycle can be divided in a reductive (k_1) and oxidative half-reaction (k_2-k_4) and is depicted below (Husain & Massey, 1979) (Scheme 3).

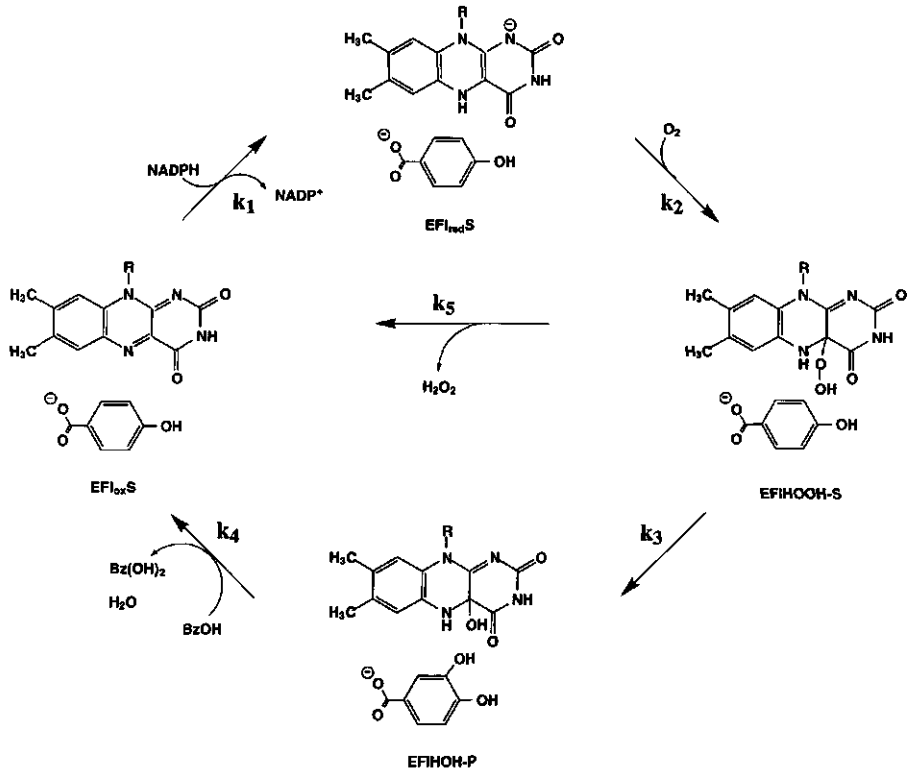

Scheme 3: Catalytic cycle of *p*-hydroxybenzoate hydroxylase.

In the first half reaction, the oxidized enzyme-substrate complex rapidly reacts with NADPH. The substrate acts as an effector by stimulating the rate of reduction up to 10^5 times. The high rate of flavin reduction correlates with the transient formation of a charge-transfer complex between the reduced flavin and $NADP^+$. After enzyme reduction, the $NADP^+$ is released.

In the second half reaction, oxygen reacts rapidly with the reduced enzyme/substrate complex to form a transient flavin (C4a)-hydroperoxide oxygenating species. The distal oxygen atom of the flavinhydroperoxide is then transferred to the substrate (electrophilic substitution) yielding the product 3,4-dihydroxybenzoate and flavin (C4a)-hydroxide. Finally, water is eliminated from this intermediate and the aromatic product is released. In the absence of substrate, or in the presence of non-substrate effectors, the flavin (C4a)-hydroperoxide intermediate decomposes to oxidized enzyme and hydrogen peroxide (NADPH oxidase activity, uncoupling of hydroxylation, k_5).

1.5.3. Crystal structure

The crystal structure of PHBH from *P. fluorescens* was initially solved at 2.5 Å resolution (Wierenga et al., 1979) and later refined to 1.9 Å resolution (Schreuder et al., 1989). Recently, the three-dimensional structure of the enzyme from *P. aeruginosa* was also determined (Lah et al., 1994). Not surprisingly, this structure is identical to that of the *P. fluorescens* enzyme. PHBH has a complex and unique folding pattern with three different domains: FAD binding domain, substrate binding domain and interface domain (Fig. 6).

Fig. 6: Ribbon diagram of *p*-hydroxybenzoate hydroxylase from *P. fluorescens* (see cover for full color representation)

The N-terminal FAD-binding domain (α/β structure, residues 1-175, in orange) contains the Rossmann fold, responsible for the interactions with the ADP portion of FAD which has an extended conformation. The substrate binding domain (α/β structure, residues 176-295, in green) is involved in most interactions with the aromatic substrate. The interface domain (α structure, residues 296-394, in blue) is necessary for the stabilization of the dimer. The active site of PHBH is buried in the interior of the protein and is surrounded by the three domains. All three domains are closely interwoven and residues from all three domains play some role in the catalytic mechanism. As noted above, structural databases classify PHBH as a two domain structure. One large domain is formed by the FAD-binding domain together with the interface domain and a loop excursion of the substrate binding domain, whereas the other smaller domain includes the substrate binding domain. This two domain structure is highly similar to the core structure of phenol hydroxylase, although the sequence identity between both enzymes is lower than 20%. Phenol hydroxylase is a

homodimer of 150 kDa, each subunit contains an extra 30 kDa domain involved in dimer association but otherwise with unknown function (Enroth et al., 1998a).

The aromatic substrate in PHBH is buried and held in the active site by multiple contacts (Fig. 7). The carboxylic moiety of the substrate interacts with the side chains of Ser212, Arg214 and Tyr222, whereas Tyr201, Pro293 and Tyr385 are involved in binding the hydroxyl moiety of the substrate.

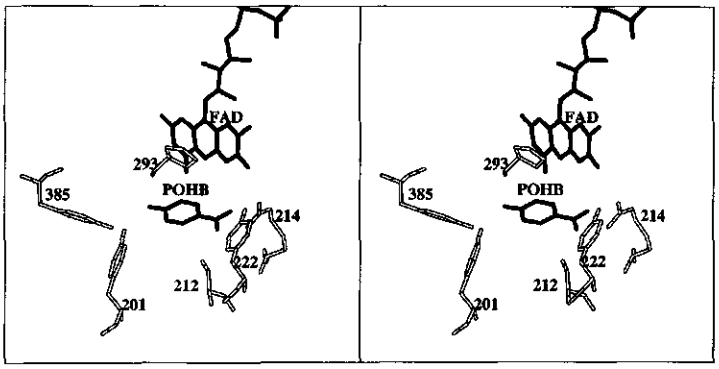

Fig. 7: Stereoview of the active site of *p*-hydroxybenzoate hydroxylase.

1.5.4. Site-directed mutagenesis

Studies from site-directed mutants have yielded a detailed insight in the role of the active site amino acid residues. Substitution by Phe showed that Tyr201 and Tyr385 play a crucial role in substrate activation (Entsch et al., 1991; Eschrich et al., 1993). A hydrogen bond network connects the 4-hydroxyl moiety of the substrate to the protein surface through Tyr201, Tyr385, structural water molecules, and His72 at the protein surface (Schreuder et al., 1994; Gatti et al., 1996). These findings together with molecular dynamics calculations suggested that the substrate *p*-hydroxybenzoate can be reversely protonated in the wild-type enzyme, with its phenolic pK_a influenced by the charge distribution of the active site and the protonation state of His72 (Gatti et al., 1996). Studies on the mutants Y201F and Y385F showed that the efficiency of hydroxylation is a competition between the rate of oxygen transfer to the substrate and the rate of hydrogen peroxide release (Entsch et al., 1991).

Furthermore, Tyr385 plays a crucial role in the regiospecificity of substrate hydroxylation (van der Bolt et al., 1997).

The ionic interaction between the side chain of Arg214 and the carboxylic moiety of the substrate is essential for catalysis. Studies on Arg214 mutants showed a lower affinity for the substrate and a strong uncoupling of hydroxylation (van Berkel et al., 1992). Tyr222, also at hydrogen bond distance of the carboxyl moiety of the substrate (Fig.6), is another residue crucial for efficient hydroxylation (Entsch et al., 1994; van Berkel et al., 1994b; Gatti et al., 1994; van der Bolt et al., 1996). Crystallographic data suggested that the uncoupling of hydroxylation in Tyr222 mutants is associated with a movement of the flavin ring out of the active site (Schreuder et al., 1994; Gatti et al., 1994; Entsch & van Berkel, 1995). This flavin motion may provide a path for the exchange of substrates and products during catalysis (Schreuder et al., 1994; Gatti et al., 1994). In the crystal structure of phenol hydroxylase a similar movement of the flavin ring was observed. However, in this enzyme an additional loop movement seems required to close the active site (Enroth et al., 1998a). Shielding the active site from solvent is necessary for stabilisation of the flavin (C4a)-hydroperoxide oxygenation species (Gatti et al., 1994).

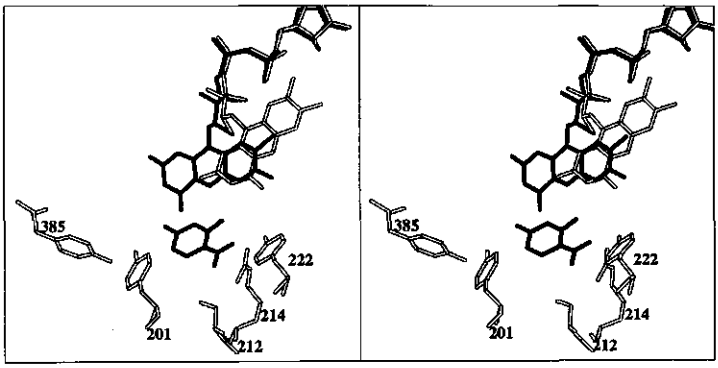

Fig. 8: Stereoview of the flavin ring movement in *p*-hydroxybenzoate hydroxylase, with the "in" (black bonds) and "out" (white bonds) conformation.

A number of residues not directly involved in substrate binding, have also been changed by site-directed mutagenesis. Table 3 summarizes the impact of the amino acid substitutions on catalysis.

Table 3. Function of PHBH amino acid residues.

Residue	Mutation(s)	Function	Reference
His72	Asn	substrate activation; flavin reduction	(Palfey, 1999)
Cys116	Ser	oxidation causes microheterogeneity	(Eschrich, 1990)
Cys152	Ser	no functional role	(van der Bolt, 1994)
Cys158	Ser	FAD binding	(van der Bolt, 1994)
Tyr201	Phe	substrate activation; flavin reduction	(Entsch, 1991; Eschrich, 1993)
Cys211	Ser	mercuration prevents substrate binding	(van der Bolt, 1994)
Ser212	Ala	substrate binding	(van Berkel, 1994)
Arg214	Lys, Gln, Ala	substrate binding	(van Berkel, 1992)
Arg220	Lys	flavin motion	(Moran, 1996)
Tyr222	Phe, Ala, Val	flavin motion	(Gatti, 1994; Schreuder, 1994; van der Bolt, 1996)
Lys297	Met	substrate activation	(Moran, 1997)
Asn300	Asp	miscellaneous (protein conformation)	(Palfey, 1994)
Cys332	Ser	no functional role	(van der Bolt, 1994)
Tyr385	Phe	substrate activation; flavin reduction; regioselectivity of hydroxylation	(Entsch, 1991; Eschrich, 1993; Lah, 1994; van der Bolt, 1997)

Except from Cys116, Cys211 and Cys332, all residues mentioned in Table 3 are strictly conserved among PHBH enzymes of known primary structure. The accessible surface residue Cys116 is highly variable and replaced by Ala, Gly and Ser in other PHBH enzymes. Replacement of Cys116 by Ser in PHBH from *P. fluorescens* made the enzyme

resistant to oxidation (Eschrich et al., 1990). In phenol hydroxylase, the conserved residues Arg287 (Arg220 in PHBH) and Tyr289 (Tyr222 in PHBH) serve a direct role in substrate binding (Enroth et al., 1998). The conservation of some active site residues and a similar folding topology of the core structure of PHBH and phenol hydroxylase might point to a common ancestor of the flavoprotein aromatic hydroxylases.

The reaction mechanism of *p*-hydroxybenzoate hydroxylase is intriguing and rather complex. Different sequential chemical reactions are mediated by the flavin as influenced by the protein environment. PHBH has a narrow substrate specificity and only benzoate derivatives with a electron donating group at the C4 position are hydroxylated. The efficiency of substrate hydroxylation depends on the chemical reactivity of the substrates, their mode of activation in the active site and the stabilisation of the flavin-C4a-hydroperoxide intermediate (van der Bolt et al., 1997). Moreover, the number of actual substrates is limited by the narrow effector specificity. Potential substrates like *p*-aminobenzoate and 2-hydroxy-4-aminobenzoate are poorly converted, because their binding, although similar to the native substrate (Schreuder et al., 1994), does hardly stimulate the rate of enzyme reduction (Table 4). The rate of reduction is not simply correlated to the conformation of the flavin ring (Table 4). This suggests that some unknown changes are involved in the reductive half reaction, and that these changes are linked to the ionic state of the substrate and the H-bond network connecting the 4-hydroxyl group with the protein surface (Palfey, 1999).

Table 4. Some characteristics of PHBH with substrate analogs.

Substrate analog	k_{red}	k_{cat}	Flavin conformer
	s^{-1}	s^{-1}	
p-hydroxybenzoate	300[a]	55[a]	in[e]
3,4-dihydroxybenzoate	4[b]	4[b]	in[f]
2,4-dihydroxybenzoate	1.1[c]	0.7[c]	out[g]
p-aminobenzoate	0.09[d]	0.09[d]	in[g]
2-hydroxy-4-aminobenzoate	0.003[a]	0.003[a]	out[g]

[a] van Berkel, 1992; [b] Eschrich, 1993; [c] van der Bolt, 1996; [d] Gatti, 1996; [e]Schreuder, 1989; [f]Schreuder, 1988; [g]Schreuder, 1994.

1.5.5. NADPH binding

The structure of *p*-hydroxybenzoate hydroxylase is unusual because there is no well-defined binding site for the NADPH coenzyme (Schreuder et al., 1991). So far, crystallographic analysis did not reveal a structure of the enzyme complexed with NADPH and soaking experiments with the coenzyme analogue ADPR resulted in displacement of FAD by ADPR (van der Laan et al., 1989). For optimal catalysis, it is essential that the flavin is rapidly reduced by NADPH. How this is achieved is as yet unknown. Spectroscopic studies showed that the nicotinamide ring binds at the *re* side of the flavin ring (Manstein et al., 1986) and that the *pro-R* hydrogen of the C4 atom is transferred to the N5 of the flavin ring (You, 1982). From these findings and chemical modification studies with 5'-*p*-fluorosulfonylbenzoyladenosine a three-dimensional model for the mode of NADPH binding was proposed (van Berkel et al., 1988). In this PhD study, this model served as a starting point to address the mode of NADPH binding in PHBH by site-directed mutagenesis.

1.6. Outline of the thesis

The aim of the research described in this thesis was to investigate the mode of NADPH binding in *p*-hydroxybenzoate hydroxylase from *P. fluorescens* by a combined site-directed mutagenesis and X-ray crystallographic approach.

In **Chapter 2** the apoenzyme of PHBH was reconstituted with a modified FAD analog present in alcohol oxidases from methylotrophic yeasts. The crystal structure of *p*-hydroxybenzoate hydroxylase with this flavin analog provided direct evidence for the presence of an arabityl sugar chain in the modified form of FAD. The flavin ring attains the "out" conformation, which could explain the partial uncoupling of substrate hydroxylation. Reduction of the arabino-FAD containing enzyme-substrate complex by NADPH was extremely fast, supporting the idea that flavin mobility is involved in NADPH recognition.

In **Chapter 3**, the properties of mutant Arg44Lys are presented. This study revealed that Arg44, located at the *si*-side of the flavin ring, is important for FAD binding and for efficient enzyme reduction.

Chapter 4 denotes the important role of the conserved Arg42 in NADPH binding. Lys42 and Ser42 replacements resulted in impaired NADPH binding. In contrast to an earlier conclusion drawn for PHBH from *Acinetobacter calcoaceticus*, substitution of Arg42 with Ser hardly disturbs FAD binding.

Chapter 5 reports a new sequence fingerprint motif in flavoprotein aromatic hydroxylases with a putative dual function in FAD and NAD(P)H binding.

Chapter 6 describes the properties of His162 and Arg269 mutants. Evidence was obtained that both residues interact with the pyrophosphate moiety of NADPH. Based on this and additional GRID calculations an interdomain binding of NADPH is proposed.

Chapter 7 provides evidence that Phe161 and Arg166 in the FAD binding domain are not directly involved in NADPH binding. The crystal structure of Arg166Ser revealed that Arg166 is structurally important for the inter/intra domain contact.

Chapter 8 describes the properties of PHBH from *Pseudomonas sp.* CBS3. This enzyme, involved in the biodegradation of 4-chlorobenzoate, represents the first PHBH with known sequence which prefers NADH over NADPH as the electron donor. Based on an isolated region of sequence divergence, it is proposed that helix H2 in PHBH is involved in determining the coenzyme specificity.

Chapter 9 reports on the role of helix H2 in determining the coenzyme specificity. Multiple amino acid changes were introduced to create a NADH-dependent enzyme.

Chapter 10 describes the crystal structures of substrate-free PHBH and in complex with the substrate analog benzoate. The results in this study shows that large protein conformational changes are not required for substrate binding.

1.7. References

Altenschmidt U, Bokranz M, Fuchs G. 1992. Novel aerobic 2-aminobenzoate metabolism. *Eur J Biochem 207*:715-722.

Anderson JJ, Dagley S. 1980. Catabolism of aromatic acids in *Trichosporon cutaneum. J Bacteriol 141*:534-543.

Baker PJ, Britton KL, Rice DW, Rob A, Stillman TJ. 1992. Structural consequences of sequence patterns in the fingerprint region of the nucleotide binding fold. *J Mol Biol 228*:662-671.

Beauty NB, Ballou DP. 1981. The oxidative half-reaction of liver microsomal FAD-containing monooxygenase. *J Biol Chem 256*:4619-4625.

Bell CE, Eisenberg D. 1996. Crystal structure of diphtheria toxin bound to nicotinamide adenine dinucleotide. *Biochemistry 35*:1137-1149.

Bellamacina CR. 1996. The nicotinamide dinucleotide binding motif: a comparison of nucleotide binding proteins. *FASEB J 10*:1257-1269.

Benson TE, Filman DJ, Walsh CT, Hogle JM. 1995. An enzyme-substrate complex involved in bacterial cell wall biosynthesis. *Nat Struct Biol 2*:644-653.

Bränden C, Tooze J. 1991. Introduction to protein structure, Garland Publishing, Inc. New York and London.

Chen Y-C, Peoples OP, Walsh C. 1988. *Acinetobacter* cyclohexanone monoooxygenase: gene cloning and sequence determination. *J Bacteriol 170*:781-789.

DiMarco AA, Averhoff BA, Kim EE, Ornston LN. 1993. Evolutionary divergence of *pobA*, the structural gene encoding *p*-hydroxybenzoate hydroxylase in an *Acinetobacter calcoaceticus* strain well-suited for genetic analysis. *Gene 125*:25-33.

Enroth C, Huang W, Waters S, Neujahr H, Lindqvist Y, Schneider G. 1994. Crystallization and preliminary X-ray analysis of phenol hydroxylase from *Trichosporon cutaneum*. *J Mol Biol 238*:128-130.

Enroth C, Neujahr H, Schneider G, Lindqvist Y. 1998a. The crystal structure of phenol hydroxylase in complex with FAD and phenol provides evidence for a concerted conformational change in the enzyme and its cofactor during catalysis. *Structure 6*:605-617.

Enroth C. 1998b. PhD. Thesis.

Entsch B, Ballou DP, Massey V. 1976. Flavin-oxygen derivatives involved in hydroxylation by *p*-hydroxybenzoate hydroxylase. *J Biol Chem 251*:255-2563.

Entsch B, Nan Y, Weaich K, Scott KF. 1988. Sequence and organization of *pob*A, the gene coding for *p*-hydroxybenzoate hydroxylase, an inducible enzyme from *Pseudomonas aeruginosa*. *Gene 71*:279-291.

Entsch B. Ballou DP. 1989. Purification, properties, and oxygen reactivity of *p*-hydroxybenzoate hydroxylase from *Pseudomonas aeruginosa*. *Biochim Biophys Acta 999*:313-322.

Entsch B, Palvey BA, Ballou DP, Massey V. 1991. Catalytic function of tyrosine residues in *para*-hydroxybenzoate hydroxylase as determined by the study of site-directed mutants. *J Biol Chem 266*:17341-17349.

Entsch B, van Berkel WJH. 1995. Structure and mechanism of para-hydroxybenzoate hydroxylase. *FASEB J 9*:476-483.

Eppink MHM, Boeren JA, Vervoort J, van Berkel WJH. 1997. Purification and properties of 4-hydroxybenzoate 1-hydroxylase (decarboxylating), a novel flavin adenine dinucleotide-dependent monooxygenase from *Candida parapsilosis* CBS604. *J Bacteriol 179*:6680-6687.

Eschrich K, van Berkel WJH, Westphal AH, de Kok A, Mattevi A, Obmolova A, Kalk KH, Hol WGJ. 1990. Engineering of microheterogeneity-resistant *p*-hydroxybenzoate hydroxylase from *Pseudomonas fluorescens*. *FEBS Lett 277*:197-199.

Eschrich K, van der Bolt FJT, de Kok A, van Berkel WJH. 1993. Role of Tyr201 and Tyr385 in substrate activation by *p*-hydroxybenzoate hydroxylase from *Pseudomonas fluorescens*. *Eur.J.Biochem 216*:137-146.

Fraaije MW, van Berkel, WJH. 1997. Catalytic mechanism of the oxidative demethylation of 4-(methoxymethyl)phenol by vanillyl-alcohol oxidase. *J Biol Chem 272*:18111-18116.

Fraaije MW, van Berkel WJH, Benen JAE, Visser J, Mattevi A. 1998. A novel oxidoreductase family sharing a conserved FAD-binding domain.

Fuji T, Kaneda T. 1985. Purification and properties of NADH/NADPH-dependent *p*-hydroxybenzoate hydroxylase from *Corynebacterium cyclohexanicum*. *Eur J Biochem 147*:97-104.

Gatti DL, Palvey BA, Lah MS, Entsch B, Massey V, Ballou DP, Ludwig ML. 1994. The mobile flavin of 4-OH benzoate hydroxylase. *Science 266*:110-114.

Gatti DL, Entsch B, Ballou DP, Ludwig ML. 1996. pH-Dependent structural changes in the active site of *p*-hydroxybenzoate hydroxylase point to the importance of proton and water movements during catalysis. *Biochemistry 35*:567-578.

Gouet P, Jouve H-M, Dideberg O. 1995. Crystal structure of *Proteus mirabilis* PR catalase with and withoud bound NADPH. *J Mol Biol 249*:933-954.

Harwood CS, Parales RE. 1996. The beta-ketoadipate pathway and the biology of self-identity. *An Rev Microb 50*:553-590.

Hecht HJ, Kalisz HM, Hendle J, Schmid RD, Schomburg D. 1993. Crystal structure of glucose oxidase from *Aspergillus niger* refined at 2.3Å resolution. *J Mol Biol 229*:153-172.

Hecht HJ, Erdmann H, Park HJ, Sprinzl M, Schmid RD. 1995. Crystal structure of NADH oxidase from *Thermus thermophilus*. *Nat Struct Biol 2*:1109-1114.

Hektor H. 1998. Ph.D. Thesis.

Hol WGJ, van Duijnen PT, Berendsen HJC. 1978. The α-helix dipole and properties of proteins. *Nature 273*:443-446.

Hosokawa K, Stanier RY. 1966. Crystallization and properties of *p*-hydroxybenzoate hydroxylase from *Pseudomonas putida*. *J Biol Chem 241*:2453-2460.

Howell LG, Spector T, Massey V. 1972. Purification and properties of *p*-hydroxybenzoate hydroxylase from *Pseudomonas fluorescens*. *J Biol Chem 247*:4340-4350.

Hurley JH, Dean AM. 1994. Structure of 3-isopropylmalate dehydrogenase in complex with NAD^+: ligand-induced loop closing and mechanism for cofactor specificity. *Structure 2*:1007-1016.

Husain M, Massey V. 1979. Kinetic studies on the reaction mechanism of *p*-hydroxybenzoate hydroxylase. Agreement of steady state and rapid reaction data. *J Biol Chem 254*:6657-6666.

Karplus PA, Daniels MJ, Herriott JR. 1991. Atomic structure of ferredoxin-$NADP^+$ reductase: prototype for a structurally novel flavoenzyme family. *Science 251*:60-66.

Karplus PA, Schulz GE. 1991. Refined three-dimensional structure of glutathione reductase. In: Müller F, ed.*Chemistry and biochemistry of flavoenzymes 2* Boca Raton, Florida: CRC Press. pp 213-228.

Kubo A, Itoh S, Itoh K, Kamataki T. 1997. Determination of FAD-binding domain in flavin-containing monooxygenase 1 (FMO1). *Arch Biochem Biophys 345*:271-277.

Lah MS, Palvey BA, Schreuder HA, Ludwig ML. 1994. Crystal structures of mutant *Pseudomonas aeruginosa* *p*-hydroxybenzoate hydroxylases: The Tyr201Phe, Tyr385Phe, and Asn300Asp variants. *Biochemisry 33*:1555-1564.

Lawrence CM, Rodwell VW, Stauffacher CV. Crystal structure of *Pseudomonas mevalonii* HMG-CoA reductase at 3.0 angstrom resolution. *Science 268*:1758-1762.

Lesk AM. 1995. NAD-binding domains of dehydrogenases. *Curr Op Struct Biol 1*:954-967.

Li R, Bianchet MA, Talalay P, Amzel LM. 1995. The three-dimensional structure of NAD(P)H:quinone reductase, a flavoprotein involved in cance chemoprotection and chemotheray: Mechanism of the two-electron reduction. *Proc NAtl Acad Sci USA 92*:8846-8850.

Lim LW, Mathews FS, Steenkamp DJ. 1988. Identification of ADP in the iron-sulfur flavoprotein trimethylamine dehydrogenase. *J Biol Chem 2633*075-3078.

Liu ZJ, Sun YJ, Rose J, Chung YJ, Hsiao CD, Chang WR, Kuo I, Perozich J, Lindahl R, Hempel J, Wang B-C. 1997. The first structure of an aldehyde dehydrogenase reveals novel interactions between NAD and the rossmann fold. *Nat Struct Biol 4*:317-326.

Maeda-Yorita K, Massey V. 1993 On the reaction mechanism of phenol hydroxylase. *J Biol Chem 268*:4134-4144.

Manstein DJ, Pai EF, Schopfer LM, Massey V. 1986. Absolute stereochemistry of flavins in enzyme-catalyzed reactions. *Biochemistry 25*:6807-6816.

Massey V. 1994. Introduction: Flavoprotein structure and mechanism. *FASEB J 9*:473-475.

Mathews FS, Chen Z-W, Bellamy HD. 1991. Three-structure of *p*-cresol methylhydroxylase (Flavocytochrome c) from *Pseudomonas putida* at 3.0-Å resolution. *Biochemistry 30*:238-247.dimensional

Mathews FS. 1991. New flavoenzymes. *Curr Opin Struct Biol 1*:954-967.

Mattevi A, Vanoni MA, Todone F, Rizzi M, Teplyakov A, Coda A, Bolognesi M, Curti, B. 1996. Crystal structure of D-amino acid oxidase: A case of active site mirror-image convergent evolution with flavocytochrome b_2. *Proc Natl Acad Sci USA 93*:7496-7501.

Mattevi A, Fraaije MW, Mozzarelli A, Olivi L, Coda A, van Berkel WJH. 1997. Crystal structures and inhibitor binding in the octameric flavoenzyme vanillyl-alcohol oxidase: the shape of the active-site cavity controls substrate specificity. *Structure 5*:907-920.

Mattevi A. 1998. The PHBH fold: Not only flavoenzymes. *Biophys J 70*:217-222.

Matthews DA, ALden RA, Freer ST, Xuong N-H, Kraut J. 1979. Dihydrofolate reductase from *Lactobacillus casei*. *J Biol Chem 254*:4144-4151.

Mathews FS. 1991. New flavoenzymes. *Curr Opin Struct Biol 1*:954-967.

Middelhoven WJ. 1993. Catabolism of benzene compounds by ascomycetes and basidiomycetous yeasts and yeastlike fungi. *A van Leeuwenhoek 63*:125-144.

Mittl PRE, Berry A, Scrutton NS, Perham RN, Schulz GE. 1994. Anatomy of an engineered NAD-binding site. *Prot Science 3*:1504-1514.

Mizutani H, Miyahara I, Hirotsu K, Nishina Y, Shiga K, Setoyama C, Miura R. 1996. Three-dimensional structure of porcine kidney D-amino acid oxidase at 3.0Å resolution. *J Biochem 120*:14-17.

Moran GR, Entsch B, Palvey BA, Ballou DP. 1996. Evidence for flavin movement in the function of *p*-hydroxybenzoate hydroxylase from studies of the mutant Arg220Lys. *Biochemistry* 35:9278-9285.

Moran GR, Entsch B, Palvey BA, Ballou DP. 1997. Electrostatic effects on substrate activation in *para*-hydroxybenzoate hydroxylase: Studies of the mutant lysine 297 methionine. *Biochemistry 36*:7548-7556.

Murzin AG. Brenner SE, Hubbard T, Chothia C. 1995. SCOP: a structural classification of proteins database for the investigation of sequences and structures. *J Mol Biol 247*:536-540.

Ornston LN, Stanier RY. 1964. Mechanism of β-ketoadipate formation by bacteria. *Nature 26*:1279-1283.

Pai EF, Karplus PA, Schulz GE. 1988. Crystallographic analysis of the binding of NADPH, NADPH fragments, and NADPH analogues to glutathione reductase. *Biochemistry 27*:4465-4474.

Palfey BA, Entsch B, Ballou DP, Massey V. 1994. Changes in the catalytic properties of *p*-hydroxybenzoate hydroxylase caused by the mutation Asn300Asp. *Biochemistry 33*:1545-1554.

Palfey BA, Moran GR, Entsch B, Ballou DP, Massey V. 1999. Substrate recognition by "Password" in *p*-hydroxybenzoate hydroxylase. *Biochemistry 38*:1153-1158.

Rondeau JM, Tête-Favier F, Podjarn A, Reymann JM, Barth P, Biellmann JF, Moras D. 1992. Novel NADPH-binding domain revealed by the crystal structure of aldose reductase. *Nature 355*:469-472.

Rossmann MG, Moras D, Olsen KW. 1974. Chemical and biological evolution of a nucleotide-binding protein. *Nature 250*:194-199.

Ryerson CC, Ballou DP, Walsh C. 1982. Mechanistic studies on cyclohexanone oxygenase. *Biochemistry 21*:2644-2655.

Schreuder HA, van der Laan JM, Hol WGJ, Drenth J. 1988. Crystal structure of *p*-hydroxybenzoate hydroxylase complexed with its reaction product 3,4-dihydroxybenzoate. *J Mol Biol 199*:637-648.

Schreuder HA, Prick PAJ, Wierenga RK, Vriend G, Wilson KS, Hol, WGJ, Drenth J. 1989. Crystal structure of the *4-hydroxybenzoate hydroxylase*-substrate complex refined at 1.9 Å resolution. *J Mol Biol 208*:679-696.

Schreuder HA, van der Laan JM, Hol WGJ, Drenth J. 1991. The structure of *p*-hydroxybenzoate hydroxylase. In: Müller F, ed.*Chemistry and biochemistry of flavoenzymes 2*. Boca Raton, Florida: CRC Press. pp 31-64.

Schreuder HA, Mattevi A, Obmolova G, Kalk KH, Hol WGJ. *1994*. Crystal structures of wild-type *p*-hydroxybenzoate hydroxylase complexed with 4-aminobenzoate, 2,4-dihydroxybenzoate, and 2-hydroxy-4-aminobenzoate and of the Tyr222Ala mutant complexed with 2-hydroxy-4-aminobenzoate. Evidence for a proton channel and a new binding mode of the flavin ring. *Biochemistry 33*:10161-10170.

Seibold B, Matthes M, Eppink MHM, Lingens F, van Berkel WJH, Müller, R. 1996. 4-Hydroxybenzoate hydroxylase from *Pseudomonas* sp.CBS3: Purification, characterization, gene cloning, sequence analysis and assignment of structural features determining the coenzyme specificity. *Eur J Biochem 239*:469-478.

Serre L, Vellieux MD, Medina M, Gomez-Moreno C, Fontecilla-Camps JC, Frey M. 1996. X-ray structure of the ferredoxin:$NADP^+$ reductase from the cyanobacterium *Anabaena* PCC 7119 at 1.8 Å resolution, and crystallographic studies of $NADP^+$ binding at 2.25 Å resolution. *J Mol Biol 263*:20-39.

Shuman B, Dix TA. 1993. Cloning, nucleotide sequence and expression of a *p*-hydroxybenzoate hydroxylase isozyme gene from *Pseudomonas fluorescens. J Biol Chem 268*:17057-17062.

Stanier RY, Ornston LN. 1973. The β-ketoadipate pathway. *Adv Microb Physiol* (Rose, A.H. and Tempest, D.W., eds.) *9*:89-151.

Stehr M, Diekmann H, Smau L, Seth O, Ghisla S, Singh M, Macheroux P. 1998. A hydrophobic sequence motif common to N-hydroxylating enzymes. *TIBS 23*:56-57.

Sterjiades R. 1993. Properties of NADH/NADPH-dependent *p*-hydroxybenzoate hydroxylase from *Moraxella* sp. *Biotechol Appl Biochem 17*:77-90.

Stura EA, Zanotti G, Babu YS, Sansom MSP, Stuart DI, Wilson KS, Johnson LN, van de Werve G. 1983. Comparison of AMP and NADH binding to glycogen phosphorylase b. *J Mol Biol 170*:529-565.

Suemori A, Kurane R, Tomizuka N. 1993. Purification and properties of three types of monohydroxybenzoate monooxygenase from *Rhodococcus erythropolis* S-1. *Biosci Biotech Biochem 57*:1487-1491.

Suemori A, Nakajima K, Kurane R, Nakamura Y. 1996. Temperature- and detergent-dependent oligomeric structures of flavoprotein monohydroxybenzoate hydroxylases from *Rhodococcus erythropolis. J Ferm Bioen 82*:174-176.

Suzuki K, Itoh M. 1986. Metabolism of *p*-hydroxybenzoate via hydroxyquinol by *Trichosporon cutaneum* WY2-2: Characterization of the pathway using superoxide dismutase as a stabilizer of hydroxyquinol. *Plant Cell Physiol 27*:1451-1460.

Tanner JJ, Lei B, Tu S-C, Krause KL. 1996. Flavin reductase P: structure of a dimeric enzyme that reduces flavin. *Biochemistry* 35:13531-13539.

Van Berkel WJH, Müller F, Jekel PA, Weijer WJ, Schreuder HA, Wierenga RK. 1988. Chemical modifcation of tyrosine-38 in *4-hydroxybenzoate hydroxylase* from *Pseudomonas fluorescens* by 5'-*p*-fluorosulfonylbenzoyladenosine: A probe for the elucidation of the NADPH binding site? *Eur.J.Biochem 176*:449-459.

Van Berkel WJH, Müller, F. 1989. The temperature and pH dependene of some properties of *p*-hydroxybenzoate hydroxylase from *Pseudomonas fluorescens. Eur J Biochem 179*:307-314.

Van Berkel WJH. 1989. PhD. Thesis.

Van Berkel WJH, Müller F. 1991. Flavin-dependent monooxygenases with special reference to 4-hydroxybenzoate hydroxylase. In: Müller F, ed.*Chemistry and biochemistry of flavoenzymes 2*. Boca Raton, Florida: CRC Press. pp 1-29.

Van Berkel WJH, Westphal A, Eschrich K, Eppink MHM, de Kok A. 1992. Substitution of Arg214 at the substrate-binding site of *p*-hydroxybenzoate hydroxylase from *Pseudomonas fluorescens. Eur J Biochem* 210:411-419.

Van Berkel WJH, Eppink MHM, Middelhoven WJ, Vervoort J, Rietjens IMCM. 1994a. Catabolism of 4-hydroxybenzoate in *Candida parapsilosis* proceeds through initial oxidative decarboxylation by a FAD-dependent 4-hydroxybenzoate 1-hydroxylase. *FEMS Microbiol Lett 121*: 207-216.

Van Berkel WJH, van der Bolt FJT, Eppink MHM, de Kok A, Rietjens IMCM, Veeger C, Vervoort J, Schreuder H. 1994b. Substrate and effector specificity of two active-site mutants of *p*-hydroxybenzoate hydroxylase from *Pseudomonas fluorescens*. In: Yagi K, Williams CH Jr, Massey V. *Flavins and flavoproteins 1993*. W. de Gruyter & Co., Berlin Germany pp 231-234.

Van Berkel WJH, Eppink MHM, van der Bolt FJT, Vervoort J, Rietjens IMCM. (1997). *p*-Hydroxybenzoate hydroxylase: Mutants and mechanism. In: Stevenson K, Williams CH Jr, Massey V. *Flavins and flavoproteins 1996*. University Press, Calgary Canada pp 305-314.

Van der Bolt FJT, Drijfhout MC, Eppink MHM, Hagen WR, van Berkel WJH. 1994. Selective cysteine -> serine replacements in *p*-hydroxybenzoate hydroxylase from *Pseudomonas fluorescens* allow the unambigous assignment of Cys211 as the site of modification by spin-labeled *p*-chloromercuribenzoate. *Prot Eng 7*:801-804.

Van der Bolt FJT, Vervoort J, van Berkel WJH. 1996. Flavin motion in *p*-hydroxybenzoate hydroxylase: Substrate and effector specificity of the Tyr222->Ala mutant. *Eur J Biochem 237*:592-600.

Van der Bolt FJT, van den Heuvel RHH, Vervoort J, van Berkel WJH. 1997. ^{19}F NMR Study on the regiospecificity of hydroxylation of tetrafluoro-4-hydroxybenzoate by wild-type and Y385F *p*-hydroxybenzoate hydroxylase: Evidence for a consecutive oxygenolytic dehalogenation mechanism. *Biochemistry 36*:14192-14201.

Van der Laan JM, Schreuder HA, Swarte MBA, Wierenga RK, Kalk KH, Hol WGJ, Drenth J. 1989. The coenzyme analogue adenosine 5-diphosphoribose displaces FAD in the active site of *p*-hydroxybenzoate hydroxylase. An X-ray crystallographic investigation. *Biochemistry 28*:7199-7205.

Vervoort J, van Berkel WJH, Müller F, Moonen CTW. 1991. NMR studies on *p*-hydroxybenzoate hydroxylase from *Pseudomonas fluorescens* and salicylate hydroxylase from *Pseudomonas putida. Eur J Biochem 200*:731-738.

Vrielink A, Lloyd LF, Blow D. 1991. Crystal structure of cholesterol oxidase from *Brevibacterium sterolicum* refined at 1.8Å resolution. *J Mol Biol 219*:533-554.

Weijer WJ, Hofsteenge J, Vereijken JM, Jekel PA, Beintema JJ. 1982. Primary structure of *p*-hydroxybenzoate hydroxylase from *Pseudomonas fluorescens. Biochim Biophys Acta 704*:385-388.

White JL, Hackert ML, Buehner M, Adams MJ, Ford GC, Lentz PJ Jr, Smiley IE, Steindel SJ, Rossmann MG. 1976. A comparison of the structures of apo *dogfish* M_4 lactate dehydrogenase and its ternary complexes. *J Mol Biol 102*:759-779.

Wierenga RK, de Jong RJ, Kalk KH, Hol WGJ, Drenth J. 1979. Crystal structure of *p*-hydroxybenzoate hydroxylase. *J Mol Biol 131*:55-73.

Wierenga RK, Drenth J, Schulz GE. 1983. Comparison of the three-dimensional protein and nucleotide structure of the FAD-binding domain of *p*-hydroxybenzoate hydroxylase with the FAD- as well as NADPH-binding domains of glutathione reductase. *J Mol Biol 167*:725-739.

Wierenga RK, Terpstra P, Drenth J. 1986. Prediction of the occurence of the ADP-binding βαβ-fold in proteins, using an amino acid sequence fingerprint. *J Mol Biol 187*:101-107.

Williams CH Jr. 1991. Lipoamide dehydrogenase, glutathione reductase, thioredoxin reductase, and mercuric ion reductase: A family of flavoenzyme transhydrogenases.

In: Müller F. ed.*Chemistry and biochemistry of flavoenzymes 2* Boca Raton, Florida: CRC Press. pp 121-211.

Wilson DK, Bohren KM, Gabbay KH, Quiocho FA. 1992. An unlikely sugar substrate site in the 1.65 Å structure of the human aldose reductase holoenzyme implicated in diabetic complications. *Science 257*:81-84.

Wong CM, Dilworth MJ, Glenn AR. 1994. Cloning and sequencing show that 4-hydroxybenzoate hydroxylase (*pobA*) is required for uptake of 4-hydroxybenzoate in *Rhizobium leguminosarum. Microbiology 140*:2775-2786.

Wright JD. 1993. Fungal degradation of benzoic acid and related compounds. *World J Microbiol Biotechnol 9*:9-16.

Xiong J-P, Xia Z-X, Wang Y. 1994. Crystal structure of trichosanthin-NADPH complex at 1.7Å resolution reveals active-site architecture. *Nat Struct Biol 1*:695-700.

You K. 1982. Stereospecificities of the pyridine nucleotide-linked enzymes. *Meth. Enzym 87*:101-126.

Yabuuchi T, Suzuki K, Sato T, Ohnishi K, Itagaki E, Morimoto Y. 1996. Crystallization and preliminary X-Ray analysis of salicylate hydroxylase from *Pseudomonas putida* S-1. *J Biochem 119*:829-831.

Yano K, Higashi N, Arima K. 1969. *p*-Hydroxybenzoate hydroxylase: conformational changes in crystals of holoenzyme vs holoenzyme-substrate complex. *Biochem Biophys Res Comm 34*:1-7.

CHAPTER 2

Crystal structure of *p*-hydroxybenzoate hydroxylase reconstituted with the modified FAD present in alcohol oxidase from methylotrophic yeasts: Evidence for an arabinoflavin

Willem J.H. van Berkel, Michel H.M. Eppink and Herman A. Schreuder

Protein Science 3: 2245-2253 (1994)

Protein Science (1994), *3*:2245-2253. Cambridge University Press. Printed in the USA.

Crystal structure of *p*-hydroxybenzoate hydroxylase reconstituted with the modified FAD present in alcohol oxidase from methylotrophic yeasts: Evidence for an arabinoflavin

WILLEM J.H. VAN BERKEL,[1] MICHEL H.M. EPPINK,[1] AND HERMAN A. SCHREUDER[2]

[1] Department of Biochemistry, Agricultural University, Dreyenlaan 3, 6703 HA Wageningen, The Netherlands
[2] Marion Merrell Dow Research Institute, 16 Rue d'Ankara, 67080 Strasbourg Cedex, France

(RECEIVED July 14, 1994; ACCEPTED September 23, 1994)

Abstract

The flavin prosthetic group (FAD) of *p*-hydroxybenzoate hydroxylase from *Pseudomonas fluorescens* was replaced by a stereochemical analog, which is spontaneously formed from natural FAD in alcohol oxidases from methylotrophic yeasts. Reconstitution of *p*-hydroxybenzoate hydroxylase from apoprotein and modified FAD is a rapid process complete within seconds. Crystals of the enzyme-substrate complex of modified FAD-containing *p*-hydroxybenzoate hydroxylase diffract to 2.1 Å resolution. The crystal structure provides direct evidence for the presence of an arabityl sugar chain in the modified form of FAD. The isoalloxazine ring of the arabinoflavin adenine dinucleotide (a-FAD) is located in a cleft outside the active site as recently observed in several other *p*-hydroxybenzoate hydroxylase complexes.

Like the native enzyme, a-FAD-containing *p*-hydroxybenzoate hydroxylase preferentially binds the phenolate form of the substrate ($pK_a = 7.2$). The substrate acts as an effector highly stimulating the rate of enzyme reduction by NADPH ($k_{red} > 500\ s^{-1}$). The oxidative part of the catalytic cycle of a-FAD-containing *p*-hydroxybenzoate hydroxylase differs from native enzyme. Partial uncoupling of hydroxylation results in the formation of about 0.3 mol of 3,4-dihydroxybenzoate and 0.7 mol of hydrogen peroxide per mol NADPH oxidized. It is proposed that flavin motion in *p*-hydroxybenzoate hydroxylase is important for efficient reduction and that the flavin "out" conformation is associated with the oxidase activity.

Keywords: apo-flavoprotein; arabino-FAD; crystal structure; flavin conformation; flavoprotein oxidases; *p*-hydroxybenzoate hydroxylase; reconstitution

In 1985, Sherry and Abeles reported that alcohol oxidase isolated from methylotrophic yeasts contains 2 different forms of FAD. One form was identified as natural FAD and the other as an optical isomer differing only in the ribityl part of the ribityldiphosphoadenosine side chain. Subsequent studies by Bystrykh et al. (1989, 1991) revealed that the content of the modified flavin in alcohol oxidase from *Hansenula polymorpha* ranges from 5 to 95% of total flavin, dependent on the culturing conditions. Furthermore, it was demonstrated that conversion of natural FAD into modified FAD is autocatalyzed by the purified enzyme and strongly inhibited in the presence of reducing agents (Bystrykh et al., 1991). From this and from NMR structural analysis of the extracted flavin it was argued that the modified FAD most probably is an arabinoflavin adenine dinucleotide (Kellog et al., 1992). The stereochemical modification of FAD changes the catalytic properties of alcohol oxidase and may be of physiological relevance (Bystrykh et al., 1991). The lack of crystallographic data for the octameric alcohol oxidases does not allow rationalization of the changes in catalysis from a structural point of view. We therefore have started studying the interaction of the modified flavin with other flavoproteins for which structural data are available. In this paper we describe some properties of *p*-hydroxybenzoate hydroxylase from *Pseudomonas fluorescens* reconstituted with the stereochemi-

Correspondence to: W.J.H. van Berkel, Department of Biochemistry, Agricultural University, Dreyenlaan 3, 6703 HA Wageningen, The Netherlands; e-mail: willem.vanberkel@fad.bc.wau.nl.

Abbreviations: a-FAD, arabinoflavin adenine dinucleotide; a-FMN, arabinoflavin mononucleotide; alcohol oxidase, alcohol:oxygen oxidoreductase (EC 1.1.3.13); catalase, hydrogen-peroxide oxidoreductase (EC 1.11.1.6); cholesterol oxidase, 3β-hydroxysteroid:oxygen oxidoreductase (EC 1.1.3.6); glucose oxidase, β-D-glucose:oxygen 1-oxidoreductase (EC 1.1.3.4); *p*-hydroxybenzoate hydroxylase, 4-hydroxybenzoate, NADPH:oxygen oxidoreductase (3-hydroxylating) (EC 1.14.13.2).

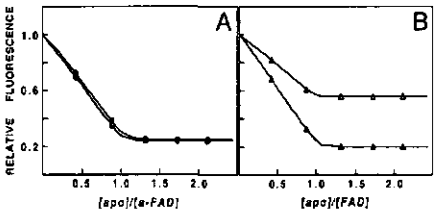

Fig. 1. Fluorescence titration of a-FAD with apo-*p*-hydroxybenzoate hydroxylase. Flavin (2 μM) was titrated with apo-*p*-hydroxybenzoate hydroxylase either in the absence or presence of 4-hydroxybenzoate. All experiments were performed at 25 °C in 100 mM Tris/sulfate, pH 8.0. Fluorescence emission was observed at 525 nm upon excitation at 450 nm. **A:** a-FAD in the absence (○) or presence (●) of 1 mM 4-hydroxybenzoate. **B:** Natural FAD in the absence (△) or presence (▲) of 1 mM 4-hydroxybenzoate.

cally modified FAD, obtained from *H. polymorpha* alcohol oxidase. By using the *p*-hydroxybenzoate hydroxylase apoprotein as a vehicle, direct crystallographic evidence is provided for the presence of an a-FAD in alcohol oxidases from methylotrophic yeasts.

Introduction of an optical isomer of FAD may give valuable additional information about the structure–function relationship of *p*-hydroxybenzoate hydroxylase. Recent crystallographic studies (Gatti et al., 1994; Schreuder et al., 1994) indicate that in *p*-hydroxybenzoate hydroxylase, flavin motion is a crucial factor for substrate binding and product release. As flavin motion requires a flexible ribityl side chain, a stereochemical modification in this side chain is expected to give more insight into the functional role of different flavin conformers. The crystal structure presented in this paper shows that the a-FAD bound to *p*-hydroxybenzoate hydroxylase is located in the "out" conformation. The rapid reduction of the arabinoflavin by NADPH lend us to propose that flavin motion in *p*-hydroxybenzoate hydroxylase is also important for an optimal positioning of the nicotinamide cofactor.

Results

Reconstitution of p-hydroxybenzoate hydroxylase

Reconstitution of holo *p*-hydroxybenzoate hydroxylase from the dimeric apoprotein and a-FAD is a rapid process. Upon addition to the apoprotein of an excess of a-FAD, the maximal activity is reached within a few seconds. The kinetics of reconstitution were not studied in detail. Activity measurements performed in the presence of nanomolar concentrations of flavin (Müller & van Berkel, 1982) indicate that binding of a-FAD is somewhat slower than with normal FAD.

The flavin fluorescence quantum yield of the a-FAD–apoprotein complex was determined from fluorescence titration experiments. Figure 1A shows that binding of the apoprotein results in a strong quenching of the fluorescence of a-FAD. The flavin fluorescence quantum yield of the a-FAD–apoprotein complex is much lower than that of the native enzyme (van Berkel & Müller, 1989). In contrast to the native enzyme (Fig. 1B), the presence of the aromatic substrate hardly influences the fluorescence quantum yield of protein-bound a-FAD (Fig. 1A).

Structural properties

The crystal structure of *p*-hydroxybenzoate hydroxylase complexed with a-FAD was solved and refined at 2.1 Å resolution (Kinemage 1). The final *R*-factor is 0.179 for 26,407 reflections between 8.0 and 2.1 Å. The almost (97.2%) complete 2.1-Å data allowed us to unambiguously establish the absolute configuration of the C2 carbon of the ribityl chain. The electron density map in Figure 2 clearly shows that the configuration at this position has changed from R to S, as has been inferred from NMR experiments (Kellog et al., 1992). The most important interaction between the modified flavin and the protein, the strong hydrogen bond with the OE1 of Gln 102, which is present both in the enzyme–substrate (Schreuder et al., 1989) and the 2,4-dihydroxybenzoate complex (Schreuder et al., 1994), is preserved in the a-FAD complex (see Fig. 3, Kinemage 1, and Table 1) despite the change in configuration. Table 1 also shows that whereas the O2′ of the natural flavin is buried between the side chain of Arg 44 and the flavin ring, it is more exposed in the a-FAD complex and contacts a bound water molecule (Wat 159).

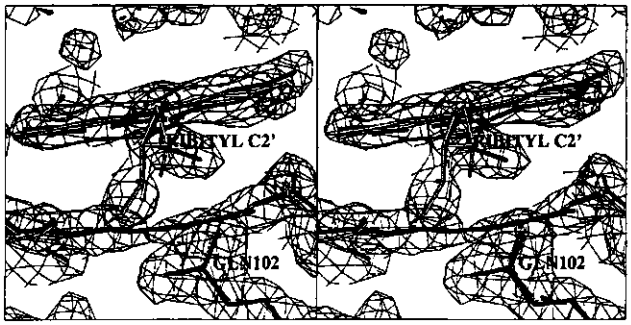

Fig. 2. Stereo diagram of the $2F_o - F_c$ electron density map of a-FAD-containing *p*-hydroxybenzoate hydroxylase in complex with 4-hydroxybenzoate. The final $2F_o - F_c$ electron density map was contoured at 1σ. The view is from the ribityl chain toward the flavin ring. The structure of the 4-hydroxybenzoate complex with a-FAD is drawn with solid bonds; the structure of the 2,4-dihydroxybenzoate complex with natural FAD is drawn with open bonds. Only the ribityl C2′ in the S-configuration (a-FAD complex, solid bonds) fits the electron density map. The side chain of Gln 102, which makes a hydrogen bond with the O2′ is visible in the lower right corner of the figure.

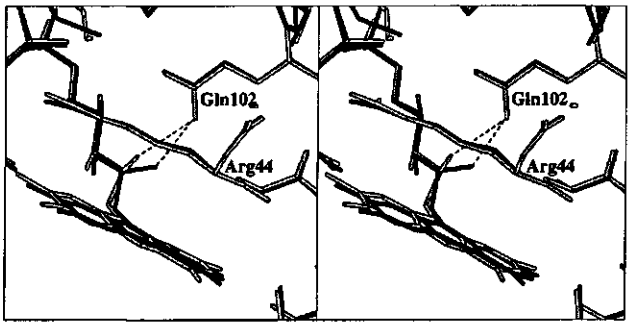

Fig. 3. Superposition of the structures of the a-FAD-containing enzyme-4-hydroxybenzoate complex and the native enzyme-2,4-dihydroxybenzoate complex. The structure of the 4-hydroxybenzoate complex with a-FAD is drawn with solid bonds; the structure of the 2,4-dihydroxybenzoate complex with natural FAD is drawn with open bonds. The view is from the flavin ring toward the ribityl chain. Broken lines indicate the hydrogen bond between the O2′ hydroxyl group and the OE1 of Gln 102, which is present in both complexes.

Binding of the modified flavin does not alter the overall structure of *p*-hydroxybenzoate hydroxylase. The RMS difference of the a-FAD-containing enzyme-substrate complex after superimposing the 391 C^{α} atoms present in the models are 0.22 Å with the native enzyme-substrate complex and 0.21 Å with the native 2,4-dihydroxybenzoate complex. These differences are of the same magnitude as the 0.2–0.3-Å mean coordinate error, which can be derived from Luzzati plots (Luzzati, 1952). The most important difference between the native enzyme-substrate complex and the a-FAD complex is that the flavin has moved to the "out" position (Fig. 4). The position of the flavin ring in the a-FAD-containing enzyme-substrate complex is almost identical to its position in the complex of the native enzyme with 2,4-dihydroxybenzoate (Schreuder et al., 1994). Figure 5 shows that in the latter complex, the flavin ring is approximately 0.7 Å further out, presumably because of a hydrogen bond contact of the 2-hydroxy group of the substrate analog (which is not present in the normal substrate) and the N3 of the flavin. The flavin ring is not completely planar in the a-FAD complex. The dimethylbenzene ring and the pyrimidine ring (the outer rings of the flavin ring system) make an angle of 7.1°. Interestingly, the flavin ring is not twisted as is the native flavin ring in the "in" position, but is bent like a butterfly. The geometry of the flavin ring is well within the range of butterfly conformations found in other flavoenzymes (Mathews, 1991).

Table 1. *Contacts (d < 3.4 Å) between the O2′ of the ribityl chain and protein or FAD atoms*[a]

a-FAD-containing 4-hydroxybenzoate complex	2,4-Dihydroxybenzoate complex[b]	4-Hydroxybenzoate complex[c]
	CD Arg 44 (3.2)	CD Arg 44 (3.4)
		CB Arg 44 (3.3)
OE1 Gln 102 (2.7)	OE1 Gln 102 (2.7)	OE1 Gln 102 (2.6)
	C9 flavin (3.3)	C9 flavin (3.2)
	C9A flavin (2.9)	C9A flavin (3.2)
N10 flavin (3.1)	N10 flavin (2.5)	N10 flavin (2.9)
O3′ ribityl (2.9)		
C4′ ribityl (2.9)	C4′ ribityl (3.1)	C4′ ribityl (3.1)
O4′ ribityl (3.4)	O4′ ribityl (2.9)	O4′ ribityl (3.1)
OW Water 159 (3.2)		

[a] Not mentioned are 1–2 and 1–3 contacts (i.e., with the ribityl C1′, C2′ and C3′ atoms). Distances in Å are given in parentheses.
[b] From Schreuder et al. (1994).
[c] From Schreuder et al. (1989).

Spectral properties

The visible absorption spectrum of free a-FAD is comparable to that of normal FAD (Table 2; Sherry & Abeles, 1985; Bystrykh et al., 1989). Binding to apo-*p*-hydroxybenzoate hydroxylase slightly influences the absorption characteristics of a-FAD. Table 2 shows that at pH 7.0, the maximum of the first absorption band is shifted from 450 to 458 nm and that the molar absorption coefficient of this band is higher than with the native enzyme. Upon binding of the aromatic substrate to the a-FAD-complexed enzyme, the intensity of the first absorption band increases with a concomitant shift of the absorption maximum to 455 nm. The intensity of the first absorption band of the a-FAD-containing enzyme-substrate complex is much higher than the corresponding band of the native enzyme-substrate complex (Table 2). Figure 6 shows a set of difference spectra recorded at pH 8.0, between the free a-FAD-containing enzyme and in the presence of increasing concentrations of 4-hydroxybenzoate. From the titration curve (inset, Fig. 6) simple 1:1 binding is observed and a dissociation constant for the a-FAD-complexed enzyme–substrate complex of about 50 μM is estimated. This value is in the same range as found for the corresponding complex of the native enzyme (van Berkel & Müller, 1989).

Bystrykh et al. (1989) reported that the CD spectrum of free a-FAD is different from natural FAD. In view of this, and because of the "out" position of the flavin observed in the crystal structure, it was of interest to study the CD properties of a-FAD-containing *p*-hydroxybenzoate hydroxylase. In the visible region, the CD spectrum of native *p*-hydroxybenzoate hydroxylase shows a negative Cotton peak around 450 nm and a positive Cotton peak around 365 nm (Fig. 7A; van Berkel & Müller, 1989). Upon binding of the aromatic substrate, the positive Cotton peak shifts to 380 nm, corresponding to the second

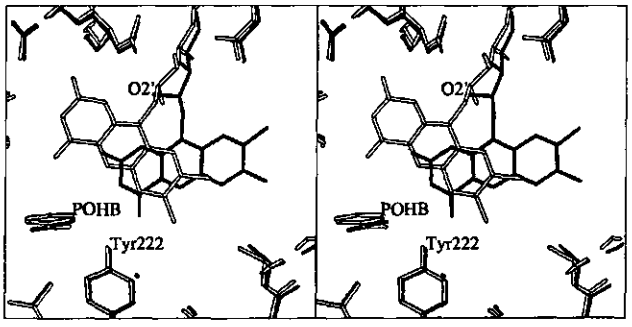

Fig. 4. Stereo diagram of the superposition of the native enzyme–substrate complex of *p*-hydroxybenzoate hydroxylase (Schreuder et al., 1989; white bonds), and the a-FAD-containing enzyme–substrate complex (this study; black bonds). The figure shows clearly how the flavin ring has moved to the "out" position.

absorption band of protein-bound FAD (Table 2). Furthermore, in the presence of the substrate both Cotton peaks become better resolved due to vibronic transitions in the 2 electronic absorption bands. Introduction of the a-FAD slightly changes the CD properties of *p*-hydroxybenzoate hydroxylase. Both Cotton peaks of the free enzyme and the enzyme–substrate complex are somewhat shifted with respect to the native enzyme (Fig. 7B). In line with the optical properties reported above, the main difference with the native enzyme is the increase in molar ellipticity of the first absorption band of the a-FAD-containing enzyme–substrate complex. At present it is not clear whether these differences in electronic transitions reflect the different flavin conformations observed in the crystal structures.

Native *p*-hydroxybenzoate hydroxylase preferentially binds the aromatic substrate in its phenolate form (Shoun et al., 1979; Entsch et al., 1991; Eschrich et al., 1993). Ionization of the 4-hydroxyl group is expected to activate the substrate for hydroxylation (Vervoort et al., 1992). Binding of the substrate to a-FAD-containing *p*-hydroxybenzoate hydroxylase also results in a large decrease in the phenolic pK_a. Figure 8 shows that binding of the substrate is accompanied by absorption changes around 290 nm and strongly dependent on the pH of the solution. The UV difference spectra observed are comparable with the corresponding spectra of the native enzyme (Eschrich et al., 1993). The estimated apparent pK_a value of 7.2 for protein-bound substrate (Fig. 8), compared to the pK_a of 9.3 for the substrate free in solution, strongly suggests that introduction of the a-FAD does not perturb the hydrogen bonding network formed by the 4-hydroxy moiety of the substrate and the side chains of Tyr 201 and Tyr 385 (Schreuder et al., 1989; Lah et al., 1994). This is in full accordance with the crystal structure presented above.

Catalytic properties

The catalytic properties of *p*-hydroxybenzoate hydroxylase reconstituted with a-FAD differ from native enzyme. Table 3 shows that replacement of normal FAD with a-FAD decreases the turnover rate (k_{cat}) and changes the reaction stoichiometry. Partial uncoupling of substrate hydroxylation results in a relatively high oxidase activity (production of hydrogen peroxide). Such an impaired hydroxylation capacity has also been observed with various mutant enzymes (Entsch et al., 1991, 1994; van Berkel et al., 1992, 1994; Eschrich et al., 1993) and with native enzyme reconstituted with artificial flavins (Entsch et al., 1980,

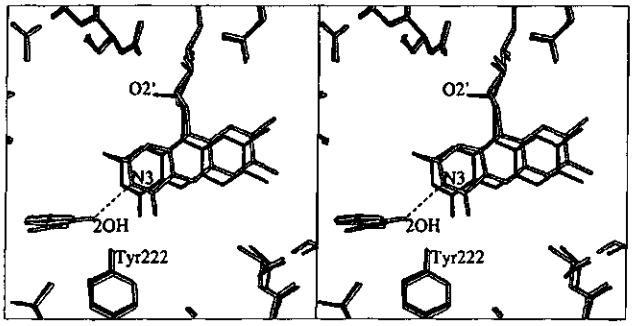

Fig. 5. Stereo diagram of the superposition of native 2,4-dihydroxybenzoate-complexed *p*-hydroxybenzoate hydroxylase (Schreuder et al., 1994; gray bonds) and the a-FAD-containing enzyme–substrate complex (black bonds). The flavin ring occupies the "out" position in both complexes, but the flavin ring is slightly further out in the 2,4-dihydroxybenzoate complex, presumably because of a hydrogen bond contact, indicated by a broken line, between the 2-hydroxy group of the substrate analog and the N3 of the flavin ring.

Table 2. *Absorption properties of free and protein-bound a-FAD*[a]

Sample	A_{max} (nm)	ϵ ($mM^{-1}\,cm^{-1}$)	A_{max} (nm)	ϵ ($mM^{-1}\,cm^{-1}$)
FAD	376	9.2	450	11.3
a-FAD	376	9.2	450	11.3
Native free enzyme[b]	373	8.5	450	10.2
a-FAD-containing free enzyme	374	8.6	458	11.3
Native ES complex[b]	380	9.1	450	10.2
a-FAD containing ES complex	378	9.1	455	12.3

[a] Molar absorption coefficients were determined at 25 °C in 50 mM sodium phosphate, pH 7.0. ES complex, enzyme–substrate complex.
[b] From van Berkel et al. (1992).

1987; Claiborne & Massey, 1983). Table 3 shows that the apparent K_m for *p*-hydroxybenzoate is in agreement with the K_d derived above, suggesting that partial uncoupling of hydroxylation is not due to weak substrate binding. Partial uncoupling of hydroxylation in the a-FAD-containing enzyme therefore most probably results from nonproductive decomposition of the C(4a)-hydroperoxyflavin intermediate (Entsch et al., 1976).

Anaerobic reduction of free *p*-hydroxybenzoate hydroxylase by NADPH is a very slow process. The rate of reduction is orders of magnitude stimulated in the presence of the aromatic substrate, acting as an effector (Nakamura et al., 1970; Howell et al., 1972). Anaerobic reduction of free a-FAD-containing *p*-hydroxybenzoate hydroxylase by NADPH ($k'_{red} = 0.1\ s^{-1}$ at 1 mM NADPH, pH 8.0, 25 °C) is considerably faster than with the native enzyme ($k'_{red} < 0.002\ s^{-1}$; van Berkel et al., 1992) as measured under the same experimental conditions. In line with this, the free a-FAD-containing enzyme possesses considerable NADPH oxidase activity. From activity experiments performed in the absence of the aromatic substrate, apparent values of $k_{cat} = 0.1\ s^{-1}$ and K_m NADPH = 1.9 mM (pH 8.0, 25 °C) are estimated. Wasteful consumption of NADPH is not observed with the native free enzyme, probably because of a nonoptimal geometry of the flavin with respect to the nicotinamide ring (van Berkel & Müller, 1991).

The substrate is a very strong effector for the a-FAD-complexed enzyme. In Figure 9, the rate of reduction of the a-FAD-containing enzyme–substrate complex at 25 °C is plot-

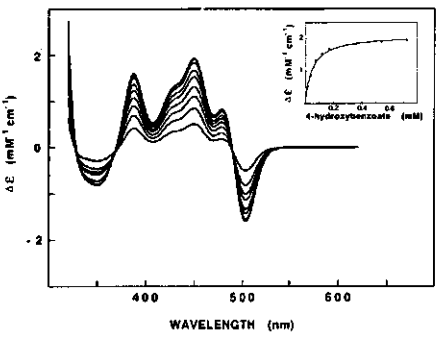

Fig. 6. Flavin absorption difference spectra observed upon binding of 4-hydroxybenzoate to a-FAD-containing *p*-hydroxybenzoate hydroxylase. The absorption spectra were recorded at 25 °C in 100 mM Tris/sulfate, pH 8.0. The enzyme concentration was 30 μM. Difference spectra are plotted between free enzyme as a reference and the same solution containing variable amounts of 4-hydroxybenzoate. The inset shows the molar absorbance difference at 450 nm as a function of the substrate concentration.

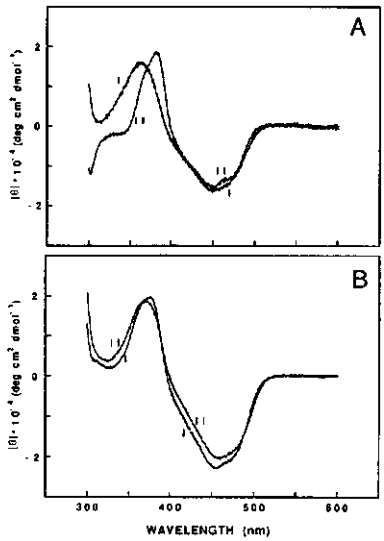

Fig. 7. CD spectra of native and a-FAD-containing *p*-hydroxybenzoate hydroxylase. The CD spectra were recorded at 25 °C in 100 mM Tris/sulfate, pH 8.0. The enzyme concentration was 40 μM. **A:** Native enzyme in the absence (I) or in the presence of 1 mM 4-hydroxybenzoate (II). **B:** a-FAD-complexed enzyme in the absence (I) or in the presence of 1 mM 4-hydroxybenzoate (II).

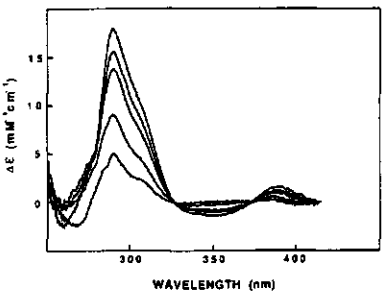

Fig. 8. UV absorption difference spectra upon binding of 4-hydroxybenzoate to a-FAD-containing *p*-hydroxybenzoate hydroxylase. Both cuvettes contained 1.0 mL 20 μM a-FAD-complexed enzyme in one compartment and 1.0 mL 200 μM 4-hydroxybenzoate in the same buffer in the other compartment. The temperature was 25 °C. For buffers used see Materials and methods. Before mixing the solutions in the 2 compartments of the sample cell, a baseline was recorded. From bottom to top: difference spectrum of a-FAD-containing *p*-hydroxybenzoate hydroxylase at pH 6.7, pH 7.2, pH 7.7, pH 8.0, and pH 8.3, respectively. From the molar absorption differences at 290 nm an apparent pK_a value of 7.2 for protein-bound substrate is estimated.

ted as a function of the concentration NADPH. The dissociation constant for NADPH as derived from this plot is in the same range as found for the native enzyme–substrate complex (Table 3). The maximal rate of reduction in the presence of 4-hydroxybenzoate is higher than found for native enzyme (Howell et al., 1972; van Berkel et al., 1992; Table 3). Interestingly, an enhanced rate of reduction with respect to the native enzyme–substrate complex has so far only been observed with *p*-hydroxybenzoate hydroxylase-containing 2-thio-FAD (Claiborne & Massey, 1983).

Discussion

This is, to our best knowledge, the first paper describing the crystal structure of a flavoenzyme reconstituted with a stereochemical analog of FAD. The high quality of the crystals shows that the immobilization technique used to prepare apo-*p*-hydroxybenzoate hydroxylase (Müller & van Berkel, 1982) is a convenient method to replace the flavin while retaining the native state of the enzyme. By using the apoenzyme of *p*-hydroxybenzoate hydroxylase as a vehicle and because the modified FAD was taken from alcohol oxidase, clear crystallographic evidence is provided for the presence of an a-FAD in alcohol oxidases from methylotrophic yeasts. The electron density map of the modified flavin containing enzyme–substrate complex shows that the absolute configuration of the C2 carbon of the ribityl chain has changed from R to S, in perfect agreement with an earlier proposal based on NMR studies (Kellog et al., 1992). Replacement of natural FAD with a-FAD in *p*-hydroxybenzoate hydroxylase does not alter the overall structure of the protein but induces the flavin ring to occupy the "out" position (Kinemage 1). This "out" conformation has been observed before in a number of crystal structures including complexes of wild-type enzyme with 2-hydroxybenzoate analogues (Schreuder et al., 1994), in mutant Tyr 222 Phe complexed with 4-hydroxybenzoate (Gatti et al., 1994), and in mutant Tyr 222 Ala complexed with 2-hydroxy-4-aminobenzoate (Schreuder et al., 1994). Superpositions have shown that in complexes with 2-hydroxybenzoate analogues, the "in" conformation is destabilized by a short contact between the 2-OH group of the substrate analogue and flavin C6, whereas the "out" conformation is stabilized by a strong hydrogen bond of the 2-OH group of the substrate analogue with the N3 of the flavin. These destabilizing/stabilizing interactions do not explain the "out" conformation in the crystals with a-FAD presented here because these crystals contain the natural substrate 4-hydroxybenzoate, which does not possess a 2-OH group. Here, the "out" conformation must have been caused by the R to S transition of the C2 carbon of the ribityl chain because this is the only difference between the crystals with the a-FAD and the crystals of the native enzyme–substrate complex (Schreuder et al., 1989). In order to assess the contacts of

Table 3. *Kinetic parameters of a-FAD complexed p-hydroxybenzoate hydroxylase*[a]

Enzyme	Product (%)	K_d NADPH (μM)	k_{red} (s^{-1})	k_{cat} (s^{-1})	K_m (μM) NADPH	K_m (μM) BzOH
Native	98 ± 2	150	300	55	70	20
a-FAD complexed	33 ± 5	115	530	11	7	56

[a] Kinetic parameters were determined at 25 °C in 100 mM Tris/SO_4^{2-}, pH 8.0. Turnover rates are maximum values (k_{cat}) determined at 0.26 mM oxygen. Dissociation constants for NADPH (K_d NADPH) were determined from rapid reaction experiments. Data for native *p*-hydroxybenzoate hydroxylase are taken from van Berkel et al. (1992). Product, 3,4-dihydroxybenzoate; BzOH, 4-hydroxybenzoate.

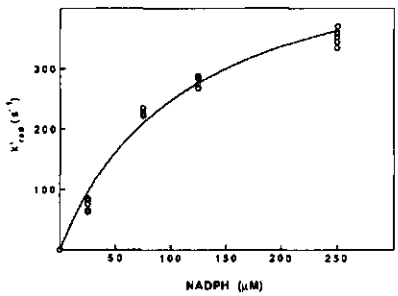

Fig. 9. Reduction of a-FAD-containing *p*-hydroxybenzoate hydroxylase by NADPH. All experiments were performed in 100 mM Tris/sulfate pH 8.0. Enzyme (18 μM) was anaerobically mixed with an equal volume of variable concentrations of NADPH in the stopped-flow spectrophotometer. Both solutions contained 1 mM 4-hydroxybenzoate. The rate of reduction of a-FAD-containing *p*-hydroxybenzoate hydroxylase at 25 °C is plotted as a function of the concentration of NADPH, as monitored at 450 nm.

a-FAD in the "in" conformation, we inverted the conformation of the ribityl C2 carbon in the structure of the native enzyme-substrate complex. The result indicates that (without adaptation of the protein) the ribityl 2-OH group would be involved in 2 short contacts: one with the CA of Leu 299 (3.0 Å) and one with the CB of Leu 299 (2.5 Å). The hydrogen bond with the side chain of Gln 102 would still be present. Only small (0.5–1.0 Å) rearrangements are needed to relieve the short contacts. These rearrangements, however, may be hindered because Leu 299 is part of helix H10. These observations point to a small difference in binding energy between the "in" and "out" conformation because the a-FAD binds in the "out" conformation in spite of apparently minor adaptations necessary to bind the "in" conformation.

The shift of the equilibrium position toward the "out" conformation, as observed in the crystal structure, explains perfectly the observed formation of considerable amounts of hydrogen peroxide during catalysis because the hydroperoxyflavin intermediate can only hydroxylate the substrate in the "in" position (Schreuder et al., 1994). A dynamic equilibrium of flavin conformers probably is also of relevance for the native enzyme because the entrance of the substrate binding site is blocked with the flavin in the "in" position and movement of the flavin to the "out" position seems to be necessary to provide a path for the substrate to enter the active site (see Gatti et al., 1994; Schreuder et al., 1994). The situation is less clear for the NADPH binding and reduction step. We have previously argued (Schreuder et al., 1994) that the flavin would most likely not be reduced in the "out" position because 2,4-dihydroxybenzoate (which also pushes the flavin toward the "out" conformation), stimulates the reduction much less than the normal substrate. However, the present data strongly suggest that the flavin is rapidly reduced in the "out" conformation. Clearly, additional data (e.g., site-directed mutants with altered NADP binding properties or a crystal structure of a complex with an NADPH analog) are needed to settle this point.

No crystal structure of methanol oxidase is available, but amino acid sequence comparisons have revealed that this enzyme belongs to the glucose-methanol-choline (GMC) oxidoreductase family (Cavener, 1992). Within this class of flavoenzymes, 2 crystal structures are known. The crystal structures of glucose oxidase from *Aspergillus niger* (Hecht et al., 1993) and cholesterol oxidase from *Brevibacterium sterolicum* (Vrielink et al., 1991; Li et al., 1993) show that the O2′ of the ribityl chain of the FAD makes a hydrogen bond with the amide nitrogen of a conserved Asn residue (Asn 107 in glucose oxidase and Asn 119 in cholesterol oxidase). The conserved Asn (Asn 98 in methanol oxidase from *H. polymorpha*; Ledeboer et al., 1985) seems to fulfill the same role as Gln 102 in *p*-hydroxybenzoate hydroxylase. Analysis of hypothetical short contacts of the ribityl O2′ after inverting the configuration of the C2 carbon reveals that for the 2 flavoprotein oxidases with known 3-dimensional structure, the short contacts would be less severe than with *p*-hydroxybenzoate hydroxylase. The shortest non-hydrogen bond-type contacts are 3.0 Å with the Cγ of Met 561 for glucose oxidase and 3.1 Å with the Cβ of Phe 487 for cholesterol oxidase, in contrast to the short contact of 2.5 Å with the Cβ of Leu 299 in *p*-hydroxybenzoate hydroxylase. These observations and the general occurrence of a-FAD in methanol oxidase suggest that the active site of this enzyme is likely to be able to accommodate the a-FAD without too many rearrangements.

Materials and methods

General

Biochemicals and chromatography resins used have been described elsewhere (van Berkel et al., 1992). Optical (difference) spectra were recorded at 25 °C, on a computer-controlled Aminco DW-2000 spectrophotometer. Fluorescence experiments were performed on an Aminco SPF-500C spectrofluorimeter at 25 °C. CD spectra were recorded on a Jobin Yvon Mark V dichrograph, essentially as described elsewhere (Benen et al., 1991). Rapid-reaction kinetics were carried out using a temperature-controlled single-wavelength stopped-flow spectrophotometer, type SF-51, from High-Tech Scientific Inc., with a 1.3-ms dead-time. The instrument was interfaced to an IBM microcomputer for data acquisition and analysis.

Purification procedures

Crude a-FAD as extracted from alcohol oxidase (Kellog et al., 1992) was a gift of Dr. L.V. Bystrykh. a-FAD was separated from natural FAD by HPLC using a Microspher C18 (20 × 300-mm) column. The elution solvent contained 15% MeOH, 85 mM ammonium bicarbonate, pH 3.7. The flow rate was 2 mL/min. Using a 10-μL sample loop, the following elution times are observed: a-FAD (4.2 min), a-FMN (5.7 min), FMN (6.3 min), and FAD (6.9 min). Micromolar quantities of pure a-FAD were obtained from repeated 50-μL injections. Purified a-FAD was desalted by reverse-phase chromatography and stored at −20 °C. FAD used in fluorescence experiments was purified by gel filtration on Biogel P-2 (Müller & van Berkel, 1982).

p-Hydroxybenzoate hydroxylase from *P. fluorescens*, as cloned in *Escherichia coli*, was purified as described (van Berkel et al., 1992). The apoprotein of *p*-hydroxybenzoate hydroxylase was prepared by covalent chromatography (Müller & van Berkel, 1982). The residual activity of the apoprotein was less than 0.2%.

Analytical methods

Fluorescence titration experiments were performed in 100 mM Tris/sulfate, pH 8.0. Flavin fluorescence emission was observed at 525 nm upon excitation at 450 nm (Müller & van Berkel, 1982). Molar absorption coefficients of protein-bound flavin were determined at 25 °C by recording absorption spectra in 50 mM sodium phosphate, pH 7.0, either in the absence or presence of 0.5% SDS (de Jong et al., 1992). Protein concentrations were determined using the following molar absorption coefficients: holo *p*-hydroxybenzoate hydroxylase, ϵ_{450} = 10.2 mM^{-1} cm^{-1} (van Berkel et al., 1992); apo-*p*-hydroxybenzoate hydroxylase, ϵ_{280} = 74 mM^{-1} cm^{-1} (Müller & van Berkel, 1982). The molar ellipticity of protein-bound flavin was determined by recording CD spectra in the visible region. The enzyme concentration was 40 μM in 50 mM potassium phosphate, 0.5 mM EDTA, pH 7.0. The ionization state of enzyme-bound 4-hydroxybenzoate was measured by recording UV absorption difference spectra as a function of substrate concentration and of pH (Eschrich et al., 1993).

p-Hydroxybenzoate hydroxylase activity was routinely assayed in 100 mM Tris/sulfate, pH 8.0, containing 0.5 mM EDTA, 150 μM NADPH, 150 μM 4-hydroxybenzoate, and

10 μM FAD (Müller & van Berkel, 1982). Kinetic parameters of *p*-hydroxybenzoate hydroxylase were determined at pH 8.0, essentially as described elsewhere (Eschrich et al., 1993). The hydroxylation efficiency of *p*-hydroxybenzoate hydroxylase was estimated from oxygen consumption experiments, either in the absence or presence of catalase (Eschrich et al., 1993). The product 3,4-dihydroxybenzoate was identified and quantified by reverse-phase HPLC (Entsch et al., 1991).

Crystallization

Crystals of a-FAD-containing *p*-hydroxybenzoate hydroxylase in complex with 4-hydroxybenzoate were obtained using the hanging drop method. The protein solution contained 10 mg/mL enzyme in 50 mM potassium phosphate buffer (pH 7.0). The reservoir solution contained 50% saturated ammonium sulfate, 0.04 mM FAD, 0.15 mM EDTA, 0.1 mM reduced glutathione, 1 mM 4-hydroxybenzoate, 60 mM sodium sulfite, and 50 mM potassium phosphate buffer, pH 7.0. Drops of 4 μL protein solution and 4 μL reservoir solution were allowed to equilibrate at 4 °C against 1 mL of reservoir solution. Crystals with dimensions of up to $0.2 * 0.3 * 0.4$ mm^3 grew within 3 days.

Data collection

X-ray diffraction data were collected using a Siemens multiwire area detector and graphite monochromated CuKα radiation from an 18-kW Siemens rotating anode generator, operating at 45 kV and 80 mA. The crystal-detector distance was 11.6 cm and the 2θ angle was 25°. Data were processed using the XDS package (Kabsch, 1988). The space group is $C222_1$ and the cell dimensions: $a = 72.1$ Å, $b = 146.4$ Å, and $c = 88.45$ Å differ only slightly from the native crystals: $a = 71.5$ Å, $b = 145.8$ Å, and $c = 88.2$ Å (Schreuder et al., 1989). A total of 102,196 observations yielded 26,934 unique reflections with an R-sym of 6.9%. The data set is 97.2% complete to 2.1 Å.

Refinement

A starting electron density map was calculated based on the structure of the *p*-hydroxybenzoate hydroxylase–substrate complex (Schreuder et al., 1989), after correcting for the slightly different cell dimensions (Schreuder et al., 1994). However, the $2F_o - F_c$ and $F_o - F_c$ electron density maps clearly indicated that the flavin does not occupy the "in" position as in the enzyme–substrate complex, but that it occupies the "out" position as observed in several other *p*-hydroxybenzoate hydroxylase complexes (Gatti et al., 1994; Schreuder et al., 1994). We decided therefore not to use the structure of the enzyme–substrate complex as starting model, but to use the structure of the enzyme-2,4-dihydroxybenzoate complex (Schreuder et al., 1994) instead. The starting R-factor, after correcting for slightly different cell dimensions, was 0.277 for data between 8.0 and 2.1 Å. The $2F_o - F_c$ and $F_o - F_c$ maps clearly indicate that the absolute configuration of the C2′ of the ribityl-chain differs from normal FAD, as has been suggested earlier on the basis of NMR experiments (Kellog et al., 1992). The ribityl chain was built and the model was inspected and corrected where necessary with the graphics program FRODO (Jones, 1985). Refinement was carried out using the program XPLOR (Brünger, 1992). The parameter set as determined by Engh and Huber (1991) was used for the protein part of the structure. For the FAD we used the parameters as described by Schreuder et al. (1994). The topology definition for the C2 of the ribityl chain was changed from R to S. The model was refined with energy minimization and temperature factor refinement. Water molecules were assigned by searching $F_o - F_c$ maps for peaks of at least 4σ, which were between 2.0 and 5.0 Å of other protein or water atoms. Water molecules with temperature factors after refinement in excess of 70 Å^2 were rejected.

The final structure was obtained after 4 cycles of map inspection and refinement and contains 284 water molecules. The final R-factor is 0.179 for 26,407 reflections between 8.0 and 2.1 Å. The *RMS* deviations are 0.008 Å for bond lengths and 1.4° for bond angles. All non-glycine residues have ϕ, ψ angles within, or close to allowed regions. The only exceptions are Arg 44 and Asp 144, which also deviate in the structures of other *p*-hydroxybenzoate hydroxylase complexes from *P. fluorescens* (Schreuder et al., 1989, 1994). The coordinates of the refined a-FAD-containing enzyme–substrate complex will be deposited in the Brookhaven Protein Data Bank.

Acknowledgments

We thank Mr. J.A. Boeren for help in HPLC experiments. This study was supported by the Netherlands Foundation for Chemical Research (SON) with financial aid from the Netherlands Organization for Scientific Research (NWO).

References

Benen JAE, van Berkel WJH, Zak Z, Visser AJWG, Veeger C, de Kok A. 1991. Lipoamide dehydrogenase from *Azotobacter vinelandii*: Site-directed mutagenesis of the His 450–Glu 455 diad. Spectral properties of wild type and mutated enzymes. *Eur J Biochem 202*:863–872.

Brünger AT. 1992. *X-PLOR, version 3.1*. New Haven, Connecticut: Yale University Press.

Bystrykh LV, Romanov VP, Steckzo J, Trotsenko YA. 1989. Catalytic variability of alcohol oxidase from the methylotrophic yeast *Hansenula polymorpha*. *Biotech Appl Biochem 11*:184–192.

Bystrykh LV, Dijkhuizen L, Harder W. 1991. Modification of flavin adenine dinucleotide in alcohol oxidase of the yeast *Hansenula polymorpha*. *J Gen Microbiol 137*:2381–2386.

Cavener DR. 1992. GMC oxidoreductases. A newly defined family of homologous proteins with diverse catalytic activities. *J Mol Biol 223*: 811–814.

Claiborne A, Massey V. 1983. Mechanistic studies of *p*-hydroxybenzoate hydroxylase reconstituted with 2-thio-FAD. *J Biol Chem 258*:4919–4925.

de Jong E, van Berkel WJH, van der Zwan RP, de Bont JAM. 1992. Purification and characterization of vanillyl-alcohol oxidase from *Penicillium simplicissimum*. A novel aromatic alcohol oxidase containing covalently bound FAD. *Eur J Biochem 208*:651–657.

Engh RA, Huber R. 1991. Accurate bond and angle parameters for X-ray protein structure refinement. *Acta Crystallogr A 47*:392–400.

Entsch B, Ballou DP, Massey V. 1976. Flavin-oxygen derivatives involved in hydroxylation by *p*-hydroxybenzoate hydroxylase. *J Biol Chem 251*: 2550–2563.

Entsch B, Husain M, Ballou DP, Massey V, Walsh C. 1980. Oxygen reactivity of *p*-hydroxybenzoate hydroxylase containing 1-deaza-FAD. *J Biol Chem 255*:1420–1429.

Entsch B, Massey V, Claiborne A. 1987. *para*-Hydroxybenzoate hydroxylase containing 6-hydroxy-FAD is an effective enzyme with modified reaction mechanism. *J Biol Chem 262*:6060–6068.

Entsch B, Palfey BA, Ballou DP, Massey V. 1991. Catalytic function of tyrosine residues in *para*-hydroxybenzoate hydroxylase as determined by the study of site-directed mutants. *J Biol Chem 266*:1734[–17349.

Entsch B, Palfey BA, Lumberg MS, Ballou DP, Massey V. 1994. The mobile flavin of *para*-hydroxybenzoate hydroxylase: A case for major structural dynamics in catalysis. In: Yagi K, ed. *Flavins and flavoproteins 1993*. Berlin: W. de Gruyter. pp 211–220.

Eschrich K, van der Bolt FJT, de Kok A, van Berkel WJH. 1993. Role of Tyr 201 and Tyr 385 in substrate activation by *p*-hydroxybenzoate hydroxylase from *Pseudomonas fluorescens*. *Eur J Biochem 216*:137–146.

Gatti DL, Palfey BA, Lah MS, Entsch B, Massey V, Ballou DP, Ludwig ML. 1994. The mobile flavin of 4OH benzoate hydroxylase. *Science 266*: *110–114*.

Hecht HJ, Kalisz HM, Hendle J, Schmid RD, Schomburg D. 1993. Crystal structure of glucose oxidase from *Aspergillus niger* refined at 2.3 Å resolution. *J Mol Biol 229*:153–172.

Howell LG, Spector T, Massey V. 1972. Purification and properties of *p*-hydroxybenzoate hydroxylase from *Pseudomonas fluorescens*. *J Biol Chem 247*:4340–4350.

Jones TA. 1985. Interactive computer graphics: FRODO. *Methods Enzymol 115*:157–171.

Kabsch W. 1988. Evaluation of single-crystal diffraction data from a position-sensitive detector. *J Appl Crystallogr 21*:916–924.

Kellog RM, Kruitzinga W, Bystrykh LV, Dijkhuizen L, Harder W. 1992. Structural analysis of a stereochemical modification of flavin adenine dinucleotide in alcohol oxidase from methylotrophic yeasts. *Tetrahedron 48*:4147–4162.

Lah MS, Palfey BA, Schreuder HA, Ludwig ML. 1994. Crystal structures of mutant *Pseudomonas aeruginosa p*-hydroxybenzoate hydroxylase: The Tyr 201 Phe, Tyr 385 Phe and Asn 300 Asp variants. *Biochemistry 33*:1555–1564.

Ledeboer AM, Edens L, Maat J, Visser C, Bos JW, Verrips CT. 1985. Molecular cloning and characterization of a gene coding for methanol oxidase in *Hansenula polymorpha*. *Nucleic Acids Res 13*:3063–3082.

Li J, Vrielink A, Brick P, Blow DM. 1993. Crystal structure of cholesterol oxidase complexed with a steroid substrate: Implications for flavin adenine dinucleotide dependent alcohol oxidases. *Biochemistry 32*: 11507–11515.

Luzzati V. 1952. Traitement statistique des erreurs dans la determination des structures cristallines. *Acta Crystallogr 5*:802–810.

Mathews FS. 1991. New flavoenzymes. *Curr Opin Struct Biol 1*:954–967.

Müller F, van Berkel WJH. 1982. A study on *p*-hydroxybenzoate hydroxylase from *Pseudomonas fluorescens*. A convenient method of preparation and some properties of the apoenzyme. *Eur J Biochem 128*:21–27.

Nakamura S, Ogura Y, Yano K, Higashi N, Arima K. 1970. Kinetic studies on the reaction mechanism of *p*-hydroxybenzoate hydroxylase. *Biochemistry 9*:3235–3242.

Schreuder HA, Mattevi A, Obmolova G, Kalk KH, Hol WGJ, van der Bolt FJT, van Berkel WJH. 1994. Crystal structures of wild-type *p-hydroxybenzoate* hydroxylase *complexed with 4-aminobenzoate*, 2,4-dihydroxybenzoate and 2-hydroxy-4-aminobenzoate and mutant Tyr 222 Ala, complexed with 2-hydroxy-4-aminobenzoate. Evidence for a proton channel and a new binding mode of the flavin ring. *Biochemistry 33*:10161–10170.

Schreuder HA, Prick P, Wierenga RK, Vriend G, Wilson KS, Hol WGJ, Drenth J. 1989. Crystal structure of the *p*-hydroxybenzoate hydroxylase-substrate complex refined at 1.9 Å resolution. *J Mol Biol 208*:679–696.

Sherry B, Abeles RH. 1985. Mechanism of action of methanol oxidase, reconstitution of methanol oxidase with 5-deazaflavin, and inactivation of methanol oxidase by cyclopropanol. *Biochemistry 24*:2594–2605.

Shoun H, Beppu T, Arima K. 1979. On the stable enzyme-substrate complex of *p*-hydroxybenzoate hydroxylase. *J Biol Chem 254*:899–904.

van Berkel WJH, Müller F. 1989. The temperature and pH dependence of some properties of *p*-hydroxybenzoate hydroxylase from *Pseudomonas fluorescens*. *Eur J Biochem 179*:307–314.

van Berkel WJH, Müller F. 1991. Flavin-dependent monooxygenases with special reference to *p*-hydroxybenzoate hydroxylase. In: Müller F, ed. *Chemistry and biochemistry of flavoenzymes, vol 2*. Boca Raton, Florida: CRC Press. pp 1–29.

van Berkel WJH, van der Bolt FJT, Eppink MHM, de Kok A, Rietjens IMCM, Veeger C, Vervoort J. 1994. Substrate and effector specificity of two active-site mutants of *p*-hydroxybenzoate hydroxylase from *Pseudomonas fluorescens*. In: Yagi K, ed. *Flavins and flavoproteins 1993*. Berlin: W. de Gruyter. pp 231–234.

van Berkel WJH, Westphal AH, Eschrich K, Eppink MHM, de Kok A. 1992. Substitution of Arg 214 at the substrate-binding site of *p*-hydroxybenzoate hydroxylase from *Pseudomonas fluorescens*. *Eur J Biochem 210*:411–419.

Vervoort J, Rietjens IMCM, van Berkel WJH, Veeger C. 1992. Frontier orbital study on the 4-hydroxybenzoate-3-hydroxylase-dependent activity with benzoate derivatives. *Eur J Biochem 206*:479–484.

Vrielink A, Lloyd LF, Blow DM. 1991. Crystal structure of cholesterol oxidase from *Brevibacterium sterolicum* refined at 1.8 Å resolution. *J Mol Biol 219*:533–554.

CHAPTER 3

Structure and function of mutant Arg44lys of 4-hydroxybenzoate hydroxylase. Implications for NADPH binding

Michel H.M. Eppink, Herman A. Schreuder and Willem J.H. van Berkel

Eur. J. Biochem 231: 157-165 (1995)

Eur. J. Biochem. 231, 157–165 (1995)

Structure and function of mutant Arg44Lys of 4-hydroxybenzoate hydroxylase
Implications for NADPH binding

Michel H. M. EPPINK[1], Herman A. SCHREUDER[2] and Willem J. H. VAN BERKEL[1]

[1] Department of Biochemistry, Agricultural University, Wageningen, The Netherlands
[2] Marion Merrel Dow Research Institute, Strasbourg, France

(Received 3 February 1995) – EJB 95 0163/3

Arg44, located at the si-face side of the flavin ring in 4-hydroxybenzoate hydroxylase, was changed to lysine by site-specific mutagenesis. Crystals of [R44K]4-hydroxybenzoate hydroxylase complexed with 4-hydroxybenzoate diffract to 0.22-nm resolution. The structure of [R44K]4-hydroxybenzoate hydroxylase is identical to the wild-type enzyme except for local changes in the vicinity of the mutation. The peptide unit between Ile43 and Lys44 is flipped by about 180° in 50% of the molecules. The ϕ,ψ angles in both the native and flipped conformation are outside the allowed regions and indicate a strained conformation. [R44K]4-Hydroxybenzoate hydroxylase has a decreased affinity for the flavin prosthetic group. This is ascribed to the lost interactions between the side chain of Arg44 and the diphosphoribose moiety of the FAD. The replacement of Arg44 by Lys does not change the position of the flavin ring which occupies the same interior position as in wild type.

[R44K]4-Hydroxybenzoate hydroxylase fully couples flavin reduction to substrate hydroxylation. Stopped-flow kinetics showed that the effector role of 4-hydroxybenzoate is largely conserved in the mutant. Replacement of Arg44 by Lys however affects NADPH binding, resulting in a low yield of the charge-transfer species between reduced flavin and $NADP^+$. It is inferred from these data that Arg44 is indispensable for optimal catalysis.

Keywords. Crystal structure; flavoprotein monooxygenase; NADPH binding; 4-hydroxybenzoate hydroxylase; site-specific mutagenesis.

FAD-dependent aromatic hydroxylases are inducible enzymes which catalyze the insertion of one atom of molecular oxygen into the substrate, using NAD(P)H as external electron donor (van Berkel and Müller, 1991). The aromatic substrates act as effectors, stimulating the rate of enzyme reduction (Hosokawa and Stanier, 1966). As the reduced enzymes react readily with oxygen, the effector role of substrates is essential to prevent the wasteful utilization of high-energy reducing equivalents (Massey and Hemmerich, 1975). FAD-dependent aromatic hydroxylases are induced in soil microorganisms able to assimilate phenolic compounds as sole carbon source. In this way many secondary plant metabolites, decomposition products of lignin as well as aromatic pollutants, are readily subject to further catabolism (Middelhoven, 1993).

4-Hydroxybenzoate hydroxylase from *Pseudomonas fluorescens* is the most extensively studied flavoprotein aromatic hydroxylase (van Berkel and Müller, 1991). The strictly NADPH-dependent enzyme catalyzes the first step of the β-ketoadipate pathway, i.e. the conversion of 4-hydroxybenzoate into 3,4-dihydroxybenzoate (Stanier and Ornston, 1973):

4-hydroxybenzoate + NADPH + O_2
$\rightarrow$ 3,4-dihydroxybenzoate + $NADP^+$ + H_2O . (1)

The reaction sequence of 4-hydroxybenzoate hydroxylase has been studied in detail (Husain and Massey, 1979) and rapid reaction kinetics have shown that hydroxylation of the substrate proceeds through the attack of a labile C(4a)-hydroperoxyflavin intermediate (Entsch et al., 1976).

The availability of a high-resolution crystal structure of the enzyme/substrate complex (Wierenga et al., 1979; Schreuder et al., 1989) and the cloning of the *pob*A gene encoding 4-hydroxybenzoate hydroxylase from *Psuedomonas aeruginosa* (Entsch et al., 1988) and *P. fluorescens* (van Berkel et al., 1992) allow us to address the role of individual amino acid residues by site-directed mutagenesis. Most mutagenesis studies performed have dealt with amino acid replacements in the substrate-binding site. In this way, much insight has been gained into the mechanism of substrate activation (Entsch and van Berkel, 1995).

The effector specificity of 4-hydroxybenzoate hydroxylase is less well understood. Recent crystallographic data indicate that subtle structural perturbations determine the poor effector role of 4-aminobenzoate derivatives (Schreuder et al., 1994). Understanding the effector specificity is limited by the fact that the binding mode of NADPH is unknown (van der Laan et al., 1989a). Stereochemical studies showed that the nicotinamide-binding pocket is located at the re-face of the flavin ring (Manstein et al., 1986). Based on these results and from crystallographic data of glutathione reductase (Pai and Schulz, 1983; Wierenga et al., 1983), a potential mode of NADPH binding was proposed (van Berkel et al., 1988). However, recent crystallo-

Correspondence to W. J. H. van Berkel, Department of Biochemistry, Agricultural University, Dreyenlaan 3, NL-6703 HA Wageningen, The Netherlands
Fax: +31 8370 84801.

Abbreviations. [R44K]4-hydroxybenzoate hydroxylase, 4-hydroxybenzoate hydroxylase with Arg44 replaced by Lys; [C116S]4-hydroxybenzoate hydroxylase, 4-hydroxybenzoate hydroxylase with Cys116 replaced by Ser; r.m.s., root-mean-squared.

Enzymes. 4-Hydroxybenzoate hydroxylase (EC 1.14.13.2); catalase (EC 1.11.1.6).

graphic data have revealed that the flavin ring can attain different orientations (Schreuder et al., 1994; Gatti et al., 1994; van Berkel et al., 1994). This leaves the intriguing possibility that flavin motion is not only essential for substrate binding and product release but also for efficient reduction by NADPH (van Berkel et al., 1994). To study this in more detail we decided to replace Arg44 with Lys by site-directed mutagenesis. Arg44 is located at the si-face of the flavin ring and is possibly involved in flavin motion and/or NADPH binding (Schreuder et al., 1994). Alteration of Arg44 is expected to yield important information about the role of this residue for the function of 4-hydroxybenzoate hydroxylase.

MATERIALS AND METHODS

General. Biochemicals and chromatography resins used have been described elsewhere (van Berkel et al., 1992). Oxygen consumption was measured at 25°C using a Clark electrode. Fluorescence binding studies were performed on an Aminco SPF-500 spectrofluorimeter. Absorption (difference) spectra were recorded on an Aminco DW 2000 spectrophotometer. Activity measurements were performed on a LKB Ultrospec III spectrophotometer. Rapid-reaction kinetics were carried out using a temperature-controlled single-wavelength stopped-flow spectrophotometer, type SF-51, from High-Tech Scientific Inc. with 1.3-ms deadtime. The instrument was interfaced to an Hyuandai 486 microcomputer for data acquisition and analysis. All spectrophotometers were maintained at 25°C, unless stated otherwise. Aromatic products were analysed with an ISCO 2300 HPLC system.

Mutagenesis and enzyme purification. *Escherichia coli* TG2 (pAW45), containing the gene encoding 4-hydroxybenzoate hydroxylase from *P. fluorescens*, has been described elsewhere (van Berkel et al., 1992). Site-directed mutagenesis, using *E. coli* RZ1032 for generation of uracil-containing single-stranded DNA, was performed in the bacteriophage M13mp18 according to the method of Kunkel et al. (1987).

The oligonucleotide 5'-GGCCGCATCAAAGCCGGCGTG-3' was used for the construction of [R44K]4-hydroxybenzoate hydroxylase. To prevent possible crystallization problems due to oxidation of Cys116 (van Berkel and Müller, 1987; van der Laan et al. 1989b), the mutation was introduced into the *E. coli* gene encoding the [C116S]4-hydroxybenzoate hydroxylase mutant (Eschrich et al., 1990; van Berkel et al., 1992). The replacement of Arg44 by Lys was confirmed by nucleotide sequencing using the M13 dideoxynucleotide chain-termination method of Sanger et al. (1977).

Mutant 4-hydroxybenzoate hydroxylase genes were expressed in transformed *E. coli* TG2 grown in 6-l batches of tryptone/yeast medium containing 75 μg/ml ampicillin at 37°C with vigorous aeration (Westphal and de Kok, 1988). Mutant enzymes were purified from *E. coli* TG2, essentially as described (van Berkel et al., 1992). The expression and yield of [R44K]4-hydroxybenzoate hydroxylase is comparable to wild-type enzyme. For convenience, and in view of identical catalytic properties (Eschrich et al., 1990), [C116S]4-hydroxybenzoate hydroxylase is referred to as wild-type enzyme.

Analytical methods. Enzyme concentrations were determined by using a molar absorption coefficient, ε_{450} of 10.2 mM^{-1} cm^{-1} for holo-4-hydroxybenzoate hydroxylase (van Berkel et al., 1992).

4-Hydroxybenzoate hydroxylase activity was routinely assayed in 100 mM Tris/sulfate, pH 8.0, containing 0.5 mM EDTA, 200 μM NADPH, 200 μM 4-hydroxybenzoate and 10 μM FAD (Müller and van Berkel, 1982). Steady-state kinetic parameters of 4-hydroxybenzoate hydroxylase were determined at pH 8.0, essentially as described (Eschrich et al., 1993). Rapid-reaction studies were performed in the stopped-flow apparatus using the single-wavelength mode. Kinetic traces of the oxidative half-reaction were analyzed according to published procedures (Entsch and Ballou, 1989; Eschrich et al., 1993). Rate constants for anaerobic flavin reduction were estimated from kinetic traces recorded at 450 nm at variable concentrations of NADPH (van Berkel et al., 1994). Rate constants for hydride transfer and $NADP^+$ dissociation were generated from best fits of stopped-flow traces (recorded at 690 nm) to the kinetic scheme of wild type (Husain and Massey, 1979) using the computer simulation program KINSIM (Barshop et al., 1983). The hydroxylation efficiency of 4-hydroxybenzoate hydroxylase was estimated from oxygen-consumption experiments, either in the absence or presence of catalase (Eschrich et al., 1993). The product 3,4-dihydroxybenzoate was identified and quantified by reverse-phase HPLC (Entsch et al., 1991). Dissociation constants of enzyme/substrate complexes were determined from flavin fluorescence-quenching experiments (van Berkel et al., 1992). The ionization state of aromatic ligands was measured by recording absorption difference spectra as a function of ligand concentration and of pH (Eschrich et al., 1993).

Crystallization. Crystals of [R44K]4-hydroxybenzoate hydroxylase in complex with 4-hydroxybenzoate were obtained using the hanging-drop method. The protein solution contained 10 mg/ml enzyme in 100 mM potassium phosphate, pH 7.0. The reservoir solution contained 39% saturated ammonium sulfate, 0.04 mM FAD, 0.15 mM EDTA, 1 mM 4-hydroxybenzoate, 60 mM sodium sulfite in 100 mM potassium phosphate, pH 7.0. Drops of 2 μl protein solution and 2 μl reservoir solution were allowed to equilibrate at 4°C against 1 ml reservoir solution. Crystals with dimensions of up to 0.2×0.3×0.1 mm grew within 5 days.

Data collection. X-ray diffraction data were collected using a Siemens multiwire area detector and graphite monochromated CuKα radiation from an 18-kW Siemens rotating-anode generator, operating at 45 kV and 100 mA. The crystal-detector distance was 11.6 cm and the 2θ angle was 20°. Data were processed using the XDS package (Kabsch, 1988). The space group is C222$_1$ and the cell dimensions were: a = 7.27 nm, b = 14.64 nm and c = 8.85 nm, differing only slightly from those of native crystals, a = 7.15 nm, b = 14.58 nm and c = 8.82 nm (Schreuder et al., 1989). A total of 92992 observations yielded 23336 unique reflections with an R-sym of 6.8%. The data set is 96.6% complete to 0.22 nm.

Refinement. A starting electron-density map was calculated based on the structure of the wild-type 4-hydroxybenzoate hydroxylase-substrate complex (Schreuder et al., 1989), after a correction had been made for the slightly different cell dimensions (Schreuder et al., 1994). The starting R-factor was 0.213 for data between 0.80 nm and 0.22 nm. The 2*Fo-Fc* and *Fo-Fc* maps clearly show the replacement of Arg44 by Lys. Arg44 in the model was changed into Lys and was fitted in the electron-density map with the graphics program FRODO (Jones, 1985). The complete protein model was inspected and corrected where necessary. Refinement was carried out by energy minimization and temperature-factor refinement using the program Xplor (Brünger, 1992). For the FAD we used the parameters as described by Schreuder et al. (1994). Water molecules were assigned by searching *Fo-Fc* maps for peaks of at least 4σ, which were between 0.20 nm and 0.50 nm of other protein or water atoms. Water molecules with temperature factors after refinement in excess of 0.7 nm^2 were rejected.

The final structure was obtained after four cycles of map inspection and refinement and contains 243 water molecules.

Table 1. Selected polar interactions (d<0.35 nm) involving Lys44 in [R44K]4-hydroxybenzoate hydroxylase and Arg44 in wild-type 4-hydroxybenzoate hydroxylase. Distances in nm are given in parentheses. HOBzH 4-hydroxybenzoate. Data for wild-type enzyme are taken from Schreuder et al. (1989).

Interactions of					
[R44K]4-hydroxybenzoate hydroxylase			wild-type enzyme		
atom 1	atom2		atom 1	atom 2	
		(nm)			(nm)
LysNZ	O4′ ribityl	(0.33)	Arg44 NH1	O4′ ribityl	(0.29)
	O Wat121	(0.32)		O1 ribose-*P*	(0.34)
Lys44O	NH1 Arg214	(0.30)		O2 ribose-*P*	(0.35)
	O2* HOBzH	(0.33)	Arg Nε	O Wat610	(0.28)
	O Wat135	(0.29)	Arg44 O	NH1 Arg214	(0.29)
				O2* HOBzH	(0.34)
				O Wat609	(0.27)

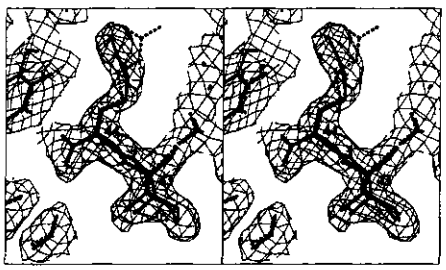

Fig. 1. Stereo diagram of the final 2*Fo*-*Fc* electron density map of [R44K]4-hydroxybenzoate hydroxylase, contoured at 1σ. The atomic model of [R44K]4-hydroxybenzoate hydroxylase is drawn in continuous bold lines, while the orientation of Arg44 in wild-type 4-hydroxybenzoate hydroxylase is indicated in broken lines. The peptide unit between Ile43 and Lys44 is disordered, and about 50% of the peptides in the crystal are rotated by about 180° with respect to wild-type enzyme. To accomodate the flipping peptide, we refined two alternate conformations for residues 43 and 44. While the two alternate conformations are virtually identical for Lys44, they differ slightly for Ile43, as is visible in the figure by the two separate side chains. Both orientations of the side chain of Ile43 fit well to the electron-density map.

The final R-factor is 0.182 for 22697 reflections between 0.80 nm and 0.22 nm. The root-mean-squared (r.m.s.) deviations are $9 \cdot 10^{-4}$ nm for bond lengths and 1.4° for bond angles. All non-glycine residues have ϕ,ψ angles within, or close to, allowed regions. The only exceptions are Lys44 and Asp144 which (with Lys44 replaced by Arg) also deviate in the structures of other complexes of 4-hydroxybenzoate hydroxylase from *P. fluorescens* (Schreuder et al., 1989, 1994). The peptide plane between Ile43 and Lys44 is disordered and two orientations have been modeled, each with half occupancy: the same orientation as in the wild-type enzyme/substrate complex, and a flipped orientation in which the peptide plane is rotated by about 180°. The consequences for the ϕ,ψ angles of Lys44 will be discussed in detail with the results.

RESULTS

Structural properties. The almost 97% complete 0.22-nm data resulted in excellent electron-density maps (Fig. 1) which allowed us to study the structure of [R44K]4-hydroxybenzoate hydroxylase in great detail. The overall structure of [R44K]4-hydroxybenzoate hydroxylase in complex with 4-hydroxybenzoate is almost identical to the structure of the wild-type enzyme/substrate complex. Superposition of the two revealed an r.m.s. difference of 0.015 nm for 391 equivalent C^{α} residues. As expected, the differences were localized in the vicinity of the mutated residue. The differences are even here not very big, which may be due to the positive charge at position 44 being preserved in the Arg to Lys mutation. However, as Table 1 shows, some subtle differences exist in the interactions of the two side chains with the protein and the FAD. Most notable, the interaction between the NH1 of Arg44 and the ribityl O4′ seemed to be strong (d = 0.29 nm), while the interaction between the N^{ζ} of Lys44 and the ribityl O4′ in the mutant appeared to be much weaker (d = 0.33 nm). This and the lost interactions with the ribitylphosphate may explain the weaker FAD binding which was observed for [R44K]4-hydroxybenzoate hydroxylase. From activity measurements performed in the absence or presence of varying amounts of FAD, an apparent K_m value for FAD of 1 μM was estimated. This value is about 20-fold higher than the corresponding value for wild type (Müller and van Berkel, 1982).

Another interesting feature is the orientation of the peptide unit between Ile43 and Lys44. The ϕ,ψ angles of Arg44 in wild-type enzyme had already attracted attention (Schreuder et al., 1989; Lah et al., 1994a) since Arg44 is located in the active-site region and its ϕ,ψ angles are far outside allowed regions. As is shown in Figs 1 and 2, the peptide between Ile43 and Lys44 was disordered in [R44K]4-hydroxybenzoate hydroxylase. Using a *Fo*-*Fc* omit map with Lys44 omitted from the calculation of *Fc* and phases, we estimated that about 53% of the peptides in the crystal were flipped and 47% had the same orientation as in wild type. These occupancies are identical within experimental error and we modeled therefore two orientations of the peptide, each with half occupancy.

The results of the refinement confirm that the Ile43-Lys44 peptide is flipped in about 50% of the molecules in the crystal. A flip of the Ile43-Arg44 peptide has also been observed by Lah et al. (1994b) after the addition of 200 mM potassium bromide to crystals of the wild-type enzyme/substrate complex. The ϕ,ψ angles in both the native conformation and the flipped conformation are outside the allowed regions and point to a strained conformation in which none of the two observed conformations is very stable. The carbonyl oxygen in the flipping peptide (belonging to Ile43) interacts in both orientations only with solvent

Table 2. Optical properties of FAD in free and 4-hydroxybenzoate-complexed 4-hydroxybenzoate hydroxylase. Molar absorption coefficients were determined at 25°C by recording absorption spectra in 50 mM sodium phosphate, pH 7.0, either in the absence or presence of 0.1% SDS (Entsch et al., 1991).

Enzyme	λ_{max}	ε	λ_{max}	ε
	nm	$mM^{-1}\ cm^{-1}$	nm	$mM^{-1}\ cm^{-1}$
Wild-type 4-hydroxybenzoate hydroxylase	373	8.5	450	10.2
Wild-type 4-hydroxybenzoate hydroxylase complexed with 4-hydroxybenzoate	380	9.1	450	10.2
[R44K]4-hydroxybenzoate hydroxylase	370	8.9	445	10.2
[R44K]4-hydroxybenzoate hydroxylase complexed with 4-hydroxybenzoate	378	9.0	450	9.6

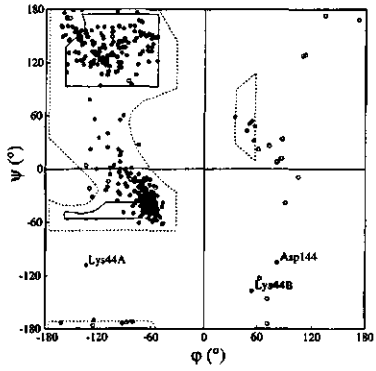

Fig. 2. ϕ,ψ plot of the structure of [R44K]4-hydroxybenzoate hydroxylase. Two ϕ,ψ values are given for Ile43 and Lys44 because of disorder of the Ile43-Lys44 peptide. Orientation A corresponds to a flipped orientation (see text), while orientation B corresponds to the conformation as observed in the wild-type enzyme/substrate complex. The ϕ,ψ angles of Lys44 are outside the allowed regions for both conformations, suggesting that both conformations are strained.

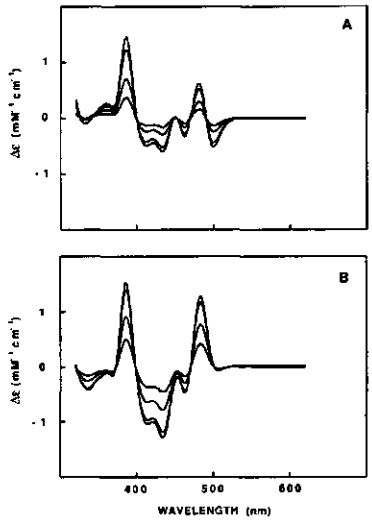

Fig. 3. Flavin absorption difference spectra observed upon binding of 4-hydroxybenzoate to 4-hydroxybenzoate hydroxylase. The absorption spectra were recorded at 25°C in 100 mM Tris/sulfate, pH 8.0. Difference spectra are plotted between 60 μM free enzyme as a reference and the same solution containing 25, 50, 110 and 165 μM 4-hydroxybenzoate, respectively. (A) wild-type (B) [R44K]4-hydroxybenzoate hydroxylase.

molecules which will not provide much stabilization for either conformation.

The reason for the strained conformation is simple. Fig. 2 shows that it is the ψ angle which is deviating, both for the native and the flipped conformation. The ψ angle was associated with the peptide between Lys44 and Ala45 and not with the peptide which flips. As has been discussed before (Schreuder et al., 1991), the 44−45 peptide is firmly held in place by a hydrogen bond of its carbonyl oxygen (belonging to residue 44) with the side chain of Arg214 and with a water molecule (Wat135 or Wat609 in Table 1) which, in turn, is fixed by hydrogen bonds to the side chains of Arg220 and Tyr222.

It is not clear from the current structural data if this flipping peptide serves any catalytic function. In either conformation, the flipping peptide between residues 43 and 44 does not have any specific interactions with the protein in the known crystal structures. In the absence of any structural information on the interaction of 4-hydroxybenzoate hydroxylase with NADPH, we do not know whether this peptide interacts with bound NADPH.

Spectral properties. The optical flavin spectrum of [R44K]4-hydroxybenzoate hydroxylase differs slightly from wild type (van Berkel et al., 1992) by showing absorption maxima at 370 nm and 445 nm (Table 2). From recording absorption spectra in the absence and presence of 0.1% SDS (Entsch et al., 1991), a value of ε_{445} of 10.2 $mM^{-1}\ cm^{-1}$ was estimated for the molar absorption coefficient of protein-bound FAD (Table 2). Fig. 3 shows the absorption difference spectra recorded upon titration of wild type (Fig. 3A) or [R44K]4-hydroxybenzoate hydroxylase (Fig. 3B) with 4-hydroxybenzoate. The shape of both sets of difference spectra indicates that the mutation induced *marginal structural changes in the substrate-binding site. This is* in full agreement with the 'in' position of the flavin observed in the crystal structure.

Binding of 4-hydroxybenzoate to [R44K]4-hydroxybenzoate hydroxylase resulted in about 70% quenching of the fluorescence of protein-bound FAD (pH 7.0). From titration of [R44K]4-hydroxybenzoate hydroxylase with 4-hydroxybenzoate, simple 1:1 binding was observed and a dissociation constant for the enzyme/substrate complex of about 40 μM was estimated. This value is in the same range as found for wild type (van Berkel et al., 1992). Wild-type 4-hydroxybenzoate hydrox-

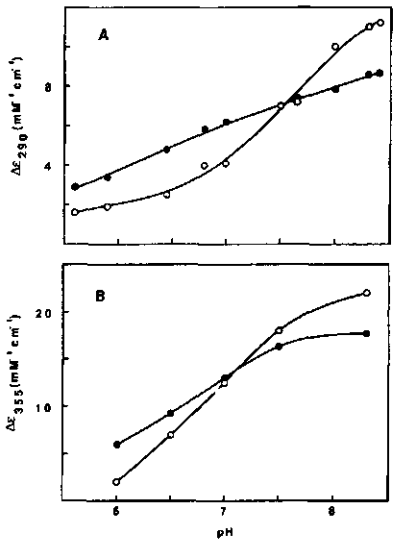

Fig. 4. pH-dependent absorption differences observed upon binding of aromatic ligands to 4-hydroxybenzoate hydroxylase. Wild-type and [R44K]4-hydroxybenzoate hydroxylase were titrated with 4-hydroxybenzoate or 4-hydroxycinnamate and the increase in absorption was monitored from recording absorption difference spectra (Eschrich et al., 1993). The molar absorption differences are extrapolated to infinite ligand concentration and plotted against pH. (A) Molar absorption increase at 290 nm upon titration of 10 μM wild-type (○) or [R44K]4-hydroxybenzoate hydroxylase (●) with 4-hydroxybenzoate. (B) Molar absorption increase at 355 nm upon titration of 20 μM wild-type (○) or [R44K]4-hydroxybenzoate hydroxylase (●) with 4-hydroxycinnamate.

ylase preferentially binds the aromatic substrate in the phenolate form with a pK_s of about 7.2 (Eschrich et al., 1993). Ionization of the 4-hydroxyl group is expected to activate the substrate for hydroxylation (Vervoort et al., 1992). Binding of 4-hydroxybenzoate to [R44K]4-hydroxybenzoate hydroxylase resulted in pH-dependent absorption changes around 290 nm (Fig. 4A), indicative for the deprotonation of the phenolic moiety of the substrate (Shoun et al., 1979). The absorption changes are smaller than found for wild type (Eschrich et al., 1993), suggesting that the mutation affects the arrangement of the hydrogen-bonding network around the 4-hydroxyl group of the substrate. These perturbations must be small, because no structural changes in this region of the active site were detectable in the crystal structure. Therefore, and because the absorption changes at 290 nm increased with increasing pH (Fig. 4A), we conclude that [R44K]4-hydroxybenzoate hydroxylase is capable of substrate activation. This conclusion is supported by the observation that the pK_s of the competitive inhibitor 4-hydroxycinnamate (pK_s = 9.3, free in solution) was decreased by more than 2 upon binding to [R44K]4-hydroxybenzoate hydroxylase (Fig. 4B). A comparable pK_s shift has also been observed upon binding of 4-hydroxycinnamate to wild type (Entsch et al., 1991; Eschrich et al., 1993).

Catalytic properties. Wild-type 4-hydroxybenzoate hydroxylase tightly couples enzyme reduction to substrate hydroxylation (Entsch et al., 1976). Replacement of Arg44 by Lys did not change the reaction stoichiometry. HPLC product analysis showed that the mutant enzyme exclusively formed 3,4-dihydroxybenzoate from 4-hydroxybenzoate with stoichiometric consumption of NADPH. In accordance with this, no production of hydrogen peroxide was detected in oxygen-consumption experiments. We therefore conclude that [R44K]4-hydroxybenzoate hydroxylase is an effective hydroxylase. This conclusion is further supported by rapid-reaction studies on the oxidative half-reaction. These studies were performed at pH 6.6 and 6°C in order to separate the individual reaction steps (Entsch and Ballou, 1989). When reduced [R44K]4-hydroxybenzoate hydroxylase complexed with 4-hydroxybenzoate is mixed with oxygen, the spectral changes and reaction rates are nearly indistinguishable from wild-type and indicative for the subsequent formation and decay of the flavin C(4a)-hydroperoxide and flavin C(4a)-hydroxide (Entsch et al., 1976).

The steady-state kinetic properties of [R44K]4-hydroxybenzoate hydroxylase were studied at pH 8.0, the pH optimum for wild-type enzyme (van Berkel and Müller, 1989). Table 3 shows that the maximum turnover rate of [R44K]4-hydroxybenzoate hydroxylase (k_{cat} = 10 s^{-1}) at 25°C was about fivefold slower than wild type. In contrast to wild type, the maximum turnover rate of [R44K]4-hydroxybenzoate hydroxylase was not influenced by decreasing the temperature to 6°C (Table 3). Table 3 also shows that the K_m NADPH for [R44K]4-hydroxybenzoate hydroxylase was about one order of magnitude higher than for wild type, suggesting that the mutation affects the binding of NADPH. As a result, the catalytic efficiency of [R44K]4-hydroxybenzoate hydroxylase (expressed as k_{cat}/K_m NADPH) was rather low (Table 3).

To investigate the interaction with NADPH in more detail, the reductive half-reaction of [R44K]4-hydroxybenzoate hydroxylase was studied by anaerobic stopped-flow experiments. In the absence of 4-hydroxybenzoate, the rate of reduction of [R44K]4-hydroxybenzoate hydroxylase by NADPH was extremely slow (k'_{red} = 0.002 s^{-1} at 1 mM NADPH) and in the same range as wild type (Eschrich et al., 1993). Reduction of [R44K]4-hydroxybenzoate hydroxylase was highly stimulated in the presence of 4-hydroxybenzoate, acting as an effector. As can be seen from Fig. 5, the rate of reduction of substrate-complexed [R44K]4-hydroxybenzoate hydroxylase was dependent both on temperature and the concentration of NADPH. Table 4 shows that under the conditions used, the maximum rate of reduction of [R44K]4-hydroxybenzoate hydroxylase was about five times slower than wild type. From Table 4 it is also evident that Arg44 plays an important role in NADPH binding. At both temperatures studied, the dissociation constant for NADPH in the ternary complex of the mutant was strongly increased with respect to wild type, making [R44K]4-hydroxybenzoate hydroxylase a rather inefficient reductase.

The reductive half-reaction of 4-hydroxybenzoate hydroxylase is assumed to involve the following sequence of events (Husain and Massey, 1979):

$$E_{ox}S + NADPH \underset{k_{-1}}{\overset{k_1}{\rightleftharpoons}} E_{ox}S\text{-}NADPH \qquad (2)$$

$$\xrightarrow{k_2} E_{red}S\text{-}NADP^+ \xrightarrow{k_3} E_{red}S + NADP^+$$

where $E_{ox}S$ is the oxidized enzyme/substrate complex and $E_{red}S$ is the reduced enzyme/substrate complex. The formation of ternary complexes was indicated by the appearance and decay of long-wavelength absorbances, presumably reflecting flavin-NADP(H) charge-transfer intermediates (Howell et al., 1972). The transient formation of long-wavelength absorption is supposed to be indicative for the proper orientation of flavin and

Table 3. Steady-state kinetic parameters of 4-hydroxybenzoate hydroxylase. Kinetic parameters were determined in air-saturated 100 mM Tris/SO_4^{2-}, pH 8.0. HOBzH, 4-hydroxybenzoate. Data for wild-type 4-hydroxybenzoate hydroxylase at 25°C are from van Berkel et al. (1992).

Enzyme	t	K_m for		k_{cat}	k_{cat}/K_m (NADPH)
		NADPH	HOBzH		
	°C	μM		s^{-1}	$M^{-1}\,s^{-1}$
Wild-type 4-hydroxybenzoate hydroxylase	6	40	30	9	2.3×10^5
[R44K]4-Hydroxybenzoate hydroxylase		520	30	10	1.9×10^4
Wild-type 4-hydroxybenzoate hydroxylase	25	50	25	55	1.1×10^6
[R44K]4-Hydroxybenzoate hydroxylase		560	30	10	1.8×10^4

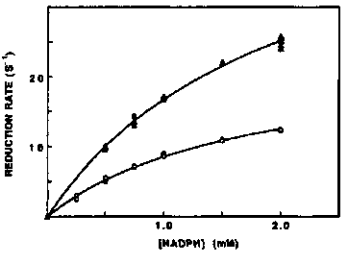

Fig. 5. NADPH and temperature dependence of the rate of reduction of [R44K]4-hydroxybenzoate hydroxylase complexed with 4-hydroxybenzoate. The experiments were performed in 100 mM Tris/sulfate, pH 8.0. 30 μM enzyme was anaerobically mixed with an equal volume of variable concentrations of NADPH in the stopped-flow spectrophotometer. Both solutions contained 1 mM 4-hydroxybenzoate. The rate of reduction of [R44K]4-hydroxybenzoate hydroxylase, as determined from the decrease of absorbance at 450 nm, is plotted as a function of the concentration of NADPH; 25°C, (△); 6°C, (○). The lines through the data points were obtained from non-linear regression analysis.

Table 4. Kinetic parameters for the reductive half-reaction of 4-hydroxybenzoate hydroxylase. For experimental details see Figs 5 and 6. For explanation of symbols see Eqn 2. Data for wild-type 4-hydroxybenzoate hydroxylase at 25°C are from van Berkel et al., 1992. n.d., not determined.

Enzyme	t	K_d NADPH	k_2	k_3
	°C	μM	s^{-1}	
Wild-type 4-hydroxybenzoate hydroxylase	6	150	80	23
[R44K]4-Hydroxybenzoate hydroxylase		2000	22	50
Wild-type 4-hydroxybenzoate hydroxylase	25	150	300	n.d.
[R44K]4-Hydroxybenzoate hydroxylase		2000	50	n.d.

nicotinamide rings allowing the rapid transfer of a hydride equivalent (Palfey et al., 1994).

Anaerobic reduction of [R44K]4-hydroxybenzoate hydroxylase complexed with 4-hydroxybenzoate involves long-wavelength absorbance changes when the reaction is performed at pH 8.0. For kinetic reasons (Howell et al., 1972; Husain and Massey, 1979), charge-transfer complex formation was studied at 6°C. In contrast to wild-type (Husain and Massey, 1979), no long-wavelength absorption was observed with [R44K]4-hydroxybenzoate hydroxylase at pH 6.6, presumably due to the slow rate of flavin reduction ($k'_{red} = 1\ s^{-1}$ at 1 mM NADPH) and the very weak binding of NADPH.

Fig. 6 compares typical reaction traces for the reduction of wild-type and [R44K]4-hydroxybenzoate hydroxylase at pH 8.0. With both enzymes, maximal charge-transfer absorption was observed at 690 nm. The intensity of charge-transfer absorbance was lower for [R44K]4-hydroxybenzoate hydroxylase (Fig. 6B) than for wild-type (Fig. 6A) and strongly dependent upon the concentration of NADPH. Using the rate and dissociation constants obtained from flavin reduction at 450 nm (Table 4), the 690 nm trace of wild type depicted in Fig. 6A is well simulated with the model presented in Eqn (2). From this simulation (Fig. 6A) it is concluded that both E_{ox}S-NADPH ($\varepsilon_{690} = 0.45\ mM^{-1}\,cm^{-1}$) and E_{red}S-NADP$^+$ ($\varepsilon_{690} = 1.5\ mM^{-1}\,cm^{-1}$) contribute to the charge-transfer absorption. As can be seen from Table 4, the simulation predicts that at pH 8.0 and 6°C, NADP$^+$ release (k_3) is much slower than flavin reduction (k_2) and most probably rate limiting in overall catalysis (Table 3). A similar conclusion was drawn for wild type, when reacted at pH 7.6 and 2°C (Howell et al., 1972; Entsch and Ballou, 1989).

For [R44K]4-hydroxybenzoate hydroxylase, the very low yield of 690-nm charge-transfer absorption (Fig. 6B) complicates the evaluation of the kinetics of the reductive half-reaction. Nevertheless, if it assumed that the molar absorption coefficients of E_{ox}S-NADPH and E_{red}S-NADP$^+$ are comparable to wild type, the 690-nm trace depicted in Fig. 6B can be satisfactorily simulated with the model presented in Eqn (2). With this simulation (Fig. 6B) and considering the rate of reduction determined at 450 nm, an optimal fit was obtained with k_2 of 14 s^{-1} and k_3 of 50 s^{-1}. This suggests that the low yield of charge-transfer absorption observed is in part due to a relatively rapid decomposition of the E_{red}S-NADP$^+$ species. From this it is tentatively concluded that at pH 8.0 and 6°C, reduction of [R44K]4-hydroxybenzoate hydroxylase is rate limiting in catalysis.

DISCUSSION

Arg44 in 4-hydroxybenzoate hydroxylase is situated in a short loop which adjoins the si-face of the isoalloxazine ring of the FAD (Schreuder et al., 1989). The conserved nature of this loop (Entsch et al., 1988; Di Marco et al., 1993; Shuman and Dix, 1993; Wong et al., 1994) and its interaction with both the substrate and the FAD (Schreuder et al., 1989) suggest that this loop plays a functional role in catalysis. This assumption is corroborated by recent crystallographic data which show that the flavin ring in 4-hydroxybenzoate hydroxylase can attain dif-

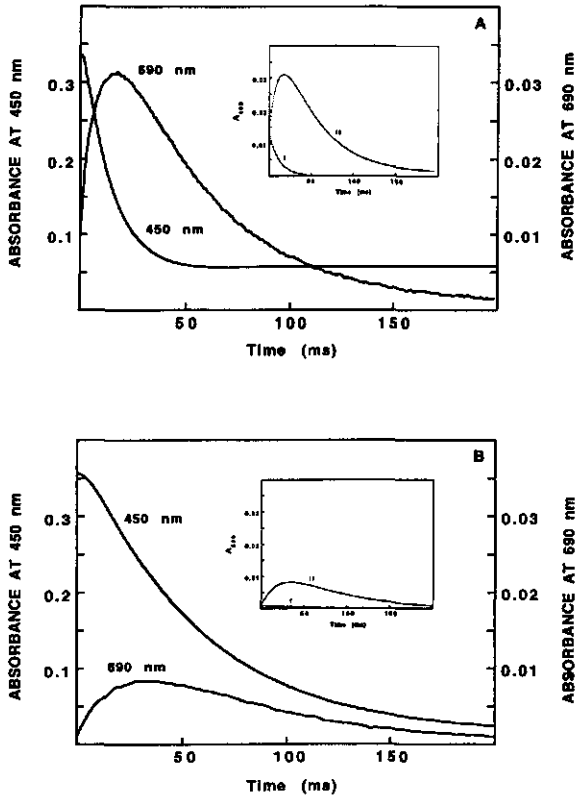

Fig. 6. Time-course of absorbance changes upon reduction of the enzyme/substrate complex of 4-hydroxybenzoate hydroxylase by NADPH. The experiments were performed at 6°C in the stopped-flow spectrophotometer. The final reaction mixture contained 30 μM enzyme, 1 mM 4-hydroxybenzoate, 1 mM NADPH in 100 mM Tris/sulfate, pH 8.0. Enzyme reduction and formation of charge-transfer absorption were monitored at 450 nm and 690 nm, respectively. (A) wild-type; (B) [R44K]4-hydroxybenzoate hydroxylase. The insets show the traces obtained from simulating the absorption changes at 690 nm. (I) E_{ox}S-NADPH complex; (II) E_{red}S-NADP$^+$ complex.

ferent conformations (Schreuder et al., 1994; Gatti et al., 1994; van Berkel et al., 1994). Flavin motion towards a more solvent-accessible region is assumed to provide a path for the substrate to enter the active site and for the product to leave (Schreuder et al., 1994; Gatti et al., 1994). Arg44 may facilitate flavin motion by stabilizing the flavin 'out' conformation through π-π stacking interactions (Schreuder et al., 1994). Studies with arabinoflavin containing 4-hydroxybenzoate hydroxylase have indicated that flavin motion may also be important for the efficient reduction of the enzyme/substrate complex by NADPH (van Berkel et al., 1994).

The data presented in this study show that Lys replacement of Arg44 does not change the overall folding of the enzyme/substrate complex. Except for local changes around the site of mutation, no structural differences are observed with respect to wild type. Lys replacement of Arg44 decreased the affinity for the FAD. From the structural data it is apparent that this is due to the weak interaction of the Lys44 side chain with its ribitylphosphate moiety. Disruption of this interaction does not influence the conformation of the flavin ring. As with wild-type (Schreuder et al., 1989), the flavin ring occupies the interior position in the active site, which is the expected conformation to allow substrate hydroxylation (Schreuder et al., 1994). The observed flipping of the Ile43-Lys44 peptide does not seem to contribute to the stabilization of the flavin 'in' position because all H-bond interactions remain virtually unaltered.

[R44K]4-Hydroxybenzoate hydroxylase tightly couples flavin reduction to substrate hydroxylation. The efficient production of 3,4-dihydroxybenzoate by [R44K]4-hydroxybenzoate hydroxylase is in agreement with the flavin 'in' conformation observed in the crystal structure. As discussed elsewhere (Schreuder et al., 1990; Entsch and van Berkel, 1995), the flavin 'in' conformation is needed for the stabilization of the flavin-(C4a)-hydroperoxide and for its correct orientation towards the

substrate. Lys replacement of Arg44 hardly influences the orientation of the substrate. Despite this, the mutation changes the absorption properties of protein-bound substrate indicating some disturbance of the hydrogen-bond network connecting the phenolic moiety of the substrate with the side chains of Tyr201 and Tyr385. The crystal structures do not show significant changes, indicating that these perturbations must be small. In analogy with mutant Tyr385Phe (Eschrich et al., 1993), the changed electronic properties of the substrate do not preclude efficient hydroxylation.

The most intriguing result from the present study is that Lys replacement of Arg44 substantially alters the binding kinetics of the reductive half-reaction. The rather high rate of reduction of [R44K]4-hydroxybenzoate hydroxylase complexed with 4-hydroxybenzoate suggests that this change in binding kinetics is not related to the effector role of the substrate. This is in accordance with the conserved mode of substrate binding observed in the crystal structure. Inefficient catalysis by Arg44Lys is mainly due to the strongly increased dissociation constant for NADPH in the ternary complex. It is not clear from the present kinetic data whether this increase in K_d NADPH reflects a change in the NADPH association-rate or dissociation-rate constant, or both. The binding mode of the NADPH molecule is unknown and it is therefore difficult to assess the exact role of Arg44 in this process. There are, however, a few possibilities. The side chain of Arg44 is located in the cleft leading towards the active site and the residue might be directly involved in NADPH binding of e.g., the ADP part of the molecule. Reduction of 4-hydroxybenzoate hydroxylase is influenced by movement of the flavin ring in and out of the active site. 4-Hydroxybenzoate hydroxylase, reconstituted with arabino-FAD binds the flavin in the out position (van Berkel et al., 1994) and is more rapidly reduced by NADPH than wild type. The mutation of Arg44 to Lys could lead to reduced stabilization of the flavin out conformation because of the absence of π-π stacking interactions, leading to less efficient reduction. The Arg44Lys mutation could lead to a change in the mutual orientation of the flavin and nicotinamide rings, inhibiting hydride transfer. The low intensity of the reduced flavin-$NADP^+$ charge-transfer species can be explained by poor binding of the NADPH/$NADP^+$ species, leading to kinetic destabilization, or by a change in the mutual orientation of the flavin and nicotinamide rings, leading to decreased orbital overlap.

For wild-type 4-hydroxybenzoate hydroxylase, the rate-limiting step in catalysis appears to vary with the reaction conditions. At pH 6.6 and low temperature, flavin reoxidation is largely responsible for determining the rate of catalysis (Husain and Massey, 1979; Entsch and van Berkel, 1995). Under optimal reaction conditions (pH 8.0, 25°C), catalysis is too fast for a clear separation of the individual reaction steps. Molecular orbital calculations suggest that under these conditions, the rate-limiting step in catalysis is dictated by the rate of substrate hydroxylation (Vervoort et al., 1992). The results presented here suggest that at pH 8.0 and 6°C, neither substrate hydroxylation or flavin reoxidation are rate limiting in catalysis, but that the overall reaction rate is dictated by the rate of $NADP^+$ release. It is noteworthy that in contrast to wild type (van Berkel and Müller, 1989), the turnover rate of [R44K]4-hydroxybenzoate hydroxylase did not increase upon raising the temperature to 25°C.

This study was supported by the Netherlands Foundation for Chemical research (SON) with financial aid from the Netherlands Organization for Scientific Research (NWO).

REFERENCES

Barshop, B. A., Wrenn, R. F. & Frieden, C. (1983) *Anal. Biochem. 130*, 134–145.

Brünger, A. T. (1992) *X-plor version 3.1. A system for the X-ray crystallography and NMR*, Yale University Press, New Haven CT.

Di Marco, A. A., Averhoff, B., Kim, E. E. & Ornston, L. N. (1993) Evolutionary divergence of *pobA*, the structural gene encoding *p*-hydroxybenzoate hydroxylase in an *Acinetobacter calcoaceticus* strain well-suited for genetic analysis. *Gene (Amst.) 125*, 25–33.

Entsch, B., Ballou, D. P. & Massey, V. (1976) Flavin-oxygen derivatives involved in hydroxylation by *p*-hydroxybenzoate hydroxylase, *J. Biol. Chem. 251*, 2550–2563.

Entsch, B., Nan, Y., Weaich, K. & Scott, K. F. (1988) Sequence and organization of *pobA*, the gene coding for *p*-hydroxybenzoate hydroxylase, an inducible enzyme from *Pseudomonas aeruginosa*, *Gene (Amst.) 71*, 279–291.

Entsch, B. & Ballou, D. P. (1989) Purification, properties, and oxygen reactivity of *p*-hydroxybenzoate hydroxylase from *Pseudomonas aeruginosa*, *Biochim. Biophys. Acta 999*, 313–322.

Entsch, B., Palfey, B. A., Ballou, D. P. & Massey, V. (1991) Catalytic function of tyrosine residues in *para*-hydroxybenzoate hydroxylase as determined by the study of site-directed mutants, *J. Biol. Chem. 266*, 17341–17349.

Entsch, B. & van Berkel, W. J. H. (1995) Structure and mechanism of *p*-hydroxybenzoate hydroxylase, *FASEB J. 9*, 476–483.

Eschrich, K., van Berkel, W. J. H., Westphal, A. H., de Kok, A., Mattevi, A., Obmolova, G., Kalk, K. H. & Hol, W. G. J. (1990) Engineering of microheterogeneity-resistant *p*-hydroxybenzoate hydroxylase from *Pseudomonas fluorescens*, *FEBS Lett. 277*, 197–199.

Eschrich, K., van der Bolt, F. J. T., de Kok, A. & van Berkel, W. J. H. (1993) Role of Tyr201 and Tyr385 in substrate activation by *p*-hydroxybenzoate hydroxylase from *Pseudomonas fluorescens*, *Eur. J. Biochem. 216*, 137–146.

Gatti, D. L., Palfey, B. A., Lah, M. S., Entsch, B., Massey, V., Ballou, D. P. & Ludwig, M. L. (1994) The mobile flavin of 4-OH benzoate hydroxylase, *Science 266*, 110–114.

Hosokawa, K. & Stanier, R. Y. (1966) Crystallization and properties of *p*-hydroxybenzoate hydroxylase from *Pseudomonas putida*, *J. Biol. Chem. 241*, 2453–2460.

Howell, L. G., Spector, T. & Massey, V. (1972) Purification and properties of *p*-hydroxybenzoate hydroxylase from *Pseudomonas fluorescens*, *J. Biol. Chem. 247*, 4340–4350.

Husain, M. & Massey, V. (1979) Kinetic studies on the reaction mechanism of *p*-hydroxybenzoate hydroxylase. Agreement of steady state and rapid reaction data, *J. Biol. Chem. 254*, 6657–6666.

Jones, T. A. (1985) Interactive computer graphics: FRODO, *Methods Enzymol. 115*, 157–171.

Kabsch, W. (1988) Evaluation of single-crystal diffraction data from a position-sensitive detector, *J. Appl. Crystallogr. 21*, 916–924.

Kunkel, T. A., Roberts, J. D. & Zakour, R. A. (1987) Rapid and efficient site-specific mutagenesis without phenotypic selection, *Methods Enzymol. 154*, 367–382.

Lah, M. S., Palfey, B. A., Schreuder, H. A. & Ludwig, M. L. (1994a) Crystal structures of mutant *Pseudomonas aeruginosa p*-hydroxybenzoate hydroxylases: The Tyr201Phe, Tyr385Phe and Asn300Asp variants, *Biochemistry 33*, 1555–1564.

Lah, M. S., Gatti, D., Schreuder, H. A., Palfey, B. A. & Ludwig, M. L. (1994b) Structures of mutant *p*-hydroxybenzoate hydroxylases: Evidence for an alternative mode of flavin binding, in *Flavins and flavoproteins* (Yagi, K., ed.) pp. 221–229, W. de Gruyter, Berlin.

Manstein, D. J., Pai, E. F., Schopfer, L. M. & Massey, V. (1986) Absolute stereochemistry of flavins in enzyme-catalyzed reactions, *Biochemistry 25*, 6807–6816.

Massey, V. & Hemmerich, P. (1975) Flavin and pteridine monooxygenases, in *The enzymes* (Boyer, P. D., ed.) vol. 12, pp. 191–252, Academic Press, New York.

Middelhoven, W. J. (1993) Catabolism of benzene compounds by ascomycetous and basidiomycetous yeasts and yeastlike fungi, *Antonie Leeuwenhoek 63*, 125–144.

Müller, F. & van Berkel, W. J. H. (1982) A study on *p*-hydroxybenzoate hydroxylase from *Pseudomonas fluorescens*. A convenient method of preparation and some properties of the apoenzyme, *Eur. J. Biochem. 128*, 21–27.

Pai, E. F. & Schulz, G. E. (1983) The catalytic mechanism of glutathione reductase as derived from X-ray diffraction analyses of reaction intermediates, *J. Biol. Chem. 258*, 1752–1757.

Palfey, B. A., Entsch, B., Ballou, D. P. & Massey, V. (1994) Changes in the catalytic properties of *p*-hydroxybenzoate hydroxylase caused by the mutation Asn300Asp, *Biochemistry 33*, 1545–1554.

Sanger, F., Nicklen, S. & Coulson, A. R. (1977) DNA sequencing with chain-terminating inhibitors, *Proc. Natl Acad. Sci. USA 74*, 5463–5472.

Schreuder, H. A., Prick, P., Wierenga, R. K., Vriend, G., Wilson, K. S., Hol, W. G. J. & Drenth, J. (1989) Crystal structure of the *p*-hydroxybenzoate hydroxylase-substrate complex refined at 1.9 Å resolution, *J. Mol. Biol. 208*, 679–696.

Schreuder, H. A., Hol, W. G. J. & Drenth, J. (1990) Analysis of the active site of the flavoprotein *p*-hydroxybenzoate hydroxylase and some ideas with respect to its reaction mechanism, *Biochemistry 29*, 3101–3108.

Schreuder, H. A., van der Laan, J. M., Hol, W. G. J. & Drenth, J. (1991) The structure of *p*-hydroxybenzoate hydroxylase, in *Chemistry and biochemistry of flavoenzymes* (Müller, F., ed.) vol. 2, pp. 31–64, CRC Press, Boca Raton.

Schreuder, H. A., Mattevi, A., Obmolova, G., Kalk, K. H., Hol, W. G. J., van der Bolt, F. J. T & van Berkel, W. J. H. (1994) Crystal structures of wild-type *p*-hydroxybenzoate hydroxylase complexed with 4-aminobenzoate, 2,4-dihydroxybenzoate and 2-hydroxy-4-aminobenzoate and mutant Tyr222Ala, complexed with 2-hydroxy-4-aminobenzoate. Evidence for a proton channel and a new binding mode of the flavin ring, *Biochemistry 33*, 10161–10170.

Shoun, H., Beppu, T. & Arima, K. (1979) On the stable enzyme-substrate complex of *p*-hydroxybenzoate hydroxylase, *J. Biol. Chem. 254*, 899–904.

Shuman, B. & Dix, T. A. (1993) Cloning, nucleotide sequence, and expression of a *p*-hydroxybenzoate hydroxylase isozyme gene from *Pseudomonas fluorescens*, *J. Biol. Chem. 268*, 17057–17062.

Stanier, R. Y. & Ornston, L. N. (1973) The β-ketoadipate pathway, *Adv. Microb. Physiol. 9*, 89–151.

van Berkel, W. J. H. & Müller, F. (1987) The elucidation of the microheterogeneity of highly purified *p*-hydroxybenzoate hydroxylase from *Pseudomonas fluorescens* by various biochemical techniques, *Eur. J. Biochem. 167*, 35–46.

van Berkel, W. J. H., Müller, F., Jekel, P. A., Weijer, W. J., Schreuder, H. A. & Wierenga, R. K. (1988) Chemical modification of tyrosine-38 in *p*-hydroxybenzoate hydroxylase from *Pseudomonas fluorescens* by 5′-*p*-fluorosulfonylbenzoyladenosine: A probe for the elucidation of the NADPH binding site? *Eur. J. Biochem. 176*, 449–459.

van Berkel, W. J. H. & Müller, F. (1989) The temperature and pH dependence of some properties of *p*-hydroxybenzoate hydroxylase from *Pseudomonas fluorescens*, *Eur. J. Biochem. 179*, 307–314.

van Berkel, W. J. H. & Müller, F. (1991) Flavin-dependent monooxygenases with special reference to *p*-hydroxybenzoate hydroxylase, in *Chemistry and biochemistry of flavoenzymes* (Müller, F., ed.) vol. 2, pp. 1–29, CRC Press, Boca Raton.

van Berkel, W. J. H., Westphal, A. H., Eschrich, K., Eppink, M. H. M. & de Kok, A. (1992) Substitution of Arg214 at the substrate-binding site of *p*-hydroxybenzoate hydroxylase from *Pseudomonas fluorescens*, *Eur. J. Biochem. 210*, 411–419.

van Berkel, W. J. H., Eppink, M. H. M. & Schreuder, H. A. (1994) Crystal structure of *p*-hydroxybenzoate hydroxylase reconstituted with the modified FAD present in alcohol oxidase from methylotrophic yeasts: Evidence for an arabinoflavin, *Protein Sci. 3*, 2245–2253.

van der Laan, J. M., Schreuder, H. A., Swarte, M. B. A., Wierenga, R. K., Kalk, K. H., Hol, W. G. J. & Drenth, J. (1989a) The coenzyme analogue adenosine 5-diphosphoribose displaces FAD in the active site of *p*-hydroxybenzoate hydroxylase. An X-ray crystallographic investigation, *Biochemistry 28*, 7199–7205.

van der Laan, J. M., Swarte, M. B. A., Groendijk, H., Hol, W. G. J. & Drenth, J. (1989b) The influence of purification and protein heterogeneity on the crystallization of *p*-hydroxybenzoate hydroxylase, *Eur. J. Biochem. 179*, 715–724.

Vervoort, J., Rietjens, I. M. C. M., van Berkel, W. J. H. & Veeger, C. (1992) Frontier orbital study on the 4-hydroxybenzoate-3-hydroxylase-dependent activity with benzoate derivatives, *Eur. J. Biochem. 206*, 479–484.

Westphal, A. H. & de Kok, A. (1988) Lipoamide dehydrogenase from *Azotobacter vinelandii*, molecular cloning, organization and sequence analysis of the gene, *Eur. J. Biochem. 172*, 299–305.

Wierenga, R. K., de Jong, R. J., Kalk, K. H., Hol, W. G. J. & Drenth, J. (1979) Crystal structure of *p*-hydroxybenzoate hydroxylase, *J. Mol. Biol. 131*, 55–73.

Wierenga, R. K., Drenth, J. & Schulz, G. E. (1983) Comparison of the three-dimensional protein and nucleotide structure of the FAD-binding domain of *p*-hydroxybenzoate hydroxylase with the FAD- as well as NADPH-binding domains of glutathione reductase, *J. Mol. Biol. 167*, 725–739.

Wong, C. M., Dilworth, M. J. & Glenn, A. R. (1994) Cloning and sequencing show that 4-hydroxybenzoate hydroxylase (*pobA*) is required for uptake of 4-hydroxybenzoate in *Rhizobium leguminosarum*, *Microbiology 140*, 2775–2786.

CHAPTER 4

Lys42 and Ser42 variants of *p*-hydroxybenzoate hydroxylase from *Pseudomonas fluorescens* reveal that Arg42 is essential for NADPH binding

Michel H.M. Eppink, Herman A. Schreuder and Willem J.H. van Berkel

Eur. J. Biochem 253: 194-201 (1998)

Eur. J. Biochem. 253, 194–201 (1998)

Lys42 and Ser42 variants of *p*-hydroxybenzoate hydroxylase from *Pseudomonas fluorescens* reveal that Arg42 is essential for NADPH binding

Michel H. M. EPPINK[1], Herman A. SCHREUDER[2] and Willem J. H. VAN BERKEL[1]

[1] Department of Biomolecular Sciences, Laboratory of Biochemistry, Wageningen Agricultural University, The Netherlands
[2] Marion Merrell Dow Research Institute Strasbourg, France

(Received 30 October 1997) – EJB 97 1535/3

The conserved Arg42 of the flavoprotein *p*-hydroxybenzoate hydroxylase is located at the entrance of the active site in a loop between helix H2 and sheet E1 of the FAD-binding domain. Replacement of Arg42 by Lys or Ser decreases the turnover rate of *p*-hydroxybenzoate hydroxylase from *Pseudomonas fluorescens* by more than two orders of magnitude. Rapid reaction kinetics show that the low activity of the Arg42 variants results from impaired binding of NADPH. In contrast to an earlier conclusion drawn for *p*-hydroxybenzoate hydroxylase from *Acinetobacter calcoaceticus*, substitution of Arg42 with Ser42 in the enzyme from *P. fluorescens* hardly disturbs the binding of FAD. Crystals of [Lys42]*p*-hydroxybenzoate hydroxylase complexed with 4-hydroxybenzoate diffract to 0.22-nm resolution. The structure of the Lys42 variant is virtually indistinguishable from the native enzyme with the flavin ring occupying the interior position within the active site. Lys42 in the mutant structure interacts indirectly via a solvent molecule with the 3-OH of the adenosine ribose moiety of FAD. Substrate perturbation difference spectra suggest that the Arg42 replacements influence the solvent accessibility of the flavin ring in the oxidized enzyme. In spite of this, the Arg42 variants fully couple enzyme reduction to substrate hydroxylation. Sequence-comparison studies suggest that Arg42 is involved in binding of the 2′-phosphoadenosine moiety of NADPH.

Keywords: crystal structure; flavoprotein monooxygenase; *p*-hydroxybenzoate hydroxylase; NADPH binding; site-specific mutagenesis.

p-Hydroxybenzoate hydroxylase is the prototype of the family of pyridine-nucleotide-dependent flavoprotein monooxygenases [1]. The enzyme catalyzes the *ortho*-hydroxylation of 4-hydroxybenzoate to 3,4-dihydroxybenzoate, an intermediate step in the degradation of aromatic compounds in soil microorganisms [2]. The *p*-hydroxybenzoate hydroxylase-mediated conversion of 4-hydroxybenzoate is a multistep reaction with three substrates and three products.

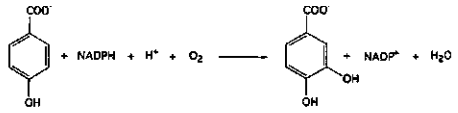

Pseudomonas p-hydroxybenzoate hydroxylase has been studied by means of many techniques, including rapid reaction kinetics [3–5], protein crystallography [6–8] and with site-directed mutagenesis [9]. As a result, many aspects of the catalytic reaction are very well known, especially the steps involving oxygen. However, many important aspects of the reductive reactions involving NADPH are unknown [10]. We do not even know the NADPH-binding site. Attempts to crystallize or soak *p*-hydroxybenzoate hydroxylase crystals with NADPH or analogs were unsuccesful. Either no NADPH binding was observed, or with the analog adenosine-5′-phosphoribose the FAD got replaced [11]. *p*-Hydroxybenzoate hydroxylase has a *βαβ* nucleotide-binding fold for the FAD, but not for NADPH [6]. *p*-Hydroxybenzoate hydroxylase has no sites with sequence or structural similarity to known NAD(P)H-binding sites [12], making it impossible to predict the binding site. Also unexplained is the mechanism behind the stimulation of the reduction rate by the substrate. In the absence of substrate, NADPH is hardly able to reduce the FAD. Substrate binding causes an acceleration of the reduction rate by more than five orders of magnitude [4]. To answer these questions, we need to know the binding mode of NADPH. In the absence of a crystal structure, we decided to identify, by means of site-directed mutagenesis, residues that are essential for NADPH binding, to provide an experimental basis for the modeling of the NADPH-binding mode.

Chemical-modification studies of *p*-hydroxybenzoate hydroxylase from *P. fluorescens* suggested that arginine residues are important for NADPH binding [13], making arginine residues an attractive target for site-directed mutagenesis. Based on the crystal structure, we selected a number of arginine residues around the active-site cleft. The first arginine we found to be important for NADPH binding was Arg44. Replacement of Arg44 by lysine strongly reduced the affinity for NADPH without disrupting the efficiency of substrate hydroxylation [14]. Arg42 is another conserved residue, possibly involved in NADPH binding. Arg42 is located at the entrance of the active site and points with its side chain towards the 2-OH and 3-OH of

Correspondence to W. J. H. van Berkel, Department of Biochemistry, Agricultural University, Dreijenlaan 3, NL-6703 HA Wageningen, The Netherlands
Fax: +31 317 484801.
E-mail: willem.vanberkel@fad.bc.wau.nl
URL: http://gcg.tran.wau.nl
Enzymes. *p*-Hydroxybenzoate hydroxylase (EC 1.14.13.2); catalase (EC 1.11.1.6).

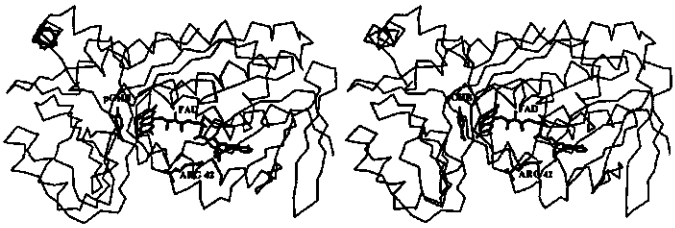

Fig. 1. Stereo drawing of the Cα backbone of the structure of the enzyme · substrate complex of *p*-hydroxybenzoate hydroxylase. The substrate (pOHB), the cofactor (FAD) and Arg42 are indicated.

the adenine-ribose moiety of FAD [7] (Fig. 1). From nucleotide sequencing of a *pobA*-deficient mutant it was proposed that replacement of Arg42 by Ser in *p*-hydroxybenzoate hydroxylase from *A. calcoaceticus* reduces FAD binding by disturbing the ADP-ribose pocket [15]. We present here studies of Arg42 variants of *p*-hydroxybenzoate hydroxylase from *P. fluorescens*, which show that Arg42 is crucial for NADPH binding rather than for FAD binding. Some of these results have been presented elsewhere [16].

MATERIALS AND METHODS

Site-specific mutagenesis. *Escherichia coli* TG2 (pAW45), harboring the gene encoding *p*-hydroxybenzoate hydroxylase from *P. fluorescens*, has been described [17]. Site-specific mutagenesis, using *E. coli* RZ1032 for generation of uracil-containing single-stranded DNA, was performed in the bacteriophage M13mp18 according to the method of Kunkel et al. [18]. Mutations were introduced in the gene encoding the microheterogeneity resistant [Ser116]*p*-hydroxybenzoate hydroxylase mutant [19]. For convenience and in view of the identical catalytic and structural properties [19], [Ser116]*p*-hydroxybenzoate hydroxylase is referred to as *p*-hydroxybenzoate hydroxylase. The mixed oligonucleotide 5'-CGTGCTCGGC$^{A}_{T}$$^{A}_{C}$ATCCGCGCC-3', which encodes the Lys42 (AAA) and Ser42 (TCC) substitutions, was used for the construction of Arg42 mutants. The mutations were confirmed by nucleotide sequencing using the M13 dideoxynucleotide chain-termination method of Sanger et al. [20].

Expression and enzyme purification. *p*-Hydroxybenzoate hydroxylase genes were expressed in transformed *E. coli* TG2 cells grown in 3-l batches of tryptone/yeast medium containing 75 μg/ml ampicillin and 20 μg/ml isopropyl thiogalactoside at 37°C with vigorous aeration [21]. The Arg42 mutants were purified by a modified procedure of the purification protocol developed for *p*-hydroxybenzoate hydroxylase [17]. The enzyme preparation obtained after protamine sulfate treatment was loaded onto a Q-Sepharose column (40 cm×2.6 cm), equilibrated in 20 mM Tris/sulfate, pH 8.0. After washing, the enzyme was eluted with 0.2 M KCl in starting buffer and dialysed against 40 mM Tris/sulfate, pH 8.0. The enzyme was loaded onto a Cibacron blue 3GA-agarose column (40 cm×2.6 cm), equilibrated in 40 mM Tris/sulfate, pH 8.0, and eluted in the wash solution. After dialysis in 7 mM potassium phosphate, pH 7.0, the enzyme was passed over a hydroxyapatite column equilibrated in 7 mM potassium phosphate, pH 7.0 [22]. The Arg42 mutants were purified to apparent homogeneity by FPLC anion-exchange chromatography [23], and stored as an 70% saturated ammonium sulfate precipitate at 4°C.

Analytical methods. Molar absorption coefficients for protein-bound FAD were determined in 50 mM sodium phosphate, pH 7.0, by recording absorption spectra in the absence and presence of 0.1% SDS [24]. *p*-Hydroxybenzoate hydroxylase activity was assayed in 100 mM Tris/sulfate, pH 8.0, containing 0.5 mM EDTA, 200 μM NADPH, 200 μM 4-hydroxybenzoate and 10 μM FAD [25]. Steady-state kinetic parameters were determined at pH 8.0, essentially as described [26]. Rapid-reaction kinetics were determined using a stopped flow spectrophotometer, type SF-51 (High-Tech Scientific Inc.) Rate constants for anaerobic flavin reduction were estimated from kinetic traces recorded at 450 nm using variable concentrations of NADPH [14]. Kinetic traces of the oxidative half-reaction were analyzed essentially as described [5]. The hydroxylation efficiency of Arg42 mutants was estimated from oxygen-consumption experiments [26]. Hydrogen peroxide formation was quantified by the addition of catalase at the end of the reaction. Aromatic products were identified and quantified by reverse-phase HPLC [24]. Dissociation constants of enzyme · substrate complexes were determined fluorimetrically [27]. Absorption difference spectra between free and substrate-complexed enzymes were recorded on an Aminco DW-spectrophotometer [17].

Crystallization and data collection. Crystals of [Lys42]*p*-hydroxybenzoate hydroxylase complexed with 4-hydroxybenzoate were obtained using the hanging-drop method. The protein solution contained 10−15 mg/ml enzyme in 100 mM potassium phosphate, pH 7.0. The reservoir solution contained 39% saturated ammonium sulfate, 0.04 mM FAD, 0.15 mM EDTA, 30 mM sodium sulfite, 1 mM 4-hydroxybenzoate 100 mM potassium phosphate, pH 7.0. Drops of 2 μl protein solution and 2 μl reservoir solution were allowed to equilibrate at 4°C against 1 ml reservoir solution. Crystals with dimensions of up to 0.2×0.3×0.1 mm³ grew within 3−5 days.

X-ray diffraction data were collected using a Siemens multiwire area detector and graphite monochromated CuKα radiation from an 18-kW Siemens rotating anode generator, operating at 45 kV and 100 mA. The crystal-detector distance was 11.6 cm and the 2θ angle was 20°. Data were processed using the XDS package [28]. The space group was C222$_1$ and the cell dimensions, a = 7.135 nm, b = 14.59 nm and c = 8.88 nm, differ only slightly from the native crystals, a = 7.15 nm, b = 14.58 nm and c = 8.82 nm [7]. A total of 78 553 observations yielded 23 174 unique reflections with an R-sym of 6.7%. The data set is 96.8% complete to 0.22 nm.

Structure refinement. A starting electron-density map was calculated based on the structure of the enzyme · substrate complex [7], after a correction had been made for the slightly different cell dimensions [29]. The starting R-factor was 0.232 for data between 0.80 nm and 0.22 nm. The $2Fo$-Fc and Fo-Fc maps show the replacement of Arg42 by Lys. Arg42 in the model was changed into Lys and was fitted in the electron-density map with the graphics program O [30]. The complete pro-

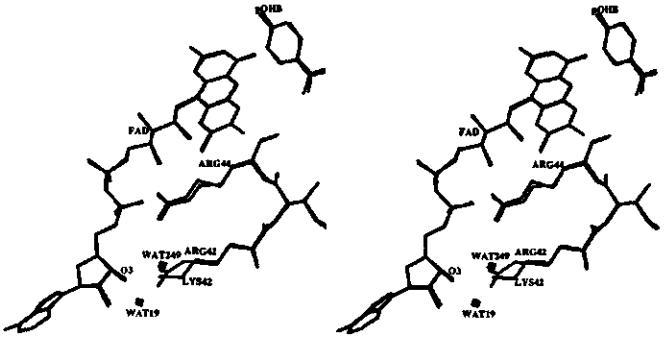

Fig. 2. Superposition of the structures of *p*-hydroxybenzoate hydroxylase and [Lys42]*p*-hydroxybenzoate hydroxylase in complexes with 4-hydroxybenzoate. The structure of *p*-hydroxybenzoate hydroxylase is drawn with solid bonds and the structure of [Lys42]*p*-hydroxybenzoate hydroxylase is shown with open bonds. The view is from the ribityl side chain towards the flavin isoalloxazine ring. The water molecules shown refer to the structure of [Lys42]*p*-hydroxybenzoate hydroxylase (Table 1).

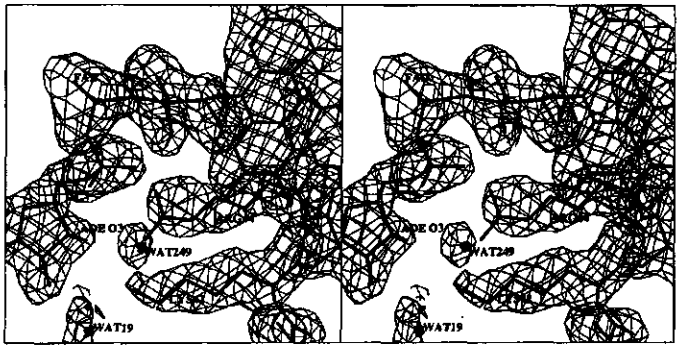

Fig. 3. Stereo diagram of the *Fo-Fc* omit map of [Lys42]*p*-hydroxybenzoate hydroxylase, contoured at 4σ. The amino acid residues are drawn in continuous bold lines, while the FAD is indicated in continuous gray lines. The orientation of the 3-OH group of the adeninosine ribose moiety of FAD (ADE O3) is indicated.

tein model was inspected and corrected where neccessary. Refinement was carried out by energy minimization and temperature-factor refinement using the program Xplor [31]. For FAD we used the parameters as described by Schreuder et al. [29]. Water molecules were assigned by searching *Fo-Fc* maps for peaks of at least 4σ, which were between 0.20 nm and 0.50 nm of other protein or water atoms. Water molecules with temperature factors after refinement in excess of 0.7 nm^2 were rejected. The final structure was obtained after four cycles of map inspection and refinement and contains 289 water molecules. The final *R*-factor was 0.175 for 22 634 reflections between 0.80 nm and 0.22 nm. The coordinates of the refined structure of the enzyme · substrate complex of [Lys42]*p*-hydroxybenzoate hydroxylase will be deposited in the Brookhaven Protein Data Bank.

RESULTS

Expression. Replacement of Arg42 by Lys or Ser in *p*-hydroxybenzoate hydroxylase from *P. fluorescens* did not significantly change the level of protein expression. With both recombinant enzymes, expression yields up to 10% of total *E. coli* protein were observed. Unlike wild-type enzyme, the Arg42 mutants displayed a rather weak interaction with Cibacron-blue agarose. In spite of this, their yields after purification were comparable to that of native *p*-hydroxybenzoate hydroxylase [17]. Moreover, the purified Arg42 mutants were bright yellow, indicative of tight binding of FAD.

Structural properties. The structure of [Lys42]*p*-hydroxybenzoate hydroxylase was very similar to the structure of native *p*-hydroxybenzoate hydroxylase [7]. The rmsd was 0.02 nm for 391 equivalent Cα atoms. The side chain of Lys42 had the same orientation as the side chain of Arg42 in the native structure (Fig. 2). A water molecule (Wat249 in the model) occupied the position of the guanidinium group of the larger arginine side chain and bridged the 3-OH of the FAD ribose and the NZ of Lys42 (Table 1). The only significant difference in the neighborhood of the modified residue was a small rotation of the Tyr38

Table 1. Selected polar interactions (d <0.32 nm) involving Lys42 in [Lys42]*p*-hydroxybenzoate hydroxylase and Arg42 in *p*-hydroxybenzoate hydroxylase. Data for *p*-hydroxybenzoate hydroxylase are taken from Schreuder et al. [7].

Enzyme	Atom 1	Atom 2	Distance
			nm
[Lys42]*p*-hydroxybenzoate hydroxylase	Lys $N\zeta$	Wat19 O	0.27
		Wat249 O	0.27
	Wat 249 O	O3 ribose	0.29
p-Hydroxybenzoate hydroxylase	Arg Nε	Wat167 O	0.28
	Arg NH1	O3 ribose	0.26
		C3 ribose	0.30
		Wat615 O	0.27

Table 2. Dissociation constants of enzyme · substrate complexes of *p*-hydroxybenzoate hydroxylase and *p*-hydroxybenzoate hydroxylase variants. Dissociation constants were determined at 25°C in 50 mM potassium phosphate pH 7.0, or 100 mM Tris/sulfate pH 8.0, by fluorimetric titration experiments. PHBH, *p*-hydroxybenzoate hydroxylase.

Substrate	pH	Dissociation constant of		
		PHBH	[Lys42]PHBH	[Ser42]PHBH
		μM		
4-Hydroxybenzoate	7.0	30 ± 5	120 ± 15	100 ± 10
	8.0	40 ± 5	120 ± 15	100 ± 10
2,4-Dihydroxybenzoate	7.0	90 ± 10	270 ± 20	250 ± 20
	8.0	90 ± 10	275 ± 25	250 ± 25

side chain, which faced the solvent. The active sites of *p*-hydroxybenzoate hydroxylase and [Lys42]*p*-hydroxybenzoate hydroxylase were identical within experimental error. However, the electron density of the guanidinium part of the Arg44 side chain was very weak in [Lys42]*p*-hydroxybenzoate hydroxylase (Fig. 3), while this side chain had strong electron density in *p*-hydroxybenzoate hydroxylase. Accordingly, the temperature factors of the Arg44 NH1 and NH2 were around 0.7 nm² for [Lys42]*p*-hydroxybenzoate hydroxylase, and around 0.43 nm² for *p*-hydroxybenzoate hydroxylase, suggesting that the Arg44 side chain has became more mobile in the Lys42 variant. Attempts to obtain high-quality crystals of [Ser42]*p*-hydroxybenzoate hydroxylase failed. The protein-flavin interaction in this mutant was therefore assessed by spectral analysis.

Spectral properties. X-ray diffraction studies have revealed that the isoalloxazine ring of the FAD in *p*-hydroxybenzoate hydroxylase can attain different conformations inside and outside the active site [29, 32, 33]. Substrate-binding studies suggest that the flavin conformation observed in the crystal structure correlates with the flavin spectral properties in solution [32]. This concept was used to study the mode of flavin binding in the Arg42 mutants in further detail. Fig. 4 shows that the shape of the difference spectrum between free and 4-hydroxybenzoate complexed [Lys42]*p*-hydroxybenzoate hydroxylase (Fig. 4A), resembled that of *p*-hydroxybenzoate hydroxylase (Fig. 4C), suggesting an 'in' position for the flavin ring, in full agreement with the crystal structure. Titration of [Lys42]*p*-hydroxybenzoate hydroxylase and [Ser42]*p*-hydroxybenzoate hydroxylase with 2,4-dihydroxybenzoate, resulted, similarly to titration of

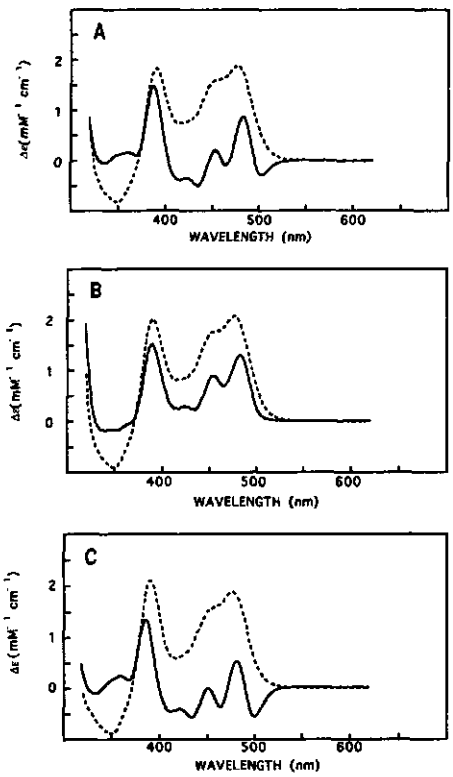

Fig. 4. Flavin absorption difference spectra observed upon binding of 4-hydroxybenzoate or 2,4-dihydroxybenzoate to *p*-hydroxybenzoate hydroxylase variants. Absorption spectra were recorded at 25°C in 50 mM sodium phosphate pH 7.0. The enzyme concentration was 30 μM. The difference spectra are extrapolated to infinite substrate concentration. ——, 4-hydroxybenzoate; – – –, 2,4-dihydroxybenzoate. (A) [Lys42]*p*-hydroxybenzoate hydroxylase; (B) [Ser42]*p*-hydroxybenzoate hydroxylase; (C) *p*-hydroxybenzoate hydroxylase.

native *p*-hydroxybenzoate hydroxylase, in difference spectra indicative for the flavin 'out' conformation [32]. Binding of 4-hydroxybenzoate to [Ser42]*p*-hydroxybenzoate hydroxylase (Fig. 4B) induced spectral changes, which deviate from those of *p*-hydroxybenzoate hydroxylase and which are intermediate between the changes observed for the flavin 'in' and 'out' spectra.

The Arg42 mutants have a somewhat lower affinity for 4-hydroxybenzoate and 2,4-dihydroxybenzoate than *p*-hydroxybenzoate hydroxylase, which was studied in more detail by fluorimetric titration experiments. For both Arg42 variants, the flavin fluorescence quantum yield was about 40% compared with that of *p*-hydroxybenzoate hydroxylase [27]. In contrast to *p*-hydroxybenzoate hydroxylase, the flavin fluorescences of [Lys42]*p*-hydroxybenzoate hydroxylase and [Ser42]*p*-hydroxybenzoate hydroxylase were not strongly quenched upon binding

Table 3. Kinetic parameters of *p*-hydroxybenzoate hydroxylase and *p*-hydroxybenzoate hydroxylase variants. Steady-state kinetic parameters were determined at 25°C in air-saturated 100 mM Tris/sulfate pH 8.0. For experimental details of the reductive half-reaction see Fig. 5. Data for *p*-hydroxybenzoate hydroxylase are from [17]. The designation greater than (>) refers to minimum values and the fact that accurate values could not be estimated because of very weak NADPH binding.

Enzyme	K_m for		k_{cat}	K_d for NADPH	k_{red}
	4-hydroxybenzoate	NADPH			
	μM		s^{-1}	μM	s^{-1}
p-Hydroxybenzoate hydroxylase	25	50	55	150	300
(Lys42]*p*-hydroxybenzoate hydroxylase	110	>500	>6	>2000	>6
[Ser42]*p*-hydroxybenzoate hydroxylase	75	>500	>0.2	>2000	>0.2

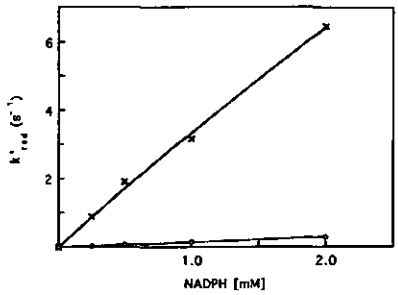

***Fig. 5.* NADPH dependence of the rate of reduction of the enzyme · substrate complexes of [Lys42]*p*-hydroxybenzoate hydroxylase and [Ser42]*p*-hydroxybenzoate hydroxylase.** The experiments were performed at 25°C in 100 mM Tris/sulfate pH 8.0. 20 μM enzyme was mixed anaerobically with an equal volume of NADPH in the stopped-flow spectrophotometer. Both solutions contained 1 mM 4-hydroxybenzoate. The rate of flavin reduction, as determined from the decrease of absorbance at 450 nm, is plotted as a function of the concentration of NADPH. ×, [Lys42]*p*-hydroxybenzoate hydroxylase; ○, [Ser42]*p*-hydroxybenzoate hydroxylase.

of 4-hydroxybenzoate. With [Lys42]*p*-hydroxybenzoate hydroxylase, the enzyme · substrate complex exhibited a fluorescence quantum yield of more than 80% of that of the free enzyme, while with [Ser42]*p*-hydroxybenzoate hydroxylase, substrate binding even resulted in a slight increase of flavin fluorescence. In both cases, substrate binding was described by simple binary · complex formation with dissociation constants in the range 100−120 μM. These values were about threefold higher than those observed with *p*-hydroxybenzoate hydroxylase (Table 2) and were in agreement with the dissociation constants derived from the absorption difference spectra. Binding of 2,4-dihydroxybenzoate to the Arg42 mutants resulted in a 50% decrease in fluorescence of protein-bound FAD with dissociation constants in the range 240−280 μM, threefold higher than with *p*-hydroxybenzoate hydroxylase (Table 2). These results confirm that the Arg42 replacements have a small but consistent effect on the binding of aromatic substrates.

Catalytic properties. Very low activities were observed when the catalytic performance of the Arg42 mutants was tested at pH 8.0 (standard assay) and at pH 7.0. This was due to a large extent to weak binding of NADPH, limiting the accurate estimation of steady-state kinetic parameters (Table 3). To confirm that the low activity was not due to FAD dissociation, we measured the turnover rate of the Arg42 mutants in the absence and presence of varying amounts of free FAD. These experiments revealed that the apparent K_m for FAD of [Lys42]*p*-hydroxybenzoate hydroxylase and [Ser42]*p*-hydroxybenzoate hydroxylase ranged from 100 nM to 200 nM, which is slightly higher than the corresponding value of 45 nM reported for *p*-hydroxybenzoate hydroxylase [25]. This, together with the structural and spectral data presented above, shows that replacement of Arg42 by Lys or Ser does not significantly disturb FAD binding.

The interaction of the Arg42 mutants with NADPH was studied by anaerobic-reduction experiments using the stopped-flow spectrophotometer. Following the disappearance of flavin absorption at 450 nm, the reaction of the uncomplexed Arg42 mutants with NADPH was as slow as with *p*-hydroxybenzoate hydroxylase (k'_{red} = 0.002 s^{-1} at 1 mM NADPH) [14]. However, reduction of the enzyme · substrate complex was much slower for the Arg42 mutants than for native *p*-hydroxybenzoate hydroxylase, taking seconds or longer (Table 3). There was an almost linear relationship between the rate of enzyme reduction and NADPH concentration (Fig. 5), suggesting impaired coenzyme binding. In agreement with this, no long-wavelength-absorbance increase, indicative of a charge-transfer complex between reduced flavin and $NADP^+$ [14, 34], was detectable. However, the effector role of the substrate was not completely lost in the Arg42 mutants. For example, at 1 mM NADPH, substrate binding stimulated the rate of flavin reduction of [Lys42]*p*-hydroxybenzoate hydroxylase by about three orders of magnitude (Table 3), which is nevertheless 100-fold less than for *p*-hydroxybenzoate hydroxylase [17] and which is rate limiting in catalysis (Table 3).

With both Arg42 mutants, HPLC analysis revealed the formation of 3,4-dihydroxybenzoate as the sole aromatic product from 4-hydroxybenzoate. The formation of 3,4-dihydroxybenzoate was stoichiometric with the consumption of 4-hydroxybenzoate and NADPH, indicative of efficient hydroxylation. Oxygen-consumption experiments performed in the absence or presence of catalase confirmed that the reduction of the Arg42 mutants by NADPH is tightly coupled to substrate hydroxylation and that no hydrogen peroxide is formed.

Stopped-flow experiments in which substrate-complexed reduced Arg42 mutants were mixed with oxygen (Fig. 6) revealed some small variations at 405 nm between [Ser42]*p*-hydroxybenzoate hydroxylase and *p*-hydroxybenzoate hydroxylase, probably due to different intrinsic absorption at that wavelength. The rapid increase of absorption at 405 nm, indicative of the formation of the flavin C(4a)-hydroperoxide, was followed by a small absorption decrease (Fig. 6), indicative for substrate hydroxylation involving the transient formation of the flavin C(4a)-hydroxide pseudobase [5]. In the final step, the latter flavin species rapidly decomposed to the oxidized enzyme as evidenced by the increase of absorption at 490 nm (Fig. 6B). For both Arg42 mutants, the individual rate constants obtained after treating the data according to a three-step reaction were in the same range as with *p*-hydroxybenzoate hydroxylase [5]. This confirms that the Arg42 replacements do not significantly affect the stabilization and reactivity of oxygenated flavin intermediates.

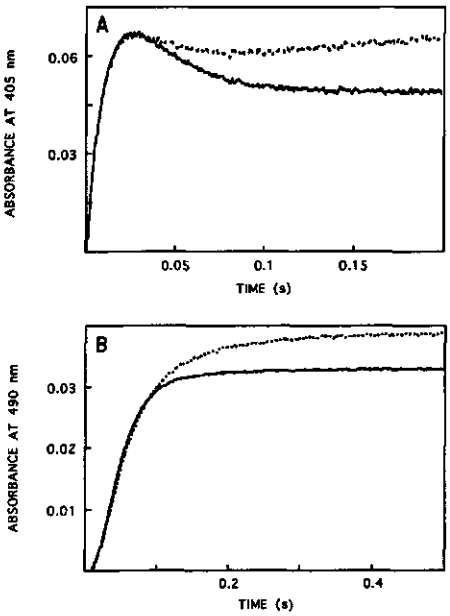

Fig. 6. Time-course of the reaction of the reduced enzyme · substrate complexes of *p*-hydroxybenzoate hydroxylase and [Ser42]*p*-hydroxybenzoate hydroxylase with oxygen. The experiments were performed at 6 °C in 50 mM potassium phosphate pH 6.6. Dithionite-reduced enzyme (15 μM) was mixed anaerobically with an equal volume of 2 mM of oxygen in the stopped-flow spectrophotometer. Both syringes contained 1 mM 4-hydroxybenzoate. The time-course of absorption was followed at 405 nm (A) and 490 nm (B). *p*-Hydroxybenzoate hydroxylase, continuous line; [Ser42]*p*-hydroxybenzoate hydroxylase, broken line.

DISCUSSION

Our studies established that Arg42 of *p*-hydroxybenzoate hydroxylase from *P. fluorescens* is essential for NADPH binding and not for FAD binding. The hydrogen bond between the NH2 of Arg42 and the 3-OH of the adenosine-ribose of the FAD does not contribute much to binding of FAD. Our conclusions disagree with those of Dimarco et al. [15], who attributed the lack of activity in cell extracts of *A. calcoaceticus* with [Ser42]*p*-hydroxybenzoate hydroxylase to impaired FAD binding of the mutant enzyme. However, this conclusion was inferred from the crystal structure of *P. fluorescens p*-hydroxybenzoate hydroxylase and no experimental data were presented to support this claim. Our experimental data and the very high sequence identity between *P. fluorescens p*-hydroxybenzoate hydroxylase and *A. calcoaceticus p*-hydroxybenzoate hydroxylase suggest that the lack of enzymatic activity in [Ser42]*p*-hydroxybenzoate hydroxylase *A. calcoaceticus* extract was either due to the extremely slow reduction rate of [Ser42]*p*-hydroxybenzoate hydroxylase by NADPH, or due to a very low expression level for the mutant protein.

Comparison of the 0.22-nm crystal structure of [Lys42]*p*-hydroxybenzoate hydroxylase with the structure of native *p*-hydroxybenzoate hydroxylase shows that both structures are virtually identical except for local changes around the site of mutation. In the Lys42 variant, the lost interaction between the guanidinium group of Arg42 and the adenosine ribose moiety of FAD is compensated by a water molecule (Wat249), which connects the NZ of Lys42 with the 3-OH of the ribose group. This bridging water molecule may explain the relatively tight binding of FAD in the Lys42 variant. The position of the substrate and interacting residues is virtually identical in both crystal structures. The decreased affinity for 4-hydroxybenzoate and 2,4-dihydroxybenzoate must therefore be due to some subtle effects beyond the experimental error of about 0.2 Å in protein crystal structures. This is possible given that a fourfold difference in affinity corresponds to a difference in binding energy of only 3.3 kJ/mol.

In spite of the decreased affinity for the aromatic substrate, the Lys42 replacement did not diminish the stabilization and hydroxylation power of the flavin (C4a)-hydroperoxide. This agrees well with the inner orientation of the flavin isoalloxazine ring in the crystal structure and with the finding that the Lys42 replacement does not disturb any of active-site residues, which leaves the hydrogen-bond network between the phenolic moiety of the substrate and the side chains of Tyr201 and Tyr385 fully intact.

The spectral properties of [Lys42]*p*-hydroxybenzoate hydroxylase are consistent with the closed conformation of the flavin in the crystal structure. The small spectral differences with respect to *p*-hydroxybenzoate hydroxylase might be explained by the significantly higher mobility of the Arg44 side chain, which normally shields the flavin ring from the solvent. Increased exposure of the flavin ring towards the solvent will cause similar spectral changes as a movement of the flavin to the 'out' position, since this leads also to an increased solvent exposure. Since the flavin conformation in the Arg42 variant does not differ significantly from that in native *p*-hydroxybenzoate hydroxylase, we cannot explain the lack of NADPH binding or flavin reduction by a shift of the flavin conformation from 'in' to 'out'.

Although no structural data for [Ser42]*p*-hydroxybenzoate hydroxylase are available it seems that in this mutant protein the interaction between the side chain of residue 42 and the adenosine-ribose moiety of FAD will be weakened with respect to the Lys42 variant. Our data show that despite this weakened interaction, FAD binding is normal. The spectral perturbations upon titration with 4-hydroxybenzoate are shifted toward the spectral changes associated with the 'out' conformation, suggesting that in [Ser42]*p*-hydroxybenzoate hydroxylase the equilibrium of flavin conformers is shifted toward the open form. However, in the absence of structural data we cannot exclude the possibility that the spectral changes are due to increased solvent exposure due to an even greater mobility of the Arg44 side chain in [Lys42]*p*-hydroxybenzoate hydroxylase.

[Lys42]*p*-hydroxybenzoate hydroxylase and [Ser42]*p*-hydroxybenzoate hydroxylase fully couple flavin reduction to substrate hydroxylation, which means that the flavin (C4a)-hydroperoxide must have the 'in' conformation [35]. In this respect, the Arg42 mutants differ from [Lys220]*p*-hydroxybenzoate hydroxylase, in which increased mobility of the flavin ring prevents product formation [36]. These observations suggest that for [Ser42]*p*-hydroxybenzoate hydroxylase the shift in flavin equilibrium, if present, must be limited to the oxidized state. This means that the electrostatic stabilization of the anionic reduced flavin in the inner position is not disturbed by the removal of the positive charge at position 42. This is not too surprising given that Arg42 is not located in the active-site region.

p-Hydroxybenzoate hydroxylase lacks a recognizable domain for binding NADPH [6, 9]. Sequence alignments suggest

that this may be a common property of the flavoprotein aromatic hydroxylases [37]. Here we show that in *P. fluorescens* *p*-hydroxybenzoate hydroxylase substitution of Arg42 with lysine or serine results in impaired NADPH binding, preventing efficient reduction of protein-bound FAD. Arg42 must therefore be important for NADPH recognition. Information about the specific function of Arg42 comes from recent studies on *p*-hydroxybenzoate hydroxylase from *Pseudomonas* CBS3 [38]. This enzyme, involved in the biodegradation of 4-chlorobenzoate, prefers NADH over NADPH. In the *Pseudomonas* CBS3 sequence, Arg42 is replaced by a threonine residue. Moreover, sequence comparison and homology-modeling studies suggest that the short helix preceding residue 42 (helix H2 in the *P. fluorescens* enzyme) [7] is involved in coenzyme specificity by binding the 2′-phosphoadenosine moiety of NADPH [38]. The poor NADPH binding in the Arg42 mutants of *p*-hydroxybenzoate hydroxylase from *P. fluorescens* supports this view and strengthens the idea that the NADPH molecule binds in a cleft leading towards the active-site between the FAD-binding domain and the substrate-binding domain [6]. The current results are in full agreement with other mutagenesis [14, 16] and modeling studies [16], which suggested that in addition to Arg42, the following residues in the active-site cleft are important for NADPH binding: Arg44 for binding the adenosine-ribose; and His162 and Arg269 for binding the pyrophosphate. However, additional protein-engineering studies and X-ray–crystallography studies are needed to unravel the molecular details of NADPH recognition by this class of flavoenzymes.

The authors wish to thank Ms Yvonne Dortmans for technical assistance.

REFERENCES

1. van Berkel, W. J. H. & Müller, F. (1991) Flavin-dependent monooxygenases with special reference to *p*-hydroxybenzoate hydroxylase, in *Chemistry and biochemistry of flavoenzymes* (Müller, F., ed.) vol. 2, pp. 1–29, CRC Press, Boca Raton.
2. van Berkel, W. J. H., Eppink, M. H. M., Middelhoven, W. J., Vervoort, J. & Rietjens, I. M. C. M. (1994) Catabolism of 4-hydroxybenzoate in *Candida parapsilosis* proceeds through initial oxidative decarboxylation by a FAD-dependent 4-hydroxybenzoate 1-hydroxylase, *FEMS Microbiol. Lett. 121*, 207–216.
3. Entsch, B., Ballou, D. P. & Massey, V. (1976) Flavin-oxygen derivatives involved in the hydroxylation by *p*-hydroxybenzoate hydroxylase, *J. Biol. Chem. 251*, 2550–2563.
4. Husain, M. & Massey, V. (1979) Kinetic studies on the reaction mechanism of *p*-hydroxybenzoate hydroxylase. Agreement of steady state and rapid reaction data, *J. Biol. Chem. 254*, 6657–6666.
5. Entsch, B. & Ballou, D. P. (1989) Purification, properties and oxygen reactivity of *p*-hydroxybenzoate hydroxylase from *Pseudomonas aeruginosa*, *Biochim. Biophys. Acta 999*, 313–322.
6. Wierenga, R. K., Drenth, J. & Schulz, G. E. (1983) Comparison of the three-dimensional protein and nucleotide structure of the FAD-binding domain of *p*-hydroxybenzoate hydroxylase with the FAD- as well as NADPH-binding domains of glutathione reductase, *J. Mol. Biol. 167*, 725–739.
7. Schreuder, H. A., Prick, P. A. J., Wierenga, R. K., Vriend, G., Wilson, K. S., Hol, W. G. J. & Drenth, J. (1989) Crystal structure of the *p*-hydroxybenzoate hydroxylase-substrate complex refined at 1.9 Å resolution, *J. Mol. Biol. 208*, 679–696.
8. Schreuder, H. A., van der Laan, J. M., Hol, W. G. J. & Drenth, J. (1991) The structure of *p*-hydroxybenzoate hydroxylase, in *Chemistry and biochemistry of flavoenzymes* (Müller, F., ed.) vol. 2, pp. 31–64, CRC Press, Boca Raton.
9. Entsch, B. & van Berkel, W. J. H. (1995) Structure and mechanism of *para*-hydroxybenzoate hydroxylase, *FASEB J. 9*, 476–483.
10. Palfey, B. A., Ballou, D. P. & Massey, V. (1997) Flavin conformational changes in the catalytic cycle of *p*-hydroxybenzoate hydroxylase substituted with 6-azido and 6-aminoflavin adenine dinucleotide, *Biochemistry 36*, 15713–15723.
11. van der Laan, J. M., Schreuder, H. A., Swarte, M. B. A., Wierenga, R. K., Kalk, K. H., Hol, W. G. J. & Drenth, J. (1989) The coenzyme analogue adenosine 5-diphosphoribose displaces FAD in the active-site of *p*-hydroxybenzoate hydroxylase. An X-ray crystallographic investigation, *Biochemistry 28*, 7199–7205.
12. Lesk, A. M. (1995) NAD-binding domains of dehydrogenases, *Curr. Opin. Struct. Biol. 5*, 775–783.
13. Wijnands, R. A., Müller, F. & Visser, A. J. W. G. (1987) Chemical modification of arginine residues in *p*-hydroxybenzoate hydroxylase from *Pseudomonas fluorescens*: a kinetic and fluorescense study, *Eur. J. Biochem. 163*, 535–544.
14. Eppink, M. H. M., Schreuder, H. A. & van Berkel, W. J. H. (1995) Structure and function of mutant Arg44Lys of 4-hydroxybenzoate hydroxylase: implications for NADPH binding, *Eur. J. Biochem. 231*, 157–165.
15. Dimarco, A. A., Averhoff, B. A., Kim, E. E. & Ornston, L. N. (1993) Evolutionary divergence of *pobA*, the structural gene encoding *p*-hydroxybenzoate hydroxylase in an *Acinetobacter calcoaceticus* strain well-suited for genetic analysis, *Gene (Amst.) 125*, 25–33.
16. van Berkel, W. J. H., Eppink, M. H. M., van der Bolt, F. J. T., Vervoort, J., Rietjens, I. M. C. M. & Schreuder, H. A. (1997) *p*-Hydroxybenzoate hydroxylase: mutants and mechanism, in *Flavins and flavoproteins* XII (Stevenson, K., Massey, V. & Williams, Ch., eds) pp. 305–314, University Press, Calgary.
17. van Berkel, W. J. H., Westphal, A. H., Eschrich, K., Eppink, M. H. M. & de Kok, A. (1992) Substitution of Arg214 at the substrate-binding site of *p*-hydroxybenzoate hydroxylase from *Pseudomonas fluorescens*, *Eur. J. Biochem. 210*, 411–419.
18. Kunkel, T. A., Roberts, J. D. & Zakour, R. A. (1987) Rapid and efficient site-specific mutagenesis without phenotypic selection, *Methods Enzymol. 154*, 367–382.
19. Eschrich, K., van Berkel, W. J. H., Westphal, A. H., de Kok, A., Mattevi, A., Obmolova, G., Kalk, K. H. & Hol, W. G. J. (1990) Engineering of microheterogeneity-resistant *p*-hydroxybenzoate hydroxylase from *Pseudomonas fluorescens*, *FEBS Lett. 277*, 197–199.
20. Sanger, F., Nicklen, S. & Coulson, A. R. (1977) DNA sequencing with chain-terminating inhibitors, *Proc. Natl Acad. Sci. USA 74*, 5463–5467.
21. Westphal, A. H. & de Kok, A. (1988) Lipoamide dehydrogenase from *Azotobacter vinelandii*, molecular cloning, organization and sequence analysis of the gene, *Eur. J. Biochem. 172*, 299–305.
22. Entsch, B. (1990) Hydroxybenzoate hydroxylase, *Methods Enzymol. 188*, 138–147.
23. van Berkel, W. J. H. & Müller, F. (1987) The elucidation of the microheterogeneity of highly purified *p*-hydroxybenzoate hydroxylase from *Pseudomonas fluorescens* by various biochemical techniques, *Eur. J. Biochem. 167*, 35–46.
24. Entsch, B., Palfey, B. A., Ballou, D. P. & Massey, V. (1991) Catalytic function of tyrosine residues in *para*-hydroxybenzoate hydroxylase as determined by the study of site-directed mutants, *J. Biol. Chem. 266*, 17341–17349.
25. Müller, F. & van Berkel, W. J. H. (1982) A study on *p*-hydroxybenzoate hydroxylase from *Pseudomonas fluorescens*. A convenient method of preparation and some properties of the apoenzyme, *Eur. J. Biochem. 128*, 21–27.
26. Eschrich, K., van der Bolt, F. J. T., de Kok, A. & van Berkel, W. J. H. (1993) Role of Tyr201 and Tyr385 in substrate activation by *p*-hydroxybenzoate hydroxylase from *Pseudomonas fluorescens*, *Eur. J. Biochem. 216*, 137–146.
27. van Berkel, W. J. H. & Müller, F. (1989) The temperature and pH dependence of some properties of *p*-hydroxybenzoate hydroxylase from *Pseudomonas fluorescens*, *Eur. J. Biochem. 179*, 307–314.
28. Kabsch, W. (1988) Evaluation of single-crystal diffraction data from a position-sensitive detector, *J. Appl. Crystallogr. 21*, 916–924.
29. Schreuder, H. A., Mattevi, A., Obmolova, G., Kalk, K. H., Hol, W. G. J., van der Bolt, F. J. T. & van Berkel, W. J. H. (1994) Crystal structures of wild-type *p*-hydroxybenzoate hydroxylase complexed with 4-aminobenzoate, 2,4-dihydroxybenzoate and 2-hydroxy-4-aminobenzoate and the Tyr222Ala mutant, complexed

with 2-hydroxy-4-aminobenzoate. Evidence for a proton channel and a new binding mode of the flavin ring, *Biochemistry 33*, 10161–10170.
30. Jones, T. A., Zou, J.-Y., Cowan, S. & Kjeldgaard, M. (1991) Improved methods for the building of protein models in electron density maps and the location of errors in these models, *Acta Cryst. A47*, 110–119.
31. Brünger, A. T. (1992) *X-plor version 3.1. A system for the X-ray crystallography and NMR*, Yale University press, New Haven.
32. Gatti, D. L., Palfey, B. A., Lah, M. S., Entsch, B., Massey, V., Ballou, D. P. & Ludwig, M. L. (1994) The mobile flavin of 4-OH benzoate hydroxylase, *Science 266*, 110–114.
33. van Berkel, W. J. H., Eppink, M. H. M. & Schreuder, H. A. (1994) Crystal structure of *p*-hydroxybenzoate hydroxylase reconstituted with the modified FAD present in alcohol oxidase from methylotrophic yeasts: evidence for an arabinoflavin, *Protein Sci. 3*, 2245–2253.
34. Howell, L. G., Spector, T. & Massey, V. (1972) Purification and properties of *p*-hydroxybenzoate hydroxylase from *Pseudomonas fluorescens*, *J. Biol. Chem. 247*, 4340–4350.
35. Schreuder, H. A., van der Laan, J. M., Swarte, M. B. A., Kalk, K. H., Hol, W. G. J. & Drenth, J. (1992) Crystal structure of the reduced form of *p*-hydroxybenzoate hydroxylase refined at 2.3 Å resolution, *Proteins Struct. Funct. Genet. 14*, 178–190.
36. Moran, G. R., Entsch, B., Palfey, B. A. & Ballou, D. P. (1996) Evidence for flavin movement in the function of *p*-hydroxybenzoate hydroxylase from studies of the mutant Arg220Lys, *Biochemistry 35*, 9278–9285.
37. Eppink, M. H. M., Schreuder, H. A. & van Berkel, W. J. H. (1997) Identification of a novel conserved sequence motif in flavoprotein hydroxylases with a putative dual role in FAD/NAD(P)H binding, *Protein Sci. 6*, 2454–2458.
38. Seibold, B., Matthes, M., Eppink, M. H. M., Lingens, F., van Berkel, W. J. H. & Müller, R. (1996) 4-Hydroxybenzoate hydroxylase from *Pseudomonas* sp. CBS3. Purification, characterization, gene cloning, sequence analysis and assignment of structural features determining the coenzyme specificity, *Eur. J. Biochem. 239*, 469–478.

CHAPTER 5

Identification of a novel conserved sequence motif in flavoprotein hydroxylases with a putative dual function in FAD/NAD(P)H binding

Michel H.M. Eppink, Herman A. Schreuder and Willem J.H. van Berkel

Protein Science 6: 2454-2458 (1997)

Protein Science (1997), 6:2454–2458. Cambridge University Press. Printed in the USA.

FOR THE RECORD

Identification of a novel conserved sequence motif in flavoprotein hydroxylases with a putative dual function in FAD/NAD(P)H binding

MICHEL H.M. EPPINK,[1] HERMAN A. SCHREUDER,[2] AND WILLEM J.H. VAN BERKEL[1]

[1]Department of Biochemistry, Agricultural University, Wageningen, The Netherlands
[2]Core Research Functions, Building G865A, Hoechst Marion Roussel, D-65926 Frankfurt, Germany

(RECEIVED May 19, 1997; ACCEPTED July 7, 1997)

Abstract: A novel conserved sequence motif has been located among the flavoprotein hydroxylases. Based on the crystal structure and site-directed mutagenesis studies of *p*-hydroxybenzoate hydroxylase (PHBH) from *Pseudomonas fluorescens*, this amino acid fingerprint sequence is proposed to play a dual function in both FAD and NAD(P)H binding. In PHBH, the novel sequence motif (residues 153–166) includes strand A4 and the N-terminal part of helix H7. The conserved amino acids Asp 159, Gly 160, and Arg 166 are necessary for maintaining the structure. The backbone oxygen of Cys 158 and backbone nitrogens of Gly 160 and Phe 161 interact indirectly with the pyrophosphate moiety of FAD, whereas it is known from mutagenesis studies that the side chain of the moderately conserved His 162 is involved in NADPH binding.

Keywords: fingerprint; flavoprotein family; NADPH-binding; *p*-hydroxybenzoate hydroxylase; sequence alignment

Flavoprotein hydroxylases are monooxygenases that catalyze the insertion of one atom of molecular oxygen into the substrate, using pyridine nucleotides as external electron donor (van Berkel & Müller, 1991). These enzymes play an important role in the biodegradation of lignin-derived aromatic compounds as well as environmental pollutants, and in the biosynthesis of sterols, antibiotics, and plant hormones. They lack a known fingerprint sequence for NAD(P)H binding, but possess two fingerprint motifs for the FAD binding. The first FAD motif identifies the dinucleotide binding $\beta\alpha\beta$-fold, which binds the ADP moiety of FAD (Wierenga et al., 1986), whereas the second motif represents residues that are in contact with the riboflavin moiety of FAD (Eggink et al., 1990).

PHBH (EC 1.14.13.2) is the prototype of FAD-dependent hydroxylases, and the only enzyme in this class of flavoproteins for which a three-dimensional structure is known in atomic detail (Schreuder et al., 1989). The strictly NADPH-dependent enzyme catalyzes the *ortho*-hydroxylation of 4-hydroxybenzoate into 3,4-dihydroxybenzoate via the transient stabilization of an oxygenated flavin intermediate (Entsch & van Berkel, 1995). The structure of PHBH is unusual because there is no NADPH-binding domain. So far, crystallographic analysis did not reveal a structure of the enzyme complexed with NADPH, and soaking experiments with the coenzyme analogue ADPR resulted in displacement of FAD by ADPR (van der Laan et al., 1989). Site-directed mutagenesis studies have pointed to the involvement of Arg 44 (Eppink et al., 1995) and His 162 (Eppink et al., 1997) in NADPH binding. From this and the properties of other mutants, a model for the mode of coenzyme binding was proposed (van Berkel et al., 1997).

In the past few years, the number of flavoprotein hydroxylase cloned genes has increased tremendously, and about 50 amino acid sequences are known currently. Therefore, and in view of the unknown binding mode of NADPH in this class of flavoenzymes, it was of interest to search for the presence of conserved sequence motifs. This report describes the identification of a novel sequence motif in flavoprotein hydroxylases, which appears to be important for the binding of both FAD and NAD(P)H.

Discussion: Sequence alignments have classified a number of gene products to flavoprotein hydroxylases (Kälin et al., 1992; Kukor & Olsen, 1992; Nakahigashi et al., 1992; Blanco et al., 1993; Filippini et al., 1995; Haigler et al., 1996; Marin et al., 1996; Seibold et al., 1996; Tsuji et al., 1996; Yang et al., 1996). These sequence data, together with that of PHBH from *Pseudomonas fluorescens* (van Berkel, 1992), were the starting points for a thorough screening of different databases. This search was performed with BEAUTY, which is an BLAST-enhanced alignment utility that integrates multiple biological information resources (Worley et al., 1995). From the 50 collected sequences, small groups were generated based on the different types of substrates: *p*-hydroxybenzoate (phb), 2-hydroxybiphenyl (biph), phenol (phe), salicylate (sal), *p*-aminobenzoate (pab), polyketide (poly), 4-methyl-5-nitrocatechol (cat), epoxide (epox), 2-methyl-3-hydroxypyridine-5-carboxylic acid (oxy), and a group of monooxygenases (mono) for which the function is largely unknown. A multiple sequence alignment was per-

Reprint requests to: W.J.H. van Berkel, Department of Biochemistry, Wageningen Agricultural University, Dreijenlaan 3, 6703 HA Wageningen, The Netherlands; e-mail: willem.vanberkel@fad.bc.wau.nl.

Table 1. *Multiple alignment of the three consensus sequences in the flavoprotein hydroxylases*[a]

Enzyme (strain)	FAD fingerprint (1)	Conserved motif	FAD fingerprint (2)	Reference
1 phh (*Pseudomonas fluorescens*)	5-VAIIGAGPSGLLLG-18	153-DYIAGCDGFHGISR-166	279-GRLFLAGDAAHIVPPTGAKGLNLAASDVSTL-309	(Weijer et al., 1982)
2 phh (*Pseudomonas aeruginosa*)	5-VAIIGAGPSGLLLG-18	153-DYIAGCDGFHGISR-166	279-GRLFLAGDAAHIVPPTGAKGLNLAASDVSTL-309	(Entsch et al., 1988)
3 phh (*Pseudomonas fluorescens*)	8-VAIIGAGPSGLLLG-21	156-DYIAGCDGFHGVAR-169	282-GRLFLLGDAAHIVPPTGAKGLNLAASDVSTL-312	(Shuman & Dix, 1993)
4 phh (*Rhizobium legominosarum* B155)	5-VAIIGSGPSGLLLG-18	153-DFIAGCDGFHGASR-166	279-GRLFLVGDAAHIVPPTGAKGLNLAASDVHYL-309	(Wong et al., 1994)
5 phh (*Rhizobium legominosarum* MNF300)	5-VAIIGSGPSGLLFG-18	153-DFIAGCDGFHGVSR-166	279-GRLFLVGDAAHIVPPTGAKGLNLAASDVHYL-309	(Wong et al., 1994)
6 phh (*Acinetobacter calcoaceticus*)	5-VAIIGSGPAGLLLG-18	152-DFIAGCDGYHGVCR-165	278-GKLFLAGDAAHIVPPTGAKGLNLAASDIAYL-308	(DiMarco et al., 1993)
7 phh (*Pseudomonas species* CBS3)	9-VGIIGAGPAGLLLS-22	156-DYVVGCDGFHGPSR-169	282-GRLLLAGDAAHIVPPTGAKGLNLAVNDVRLL-312	(Seibold et al., 1996)
8 biph (*Pseudomonas azelaica* HBP1)	9-VLIVGAGPAGAMSA-22	172-KYIIGADGAHSLVA-185	306-GRVFCMGDAVHRHTPMGGLGLNTSVQDAYNL-336	(Schmid & van der Meer, 1997)
9 phe (*Flavobacterium* species)	17-VLIVGGGPTGLIAA-30	167-RWVIGADGVRSRVR-180	291-GNVFLAGDAAHCHSPSGGSGMNVGMQDAFNL-321	(Orser et al., 1993)
10 phe (*Sphingomonas chlorophenolica*)	17-VLIVGGGPTGLIAA-30	167-RWVIGADGVRSRVR-180	291-GNVFLAGDAAHCHSPSGGSGMNVGMQDAFNL-321	(Ederer et al., 1996)
11 phe (*Alcaligenes eutrophus*)	9-VLVVGTGPAGASAG-22	172-KYLIGADGANSRVV-185	304-GRVFCAGDAVHRHPPTNGLGSNTSIQDSFNL-334	(Perkins et al., 1990)
12 phe (*Ralstonia eutropha*)	12-VLVVGTGPAGAAST-25	175-KYLIGADGANSRIV-188	307-KRVFCMGDAVHRHPPTNGLGSNTSIQDAFNL-337	(van der Meer, 1997)
13 phe (*Pseudomonas putida* pEST4011)	12-VLVVGSGPAGAAST-25	175-KYLIGADGANSQVV-188	307-NRVFCMGDAVHRHPPTNGLGSNTSIQDAFNL-337	(Köiv et al., 1996)
14 phe (*Pseudomonas* species EST1001)	37-VLIVGSGPAGSSAA-50	200-KYLIGADGARSKVA-213	321-GRVCCAGDAIHKHPPSHGLGSNTSIQDSYNL-351	(Nurk et al., 1991)
15 phe (*Trichosporon cutaneum*)	10-VLIVGAGPAGLMAA-23	219-KYVIGCDGGHSWVR-232	350-ERVFIAGDACHTHSPKAGQGMNTSMMDTYNL-380	(Kälin et al., 1992)
16 poly (*Streptomyces coelicolor*)	23-VLVVGGSLVGLSTS-36	184-DYLVAADGPRSPVR-197		(Blanco et al., 1993)
17 poly (*Streptomyces halstedii*)	17-VLVVGGSLVGLSTS-30	171-DYLVAADGPRSPVR-184	306-GRVFLAGDSAHEMSPTGAFGSNTGIQDAHNL-336	(Blanco et al., 1993)
18 poly (*Streptomyces peucetius*)	10-VLVVGGGLGGLSTA-23	173-RYLVAADGPRSAIR-186	301-GPVLLVGDAAKVTPPTGGMGGNTAIGDGFDV-331	(Filippini et al., 1995)
19 poly (*Streptomyces peucetius caesius*)	10-VLVVGGGLGGLSTA-23	173-RYLVAADGPRSAIR-186	301-GPVLLVGDAAKVTPPTGGMGGNTAIGDGFDV-331	(Hong et al., 1994)
20 poly (*Streptomyces purpurascens*)	8-VLVVGAGLGGLSTA-21	173-GYLVGADGNRSLVR-186	301-GRVFLAGDAAKVTPPTGGMSGNAAVADGFDL-331	(Niemi & Mäntsälä, 1995)
21 poly (*Streptomyces glaucescens*)	19-VLIVGGGLTGLSAA-32	191-RYLIAADGVRSPVR-204	328-GRVFLAGDAAHVHPPAGAFGANGGIQDAHNL-358	(Decker et al., 1993)
22 poly (*Streptomyces fradiae*)	5-VIVAGAGPTGLMLA-18	147-PYLVGCDGGRSTVR-160	270-GRVLLAGDAAHIHLPAGGQGMNTGIQDAVNL-301	(Decker & Haag, 1995)
23 poly (*Streptomyces venezuelae*)	28-VVVIGAGPTGLMLA-41	170-RYAVGCDGERTTVR-183	290-GRVLWAGDAAHQQMPIGGQALNLGLQDAVNL-320	(Yang et al., 1996)
24 poly (*Streptomyces aureofaciens*)	1-MVVAGAGPTGLMLA-14	137-RYLVGCDGG-STVR-149	246-GRVLLAGDAAHIHLPAGGQGLNLGFQDAVNL-276	(Dairi et al., 1995)
25 cat (*Burkholderia species* DNT)	14-VLIVGGSMVGLSTA-27	180-RYLVASDGWRSQRR-193	306-GRIFLRGDAAHVVPPYGGFGGNTGVQDAHNL-336	(Haigler et al., 1996)
26 oxy (*Pseudomonas* MA-1)	14-AEVAGGGFAFLTAA-27	150-DLIVGADGVGSKVR-163	281-GKVALVGDAAHAMCPALAQGAGCAMVNAFSL-311	(Chaiyen et al., 1997)
27 sal (*Pseudomonas putida* NAH7)	10-IGIVGGGISGVALA-23	157-DLLIGADGIKSALR-170	308-GRVVLIGDAAHAMLPHQGAGAGQGLEDAYFL-338	(You et al., 1991)
28 sal (*Pseudomonas putida*)	10-IGIIGGGISGVALA-23	156-DLLIGADGIKSALR-169	307-GRVVLIGDAAHAMLPHQGAGAAQGLEDAYFL-337	(Darby et al., 1995)
29 sal (*Pseudomonas putida* KF715)	13-VAIVGGGISGLALA-26	158-DLLIGRDGIKSALR-171	308-GRVALIGDAAHAMLPHQGAGAGQGLEDAYFL-338	(Lee et al., 1996)
30 sal (*Pseudomonas putida* S-1)	8-VAVIGGGIAGTALA-21	154-DVAIAADGIKSSMR-167	305-GRVALIGDAAHAMLPHQGAGAGQGLEDAYFM-335	(Suzuki et al., 1996b)
31 sal (*Sphingomonas* species AJ1)	3-IAIIGAGIGGLALA-16	153-DVVIGADGVRSVIR-166	286-GPAVLIGDAAHAMLPHHGQGANTSIEDACVL-316	(Iwabuchi, 1997)
32 pub (*Agaricus bisporus*)	9-VAIVGAGIVGLTLA-22	175-DILVGADGIKSTLR-188	326-GRVFLMGDAAHAMLPHLGAGAHVGMEDAYIL-356	(Tsuji et al., 1996)
33 epox (*Lycopersicon esculentum*)	88-VLVAGGGIGGLVFA-101	242-DLLVGADGIRSKVR-255	371-GRVTLLGDSVHAMQPNLGQGGCMAIEDSYQL-401	(Burbidge, 1997)
34 epox (*Nicotiana plumbaginifolia*)	82-VLVAGGGIGGLVFA-95	236-DLLVGADGIRSKVR-249	365-GRVTLLGDSVHAMQPNLGQGGCMAIEDSYQL-395	(Marin et al., 1996)
35 epox (*Capsicum annuum*)	83-VLVAGGGIGGLVFA-96	236-DLLVGADGIRSKVR-249	366-GRVTLLGDSVHAMQPNLGQGGCMAIEDSYQL-396	(Bouvier et al., 1996)
36 epox (*Saccharomyces cerevisiae*)	21-AIVIGAGVIGPCVA-34	203-HLTFICDGIFSRFR-216	328-TGMCVIGDAALNMRHPLTGGGMTVGLHDVVLL-358	(Jandrositz et al., 1991)
37 epox (Rat)	125-VIIIGSGVLGSALA-138	278-PLTVVADGLFSKFR-290	401-RGVLLLGDAYNLRHPLTGGGMTVALKDIKIW-431	(Sakakibara et al., 1995)
38 mono (*Rhodococcus equi*)	4-VIIVGAGPTGLMLA-17	145-RYLVGCDGGRSTVR-158	271-DRVFLAGDAAHIHPPMGGQGLNLGVQDAFNL-301	(Andersen et al., 1997)
39 mono (*Pseudomonas aeruginosa*)		50-SLVVGADGIRSSVR-63	178-GRVVLIGDAAHAMTPNLGQGAAMALEDAFLL-208	(Kinscherf & Willis, 1995)
40 mono (*Escherichia coli* K-12 CS520)	18-VAIAGAGPVGLMMA-31	168-QWLVACDGGASFVR-181	288-DRVLLAGDAAHIMPVWQGQGYNSGMRDAFNL-318	(Ferrandez et al., 1996)
41 mono (*Escherichia coli* K-12 W3110)	18-VAIAGAGPVGLMMA-31	168-QWLVACDGGASFVR-181	288-DRVLLAGDAAHIMPVWQGQGYNSGMRDAFNL-318	(Kawanuukai, 1996)
42 mono (*Escherichia coli* K-12 visC)	6-VAIVGGGMVGLAVA-19	150-RLVIGADGANSWLR-163	274-IIRLALVGDAAHTIHPLAGQGVNLGFMDAAEL-304	(Nakahigashi et al., 1992)
43 mono (*Escherichia coli* K-12 ubiH)	3-VIIVGGGMAGATLA-16	147-RVLVAADGTHSALA-160	270-HRTVLVGNAAQTLHPIAGQGFNLGMRDVMSL-300	(Nakahigashi et al., 1992)
44 mono (*Saccharomyces cerevisiae*)	5-VAIIGAGLVGCLAA-18	162-DFVIGCDGAYSATR-175	307-GKAILLGDAAHAMVPFYGQGMNCGFEDVRIL-337	(Domdey et al., 1994)
45 mono (*Caenorhabditis elegans* R07B7.4)	4-VVIAGGGLVGSANA-17	155-DLFLACDGAHSSIR-168	291-DKLVLMGDAAHAMVPFNGQGVNCGFEDCLVL-321	(Wilson et al., 1994)
46 mono (*Caenorhabditis elegans* R07B7.5)	4-VAIAGAGLVGALNA-17	171-DLILACDGAYSAVR-184	308-DNLVLMGDAAHAMVPFYGQGMNCGFEDCLVR-338	(Wilson et al., 1994)
47 mono (*Bacillus subtilis*)	4-MLIAGGGIGGLSAA-17	149-DILAGFDGIHSVVR-162	278-GRVIGGDAAHAGAPTLAQGAAMAIEDAIVL-308	(Sekiguchi, 1996)
48 mono (*Mycobacterium tuberculosis* H37Rv)	4-VVVSGASVAGTAAA-17	150-DLVIGADGLHSNVR-163	282-GRVALVGDAGYCCSPLSGQGTSVALLGAYIL-312	(Barrell et al., 1996)
Consensus sequence	VhhhGsGhhGhhhs	chhhssDGxcSxhR	GxhhLhGDAAHxxxPxxGxGxNxsxxDsxxL	

[a]*This multiple alignment was obtained from 48 sequences with* MACAW *and* ClustalW using the BLOSUM62 matrix. The consensus profiles shown underneath the alignment include strictly conserved residues as well as those profiles in which there are not more than 10 violations. Uppercase letters in the profile are amino acid residues, lowercase letters and symbols are: h = hydrophobic residues; s = small residues; c = charged residues; x = all residues; - = gap.

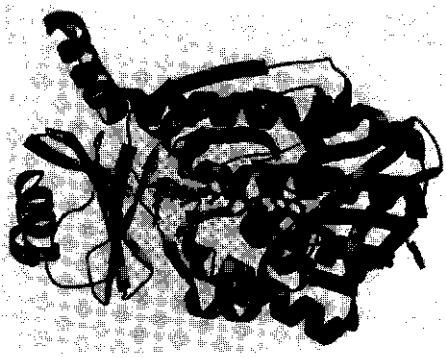

Fig. 1. Ribbon structure of *p*-hydroxybenzoate hydroxylase from *Pseudomonas fluorescens*. MOLSCRIPT (Kraulis, 1991) picture highlighting the conserved regions of the protein. GXGXXG sequence in red; DG sequence in blue; GD sequence in green. The FAD and aromatic substrate are depicted in ball and stick representation.

formed with the programs MACAW (Schuler et al., 1991) and ClustalW (Thompson et al., 1994) using the Blosum matrixes (Henikoff & Henikoff, 1992). From the alignment of 50 flavoprotein hydroxylase sequences, three conserved regions could be deduced, which are shown in Table 1.

The first FAD fingerprint sequence, shown in Table 1, is the well-known Rossmann fold or $\beta\alpha\beta$-fold (containing the GXGXXG sequence), a common motif among FAD- and NAD(P)H-dependent oxidoreductases (Wierenga et al., 1986). In PHBH, this fingerprint (residues 5–19) is important for binding the ADP moiety of FAD (Fig. 1). The structural properties of this dinucleotide binding fold were reported more than 10 years ago (Wierenga et al., 1983, 1985, 1986).

The second FAD binding motif contains the GD sequence (Table 1) with the highly conserved Asp residue, which contacts the O3′ of the ribose moiety of FAD (Eggink et al., 1990). This common fingerprint sequence among the family of FAD-dependent oxidoreductases differs somewhat between the disulfide oxidoreductases and flavoprotein hydroxylases because the latter enzymes have more conserved residues downstream from the GD sequence (DiMarco et al., 1993). In PHBH, this fingerprint sequence (residue 278–308) is located partly at the *re*-side of the isoalloxazine ring of FAD, near the binding site of the aromatic substrate (Fig. 1; Schreuder et al., 1989).

Table 1 shows that the newly defined DG amino acid sequence is highly conserved among all flavoprotein hydroxylases studied. In PHBH, this short sequence motif comprises strand A4 and the N-terminal part of helix H7 (residues 153–166) of the FAD binding domain, and is situated near the cleft leading toward the active site (Fig. 1). Strand A4 (residue 154–157) is completely buried and multiple contacts are made with residues of both the FAD binding domain and a long excursion of the substrate binding domain. However, as one of the referees pointed out, one could argue that this excursion, together with the FAD and the interface domain, forms one large globular domain and that the contacts of strand A4 are important for maintaining the integrity of this domain. The large turn (residues 158–163) that connects strand A4 and helix H7 contains the strictly conserved residues Asp 159 and Gly 160. This Gly 160 faces the putative NADPH binding cleft and its Phi/Psi angles (62.1/−174.8) are allowed for glycines, whereas they are disallowed for other residues. Also, a side chain at this position would probably hinder binding of the cofactor. The structurally important and tightly packed residues Asp 159 and Gly 160 form hydrogen bonds with the backbone atoms of residues 163–165 (Fig. 2). Indirect hydrogen bonds exist between the backbone oxygen of Cys 158 and backbone nitrogen of Gly 160, with the pyrophosphate moiety of FAD via protonated water molecules (Schreuder et al., 1989). From site-directed mutagenesis studies, it is known that replacement of Cys 158 by Ser decreases the affinity for FAD, probably by influencing the solvation of the pyrophosphate moiety of FAD (van der Bolt et al., 1994). Mutagenesis studies also revealed that His 162 is very important for the binding of NADPH (Eppink et al., 1997). Table 1 shows that this position in the conserved sequence motif almost always contains a positively charged residue. Chemical modification of salicylate hydroxylase has suggested that Lys 165, the equivalent of His 162 in

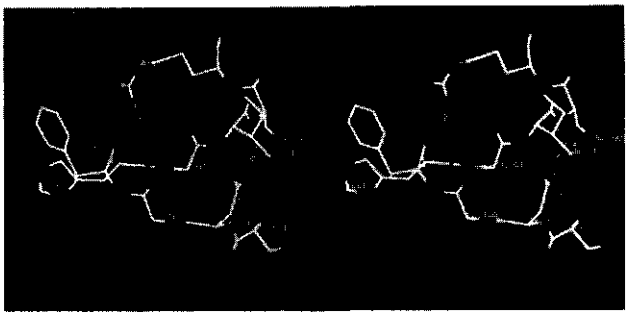

Fig. 2. Stereo picture of the novel conserved sequence motif in *p*-hydroxybenzoate hydroxylase. Close view of the turn region from amino acid 158–166, including the strong intradomain hydrogen bonds.

PHBH, is important for binding the pyrophosphate moiety of NADH (Suzuki et al., 1996a). Phe 161 in PHBH is not conserved in the fingerprint. Mutagenesis studies confirmed that replacement of Phe by Ala weakens NADPH binding, but that Phe 161 is not structurally important (van Berkel et al., 1997). Helix H7 is not regular (Schreuder et al., 1989) but, as in regular α-helices, all peptide dipoles point in approximately the same direction, giving rise to an overall helix dipole moment (Hol et al., 1978). This helix H7 (residues 164–169) is located near the protein surface (Fig. 1). The highly conserved residue Arg 166 in this helix forms strong inter- and intradomain contacts with the backbone oxygens of Phe 161 and Ala 287 (Fig. 2). Substitution of Arg 166 by Ser led to significant structural changes in the Cα-backbone and destabilization of the mutant (van Berkel et al., 1997).

In conclusion, a unique short amino acid sequence motif for flavoprotein hydroxylases is presented that seems to serve a dual function. Crystallographic analysis and site-directed mutagenesis studies of PHBH from *P. fluorescens* suggest that this sequence is involved indirectly in binding the pyrophosphate moiety of FAD and that it is also necessary for the recognition of the NADPH cofactor. Although the mode of NADPH binding in PHBH is still unknown, helix H7 might be involved in binding the pyrophosphate moiety of the pyridine nucleotide cofactor. There are two common characteristics of a dinucleotide binding fold (Wierenga et al., 1985) that probably also occur here. (1) A glycine residue near the N-terminus of a helix, to allow close contact with the pyrophosphate moiety: Gly 160 is located at such a position near the N-terminus of helix H7. (2) Favorable interaction of the helix dipole with the negatively charged pyrophosphate moiety: In the proposed model, the pyrophosphate moiety of NADPH is located near the positive end of the dipole of helix H7 (van Berkel et al., 1997). The newly identified fingerprint is highly specific for flavoprotein hydroxylases. Running BEAUTY with the sequence DFLVGADGIHSXVR (based on the alignment results and where X denotes all possibilities) yielded 48 of 52 flavoprotein hydroxylases present in the databases, and 5 unrelated proteins. Our fingerprint recognizes all different types of flavoprotein hydroxylases that are encoded by a single gene, something the current fingerprints cannot recognize. This shows that our fingerprint is able to detect unambiguously flavoprotein hydroxylases, which will allow the identification of such enzymes among the millions of genes that are produced currently by the large scale whole-genome sequencing efforts.

References

Andersen SJ, Quan S, Gowan B, Dabbs ER. 1997. Monooxygenase-like sequence of a *Rhodococcus equi* gene conferring increased resistance to rifampin by inactivating this antibiotic. *Antimicrob Agents Chemother 41*:218–221.

Barrell BG, Rajandream MA, Walsh SV. 1996. *Mycobacterium tuberculosis* monooxygenase gene. Direct submission to GenBank (MTCY50).

Blanco G, Pereda A, Brian P, Méndez C, Chater KF, Salas JA. 1993. A *hydroxylase-like gene product contributes to synthesis of a polyketide pigment in Streptomyces halstedii*. *J Bacteriol 175*:8043–8048.

Bouvier F, d'Harlingue A, Hugueney P, Marin E, Marion-Polin A, Camara B. 1996. Xanthophyll biosynthesis. Cloning, expression, functional reconstitution, and regulation of β-cyclohexenyl carotenoid epoxidase from pepper (*Capsicum annuum*). *J Biol Chem 271*:28861–28867.

Burbidge A. 1997. *Lycopersicon esculentum* mRNA for zeaxanthin epoxidase. Direct submission to GenBank (LEZEAXAT).

Chaiyen P, Ballou DP, Massey V. 1997. Gene cloning, sequence analysis, and expression of 2-methyl-3-hydroxypyridine-5-carboxylic acid (MHPC) oxygenase. *Proc Natl Acad Sci USA*, pp 7233–7238.

Dairi T, Nakano T, Aisaka K, Katsumata R, Hasegawa M. 1995. Cloning and nucleotide sequence of the gene responsible for chlorination of tetracycline. *Biosci Biotech Biochem 59*:1099–1106.

Darby RM, Bi YM, Doig S, Firek S, Draper J. 1995. *Pseudomonas putida* nahG gene for salicylate hydroxylase. Direct submission to GenBank (PPNAHGG).

Decker H, Haag S. 1995. Cloning and characterization of a polyketide synthase gene from *Streptomyces fradiae* Tü2717, which carries the genes for biosynthesis of the angucycline antibiotic urdamycin A and a gene probably involved in its oxygenation. *J Bacteriol 177*:6126–6136.

Decker H, Motamedi H, Hutchinson CR. 1993. Nucleotide sequences and heterologous expression of *tcmG* and *tcmP*, biosynthesis genes for tetracenomycin C in *Streptomyces glaucescens*. *J Bacteriol 175*:3876–3886.

DiMarco AA, Averhoff BA, Kim EE, Ornston LN. 1993. Evolutionary divergence of *pobA*, the structural gene encoding *p*-hydroxybenzoate hydroxylase in an *Acinetobacter calcoaceticus* strain well-suited for genetic analysis. *Gene 125*:25–33.

Domdey H, Gassenhuber H, Obermaier B, Piravandi E. 1994. *Saccharomyces cerevisiae* chromosome II reading frame ORF YBL098w. Direct submission to GenBank (SCYBL098W).

Ederer MM, Crawford RL, Orser CS. 1996. *Sphingomonas chlorophenolica* strain ATCC 33790 PCP-4-monooxygenase(pcpB) gene. Direct submission to GenBank (SCU60175).

Eggink G, Engel H, Vriend G, Terpstra P, Witholt B. 1990. Rubredoxin reductase of *Pseudomonas oleovorans*. Structural relationship to other flavoprotein oxidoreductases based on one NAD and two FAD fingerprints. *J Mol Biol 212*:135–142.

Entsch B, Nan Y, Weaich K, Scott KF. 1988. Sequence and organization of *pobA*, the gene coding for *p*-hydroxybenzoate hydroxylase, an inducible enzyme from *Pseudomonas aeruginosa*. *Gene 71*:279–291.

Entsch B, van Berkel WJH. 1995. Structure and mechanism of *p*-hydroxybenzoate hydroxylase. *FASEB J* 9:476–483.

Eppink MHM, Jacobs D, van Berkel WJH. 1997. Involvement of His162 in NADPH binding of *p*-hydroxybenzoate hydroxylase. In: Stevenson K, Massey V, Williams Ch, eds. *Flavins and flavoproteins XII*. Calgary: University Press, pp 315–318.

Eppink MHM, Schreuder HA, van Berkel WJH. 1995. Structure and function of mutant Arg44Lys of 4-hydroxybenzoate hydroxylase. Implications for NADPH binding. *Eur J Biochem 231*:157–165.

Ferrandez A, Garcia JL, Diaz E. 1996. *Escherichia coli* mhp cluster for 3-hydroxyphenylpropionic acid degradation. Direct submission to GenBank (ECMHP).

Filippini S, Solinas MM, Breme U, Schlüter MB, Gabellini D, Biamonti G, Colombo AL, Garofano L. 1995. *Streptomyces peucetius* daunorubicin biosynthesis gene, *dnrF*: Sequence and heterologous expression. *Microbiology 141*:1007–1016.

Haigler BE, Suen WC, Spain JC. 1996. Purification and sequence analysis of 4-methyl-5-nitrocatechol oxygenase from *Burkholderia* sp. strain DNT. *J Bacteriol 178*:6019–6024.

Henikoff S, Henikoff JG. 1992. Amino acid substitution matrices from protein blocks. *Proc Natl Acad Sci USA 89*:10915–10919.

Hol WGJ, van Duijnen PTh, Berendsen HJC. 1978. The α-helix dipole and properties of proteins. *Nature (Lond) 273*:443–446.

Hong YS, Hwang CK, Hong SK, Kim YH, Lee JJ. 1994. Molecular cloning and characterization of the aklavinone 11-hydroxylase gene of *Streptomyces peucetius* subsp. *caesius* ATCC 27952. *J Bacteriol 176*:7096–7101.

Iwabuchi T. 1997. *Sphingomonas* sp. DNA for salicylate hydroxylase. Direct submission to GenBank (AB000564).

Jandrositz A, Turnowsky F, Högenauer F. 1991. The gene encoding squalene epoxidase from *Saccharomyces cerevisiae*: Cloning and characterization. *Gene 107*:155–160.

Kälin M, Neujahr HY, Weissmahr RN, Sejlitz T, Jöht R, Fiechter A, Reiser J. 1992. Phenol hydroxylase from *Trichosporon cutaneum*: Gene cloning, sequence analysis, and functional expression in *Escherichia coli*. *J Bacteriol 174*:7112–7210.

Kawamukai M. 1996. *Escherichia coli* genes for MhpR, MhpA, MhpB, MhpC, MhpD, MhpE and MhpF, complete sequence of the mhp operon. Direct submission to GenBank (D86239).

Kinscherf TG, Willis DK. 1995. *Pseudomonas aeruginosa FAD binding protein* homolog gene. Direct submission GenBank (PAU29897).

Kõiv V, Marits R, Heinaru A. 1996. Sequence analysis of the 2,4-dichlorophenol hydroxylase gene *tfdB* and 3,5-dichlorocatechol 1,2-dioxygenase gene *tfdC* of 2,4-dichlorophenoxyacetic acid degrading plasmid pEST4011. *Gene 174*:293–297.

Kraulis PJ. 1991. MOLSCRIPT: A program to produce both detailed and schematic plots of protein structures. *J Appl Crystallogr 24*:946–950.

Lee J, Oh J, Min KR, Kim Y. 1996. Nucleotide sequence of salicylate hydroxylase gene and its 5'-flanking region of *Pseudomonas putida* KF715. *Biochem Biophys Res Commun 218*:544–548.

Marin E, Nussaume L, Quesada A, Gonneau M, Sotta B, Hugueney P, Frey A,

Marion-Poll A. 1996. Molecular identification of zeaxanthin epoxidase of *Nicotiana plumbaginifolia*, a gene involved in abscisic acid biosynthesis and corresponding to the ABA locus of *Arabidopsis thaliana*. *EMBO J 15*:2331–2342.

Nakahigashi K, Miyamoto K, Nishimura K, Inokuchi H. 1992. Isolation and characterization of a light-sensitive mutant of *Escherichia coli* K-12 with a mutation in a gene that is required for the biosynthesis of ubiquinone. *J Bacteriol 174*:7352–7359.

Niemi J, Mäntsälä P. 1995. Nucleotide sequences and expression of genes from *Streptomyces purpurascens* that cause the production of new anthracyclines in *Streptomyces galilaeus*. *J Bacteriol 177*:2942–2945.

Nurk A, Kasak L, Kivisaar M. 1991. Sequence of the gene (*pheA*) encoding phenol monooxygenase from *Pseudomonas* sp. EST1001: Expression in *Escherichia coli* and *Pseudomonas putida*. *Gene 102*:13–18.

Orser CS, Lange CC, Xun L, Zahrt T, Schneider BJ. 1993. Cloning, sequence analysis, and expression of the *Flavobacterium* pentachlorophenol-4-monooxygenase gene in *Escherichia coli*. *J Bacteriol 175*:411–416.

Perkins EJ, Gordon MP, Caceres O, Lurquin PF. 1990. Organization and sequence analysis of the 2,4-dichlorophenol hydroxylase and dichlorocatechol oxidative operons of plasmid pJP4. *J Bacteriol 172*:2351–2359.

Sakakibara J, Watanabe R, Kanai Y, Ono T. 1995. Molecular cloning and expression of rat squalene epoxidase. *J Biol Chem 270*:17–20.

Schmid A, van der Meer JR. 1997. 2-Hydroxybiphenyl 3-monooxygenase from *Pseudomonas azelaica* HBP1. Direct submission to GenBank (PAU73900).

Schreuder HA, Prick PAJ, Wierenga RK, Vriend G, Wilson KS, Hol WGJ, Drenth J. 1989. Crystal structure of the *p*-hydroxybenzoate hydroxylase–substrate complex refined at 1.9 Å resolution. *J Mol Biol 208*:679–696.

Schuler GD, Altschul SF, Lipman DJ. 1991. A workbench for multiple alignment construction and analysis. *Proteins Struct Funct Genet 9*:180–190.

Seibold B, Matthes M, Eppink MHM, Lingens F, van Berkel WJH, Müller R. 1996. 4-Hydroxybenzoate hydroxylase from *Pseudomonas* sp. CBS3. Purification, characterization, gene cloning, sequence analysis and assignment of structural features determining the coenzyme specificity. *Eur J Biochem 239*:469–478.

Sekiguchi J. 1996. *Bacillus subtilis* monooxygenase gene. Direct submission to GenBank (YfnL).

Shuman B, Dix TA. 1993. Cloning, nucleotide sequence and expression of a *p*-hydroxybenzoate hydroxylase isozyme gene from *Pseudomonas fluorescens*. *J Biol Chem 268*:17057–17062.

Suzuki K, Mizuguchi M, Gomi T, Itagaki E. 1996a. Identification of a lysine residue in the NADH-binding site of salicylate hydroxylase from *Pseudomonas putida* S-1. *J Biochem 117*:579–585.

Suzuki K, Mizuguchi M, Ohnishi K, Itagaki E. 1996b. Structure of chromosomal DNA coding for *Pseudomonas putida S-1* salicylate hydroxylase. *Biochim Biophys Acta 1275*:154–156.

Thompson JD, Higgins DG, Gibson TJ. 1994. CLUSTAL W: Improving the sensitivity of progressive multiple sequence alignment through sequence weighting, positions-specific gap penalties and weight matrix choice. *Nucleic Acids Res 22*:4673–4680.

Tsuji H, Oka T, Kimoto M, Hong YM, Natori Y, Ogawa T. 1996. Cloning and sequencing of cDNA encoding 4-aminobenzoate hydroxylase from *Agaricus bisporus*. *Biochim Biophys Acta 1309*:31–36.

van Berkel WJH, Eppink MHM, van der Bolt FJT, Vervoort J, Rietjens IMCM, Schreuder HA. 1997. *p*-Hydroxybenzoate hydroxylase: Mutants and mechanism. In: Stevenson K, Massey V, Williams Ch, eds. *Flavins and flavoproteins XII*. Calgary: University Press. pp 305–314.

van Berkel WJH, Müller F. 1991. Flavin-dependent monooxygenases with special references to *p*-hydroxybenzoate hydroxylase. In: Müller F, ed. *Chemistry and biochemistry of flavoenzymes 2*. Boca Raton, Florida: CRC Press. pp 1–29.

van Berkel WJH, Westphal AH, Eschrich K, Eppink MHM, de Kok A. 1992. Substitution of Arg214 at the substrate-binding site of *p*-hydroxybenzoate hydroxylase from *Pseudomonas fluorescens*. *Eur J Biochem 210*:411–419.

van der Bolt FJT, Drijfhout MC, Eppink MHM, Hagen WR, van Berkel WJH. 1994. Selective cysteine → serine replacements in *p*-hydroxybenzoate hydroxylase from *Pseudomonas fluorescens* allow the unambiguous assignment of Cys211 as the site of modification by spin-labeled *p*-chloromercuribenzoate. *Protein Eng 7*:801–804.

van der Laan JM, Schreuder HA, Swarte MBA, Wierenga RK, Kalk KH, Hol WGJ, Drenth J. 1989. The coenzyme analogue adenosine 5-diphosphoribose displaces FAD in the active site of *p*-hydroxybenzoate hydroxylase. An X-ray crystallographic investigation. *Biochemistry 28*:7199–7205.

van der Meer JR. 1997. Chlorophenol monooxygenase from *Ralstonia eutropha* JMP134. Direct submission to GenBank (REU16782).

Weijer WJ, Hofsteenge J, Vereijken JM, Jekel PA, Beintema JJ. 1982. Primary structure of *p*-hydroxybenzoate hydroxylase from *Pseudomonas fluorescens*. *Biochim Biophys Acta 704*:385–388.

Wierenga RK, De Maeyer MCH, Hol WGJ. 1985. Interaction of pyrophosphate moieties with α-helixes in dinucleotide binding proteins. *Biochemistry 24*:1346–1357.

Wierenga RK, Drenth J, Schulz G. 1983. Comparison of the three-dimensional protein and nucleotide structure of the FAD-binding domain of *p*-hydroxybenzoate hydroxylase with the FAD- as well as NADPH-binding domains of glutathione reductase. *J Mol Biol 167*:725–739.

Wierenga RK, Terpstra P, Hol WGJ. 1986. Prediction of the occurrence of the ADP-binding βαβ-fold in proteins, using an amino acid sequence fingerprint. *J Mol Biol 187*:101–107.

Wilson R et al. 1994. 2.2 Mb of contiguous nucleotide sequence from chromosome III of *C. elegans*. *Nature 368*:32–38. Direct submission GenBank (CER07B7).

Wong CM, Dilworth MJ, Glenn AR. 1994. Cloning and sequencing show that 4-hydroxybenzoate hydroxylase (*pobA*) is required for uptake of 4-hydroxybenzoate in *Rhizobium leguminosarum*. *Microbiology 140*:2775–2786.

Worley KC, Wiese BA, Smith RF. 1995. BEAUTY: An enhanced BLAST-based search tool that integrates multiple biological information resources into sequence similarity search results. *Genome Research 5*:173–184.

Yang K, Han L, Ayer SW, Vining LC. 1996. Accumulation of the angucycline antibiotic rabelomycin after disruption of an oxygenase gene in the jadomycin B biosynthesis gene cluster of *Streptomyces venezuelae*. *Microbiology 142*:123–132.

You IS, Ghosa D, Gunsalus IC. 1991. Nucleotide sequence analysis of the *Pseudomonas putida* PpG7 salicylate hydroxylase gene (*nahG*) and its 3'-flanking region. *Biochemistry 30*:1635–1641.

CHAPTER 6

Interdomain binding of NADPH in *p*-hydroxybenzoate hydroxylase as suggested by kinetic, crystallographic and modeling studies of histidine 162 and arginine 269 variants

Michel H.M. Eppink, Herman A. Schreuder, and Willem J.H. van Berkel

J. Biol. Chem. 273: 21031-21039 (1998)

THE JOURNAL OF BIOLOGICAL CHEMISTRY

Interdomain binding of NADPH in *p*-Hydroxybenzoate Hydroxylase as Suggested by Kinetic, Crystallographic and Modeling Studies of Histidine 162 and Arginine 269 Variants*

(Received for publication, January 21, 1998, and in revised form, April 9, 1998)

Michel H. M. Eppink‡, Herman A. Schreuder§, and Willem J. H. van Berkel‡¶

From the ‡Department of Biomolecular Sciences, Laboratory of Biochemistry, Wageningen Agricultural University, Dreijenlaan 3, 6703 HA Wageningen, The Netherlands and §Hoechst Marion Roussel, Core Research Functions, building G865A, D-65926 Frankfurt, Germany

The conserved residues His-162 and Arg-269 of the flavoprotein *p*-hydroxybenzoate hydroxylase (EC 1.14.13.2) are located at the entrance of the interdomain cleft that leads toward the active site. To study their putative role in NADPH binding, His-162 and Arg-269 were selectively changed by site-specific mutagenesis. The catalytic properties of H162R, H162Y, and R269K were similar to the wild-type enzyme. However, less conservative His-162 and Arg-269 replacements strongly impaired NADPH binding without affecting the conformation of the flavin ring and the efficiency of substrate hydroxylation.

The crystal structures of H162R and R269T in complex with 4-hydroxybenzoate were solved at 3.0 and 2.0 Å resolution, respectively. Both structures are virtually indistinguishable from the wild-type enzyme-substrate complex except for the substituted side chains. In contrast to wild-type *p*-hydroxybenzoate hydroxylase, H162R is not inactivated by diethyl pyrocarbonate. NADPH protects wild-type *p*-hydroxybenzoate hydroxylase from diethylpyrocarbonate inactivation, suggesting that His-162 is involved in NADPH binding. Based on these results and GRID calculations we propose that the side chains of His-162 and Arg-269 interact with the pyrophosphate moiety of NADPH. An interdomain binding mode for NADPH is proposed which takes a novel sequence motif (Eppink, M. H. M., Schreuder, H. A., and van Berkel, W. J. H. (1997) *Protein Sci.* 6, 2454–2458) into account.

p-Hydroxybenzoate hydroxylase is the most thoroughly characterized member of a group of inducible flavoprotein monooxygenases which are involved in the biodegradation of aromatic compounds by soil microorganisms (1). The enzyme catalyzes the hydroxylation of 4-hydroxybenzoate to 3,4-dihydroxybenzoate, *i.e.* the first step of the β-ketoadipate pathway (2), using NAD(P)H as electron donor shown in Scheme 1. The dihydroxylated aromatic product is readily subject to ring fission and further catabolism, allowing the microbes to grow (2). *p*-Hydroxybenzoate hydroxylase has been isolated from many microorganisms, and several gene sequences are presently known (3). However, most information regarding its structure and function comes from studies on the strictly NADPH-dependent enzymes from *Pseudomonas* strains (4). The kinetic properties of *p*-hydroxybenzoate hydroxylase have been elucidated (5), together with the catalytic mechanism (6, 7). The catalytic cycle of *p*-hydroxybenzoate hydroxylase and related flavoenzymes can be separated in two half-reactions, both involving ternary complex formation. In the reductive part of the reaction, the substrate acts as an effector, highly stimulating the rate of flavin reduction by NADPH (8). After $NADP^+$ release, the substrate is hydroxylated in the oxidative part of the reaction through electrophilic attack of a transiently stable oxygenated flavin intermediate (6). Efficient hydroxylation requires substrate activation upon binding (4). This prevents the uncoupling of the hydroxylation reaction from oxygen reduction which would result in the production of potential harmful hydrogen peroxide.

The crystal structure of the enzyme-substrate complex of *p*-hydroxybenzoate hydroxylase is known in atomic detail (9, 10). The enzyme is a homodimer of two independently acting 44-kDa polypeptide chains containing a noncovalently bound FAD molecule (11). Each subunit is built up from three domains, the FAD binding domain containing a characteristic βαβ-fold (12), the substrate binding domain, and the interface domain (10). The substrate is deeply buried in the interior of the protein (Fig. 1) and residues from all three domains are involved in catalysis. Crystallographic studies have revealed that the flavin ring can attain different orientations in and out of the active site (13–15). The mobility of the flavin cofactor is thought to be essential for the exchange of substrate and product during catalysis (13, 14) and for the recognition of NADPH (15). In contrast to many other pyridine nucleotide-dependent enzymes, *p*-hydroxybenzoate hydroxylase lacks a well defined domain for binding the coenzyme. Sequence alignments suggest that this might be a common property of the family of flavoprotein aromatic hydroxylases (16). So far, no crystal structures of *p*-hydroxybenzoate hydroxylase with NADP(H) or pyridine nucleotide analogs have been obtained (17).

Chemical modification studies of wtPHBH[1] from *Pseudomonas fluorescens* have indicated the involvement of histidine (18), arginine (19), and tyrosine (20) residues in NADPH binding. Based on this information and the available crystallographic data, a potential mode of NADPH binding was proposed (20). In this model, the pyrophosphate moiety of NADPH binds in a cleft leading toward the active site and interacts with the side chains of His-162 of the FAD-binding domain and Arg-269 of the substrate binding domain (12). Despite their

* The costs of publication of this article were defrayed in part by the payment of page charges. This article must therefore be hereby marked "*advertisement*" in accordance with 18 U.S.C. Section 1734 solely to indicate this fact.

¶ To whom correspondence should be addressed: Dept. of Biomolecular Sciences, Laboratory of Biochemistry, Wageningen Agricultural University, Dreijenlaan 3, 6703 HA Wageningen, The Netherlands. Tel.: 31-317-482868; Fax: 31-317-484801; E-mail: willem.vanberkel@fad.bc.wau.nl.

This paper is available on line at http://www.jbc.org

[1] The abbreviations used are: wtPHBH, wild-type *p*-hydroxybenzoate hydroxylase; Mes, 4-morpholineethanesulfonic acid; POHB, 4-hydroxybenzoate; HPLC, high performance liquid chromatography.

location near the protein surface (Fig. 1), both residues are highly conserved in *p*-hydroxybenzoate hydroxylase enzymes of known primary structure (3).

To investigate the validity of the proposed NADPH binding mode in more detail, we have undertaken the characterization of His-162 and Arg-269 variants of *p*-hydroxybenzoate hydroxylase from *P. fluorescens*. In this work we show that the His-162 and Arg-269 replacements weaken the NADPH binding without affecting the protein structure and the efficiency of substrate hydroxylation. Based on these and additional experiments, a refined model for the interdomain binding of NADPH is proposed. A preliminary account of this work has been presented elsewhere (1, 21).

EXPERIMENTAL PROCEDURES

Materials—Diethylpyrocarbonate was purchased from Janssen Chemicals. All other chemicals have been described elsewhere (22).

Site-specific Mutagenesis—Site-specific mutagenesis of the gene encoding wtPHBH from *P. fluorescens* was performed in bacteriophage M13mp18 according to the method of Kunkel *et al.* (23). The oligonucleotide 5′-GCGATGGCTTC*XXX*GGCATCTCG-5′ (where *XXX* denotes the replacement of CAC for GAC (H162D), AAC (H162N), TCC (H162S), ACC (H162T), TAC (H162Y), and AGG (H162R), respectively) was used as primer for the construction of His-162 mutants. The oligonucleotide 5′-GCGCCGCTG*XXX*AGCTTCGTGG-3′ (where *XXX* denotes the replacement of CGC for GAC (R269D), AAA (R269K), AAC (R269N), TCC (R269S), ACC (R269T), and TAC (R269Y), respectively) were used as primers for the construction of Arg-269 mutants. The mutations were introduced into the *Escherichia coli* gene encoding the microheterogeneity-resistant mutant C116S (24). All mutations were confirmed by nucleotide sequencing according to Sanger *et al.* (25). For convenience and in view of identical catalytic properties (26), C116S is further referred to as wtPHBH.

Enzyme Purification—Mutated *p*-hydroxybenzoate hydroxylase genes were expressed in transformed *E. coli* TG2 grown in 5-liter batches of tryptone/yeast medium containing 100 μg/ml ampicillin and 20 μg/ml isopropyl-1-thio-β-D-galactopyranoside at 37 °C under vigorous aeration. The mutant enzymes were purified by a slightly modified procedure of the purification protocol developed for wtPHBH (26). The enzyme solution obtained after protamine sulfate treatment was loaded onto Q-Sepharose FF, equilibrated in 20 mM Tris/sulfate, pH 8.0. After washing, the enzyme was eluted with 0.2 M KCl and dialyzed against the starting buffer. The enzyme was then loaded onto Cibacron blue 3GA-agarose, equilibrated in 40 mM Tris/sulfate, pH 8.0. R269D, R269N, R269S, R269T, and R269Y eluted during washing, whereas R269K and all His-162 mutants eluted with 0.2 M KCl. After dialysis in 7 mM potassium phosphate buffer, pH 7.0, the mutant enzymes were passed through a hydroxyapatite column (27) and purified to apparent homogeneity by fast protein liquid anion exchange chromatography (28). Purified enzymes were stored as ammonium sulfate precipitates at 4 °C.

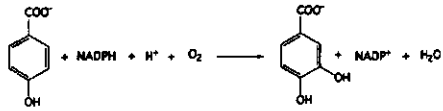

SCHEME 1

Analytical Methods—Molar absorption coefficients of protein-bound flavin were determined in 50 mM sodium phosphate buffer, pH 7.0, by recording absorption spectra in the absence and presence of 0.1% SDS (29). Difference spectra with Cibacron blue 3GA were recorded with an automated Aminco DW-2000 spectrophotometer, essentially as described by Thompson and Stellwagen (30). Dissociation constants of enzyme-ligand complexes were determined fluorimetrically (31). Oxygen consumption experiments were performed as described previously (3). Aromatic product formation was analyzed by reverse phase HPLC (29). Kinetic experiments were performed at 25 °C in 100 mM Tris/sulfate pH 8.0, unless stated otherwise. The standard activity of *p*-hydroxybenzoate hydroxylase was measured as reported earlier (32). Steady-state kinetic parameters were determined as described previously (33). Rapid-reaction kinetics were performed with a High-Tech Scientific SF-51 stopped flow spectrophotometer (Salisbury, Wilts, United Kingdom), equipped with an anaerobic kit and interfaced to an Hyundai 486 microcomputer for data acquisition and analysis (22). pH-dependent rapid reaction experiments were performed in 40 mM Mes, pH 6–7, or 40 mM Hepes, pH 7–8. The ionic strength of buffers was adjusted to 50 mM with added sodium sulfate (34).

Chemical Modification with Diethylpyrocarbonate—Ethoxyformylation of histidine residues was performed by adding 0.5 mM diethylpyrocarbonate to 20 μM enzyme in 50 mM Mes, pH 5.8 (I = 0.1 M) (18). Chemical modification was interrupted by dilution or Bio-Gel P6DG filtration after addition of excess imidazole. The amount of modified histidines was determined at 244 nm ($\Delta\varepsilon_{244}$ = 3.6 mM^{-1} cm^{-1}).

Crystallization—Crystals of POHB complexed H162R and R269T were obtained using the hanging drop vapor diffusion method. The protein solutions contained 10–15 mg/ml enzyme in 100 mM potassium phosphate buffer, pH 7.0. The reservoir solution contained 40% saturated ammonium sulfate, 0.04 mM FAD, 0.15 mM EDTA, 2 mM POHB, and 30 mM sodium sulfite in 100 mM potassium phosphate, pH 7.0. Drops of 2 μl of protein solution and 2 μl of reservoir solution were allowed to equilibrate at 4 °C against 1 ml of reservoir solution. Crystals with dimensions of up to 0.3 × 0.2 × 0.1 mm^3 grew within 5 days.

Data Collection—X-ray diffraction data were collected using a Siemens multiwire area detector and graphite monochromated CuKα radiation from an 18-kW Siemens rotating anode generator, operating

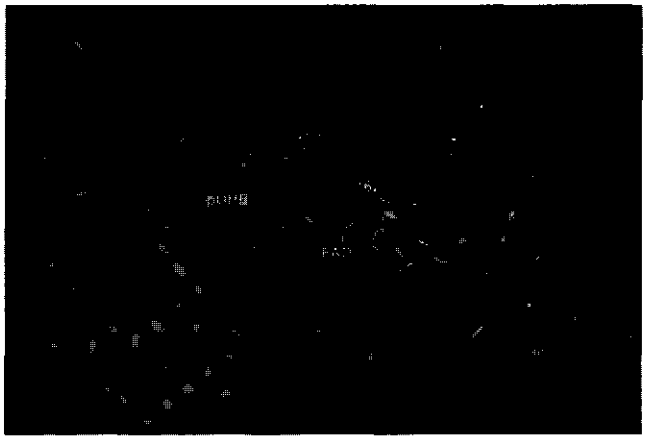

FIG. 1. **Domain structure of *p*-hydroxybenzoate hydroxylase.** The FAD domain (*orange*), substrate domain (*green*), and interface domain (*blue*) are indicated. The substrate (POHB) is in *red* and the FAD in *yellow*. The amino acid residues His-162 and Arg-269 are depicted in *magenta*. Data were taken from the crystal structure of the enzyme-substrate complex refined at 1.9 Å resolution (10).

TABLE I
X-ray diffraction data and refinement statistics of H162R and R269T

	$C222_1$	
Enzyme	H162R	R269T
Space group	$C222_1$	$C222_1$
Cell dimensions (Å)		
a	71.8	72.0
b	146.0	146.3
c	88.3	88.6
Unique reflections	6695	26122
Resolution (Å)	3.0	2.0
R_{sym} (%)	13.0	4.5
Completeness (%)	72.4	92.2
Starting model	POHB[a]	POHB[a]
Initial *R* factor (%)	22.7	22.5
Final *R* factor (%)	12.8	17.7
Water molecules	218	289
Root mean square bond lengths (Å)	0.010	0.010
Root mean square bond angles (degrees)	1.52	1.45
Average B factors (Å^2)		
Protein	26.6	26.7
Flavin ring	16.5	15.8
POHB	16.3	15.1

[a] wtPHBH-POHB complex (10).

at 45 kV and 100 mA. Data were processed using the XDS package (35). Data collection statistics are given in Table I.

Refinement—A starting electron density map was calculated for H162R based on the structure of the wtPHBH·POHB complex (10), after a correction had been made for the slightly different cell dimensions (13). The $2F_o$–F_c and F_o–F_c maps clearly showed the replacement of His-162 by Arg. His-162 was changed into Arg and fitted in the electon density map with the graphics program O (36). The complete protein model was inspected and corrected where necessary. Refinement consisted of four macrocycles of map inspection and rebuilding using O with subsequent energy minimization and temperature factor refinement using the *X-plor* package (37). For the FAD we used the parameters as described by Schreuder *et al.* (13). Water molecules were assigned by searching F_o–F_c maps for peaks of at least 4σ, which were between 2.0 and 5.0 Å of other protein or water atoms. Water molecules with temperature factors after refinement in excess of 70 Å^2 were rejected. The refined structure has an *R* factor of 12.8% for 6695 reflections between 8.0 and 3.0 Å and contains 218 water molecules. The root mean square deviations from ideal values are 0.010 Å for bond lengths and 1.52° for bond angles.

The same procedure as described above was used for the refining of the R269T structure, but the reflections were scaled by applying overall anisotropic B factor refinement, resulting in the following B factors: B11 = −0.798 Å^2; B22 = −1.849 Å^2; B33 = 0.983 Å^2. The $2F_o$–F_c and F_o–F_c maps clearly showed the replacement of Arg-269 by Thr. The final structure was obtained after four cycles of map inspection and refinement and contains 289 water molecules. The final *R* factor is 17.7% for 26122 reflections between 8.0 and 2.0 Å. The root mean square deviations from ideal values are 0.010 Å for bond lengths and 1.45° for bond angles. The refinements statistics of H162R and R269T are summarized in Table I.

GRID Calculations—Energetically favorable binding sites for the pyrophosphate moiety of NADPH in wtPHBH were computed with the GRID program (38) using HPO_4^{2-} and PO_4^{3-} as probe groups on a Silicon graphics Indigo workstation. The parameters used to evaluate the nonbonded interactions (including electrostatic, hydrogen bond, and Lennard-Jones functions) of probe groups are based on the "extended" atom concept used for the program CHARMM (39). Three-dimensional contour surfaces generated at selected energy levels were displayed with the program O (36) together with wtPHBH (10).

NADPH Model—The contour surfaces of the GRID calculations were used as a start for building a three-dimensional model of the enzyme-substrate complex in the presence of NADPH. The pyrophosphate part of the NADPH molecule was fitted on the position of the GRID contours with the graphics program O. The nicotinamide ring was placed at the *re*-side of the flavin ring by rotating around single bonds. Similarly, the 2′-phosphate group was placed next to helix H2 as indicated by mutagenesis studies (1). The model was then energy minimized by using the conjugate gradient method using the XPLOR package (37). The ternary complex was minimized allowing both NADPH and enzyme-substrate complex to move, but the protein Cα-atoms were fixed. The parameter set as determined by Engh and Huber (40) was used for the protein part of the structure. The POHB, NADPH, and FAD parameters were originally derived from CHARMM parameters (39). During energy minimization the charges of the residues Arg, Lys, Glu, and Asp were removed. The final model was obtained after 120 minimization cycles with an initial drop in the energy of 40 kcal/mol.

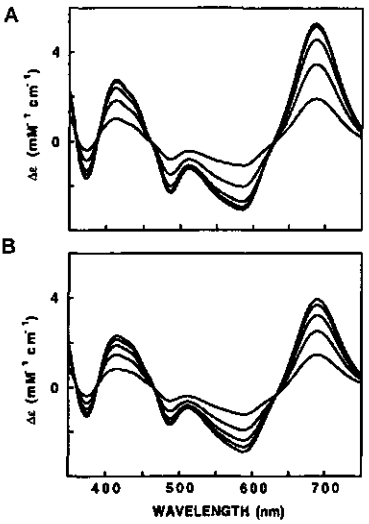

FIG. 2. **Absorption perturbation difference spectra of wtPHBH and R269T with Cibacron blue 3GA.** The experiments were performed in 0.1 M Tris/sulfate, pH 8.0, at 25 °C. A 1.0-ml sample solution containing 15 μM enzyme and a 1.0 ml of reference buffer solution were titrated with 5.0, 9.9, 14.7, 19.5, and 24.3 μM Cibacron blue 3GA. The difference spectra thus obtained were corrected for dilution and the absorbance of the free enzyme. *A*, wtPHBH; *B*, R269T.

RESULTS

Enzyme Purification—All His-162 mutants were expressed at high levels (5–10% of total protein) in *E. coli* TG2, and their yield after purification was comparable to that of wtPHBH (26). Comparable levels of protein expression were observed with the Arg-269 variants. However, with the exception of R269K, the Arg-269 variants were not retained on the Cibacron blue 3GA column used in the standard purification protocol. Such change in binding characteristics has also been observed with malate dehydrogenase variants (41). Since Cibacron blue 3GA is a strong inhibitor of wtPHBH, competitive with respect to NADPH (42), it was of interest to study the interaction of the His-162 and Arg-269 variants with the dye free in solution. Fig. 2 shows that the absorption perturbation difference spectra of wtPHBH and R269T, recorded in the presence of increasing concentrations of Cibacron blue 3GA, were nearly identical. It has been suggested that the shape of these difference spectra is indicative of electrostatic enzyme-dye interactions (43, 44). From analyzing the spectral data of Fig. 2 according to the procedure described by Thompson and Stellwagen (30), it was deduced that the dissociation constant of the wtPHBH-Cibacron blue 3GA complex (K_d = 0.34 ± 0.05 μM) is about one order of magnitude lower than the dissociation constant of the R269T-Cibacron blue 3GA complex (K_d = 4.6 ± 1.2 μM). Similar results as with wtPHBH were obtained for R269K and the His-162 variants. However, the affinity between Cibacron blue 3GA and the other Arg-269 mutants compared more favorable with that of R269T (not shown). Neither the dissociation con-

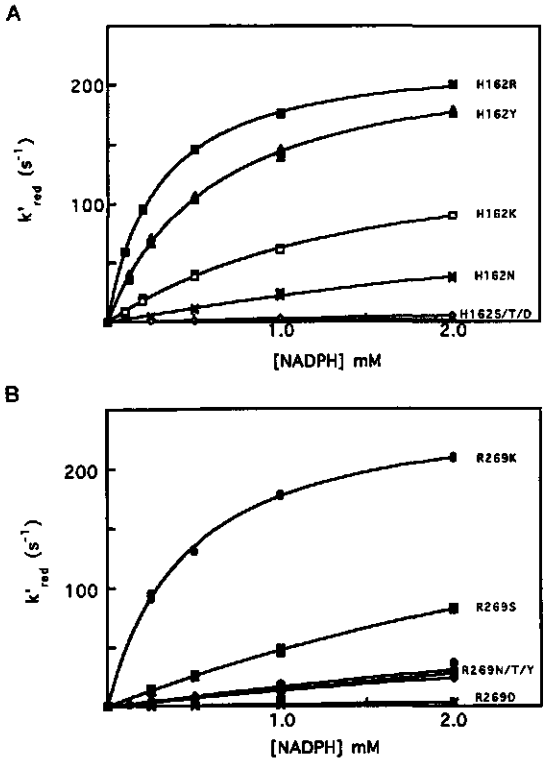

FIG. 3. **Kinetics of the reductive half-reaction of His-162 and Arg-269 mutants.** The experiments were performed in 100 mM Tris/sulfate, pH 8.0, at 25 °C. 30 μM enzyme was anaerobically mixed with varying concentrations of NADPH. Both solutions contained 1 mM POHB. The apparent rate constant of flavin reduction (k'_{red}) as determined from the decrease in absorbance at 450 nm is plotted as a function of the NADPH concentration. *A*, His-162 mutants; *B*, Arg-269 mutants.

stant of the enzyme-dye complexes nor the shape of the difference spectra changed significantly in the presence of 1 mM POHB or 1 mM NADPH. The dissociation constants of the enzyme-dye complexes were also determined from fluorimetric binding studies, using an enzyme concentation of 2 μM. With all His-162 and Arg-269 variants and similar to wtPHBH, quenching of flavin fluorescence was observed. From the titration curves and treating the data according to 1:1 binding (30), dissociation constants of 0.22 ± 0.05 μM and 1.2 ± 0.3 μM were estimated for the wtPHBH-Cibacron blue 3GA and R269T-Cibacron blue 3GA complex, respectively. These values are in reasonable agreement with the values deduced from the absorption difference spectral analysis. Altogether, the binding studies with Cibacron blue 3GA suggest that there is a corrrelation between the affinity of the mutant enzymes with the free and the immobilized dye. However, it is clear that the binding characteristics of the free dye do not simply predict the affinity of the mutant enzymes with the immobilized dye.

Substrate Binding—The His-162 and Arg-269 replacements did not change the optical properties of the flavin prosthetic group. The flavin absorption spectra of all mutants were identical to wtPHBH (26). Moreover, the flavin perturbation difference spectra in the presence of POHB indicated the flavin "in" conformation (14). Similar to the wild-type enzyme (26), the flavin fluorescence of the His-162 and Arg-269 mutants strongly decreased upon POHB binding. For all mutants, substrate binding could be described by simple binary complex formation with dissociation constants ranging from 20 to 40 μM.

Reaction Stoichiometry—Oxygen consumption experiments revealed that in the presence of excess POHB and limiting NADPH, equal amounts of oxygen and NADPH were consumed. No hydrogen peroxide formation was detected when catalase was added at the end of the reactions. HPLC product analysis confirmed that all His-162 and Arg-269 mutants fully coupled enzyme reduction to substrate hydroxylation with stoichiometric formation of 3,4-dihydroxybenzoate.

Steady-state Kinetics—The steady-state kinetic parameters of the His-162 and Arg-269 mutants were studied at pH 8.0, the optimum pH for turnover of wtPHBH (31). In agreement with the dissociation constants reported above, no significant changes in apparent K_m values for POHB were observed (Table II). However, the apparent K_m values for NADPH varied strongly (Table II), indicating that the type of amino acid residue engineered at position 162 or 269 drastically affects coenzyme binding. As can be seen from Table II, H162R, H162Y, and R269K are rather efficient enzymes with similar catalytic properties as wtPHBH. H162K and R269S are less efficient due to a clear increase in the apparent K_m for NADPH. With H162D, H162N, H162S, H162T, R269D, R269N, R269T, and R269Y no reliable turnover rates could be estimated due to impaired NADPH binding.

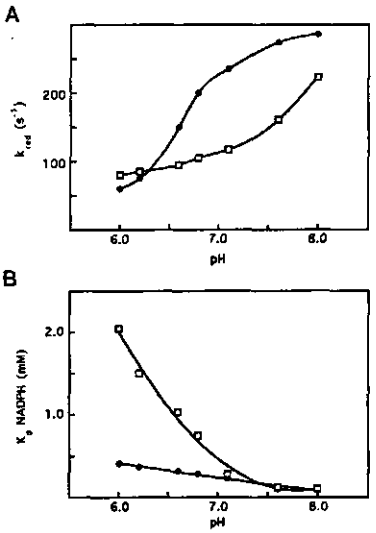

FIG. 4. **pH dependence of the reductive half-reaction of wtPHBH and H162R.** The experiments were performed at 25 °C in Mes and Hepes buffers of constant ionic strength (I = 50 mM). For other conditions see Fig. 3. *A*, maximal reduction rate constants (k_{red}) and *B*, dissociation constants (K_d NADPH) are plotted as a function of pH. wtPHBH (●), H162R (□).

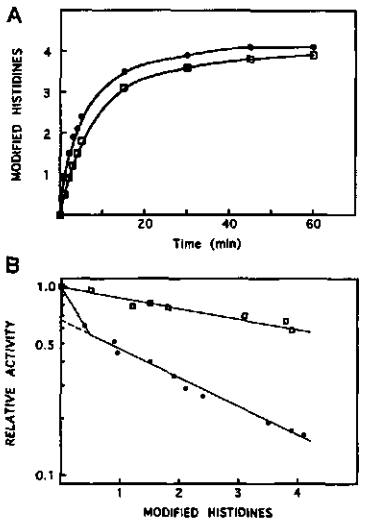

FIG. 5. **Chemical modification of wtPHBH and H162R with diethylpyrocarbonate.** *20 μM enzyme was incubated in 80 mM Mes,* pH 6.0 (I = 0.1 M), with 0.5 mM diethylpyrocarbonate at 25 °C, and the absorbance increase at 244 nm was recorded with time. At time intervals, aliquots were withdrawn from the incubation mixtures and assayed for residual activity. *A*, time dependence of ethoxyformylation: *wtPHBH (●); H162R (□). B, residual enzyme activity as a function of* modified histidines: wtPHBH (●); H162R (□).

Pre-steady-state Kinetics—The NADPH binding was further investigated by stopped-flow kinetics (pH 8.0, 25 °C). In these experiments, the anaerobic reduction of the enzyme-substrate complex was followed by measuring the decrease in FAD absorption at 450 nm with time as a function of the NADPH concentration (22, 45). The rate constant of reduction of the His-162 mutants is strongly dependent on the type of amino acid residue engineered (Fig. 3*A*). With H162R, the rate constant of flavin reduction strongly increased with increasing concentrations of NADPH and a maximal reduction rate constant of about 240 s^{-1} and an apparent K_d for NADPH of 0.23 mM were estimated. These values are in the same range as reported for the wild-type enzyme (26) (Table II), suggesting that the H162R replacement does not significantly affect the effector role of POHB and the mode of NADPH binding. With H162Y and to a lesser extent with H162K, a high rate constant of reduction was found but with a modestly elevated K_d for NADPH, revealing poor NADPH binding (Table II). With the other His-162 mutants, the rate constant of flavin reduction increased slightly with increasing NADPH concentrations (Fig. 3*A*), and the almost linear dependence of the reduction rate constant with NADPH concentration confirmed that these mutants have lost the ability of proper coenzyme binding. In agreement with the steady-state kinetic data, drastic changes in catalysis were observed when the reductive half-reactions of the Arg-269 mutants were studied. Except for R269K, all Arg-269 mutants were rather slowly reduced due to impaired coenzyme binding (Fig. 3*B*, Table II).

Because the ionization state of His-162 seems to play a role in NADPH binding (31), it was of interest to compare the pH dependence of the reductive half-reaction of wtPHBH with that of H162R. As can be seen from Fig. 4*A*, the rate constant of reduction of substrate-complexed wtPHBH increased about 2-fold between pH 6 and 7. For H162R, a similar enhancement in rate constant of reduction was observed between pH 7 and 8 (Fig. 4*A*). Interestingly, wtPHBH showed only a modest increase in K_d NADPH between pH 8 and pH 6, whereas the affinity of H162R for NADPH strongly decreased with decreasing pH (Fig. 4*B*).

Chemical Modification Studies—wtPHBH is readily inactivated by diethylpyrocarbonate at pH 6 (18). This inactivation was tentatively ascribed to the cooperative modification of His-162 and His-289, possibly both involved in NADPH binding (18). Similar to wtPHBH, incubation of H162R with diethylpyrocarbonate at pH 6 led to the modification of about four histidines (Fig. 5*A*). However, in the wild-type enzyme, the initial rate constant of ethoxyformylation is higher than with H162R and is accompanied with a much stronger decline in enzyme activity (Fig. 5*B*). During the initial stage of the chemical modification reactions, the ethoxyformylation of one histidine residue resulted in a loss of activity of more than 50% in wtPHBH and less than 10% in H162R (Fig. 5*B*). In contrast to wtPHBH (K'_m NADPH modified enzyme >100 μM), ethoxyformylation of H162R did not change the apparent K_m NADPH (*cf.* Table II), suggesting that His-162 is a main target of diethylpyrocarbonate modification which is involved in NADPH binding.

Structural Properties—All His-162 and Arg-269 variants were tested by crystallization assays. Crystals with high and moderate quality diffraction properties were obtained for R269T and H162R, both in complex with POHB. The electron density maps of H162R and R269T clearly identified the side chain substitutions (Figs. 6 and 7). The refined three-dimensional structures of H162R and R269T are very similar to the structure of wtPHBH (10) with root mean square differences of

TABLE II

Kinetic parameters of p-hydroxybenzoate hydroxylase variants

Steady-state kinetic parameters were determined at 25 °C in air-saturated 100 mM Tris/sulfate, pH 8.0. Turnover rates (k_{cat}) are apparent maximum values extrapolated to infinite concentrations of POHB and NADPH. Dissociation constants (K_d NADPH) and maximal reduction rate constants (k_{red}) were determined from anaerobic reduction experiments as described in the legend of Fig. 3. Kinetic constants have maximum error values of 10%.

Enzyme	K_m		k_{cat}	K_d NADPH	k_{red}
	POHB	NADPH			
	mM		s^{-1}	*mM*	s^{-1}
PHBH	0.02	0.03	55	0.15	300
H162R	0.03	0.05	55	0.23	240
H162Y	0.03	0.07	45	0.58	230
H162K	0.03	0.20	40	1.50	180
H162N	0.04	>0.5	>10	>5	>70
H162S	0.04	>0.5	>10	>5	>10
H162T	0.04	>0.5	>10	>5	>10
H162D	0.04	>0.5	>10	>5	>10
R269K	0.03	0.07	55	0.45	260
R269Y	0.03	>0.5	>30	>5	>30
R269N	0.03	>0.5	>30	>5	>30
R269S	0.03	0.32	40	>5	>80
R269T	0.03	>0.5	>30	>5	>30
R269D	0.06	>0.5	>10	>5	>10

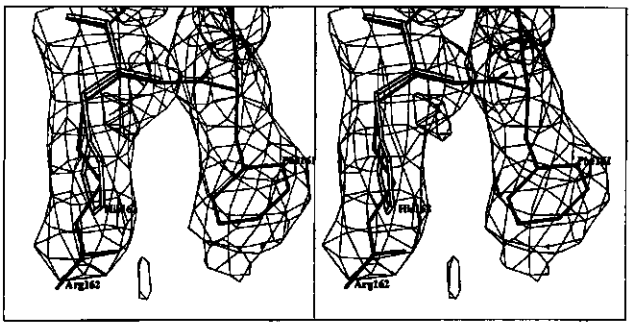

FIG. 6. **Stereo drawing of an F_o-F_c omit map of H162R, contoured at 3 σ.** The atomic model of H162R with residue Arg-162 is drawn in *black bonds*, while the orientation of His-162 in wtPHBH is drawn in *open bonds*.

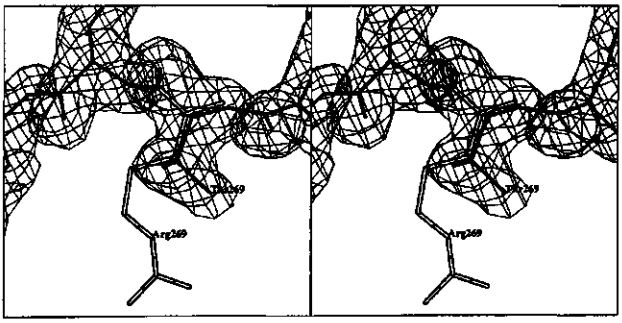

FIG. 7. **Stereo drawing of an F_o-F_c omit map of R269T, contoured at 4 σ.** The atomic model of R269T with residue Thr-269 is drawn in *black bonds*, while the orientation of Arg-269 in wtPHBH is drawn in *open bonds*.

respectively 0.25 and 0.20 Å for 391 equivalent Cα atoms. The His-162 and Arg-269 side chains are situated near the protein surface (Fig. 1) and do not form strong hydrogen bonds with other residues. This feature is conserved in H162R and R269T, leaving the local structure near the sites of mutation unchanged. However, the high B factors of the Arg-162 side chain suggest that this side chain is much more flexible than the His-162 side chain in the wild-type enzyme.

GRID Calculations and Model Building—To get more insight in the binding mode of the pyrophosphate moiety of NADPH, we searched for energetically favored binding sites of the "extended" phosphate groups HPO_4^{2-} and PO_4^{3-} in the wild-type enzyme (10). These calculations were performed with the program GRID (38). Using a GRID spacing of 1 Å we observed one large and a few small density peaks (contoured at an energy level of −15 kcal/mol) in the active site cleft. By

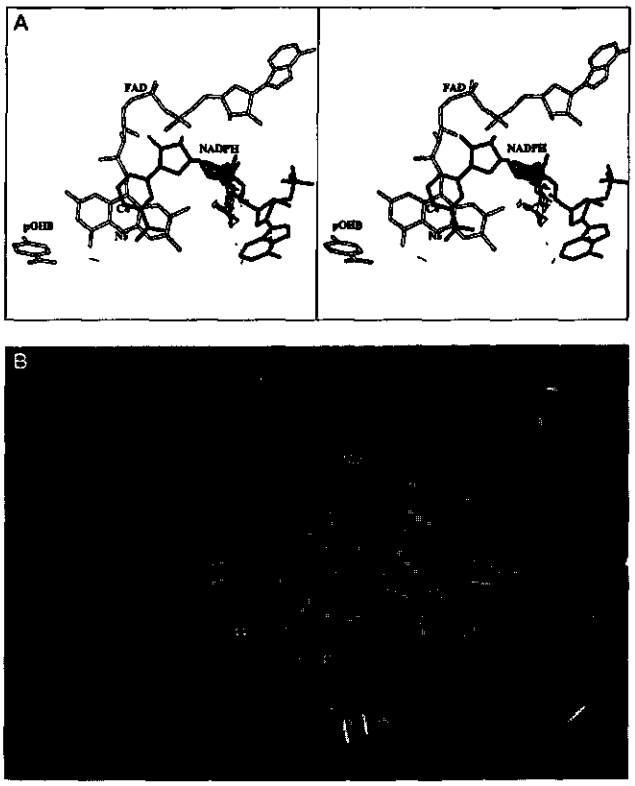

FIG. 8. **Proposed interdomain binding of NADPH.** *A*, Stereo drawing of the three-dimensional model of the ternary wtPHBH-POHB-NADPH complex with POHB and FAD in *open bonds*. The phosphate contours of the GRID calculations are at -15 kcal mol^{-1} and the NADPH molecule (in *dark gray bonds*) was modeled on the positions of GRID peaks. The close interaction between C-4 of the nicotinamide moiety of NADPH and N-5 of the flavin ring is indicated. *B*, closeup of the interdomain cleft leading toward the active site with Arg-33, Arg-42, Arg-44, His-162, and Arg-269 in *magenta*, whereas Tyr-38 is shown in *white*. NADPH is colored in *cyan*, and FAD, POHB, and the protein domains are similarly colored as in Fig. 1.

using the graphics program O (36), the pyrophosphate moiety of NADPH was modeled in the position of an extended GRID peak closely located to His-162 and Arg-269 (Fig. 8*A*). Based on this position, the other parts of the NADPH molecule were modeled in an extended conformation, similar to other NAD(P) complexes (46). In this model, the cofactor reaches the active site through a cleft between the FAD binding and substrate binding domains (Fig. 8*B*). This mode of interdomain binding is new among known NAD(P)-dependent enzymes (46). The nicotinamide was placed at the *re*-side (47) and parallel to the flavin ring (Fig. 8*A*). Attempts to place the nicotinamide such that the pro-*S* hydrogen would be transferred were unsuccessful due to steric hindrance of Pro-293. In the pro-*R* configuration, the nicotinamide ring fitted well, in full agreement with previous studies (48).

There has been discussion about whether the flavin ring would be reduced in the "in" or in the "out" position. In the in position, small protein conformational changes are necessary, because too short contacts exist between the nicotinamide ring of NADPH and residues 290–297 which are part of the highly conserved active site loop (16). In the out position, no such short contacts exist, and the NADPH complex was therefore modeled in the out position. The C-4 atom is 3.9 Å apart from the N-5 of the flavin ring to allow hydride transfer (Fig. 8*A*). Recent results supported the finding that mobility of the flavin ring is necessary for optimal reduction by NADPH (15) and that NADPH reduces the flavin ring probably in the out conformation (49). In the final model, the carboxamide moiety of the nicotinamide ring is in hydrogen bonding distance with Ala-266 and Pro-293 at the *re*-side of the flavin ring and the nicotinamide-ribose part is situated in the entrance toward the active site pocket and interacts via its hydroxyl groups with the highly conserved Asp-286 of the active site loop and with the ribityl moiety of FAD.

As mentioned before, the pyrophosphate moiety of NADPH is situated between His-162 and the highly mobile Arg-269 side chain. Additionally favorable interactions of the helix H7 dipole moment may occur with the negatively charged pyrophosphate

moiety (16). The pyrophosphate moiety also interacts with Arg-44, Phe-161, and is close to His-162. The adenine ring of the adenosine moiety interacts with Tyr-38. Finally, the 2'-phosphate of the adenine-ribose is placed in the helix H2 region and interacts closely with Arg-33 and to a lesser extent with Tyr-38 and Arg-42 (distance of about 4–5 Å). Site-directed mutagenesis studies have shown that these residues play an important role in NADPH binding (1, 22, 50) and that helix H2 is involved in determining the coenzyme specificity (3).

DISCUSSION

In this report we have described the catalytic and structural properties of His-162 and Arg-269 variants of *p*-hydroxybenzoate hydroxylase from *P. fluorescens*. The results clearly establish that His-162 and Arg-269 play an important role in NADPH recognition. Flavin spectral analysis and substrate hydroxylation experiments revealed no significant changes in the active site. From this and the structural properties of H162R and R269T it is concluded that the poor catalytic efficiency of the majority of the mutant proteins can be ascribed to impaired NADPH binding.

His-162 is part of a novel conserved sequence motif in flavoprotein hydroxylases with a putative role in FAD and NAD(P)H binding (16). In *p*-hydroxybenzoate hydroxylase, this sequence motif (residues 153–166) extends from strand A4 to helix H7 and includes a large turn (residues 158–163), with His-162 and the structurally important Asp-159 and Gly-160. His-162 is conserved in *p*-hydroxybenzoate hydroxylases of known sequence and a positive charged residue is present at this position in other flavoprotein hydroxylases (16). Replacement of His-162 by Ser, Thr, Asn, and Asp results in inefficient flavin reduction due to impaired coenzyme binding. NADPH binding is only moderately affected in the H162R, H162Y, and H162K variants, suggesting that both the bulkiness and hydrogen bonding capacity of residue 162 are of importance in NADPH recognition. Our results agree with a chemical modification study of salicylate hydroxylase, which suggested that Lys-165, the equivalent of His-162 in *p*-hydroxybenzoate hydroxylase, is involved in binding the pyrophosphate moiety of NADH (51).

At pH 6, H162R interacts much weaker with NADPH than wtPHBH, while at pH 8, the interaction is about the same. Groups with a pK_a value in this range are His-162 (free $pK_a \sim 6.2$) and the 2'-phosphate moiety of NADPH ($pK_a \sim 6.5$) (52). A possible explanation could be the following. At pH 6, His-162 is protonated which leads to a stronger interaction with the pyrophosphate moiety of NADPH. However, the 2'-phosphate of NADPH is also protonated which leads to a weaker interaction with Arg-33 and Arg-44 (Fig. 8*B*). At pH 8, the situation is reversed; His-162 is uncharged which leads to weaker interaction, while deprotonation of the 2'-phosphate of NADPH leads to a stronger interaction. These two effects are compensatory and may explain the nearly constant binding between pH 6 and 8 of NADPH and wtPHBH. For H162R, the situation is different. Arg-162 is protonated at both pH 6 and 8, favoring the interaction with the pyrophosphate of NADPH at both values of pH. At pH 8, also the deprotonated 2'-phosphate of NADPH will contribute to the binding strength. At this pH, the binding of NADPH to H162R is about as strong as with wtPHBH, suggesting that the extra ionic interaction of Arg-162 with the pyrophosphate compensates the intrinsic weaker NADPH binding of H162R. At pH 6, the 2'-phosphate of NADPH gets protonated, leading to weaker interaction not compensated by the creation of an additional ionic interaction elsewhere, which would nicely explain the observed weaker NADPH binding of H162R at pH 6.

Arg-269, located in the substrate binding domain, proved to be even more essential for NADPH recognition. Except for R269K, all Arg-269 variants have lost the ability of proper NADPH binding. This is in agreement with the poor catalytic properties of the R269A isoenzyme from *P. fluorescens* (53), and points to an electrostatic interaction between Arg-269 and NADPH. Furthermore, the high resolution x-ray structure of R269T shows that impaired NADPH binding is not caused by structural changes.

GRID calculations revealed an energetically favorable binding site for dianionic pyrophosphate near the N terminus of helix H7, supporting our earlier proposal (16) that the positive dipole of this helix is important for binding the pyridine nucleotide cofactor. The properties of the His-162 and Arg-269 variants and the GRID calculations suggest that the pyrophosphate moiety of NADPH interacts with the side chains of His-162 and Arg-269. This interdomain binding mode is in agreement with the involvement of Arg-42 (50) and Arg-44 (22) in NADPH binding, and the role of helix H2 in determining the coenzyme specificity (3).

Recent studies have shown that the flavin ring is mobile and that it can move in and out of the active site (13–15). In our model, we assumed that the flavin is in the out conformation in the NADPH complex. However, while our model fully explains all available mutagenesis and biochemical data, it is still very well possible that the flavin ring assumes an intermediate conformation in the NADPH complex. Further studies will be necessary to firmly establish the position of the flavin in the NADPH complex.

In conclusion, this report lends strong support for an interdomain binding of NADPH in *p*-hydroxybenzoate hydroxylase. There are only a few "non-Rossmann" fold enzymes of known three-dimensional structure with an interdomain binding mode of the pyridine nucleotide cofactor. These enzymes include isocitrate dehydrogenase from *E. coli* (54, 55), isopropylmalate dehydrogenase from *Thermus thermophilus* (56), the ribosome-inactivating protein trichosanthin isolated from root tuber (57), beef liver catalase (58), catalase from *Proteus mirabilis* (59), and glycogen phosphorylase *b* (60). In some of these proteins, a high flexibility of the nicotinamide nucleoside moiety is observed. In *p*-hydroxybenzoate hydroxylase, such flexibility could be essential for the recognition of the flavin ring, leading to the unique effector specificity (8).

Acknowledgment—We thank Denise Jacobs for assistance in the chemical modification experiments.

REFERENCES

1. Van Berkel, W. J. H., Eppink, M. H. M., Van der Bolt, F. J. T., Vervoort, J., Rietjens, I. M. C. M. & Schreuder, H. A. (1997) in *Flavins and Flavoproteins XII* (Stevenson, K., Massey, V., Williams, Ch., Jr., eds) University Press, Calgary, pp. 305–314
2. Stanier, R. Y. & Ornston, L. N. (1973) *Adv. Microb. Physiol.* **9**, 89–151
3. Seibold, B., Matthes, M., Eppink, M. H. M., Lingens, F., Van Berkel, W. J. H. & Müller, R. (1996) *Eur. J. Biochem.* **239**, 469–478
4. Entsch, B. & van Berkel, W. J. H. (1995) *FASEB J.* **9**, 476–483
5. Husain, M. & Massey, V. (1979) *J. Biol. Chem.* **254**, 6657–6666
6. Entsch, B., Ballou, D. P. & Massey, V. (1976) *J. Biol. Chem.* **251**, 2550–2563
7. Entsch, B. & Ballou, D. P. (1989) *Biochim. Biophys. Acta* **999**, 313–322
8. Spector, T. & Massey, V. (1972) *J. Biol. Chem.* **247**, 4679–4687
9. Wierenga, R. K., de Jong, R. J., Kalk, K. H., Hol, W. G. J. & Drenth, J. (1979) *J. Mol. Biol.* **131**, 55–73
10. Schreuder, H. A., Prick, P. A. J., Wierenga, R. K., Vriend, G., Wilson, K. S., Hol, W. G. J. & Drenth, J. (1989) *J. Mol. Biol.* **208**, 679–696
11. Müller, F., Voordouw, G., Van Berkel, W. J. H., Steennis, P. J., Visser, S. & Van Rooijen, P. (1979) *Eur. J. Biochem.* **101**, 235–244
12. Wierenga, R. K., Drenth, J. & Schulz, G. E. (1983) *J. Mol. Biol.* **167**, 725–739
13. Schreuder, H. A., Mattevi, A., Obmolova, G., Kalk, K. H., Hol, W. G. J., Van der Bolt, F. J. T. & Van Berkel, W. J. H. (1994) *Biochemistry* **33**, 10161–10170
14. Gatti, D. L., Palfey, B. A., Lah, M. S., Entsch, B., Massey, V., Ballou, D. P. & Ludwig, M. L. (1994) *Science* **266**, 110–114
15. Van Berkel, W. J. H., Eppink, M. H. M. & Schreuder, H. A. (1994) *Protein Sci.* **3**, 2245–2253
16. Eppink, M. H. M., Schreuder, H. A. & van Berkel, W. J. H. (1997) *Protein Sci.* **6**, 2454–2458
17. Van der Laan, J. M., Schreuder, H. A., Swarte, M. B. A., Wierenga, R. K., Kalk, K. H., Hol, W. G. J. & Drenth, J. (1989) *Biochemistry* **28**, 7199–7205

18. Wijnands, R. & Müller, F. (1982) *Biochemistry* **21**, 6639–6646
19. Wijnands, R. A., Müller, F. & Visser, A. J. W. G. (1987) *Eur. J. Biochem.* **163**, 535–544
20. Van Berkel, W. J. H., Müller, F., Jekel, P. A., Weijer, W. J., Schreuder, H. A. & Wierenga, R. K. (1988) *Eur. J. Biochem.* **176**, 449–459
21. Eppink, M. H. M., Jacobs, D. & van Berkel, W. J. H. (1997) in *Flavins and Flavoproteins XII* (Stevenson, K., Massey, V., Williams, Ch. Jr., eds) University Press, Calgary, pp. 315–318
22. Eppink, M. H. M., Schreuder, H. A. & Van Berkel, W. J. H. (1995) *Eur. J. Biochem.* **231**, 167–165
23. Kunkel, T. A., Roberts, J. D. & Zakour, R. A. (1987) *Methods Enzymol.* **154**, 367–382
24. Eschrich, K., van Berkel, W. J. H., Westphal, A. H., de Kok, A., Mattevi, A., Obmolova, G., Kalk, K. H. & Hol, W. G. J. (1990) *FEBS Lett.* **277**, 197–199
25. Sanger, F., Nicklen, S. & Coulson, A. R. (1977) *Proc. Natl. Acad. Sci. U. S. A.* **74**, 5463–5467
26. Van Berkel, W. J. H., Westphal, A. H., Eschrich, K., Eppink, M. H. M. & de Kok, A. (1992) *Eur. J. Biochem.* **210**, 411–419
27. Entsch, B. (1990) *Methods Enzymol.* **188**, 138–147
28. Van Berkel, W. J. H. & Müller, F. (1987) *Eur. J. Biochem.* **167**, 35–46
29. Entsch, B., Palfey, B. A., Ballou, D. P. & Massey, V. (1991) *J. Biol. Chem.* **266**, 17341–17349
30. Thompson, S. T. & Stellwagen, E. (1976) *Proc. Natl. Acad. Sci. U. S. A.* **73**, 361–365
31. Van Berkel, W. J. H. & Müller, F. (1989) *Eur. J. Biochem.* **179**, 307–314
32. Müller, F. & Van Berkel, W. J. H. (1982) *Eur. J. Biochem.* **128**, 21–27
33. Eschrich, K., Van der Bolt, F. J. T., De Kok, A. & Van Berkel, W. J. H. (1993) *Eur. J. Biochem.* **216**, 137–146
34. Wijnands, R. A., Van der Zee, J., Van Leeuwen, J. W., Van Berkel, W. J. H. & Müller, F. (1984) *Eur. J. Biochem.* **139**, 637–644
35. Kabsch, W. (1988) *J. Appl. Crystallogr.* **21**, 916–924
36. Jones, T. A., Zou, J.-Y., Cowan, S. & Kjeldgaard, M. (1991) *Acta Crystallogr. Sec. A* **47**, 110–119
37. Brünger, A. T. (1992) *X-plor*, Version 3.1, a system for the X-ray crystallography and NMR, Yale University Press, New Haven, CT
38. Goodford, P. J. (1985) *J. Med. Chem.* **28**, 849–857
39. Brooks, B. R., Bruccoleri, R. E., Olafson, B. D., States, D. J., Swiminathan, S. & Karplus, M. (1983) *J. Comp. Chem.* **4**, 187–217
40. Engh, R. A. & Huber, R. (1991) *Acta Crystallogr. Sec. A* **47**, 392–400
41. Breiter, D. R., Resnik, E. & Banaszak, L. J. (1994) *Protein Sci.* **3**, 2023–2032
42. Müller, F., Van Berkel, W. J. H. & Steenus, P. J. (1983) *Biochem. Int.* **7**, 115–122
43. Subramanian, S. (1982) *CRC Crit. Rev. Biochem.* **16**, 169–205
44. Prestera, T., Prochaska, H. J. & Talalay, P. (1992) *Biochemistry* **31**, 824–833
45. Howell, L. G., Spector, T. & Massey, V. (1972) *J. Biol. Chem.* **247**, 4340–4350
46. Bell, C. E., Yeates, T. O. & Eisenberg, D. (1997) *Protein Sci.* **6**, 2084–2096
47. Manstein, D. J., Pai, E. F., Schopfer, L. M. & Massey, V. (1986) *Biochemistry* **25**, 6807–6816
48. You, K.-S. (1985) *Crit. Rev. Biochem.* **17**, 313–451
49. Palfey, B. A., Ballou, D. P. & Massey, V. (1997) *Biochemistry* **36**, 15713–15723
50. Eppink, M. H. M., Schreuder, H. A. & Van Berkel, W. J. H. (1998) *Eur. J. Biochem.* **253**, 194–201
51. Suzuki, K., Mizuguchi, M., Gomi, T. & Itagaki, E. (1996) *J. Biochem.* **117**, 579–585
52. Mas, M. T. & Colman, R. F. (1984) *Biochemistry* **23**, 1675–1683
53. Shuman, B. & Dix, T. A. (1993) *J. Biol. Chem.* **268**, 17057–17062
54. Hurley, J. H., Dean, A. M., Koshland Jr., D. E. & Stroud, R. M. (1991) *Biochemistry* **30**, 8671–8678
55. Stoddard, B. L., Dean, A. & Koshland, D. E., Jr. (1993) *Biochemistry* **32**, 9310–9316
56. Hurley, J. H., Dean, A. M. (1994) *Structure* **2**, 1007–1016
57. Xiong, J-P., Xia, Z-X. & Wang, Y. (1994) *Nat. Struct. Biol.* **1**, 695–700
58. Fita, I. & Rossmann, M. G. (1985) *Proc. Natl. Acad. Sci. U. S. A.* **82**, 1604–1608
59. Gouet, P., Jouve, H-M. & Dideberg, O. (1995) *J. Mol. Biol.* **249**, 933–954
60. Stura, E. A., Zanotti, G., Babu, Y. S., Sansom, M. S. P., Stuart, D. I., Wilson, K. S. & Johnson, L. N. (1983) *J. Mol. Biol.* **170**, 529–565

CHAPTER 7

Phe161 and Arg166 variants of *p*-hydroxybenzoate hydroxylase. Implications for NADPH recognition and structural stability

Michel H.M. Eppink, Christine Bunthof, Herman A. Schreuder, and Willem J.H. van Berkel

FEBS Lett. 443: 151-155 (1999)

Phe^{161} and Arg^{166} variants of *p*-hydroxybenzoate hydroxylase

Implications for NADPH recognition and structural stability

Michel H.M. Eppink[a], Christine Bunthof[a], Herman A. Schreuder[b], Willem J.H. van Berkel[a,*]

[a] *Department of Biomolecular Sciences, Laboratory of Biochemistry, Wageningen University Research Centre, Dreijenlaan 3, 6703 HA Wageningen, The Netherlands*
[b] *Core Research Functions, Hoechst Marion Roussel, D-65926 Frankfurt, Germany*

Received 9 November 1998; received in revised form 16 December 1998

Abstract **Phe^{161} and Arg^{166} of *p*-hydroxybenzoate hydroxylase from *Pseudomonas fluorescens* belong to a newly discovered sequence motif in flavoprotein hydroxylases with a putative dual function in FAD and NADPH binding [1]. To study their role in more detail, Phe^{161} and Arg^{166} were selectively changed by site-directed mutagenesis. F161A and F161G are catalytically competent enzymes having a rather poor affinity for NADPH. The catalytic properties of R166K are similar to those of the native enzyme. R166S and R166E show impaired NADPH binding and R166E has lost the ability to bind FAD. The crystal structure of substrate complexed F161A at 2.2 Å is indistinguishable from the native enzyme, except for small changes at the site of mutation. The crystal structure of substrate complexed R166S at 2.0 Å revealed that Arg^{166} is important for providing an intimate contact between the FAD binding domain and a long excursion of the substrate binding domain. It is proposed that this interaction is essential for structural stability and for the recognition of the pyrophosphate moiety of NADPH.**

Key words: *p*-Hydroxybenzoate hydroxylase; Flavoprotein monooxygenase; Crystal structure; NADPH binding; Sequence motif; Site-directed mutagenesis

1. Introduction

p-Hydroxybenzoate hydroxylase (PHBH) from *Pseudomonas fluorescens* is a member of the family of NAD(P)H-dependent flavoprotein monooxygenases [2]. The enzyme catalyzes the conversion of 4-hydroxybenzoate (POHB) into 3,4-dihydroxybenzoate, an intermediate step in the degradation of aromatic compounds in soil microorganisms [3].

The crystal structure of the enzyme-substrate complex of PHBH is known in atomic detail [4] but the binding mode of NADPH is unclear. In contrast to many dehydrogenases and reductases, PHBH and related enzymes lack a well-defined domain for binding the pyridine nucleotide cofactor [5]. Site-specific modifications of PHBH have provided some insight into the mode of NADPH binding [6–8]. From these studies it was proposed that the pyrophosphate moiety of NADPH interacts with His^{162} of the FAD binding domain and Arg^{269} of the substrate binding domain and that helix H2 is involved in binding the 2′-phosphate ribose moiety of NADPH [8]. Earlier modelling studies suggested that the 2′-phosphate of NADPH interacts with Arg^{166} [9–11], and that Phe^{161} shields NADPH from entering the active site [12]. Both these residues are located near the protein surface (Fig. 1) and belong to a recently discovered sequence motif presumably involved in both FAD and NADPH binding [1]. Within this so-called DG sequence, Phe^{161} is variable whereas Arg^{166} is highly conserved [1].

To study their role in NADPH binding, we selectively altered Phe^{161} and Arg^{166} of PHBH by site-directed mutagenesis. The catalytic properties of the mutant proteins are described together with the crystal structures of F161A and R166S. It is shown that both residues are involved in NADPH binding and that Arg^{166} is important for structural stability. The implications for NADPH binding are discussed. Some preliminary results have been presented elsewhere [13].

2. Materials and methods

2.1. Mutagenesis and enzyme purification

Mutations were introduced in the *pobA* gene encoding PHBH, essentially as described elsewhere [14]. The oligonucleotide 5′-GGCATCTCGXXXCAATCGATCC-3′ (where XXX describes the replacement of CGG for AAA (R166K), GAA (R166E) and AGT (R166S), respectively), and the oligonucleotide 3′-GCGATGGCXXXCACGGCATCTCGC-5′, where XXX describes the replacement of TTC for GCC (F161A) and GGC (F161G), respectively), were used for the construction of the mutant proteins. All mutations were confirmed by nucleotide sequencing according to the method of Sanger et al. [15]. Purification of PHBH variants was done according to procedures reported earlier [6,16]. The expression levels and yields of F161A, F161G and R166K were comparable to the wild-type enzyme [16]. For R166S and R166E, a rather poor expression was observed, which resulted in a 10- and 100-fold lower yield of pure enzyme, respectively.

2.2. Analytical and physical methods

Molar absorption coefficients for protein-bound FAD were determined in 50 mM sodium phosphate, pH 7.0 by recording absorption spectra in the absence and presence of 0.1% SDS [17]. Absorption difference spectra between free and substrate complexed enzymes were recorded as reported earlier [7]. Dissociation constants of enzyme-substrate complexes were determined fluorimetrically [18]. PHBH activity was routinely assayed in 100 mM Tris/sulfate, pH 8.0, containing 0.5 mM EDTA, 0.2 mM NADPH, 0.2 mM POHB and 10 μM FAD [19]. Steady-state kinetic parameters were determined at pH 8.0 [20]. Rapid-reaction kinetics were carried out using a stopped flow spectrophotometer, type SF-51, from High-Tech Scientific Inc. Rate constants for anaerobic flavin reduction were estimated from kinetic traces recorded at 450 nm (pH 8.0, 25°C) [6]. Uncoupling of substrate hydroxylation was quantified by oxygen consumption experiments performed in the absence and presence of catalase [20]. Aromatic products were identified by reverse-phase HPLC [17]. The thermal stability of PHBH variants was studied in 50 mM potassium phosphate, pH 7.0, essentially as described elsewhere [18].

2.3. Crystallization, data collection and structural refinement

Crystallization of substrate complexed F161A and R166S and collection of X-ray diffraction data were performed as reported earlier

*Corresponding author. Fax: (31) (317) 484801.
E-mail: willem.vanberkel@fad.bc.wau.nl

PII: S0014-5793(98)01726-8

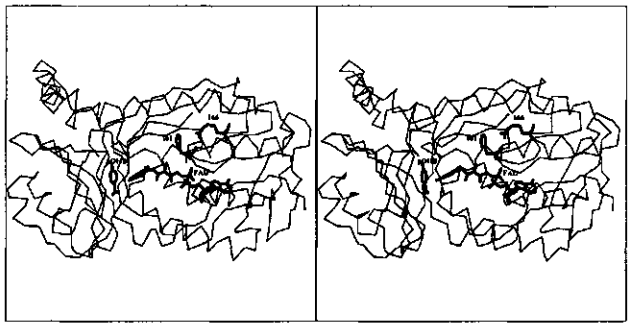

Fig. 1. Stereoview of the Cα backbone of the enzyme-substrate complex of PHBH. 4-Hydroxybenzoate (POHB), cofactor (FAD), Phe^{161} and Arg^{166} are indicated.

[6]. With R166E, no suitable crystals were obtained. A starting electron density map was calculated based on the structure of the wild-type enzyme/substrate complex [4], after a correction had been made for the slightly different cell dimensions (Table 1). The starting *R*-factor was 0.244 for F161A for data between 8.0 Å and 2.2 Å, and 0.245 for R166S for data between 8.0 Å and 2.0 Å. The F_o-F_c omit maps clearly showed the replacement of Phe^{161} by Ala in F161A (Fig. 2A), and Arg^{166} by Ser in R166S (Fig. 3A). With the graphics program *O* [21], the mutated residues were changed and fitted in the electron-density map. The complete protein models were inspected and corrected where necessary. Refinement was carried out by energy minimization and temperature-factor refinement using the program XPLOR [22]. For F161A overall anisotropic *B*-factors were refined and applied to the dataset, with the following *B*-factors: $B11 = 1.08$ Å^2; $B22 = -1.01$ Å^2; $B33 = -0.06$ Å^2. The final structures were obtained after five cycles of map inspection and refinement. The final *R*-factors are 0.179 and 0.183 for F161A and R166S, respectively. The X-ray diffraction data and refinement statistics are summarized in Table 1. The coordinates will be deposited in the Brookhaven Protein Data Bank.

3. Results

3.1. Structural properties

The overall structures of F161A and R166S are very similar to the structure of wild-type PHBH [4], with root mean square differences of respectively 0.18 Å and 0.22 Å for 391 equivalent Cα atoms. Fig. 2B shows that substitution of Phe^{161} for Ala results in a weaker interaction between the backbone oxygen of Phe^{161} and the NH1 atom of Arg^{166} (2.7→3.1 Å). Furthermore, a slight shift of the side chain of Arg^{269} was observed. This shift is most probably caused by the lost van der Waals contact between the NH1 of Arg^{269} and CE2 of Phe^{161} (3.1 Å) increasing the mobility of the Arg^{269} side chain as indicated by the temperature factors (52 Å^2→70 Å^2). The structure of R166S clearly revealed a backbone movement (Fig. 3B). The removal of the hydrogen bond interactions between the NH1 of Arg^{166} and the backbone oxygens of Phe^{161} and Ala^{287} results in a shift of helix H7 and adjoining loops, including residues 160–173, of about 0.5–1.0 Å. Consequently, weaker hydrogen bond interactions were present in this region, resulting in higher flexibility of this part of the protein as indicated by increased average temperature factors of 42.0 Å^2 instead of 27.5 Å^2 for wild-type PHBH.

3.2. Physical properties

Fluorescence binding studies revealed that the dissociation constant of the enzyme-substrate complex was not affected by the Phe^{161} and Arg^{166} replacements. With all mutants, K_d values of 30 ± 5 μM (pH = 7.0) were estimated, values similar to the wild-type enzyme [18]. Moreover, the nearly identical shape and intensity of flavin absorption difference spectra between the free enzymes and the enzyme-substrate complexes (not shown) suggest that the mode of flavin and substrate binding in the mutant proteins compares favorably with that of wild-type PHBH [23]. The only exception is R166E where no reliable absorption difference spectrum could be obtained due to impaired FAD binding.

3.3. Catalytic properties

The catalytic properties of the mutant proteins were studied at pH 8.0, the optimum pH for turnover of the wild-type enzyme [18]. No hydrogen peroxide production was detected in oxygen consumption experiments, showing that the Phe^{161} and Arg^{166} mutants tightly couple oxygen reduction to sub-

Table 1
Data collection and refinement statistics of the enzyme-substrate complexes of F161A and R166S

Complex	F161A	R166S
Cell dimensions (Å)		
a	71.7	72.2
b	146.3	146.8
c	88.5	88.9
Space group	$C222_1$	$C222_1$
Unique reflections	27 343	22 860
Resolution (Å)	2.0	2.2
R_{sym} (%)	4.9	5.5
Completeness (%)	94.4	92.5
Initial *R*-factor	24.4	24.5
Final *R*-factor	17.9	18.5
Water molecules	292	218
rms of bond lengths (Å)	0.009	0.009
rms of bond angles (deg)	1.43	1.46
Average *B*-factors (Å^2)		
protein	27.2	30.3
flavin ring	14.2	19.2
substrate	14.0	21.6

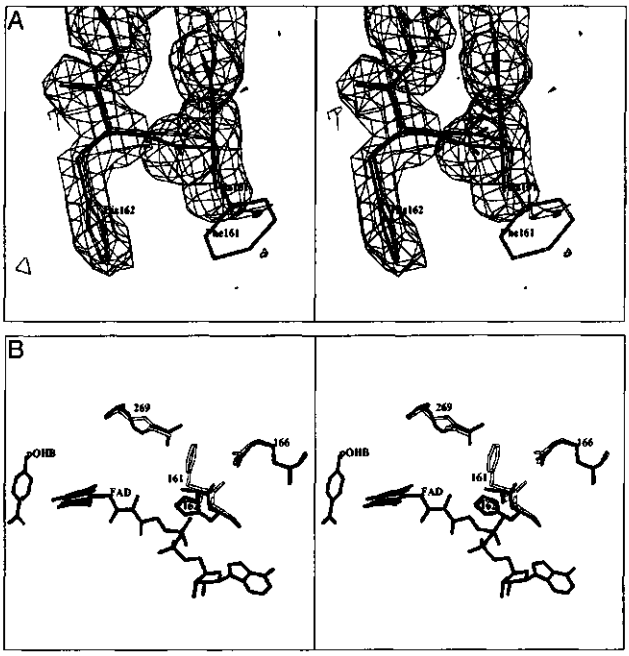

Fig. 2. Crystal structure of F161A in complex with POHB. A: Stereo diagram of the omit map of F161A, contoured at 3σ, with the residues 160–164 omitted from the map. The atomic model of F161A is drawn in bold lines, while Phe[161] of wild-type PHBH is indicated in open lines. B: Superposition of the structures of wild-type PHBH and F161A in complex with POHB. The structure of the wild-type enzyme is drawn in open bonds and the structure of F161A is shown in solid bonds.

strate hydroxylation. As can be seen from Table 2, the Phe[161] and Arg[166] replacements did not strongly affect the apparent K_m POHB. However, with some of the mutant proteins, the apparent K_m NADPH was considerably higher than with the wild-type enzyme. The most profound effects were observed with F161A, R166S and R166E, which all showed a more than five-fold increase in K_m NADPH (Table 2). With all mutants, no activity was found with NADH. With the exception of R166E, all mutants showed turnover rates comparable to wild-type enzyme. The very low turnover rate observed for R166E must be due to some structural effect since this mutant binds poorly FAD. Activity measurements in the absence and presence of varying amounts of FAD revealed an apparent K_m FAD for R166E of about 5 μM. This value is about two orders of magnitude higher than the corresponding value for the wild-type enzyme [19].

Stopped flow kinetics were performed to follow the anaerobic reduction of the enzyme-substrate complex with time as a function of the NADPH concentration. Table 2 shows that the reduction rates of the mutants are similar to that of the wild-type enzyme and not rate limiting in catalysis. However, in agreement with the results from steady-state kinetics, a 5–10-fold weaker NADPH binding was observed for F161A and R166S. As a consequence of the weak FAD binding, no reliable kinetic parameters could be determined for the reductive half-reaction of R166E.

3.4. Thermal stability

The poor expression of R166S and R166E was taken as a first indication that these mutants are less stable than the wild-type enzyme. This was confirmed by thermoinactivation studies. Fig. 4 compares the time-dependent inactivation of wild-type PHBH and the Arg[166] mutants at pH 7.0, 50°C. From this comparison it is clear that, like wild-type enzyme [18], the substrate complexed Arg[166] mutants are more thermostable than the free enzymes. Moreover, in the absence of substrate wild-type PHBH and R166K are far more stable than R166S and R166E (Fig. 4). This supports the idea that a positively charged residue at position 166 is required for structural stability.

4. Discussion

Phe[161] and Arg[166] of PHBH belong to a newly discovered conserved sequence motif in flavoprotein hydroxylases [1]. These residues are located in a surface accessible loop structure (residues 158–174), including helix H7, with a strained conformation [4]. The side chain of Arg[166] contacts the back-

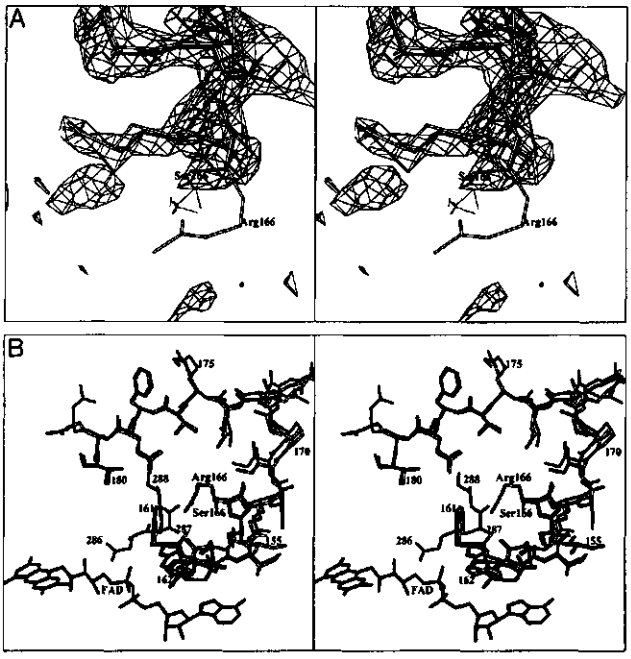

Fig. 3. Crystal structure of R166S in complex with POHB. A: Stereo diagram of the omit map of R166S, contoured at 3σ, with the residues 164–168 omitted from the map. The atomic model of R166S is drawn in bold lines, while Arg^{166} of wild-type PHBH is indicated in open lines. B: Superposition of the structures of wild-type PHBH and R166S in complex with POHB. Wild-type structure is drawn in open bonds and the structure of R166S is shown in solid bonds.

bone oxygen of both Phe^{161} (FAD binding domain) and Ala^{287} (substrate binding domain), whereas the side chain of Phe^{161} interacts with the side chain of Phe^{271} and is situated between the guanidinium groups of Arg^{166} and Arg^{269}. Removal of the aromatic side chain at position 161 slightly weakens the enzyme-NADPH interaction. The crystal structure of F161A at 2.0 Å resolution suggests that this is due to the lost contact between Arg^{269} and Phe^{161}, increasing the mobility of Arg^{269}. Recent mutagenesis studies have indicated that Arg^{269} is of crucial importance for binding the pyrophosphate moiety of NADPH [8]. The catalytic properties of Phe^{161} indicate that Phe^{161} is not essential for NADPH binding. This is in agreement with the recent finding that Phe^{161} is not conserved among flavoprotein hydroxylases [1].

More profound effects on catalysis and in particular on NADPH binding were observed with the Arg^{166} variants. R166K is an efficient enzyme, but the introduction of Ser^{166} significantly decreases the affinity for NADPH. Replacement of Arg^{166} by Glu causes structural perturbations, and impaired binding of NADPH and FAD. We therefore conclude that the catalytic performance and stability of PHBH depends strongly on the ionic character of residue 166. In this respect it is interesting to note that in phenol hydroxylase from the yeast *Trichosporon cutaneum*, the conformation and backbone interactions of the side chain of Arg^{232} are highly similar to its

Table 2
Kinetic parameters of Phe^{161} and Arg^{166} variants of PHBH from *Pseudomonas fluorescens*

Enzyme	K_m POHB (μM)	K_m NADPH (μM)	k_{cat} (s^{-1})	K_i NADPH (μM)	k_{red} (s^{-1})
Wild-type	15	34	55	230	300
F161G	31	112	37	330	300
F161A	18	180	38	1100	300
R166K	30	67	50	220	285
R166S	31	290	40	2200	240
R166E	21	360	5	n.m.	n.m.

The maximum standard error is 10%. n.m.=not measurable.

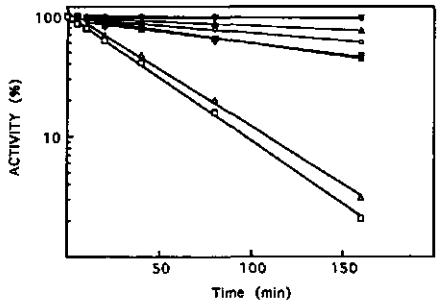

Fig. 4. Time-dependent thermoinactivation of Arg^{166} variants of PHBH. The thermoinactivation of 2 μM enzyme was studied in 50 mM potassium phosphate pH 7.0 at 50°C, in either the absence (open symbols) or presence of 1 mM POHB (filled symbols). Aliquots were withdrawn from the incubation mixtures at intervals and assayed at 25°C, pH 8.0. The remaining activity is plotted as a function of time. Wild-type PHBH (○,●), R166K (▽,▼), R166S (△,▲) and R166E (□,■).

Arg^{166} equivalent of PHBH [24]. The crystal structure of R166S shows a clear shift in the loop structure between residues 159 and 174, comprising helix H7. This movement is caused by the absence of interaction between Ser^{166} and the backbone oxygens of Phe^{161} and Ala^{287} (Fig. 2B). In R166K, the positively charged Lys side chain probably preserves the interactions with the backbone oxygens of Phe^{161} and Ala^{287}. The crystallographic analysis also established that the loop structure comprising residues 160–173 is far more flexible in the R166S mutant than in the wild-type enzyme. The flexibility of this loop decreases the overall structural stability as indicated by the low level of protein expression and the increased rate of thermoinactivation. In line with this, mutant R166E has lost the ability to bind FAD. Residue 166 is at least 10 Å away from the FAD, supporting the idea that the Glu^{166} mutation influences the structural integrity of the FAD binding domain.

In conclusion, the results presented here show that Arg^{166} in PHBH is structurally important and that both Phe^{161} and Arg^{166} are involved in NADPH recognition. However, our studies provide no evidence that Phe^{161} and Arg^{166} interact directly with NADPH. It cannot be excluded that the poor affinity for NADPH in the mutant proteins is caused by the increased flexibility of the loop structure comprising residues 160–173. This loop also contains His^{162}, a residue that is of utmost importance for binding the pyrophosphate moiety of NADPH [8].

References

[1] Eppink, M.H.M., Schreuder, H.A. and van Berkel, W.J.H. (1997) Protein Sci. 6, 2454–2458.
[2] Van Berkel, W.J.H. and Müller, F. (1991) In: Chemistry and Biochemistry of Flavoenzymes (Müller, F., Ed.), Vol. 2, pp. 1–29, CRC Press, Boca Raton, FL.
[3] Harwood, C.S. and Parales, R.E. (1996) Annu. Rev. Microbiol. 50, 553–590.
[4] Schreuder, H.A., Prick, P.A.J., Wierenga, R.K., Vriend, G., Wilson, K.S., Hol, W.G.J. and Drenth, J. (1989) J. Mol. Biol. 208, 679–696.
[5] Entsch, B. and van Berkel, W.J.H. (1995) FASEB J. 9, 476–483.
[6] Eppink, M.H.M., Schreuder, H.A. and van Berkel, W.J.H. (1995) Eur. J. Biochem. 231, 157–165.
[7] Eppink, M.H.M., Schreuder, H.A. and van Berkel, W.J.H. (1998) Eur. J. Biochem. 253, 194–201.
[8] Eppink, M.H.M., Schreuder, H.A. and van Berkel, W.J.H. (1998) J. Biol. Chem. 273, 21031–21039.
[9] Wierenga, R.K., Drenth, J. and Schulz, G.E. (1983) J. Mol. Biol. 167, 725–739.
[10] Van Berkel, W.J.H., Müller, F., Jekel, P.A., Weijer, W.J., Schreuder, H.A. and Wierenga, R.K. (1988) Eur. J. Biochem. 176, 449–459.
[11] Chaiyen, P., Ballou, D.P. and Massey, V. (1997) Proc. Natl. Acad. Sci. USA 94, 7233–7238.
[12] Van der Laan, J.M. (1986) Ph.D. Thesis, University of Groningen, Groningen.
[13] Van Berkel, W.J.H., Eppink, M.H.M., van der Bolt, F.J.T., Vervoort, J., Rietjens, I.M.C.M. and Schreuder, H.A. (1997) In: Flavins and Flavoproteins 1996 (Stevenson, K., Williams, C.H. Jr. and Massey, V., Eds.), pp. 305–314, University Press, Calgary, Alta.
[14] Eschrich, K., van Berkel, W.J.H., Westphal, A., de Kok, A., Matteva, A., Obmolova, G., Kalk, K.H. and Hol, W.G.J. (1990) FEBS Lett. 277, 197–199.
[15] Sanger, F., Nicklen, S. and Coulson, A.R. (1977) Proc. Natl. Acad. Sci. USA 74, 5463–5467.
[16] Van Berkel, W.J.H., Westphal, A., Eschrich, K., Eppink, M. and De Kok, A. (1992) Eur. J. Biochem. 210, 411–419.
[17] Entsch, B., Palfey, B.A., Ballou, D.P. and Massey, V. (1991) J. Biol. Chem. 266, 17341–17349.
[18] Van Berkel, W.J.H. and Müller, F. (1989) Eur. J. Biochem. 179, 307–314.
[19] Müller, F. and van Berkel, W.J.H. (1982) Eur. J. Biochem. 128, 21–27.
[20] Eschrich, K., van der Bolt, F.J.T., de Kok, A. and van Berkel, W.J.H. (1993) Eur. J. Biochem. 216, 137–146.
[21] Jones, T.A., Zou, J.Y., Cowan, S.W. and Kjeldgaard, M. (1991) Acta Crystallogr. A47, 110–119.
[22] Brünger, A.T. (1992) X-PLOR: Version 3.1, A System for X-ray Crystallography and NMR, Yale University Press, New Haven, CT.
[23] Gatti, D.L., Palfey, B.A., Lah, M.S., Entsch, B., Massey, V., Ballou, D.P. and Ludwig, M.L. (1994) Science 266, 110–114.
[24] Enroth, C., Neujahr, H., Schneider, G. and Lindqvist, Y. (1998) Structure 6, 605–617.

CHAPTER 8

4-Hydroxybenzoate hydroxylase from *Pseudomonas* sp. CBS3

Purification, characterization, gene cloning, sequence analysis and assignment of structural features determining the coenzyme specificity

Birgit Seibold, Martina Matthes, Michel H.M. Eppink, Franz Lingens,

Willem J.H. van Berkel and Rudolf Müller

Eur. J. Biochem. 239:469-478 (1996)

Eur. J. Biochem. 239, 469–478 (1996)

4-Hydroxybenzoate hydroxylase from *Pseudomonas* sp. CBS3

Purification, characterization, gene cloning, sequence analysis and assignment of structural features determining the coenzyme specificity

Birgit SEIBOLD[1], Martina MATTHES[2], Michel H. M. EPPINK[3], Franz LINGENS[1], Willem J. H. VAN BERKEL[3] and Rudolf MÜLLER[1]

[1] Institute of Microbiology, Hohenheim University, Stuttgart, Germany
[2] Technical University Hamburg-Harburg, Hamburg, Germany
[3] Department of Biochemistry, Agricultural University, Wageningen, The Netherlands

(Received 4 March 1996) – EJB 96 0301/3

4-Hydroxybenzoate hydroxylase from *Pseudomonas* sp. CBS3 was purified by five consecutive steps to apparent homogeneity. The enrichment was 50-fold with a yield of about 20%. The enzyme is a homodimeric flavoprotein monooxygenase with each 44-kDa polypeptide chain containing one FAD molecule as a rather weakly bound prosthetic group. In contrast to other 4-hydroxybenzoate hydroxylases of known primary structure, the enzyme preferred NADH over NADPH as electron donor. The pH optimum for catalysis was pH 8.0 with a maximum turnover rate around 45°C. Chloride ions were inhibitory, and competitive with respect to NADH.

4-Hydroxybenzoate hydroxylase from *Pseudomonas* sp. CBS3 has a narrow substrate specificity. In addition to the transformation of 4-hydroxybenzoate to 3,4-dihydroxybenzoate, the enzyme converted 2-fluoro-4-hydroxybenzoate, 2-chloro-4-hydroxybenzoate, and 2,4-dihydroxybenzoate. With all aromatic substrates, no uncoupling of hydroxylation was observed.

The gene encoding 4-hydroxybenzoate hydroxylase from *Pseudomonas* sp. CBS3 was cloned in *Escherichia coli*. Nucleotide sequence analysis revealed an open reading frame of 1182 bp that corresponded to a protein of 394 amino acid residues. Upstream of the *pobA* gene, a sequence resembling an *E. coli* promotor was identified, which led to constitutive expression of the cloned gene in *E. coli* TG1. The deduced amino acid sequence of *Pseudomonas* sp. CBS3 4-hydroxybenzoate hydroxylase revealed 53% identity with that of the *pobA* enzyme from *Pseudomonas fluorescens* for which a three-dimensional structure is known. The active-site residues and the fingerprint sequences associated with FAD binding are strictly conserved. This and the conservation of secondary structures implies that the enzymes share a similar three-dimensional fold. Based on an isolated region of sequence divergence and site-directed mutagenesis data of 4-hydroxybenzoate hydroxylase from *P. fluorescens*, it is proposed that helix H2 is involved in determining the coenzyme specificity.

Keywords: cloning; coenzyme specificity; flavoprotein hydroxylase; haloaromatic biodegradation; sequence alignment.

Pseudomonas sp. CBS3 utilizes 4-chlorobenzoate as sole source of carbon and energy (Klages and Lingens, 1980). In this strain, a hydrolytic dechlorination occurs as the initial degradation step, leading to 4-hydroxybenzoate (Müller et al., 1984). This product is then converted in the next step to 3,4-dihydroxybenzoate before the ring is cleaved at the *ortho* position (Klages and Lingens, 1980). The three component enzyme system involved in the conversion of 4-chlorobenzoate to 4-hydroxybenzoate has been thoroughly characterized during the last few years (Elsner et al., 1991a; Chang et al., 1992; Löffler et al., 1995) and 4-chlorobenzoate dehalogenase of *Pseudomonas* sp. CBS3 has been the subject of intensive genetic analysis (Savard et al., 1986; Elsner et al., 1991b; Babbitt et al., 1992). No information is available about the biochemical properties and genetic background of the enzyme converting 4-hydroxybenzoate. To date, the DNA sequences of the *pobA* genes encoding 4-hydroxybenzoate hydroxylase from *Pseudomonas aeruginosa* (Entsch et al., 1988), *Pseudomonas fluorescens* (van Berkel et al., 1992; Shuman and Dix, 1993), *Acinetobacter calcoaceticus* (DiMarco et al., 1993), and *Rhizobium leguminosarum* (Wong et al., 1994) have been reported. However, none of these FAD-dependent hydroxylases are involved in the biodegradation of a halogenated aromatic compound.

The structure and mechanism of 4-hydroxybenzoate hydroxylase from *P. fluorescens* has been studied in great detail (van Berkel and Müller, 1991; Entsch and van Berkel, 1995; Gatti et al., 1996). As a result, this strictly NADPH-dependent enzyme has become the primary model for flavoprotein aromatic hydroxylases that have many characteristics in common. The structure

Correspondence to W. J. H. van Berkel, Department of Biochemistry, Agricultural University, Dreijenlaan 3, NL-6703 HA, Wageningen, The Netherlands
Fax: +31 317 484801.

Enzymes. 4-Hydroxybenzoate 3-monooxygenase [4-hydroxybenzoate, NADPH: oxygen oxidoreductase (3-hydroxylating)] (EC 1.14.13.2); 4-hydroxybenzoate 3-monooxygenase [4-hydroxybenzoate, NAD(P)H: oxygen oxidoreductase (3-hydroxylating)] (EC 1.14.13.33); catalase (EC 1.11.1.6); alkaline phosphatase (EC 3.1.3.1); DNA polymerase I (Klenow fragment) (EC 2.7.7.7); type II site-specific deoxyribonucleases (*Ball*, *Bam*HI, *Eco*RI, *Hin*dIII, *Sau*3A) (EC 3.1.21.4).

Note. The novel nucleotide sequence data published here have been submitted to the EMBL, GeneBank, and DDBJ nucleotide sequence databases and are available under accession number X74827.

of 4-hydroxybenzoate hydroxylase is unusual because there is no well-defined binding site for the NADPH coenzyme (Schreuder et al., 1991). Here, we describe the purification, biochemical characterization, cloning, and sequence analysis of 4-hydroxybenzoate hydroxylase from *Pseudomonas* sp. CBS3. The results show that the enzyme is structurally similar to 4-hydroxybenzoate hydroxylase from *P. fluorescens* but prefers NADH as electron donor. Special emphasis is given to the structural features that determine the coenzyme specificity.

MATERIALS AND METHODS

General. Q-Sepharose FF, Superdex PG-200, Superdex 200 HR 10/30, restriction endonucleases, T4 DNA ligase, the double-stranded deletion kit, the T7 sequencing kit, and deaza T7 sequencing mixes were purchased from Pharmacia LKB; shrimp alkaline phosphatase was from United States Biochemicals; the Geneclean II kit was from Dianova; [^{35}S]dATP[αS] was from Amersham; Good buffers and Cibacron blue 3GA agarose were from Sigma. Bio-Gel P6DG and Bio-Gel HT hydroxyapatite were purchased from Bio-Rad, and benzoate derivatives were obtained from Aldrich; 2-fluoro-4-hydroxybenzoate was synthesized and purified as reported earlier (van Berkel et al., 1994).

Bacterial strains and vectors. *Pseudomonas* sp. CBS3 was originally isolated from garden soil with 4-chlorobenzoate as sole carbon source (Klages and Lingens, 1980). The strain was grown with 5 mM 4-chlorobenzoate as substrate as described. In addition, the bacterial strains *E. coli* JM 107 (Yanisch-Perron et al., 1985) and *E. coli* TG1 (Sambrook et al., 1989) were used in this study. Plasmids used included the broad host-range cosmid pLAFR3 (Friedman et al., 1982) for the construction of the genomic library and high-copy-number plasmid pUC18 as a cloning vector (Yanisch-Perron et al., 1985). M13 vectors mp18 and mp19 were used for DNA sequencing (Yanisch-Perron et al., 1985). *E. coli* strains were grown at 37°C in L-broth (Sambrook et al., 1989). Antibiotics for selective media were used at the following concentrations: ampicillin (100 μg/ml) and tetracycline (12.5 μg/ml). To test *E. coli* clones for the presence of 4-chlorobenzoate dehalogenase activity, cells were incubated in liquid medium containing 4-chlorobenzoate. Positive clones were identified by an increase in chloride concentration during the incubation time. To test *E. coli* clones for 4-hydroxybenzoate hydroxylase activity, cells were incubated in liquid medium containing 4-hydroxybenzoate. After 2 days, all cultures were examined for the product 3,4-dihydroxybenzoate by the method of Arnow (1937).

Preparation, analysis, and manipulation of DNA. Total DNA of *Pseudomonas* sp. CBS3 was prepared according to the method of Marmur (1961). Preparative amounts of plasmid or cosmid DNA were obtained by the method of Birnboim and Doly (1979) and the method of Clewell and Helinski (1969), respectively. For analytical purposes, recombinant plasmid DNA of *E. coli* was isolated by the alkaline lysis method (Sambrook et al., 1989). DNA fragments were isolated from agarose gels with the Geneclean II kit according to the recommendations of the supplier. Transformation of *E. coli* with plasmid DNA was performed by the $CaCl_2$ procedure (Mandel and Higa, 1970).

Analytical methods. 4-Hydroxybenzoate hydroxylase activity was routinely assayed in 100 mM Tris/sulfate, pH 8.0, containing 1 mM 4-hydroxybenzoate, 0.2 mM NADH, 0.5 mM EDTA and 10 μM FAD. The enzyme was preincubated with FAD and NADH for 5 min at 37°C. The reaction was subsequently started by the addition of 4-hydroxybenzoate and the NADH oxidation was followed by recording the absorption decrease at 340 nm. For the determination of the stoichiometry of the reaction, oxygen consumption in the above-mentioned mixture was measured in a closed chamber with a Clark electrode. At the end of the reaction, a catalytic amount of catalase was added to estimate the efficiency of hydroxylation (Eschrich et al., 1993). The aromatic product was identified and quantified by HPLC analysis, using a RP-18 column (20 cm×0.4 cm) that was run in 50 mM sodium-potassium phosphate, pH 5.5/2-propanol (90:10, by vol.). Alternatively, 3,4-dihydroxybenzoate was determined in a colorimetric assay with molybdate-nitrite reagent according to Arnow (1937). Free chloride ions were determined by a Marius chlor-o-counter (Labo International, Delft, the Netherlands) as described by Slater et al. (1985).

Steady-state kinetic parameters of 4-hydroxybenzoate hydroxylase were determined at pH 8.0, essentially as described (Eschrich et al., 1993). pH-dependent activity measurements were performed in 80 mM Mes, pH 5–7, 80 mM Hepes, pH 7–8, 80 mM Hepps, pH 7.5–8.5, and 80 mM Ches, pH 8.5–9.5. The ionic strength of the Good buffers was adjusted to 100 mM with added sodium sulfate (Wijnands et al., 1984). The inhibition by monovalent anions was studied, essentially as described before (Steennis et al., 1973). For the determination of the temperature optimum, the enzyme solution together with FAD and NAD(P)H was preincubated in 80 mM Hepps, pH 8.0 (I = 0.1 M) for 5 min at temperatures between 10°C and 90°C. The reaction was started by the addition of 4-hydroxybenzoate and the measuring time was 5 min.

Absorption spectra were recorded at 25°C on an Aminco DW2000 spectrophotometer. SDS/PAGE and analytical gel filtration (Superdex 200 HR 10/30) were carried out, essentially as reported earlier (van Berkel and Müller, 1987). Protein concentrations were determined by the enhanced alkaline copper assay (Lowry et al., 1951) using bovine serum albumin as a standard. For the identification of the prosthetic group, an aliquot of the enzyme (purified in the absence of FAD) was boiled for 10 min. The protein precipitate was removed by centrifugation at 10000 *g* for 5 min and the yellow supernatant was subjected to HPLC analysis, using a RP-18 column (20 cm×0.4 cm) that was run in 100 mM ammonium acetate, pH 4.8/methanol (80:20, by vol.). The cofactor eluted at the same position as FAD after 9.1 min, whereas FMN eluted after 15.3 min.

The N-terminal sequence of 4-hydroxybenzoate hydroxylase from *Pseudomonas* sp. CBS3 was determined by automated Edman degradation on a Biosystems model 477A gas-phase protein sequencer. This analysis was generously carried out by Dr B. Hauer from BASF AG, Ludwigshafen. Prior to sequencing, 0.5 mg protein was precipitated with trichloroacetic acid, washed with water, dried and finally dissolved in formic acid. The N-terminal sequence (MKTVTRTQVGIIGAGPAGLL) was identical to that deduced from the DNA sequence of the cloned gene. Nucleotide sequence analysis was performed by the dideoxynucleotide chain-terminating method of Sanger et al. (1977). The nucleotide sequences were analysed with the GENMON program (Gesellschaft für Biotechnologische Forschung, Braunschweig, Germany).

Enzyme purification. 50 g frozen *Pseudomonas* sp. CBS3 cells were suspended in 50 ml 50 mM potassium phosphate, pH 7.5, containing 1 mM 4-hydroxybenzoate, 0.5 mM phenylmethylsulfonyl fluoride, 0.5 mM EDTA, 0.5 mM dithiothreitol and 1 mg deoxyribonuclease. Cells were disrupted through a precooled French press and cell debris was removed by centrifugation at 16000 *g* for 20 min. The clarified cell extract was heated under continuous stirring in a 90°C water bath until the temperature of the extract had reached 55°C. The extract was

transferred to a 55 °C water bath and kept there for 5 min. After cooling on ice, the resulting precipitate was removed by centrifugation at 16000 *g* for 30 min. All further operations were performed at 4 °C in buffers containing 0.5 mM dithiothreitol. The supernatant from the heat treatment was diluted twice and applied to a Q-Sepharose FF column (2.5 cm×20 cm) equilibrated with 20 mM Tris/sulfate, pH 7.5. After washing with starting buffer, the enzyme was eluted with a linear gradient of NaCl (0–0.5 *M in 500 ml). Fractions containing the* 4-hydroxybenzoate hydroxylase activity (0.3–0.4 M NaCl) were pooled, and concentrated in an Amicon ultrafiltration cell with YM 30 membrane to about 30 ml. After dialysis against 20 mM Tris/sulfate, pH 7.5, containing 20 µM FAD, the enzyme solution was passed through a Cibacron blue 3GA agarose column (2.5 cm×20 cm) equilibrated in 20 mM Tris/sulfate, pH 7.5. After washing with two volumes of starting buffer, the collected enzyme fraction was concentrated by ultrafiltration to about 8 ml and dialyzed *against 10 mM potassium phosphate, pH 7.6, containing 20 µM* FAD. The enzyme solution was then passed through a hydroxyapatite column (2.5×10 cm), equilibrated in 10 mM potassium phosphate, pH 7.6. After washing with two volumes of starting buffer, the collected enzyme fraction was subjected to a 40–60% ammonium sulfate fractionation. The 60% ammonium sulfate precipitate was collected by centrifugation and dissolved in 3 ml 100 mM potassium phosphate, pH 7.6, containing 100 mM NaCl and 20 µM FAD. In the final step, the enzyme solution was *applied to a Superdex PG-200 column (2.5 cm×100 cm),* equilibrated in 100 mM potassium phosphate, pH 7.6, containing 100 mM NaCl. Active fractions were pooled, concentrated by ultrafiltration to about 6 ml and stored as a 60% ammonium sulfate precipitate at 4 °C.

Cloning and sequence analysis. Total DNA of *Pseudomonas* sp. CBS3 was partially digested with *Sau*3A to generate predominantly 20–35-kb fragments. pLAFR3 DNA was digested with *Hin*dIII and *Eco*RI. The linear cosmid was cut with *Bam*HI and dephosphorylated. Ligation was carried out with 8 µg total DNA fragments and 0.8 µg of left and right cosmid arms. The recombinant DNA was packaged in λ phage using a DNA packaging kit from Boehringer Mannheim. *E. coli* JM 107 was infected with the cosmid-containing phages and transfectants were selected on AM3-plates supplemented with tetracycline (12.5 µg/ml), 5-bromo-4-chloro-3-indolyl-β-D-galactopyranoside and isopropyl thio β-D-galactoside. This selection yielded 2632 recombinant clones, which were screened for the presence of 4-chlorobenzoate dehalogenase activity.

Each of the clones of the genomic library was inoculated in 200 µl liquid medium containing 5 g/l tryptone, 2.5 g/l yeast extract, and 5 mM 4-chlorobenzoate. After seven days at 37 °C, the cultures were checked quantitatively for chloride release. By this method, one clone designated pLAFR3 45–10 C was detected, which was able to dehalogenate 4-chlorobenzoate. During the incubation time, a metabolite accumulated in the culture medium of this clone, which was identified as 3,4-dihydroxybenzoate by HPLC analysis. These results showed that pLAFR3 45–10C carried the genes specifying 4-chlorobenzoate dehalogenation as well as the gene encoding for 4-hydroxybenzoate hydroxylase, and that these genes must be clustered in *Pseudomonas* sp. CBS3. The sequences and properties of the dehalogenase genes have been published by other groups using our strain (Savard et al., 1986; Babbitt et al., 1992).

Subcloning of plasmid pLAFR3 45-10C in pUC18 yielded a 2.8-kb *Pst*I–*Kpn*I fragment as the smallest insert expressing 4-hydroxybenzoate hydroxylase activity. To further localize the *pobA* gene on this fragment, we constructed a series of mutants, which were deleted unidirectionally with exonuclease III and S1 nuclease. The smallest insert containing the intact 4-hydroxybenzoate hydroxylase gene was a 1.6-kb fragment, as judged from 4-hydroxybenzoate hydroxylase activity experiments.

Restriction fragments of the 1.6-kb insert of pUC18 38/1 containing *pobA* from *Pseudomonas* sp. CBS3 and a series of deletion clones were used for sequence determination. A total of 1593 bp, which corresponds to the region between the *Pst*I and the *Eco*RI restriction site, was sequenced. The nucleotide sequence was determined in both directions. Only one open reading frame of appropriate length was found in this fragment, which extends from nucleotides 337 to 1521.

Structure homology modelling. The globular fold of 4-hydroxybenzoate hydroxylase from *Pseudomonas* sp. CBS3 was predicted using the ProMod package, implemented under the Swiss-Model automated protein modelling server (Peitsch, 1995). The three-dimensional model of the crystal structure of the enzyme-substrate complex of 4-hydroxybenzoate hydroxylase from *P. fluorescens* refined at 0.19-nm resolution (Brookhaven Protein Data Bank file 1PBE; Schreuder et al., 1989) served as the template file. Dimer formation of 4-hydroxybenzoate hydroxylase from *Pseudomonas* sp. CBS3 was obtained by superimposing the monomeric model onto a monomer of 4-hydroxybenzoate hydroxylase from *P. fluorescens* and performing a symmetry operation using the cell dimensions of the *P. fluorescens* enzyme (Schreuder et al., 1989). The quality of the predicted three-dimensional protein model of dimeric 4-hydroxybenzoate hydroxylase from *Pseudomonas* sp. CBS3 was assessed by determining the 3D-1D profile score (Lüthy et al., 1992).

Table 1. Purification scheme of 4-hydroxybenzoate hydroxylase from *Pseudomonas* sp. CBS3.

Step	Volume	Protein	Activity	Specific activity	Yield
	ml	mg	U	U/mg	%
Cell extract	100	3170	670	0.2	100
Heat treatment	90	1190	640	0.5	96
Q-Sepharose	160	218	480	2.2	72
Cibacron blue agarose	32	76	310	4.1	46
Hydroxyapatite	10	36	230	6.4	34
Superdex 200	50	15	150	10.0	22

RESULTS

Enzyme purification. Extracts of *Pseudomonas* sp. CBS3 cells, grown with 4-chlorobenzoate as carbon source, catalyzed the NAD(P)H-dependent conversion of 4-hydroxybenzoate to 3,4-dihydroxybenzoate (Klages and Lingens, *1980). In* extracts from cells grown with glucose, no 4-hydroxybenzoate hydroxylase activity was detectable, which indicates that the enyme was inducible. A heat treatment step at 55 °C was necessary to destroy interfering NAD(P)H oxidase activity present in the cell extract. Initial purification of the 4-hydroxybenzoate hydroxylase resulted in substantial loss of activity. Increased enzyme recovery was achieved by purification in the presence of FAD. The results of a typical purification are summarized in Table 1. In contrast to 4-hydroxybenzoate hydroxylase from *P. fluorescens* (Müller et al., 1979), the enzyme was not retarded on Cibacron-blue 3GA agarose. Analysis of the purified enzyme by SDS/PAGE revealed the presence of a single band, which corresponded to

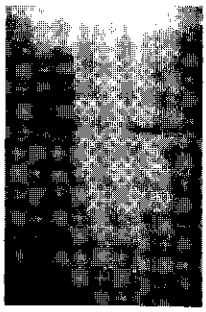

Fig. 1. SDS/PAGE analysis of purified 4-hydroxybenzoate hydroxylase from *Pseudomonas* sp. CBS3. Left lane, marker proteins (from top to bottom: phosphorylase *b*, 94 kDa; bovine serum albumin, 67 kDa; ovalbumin, 43 kDa; carbonic anhydrase, 29 kDa; trypsin inhibitor, 20 kDa; α-lactalbumin, 14.4 kDa); Right lane, purified *p*-hydroxybenzoate hydroxylase from *Pseudomonas* sp. CBS3.

Table 2. Steady-state kinetic parameters of 4-hydroxybenzoate hydroxylase from *Pseudomonas* sp. CBS3. All experiments were performed in air-saturated 80 mM Hepps pH 8.0 (I = 0.1 M), containing 10 μM FAD and 0.5 mM EDTA. Turnover rates (K'_{cat}) and Michaelis constants (K'_m) are apparent values determined at fixed concentrations of either 4-hydroxybenzoate (1 mM) or NADH (0.2 mM).

Substrate	t	K'_{cat}	K'_m
	°C	s^{-1}	μM
4-Hydroxybenzoate	35	7.4 ± 0.4	75 ± 10
NADH	25	6.8 ± 0.4	80 ± 10
	35	11.6 ± 0.5	120 ± 20
	45	16.9 ± 0.8	180 ± 30
NADPH	25	6.6 ± 0.5	140 ± 20
	35	8.6 ± 0.7	160 ± 30
	45	13.3 ± 0.9	200 ± 40

a polypeptide chain molecular mass of about 44 kDa (Fig. 1). Analytical gel filtration resulted in a single symmetrical peak with a retention time identical to that of 4-hydroxybenzoate hydroxylase from *P. fluorescens* (van Berkel and Müller, 1987). From this and running calibration proteins in parallel, a relative molecular mass of about 90 kDa was estimated, which suggests that 4-hydroxybenzoate hydroxylase from *Pseudomonas* sp. CBS3 is a dimer composed of identical subunits.

Catalytic properties. Oxygen consumption experiments revealed that 4-hydroxybenzoate hydroxylase from *Pseudomonas* sp. CBS3 catalyzed the conversion of 4-hydroxybenzoate with the consumption of equimolar concentrations of NAD(P)H and oxygen. The addition of FAD was essential to achieve optimal turnover. From activity experiments performed in the absence or presence of varying amounts of FAD, an apparent K_m value for FAD of 150 nM was estimated. FMN had no effect on the activity. The pH optimum for catalysis was around pH 8 and a maximum turnover rate was observed at 45°C. As can be observed from the kinetic parameters recorded in Table 2, the catalytic efficiency (expressed as K'_{cat}/K'_m NADH) was relatively constant

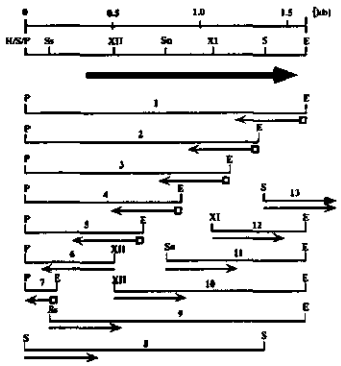

Fig. 2. Restriction map and sequence strategy of the 1.6-kb fragment containing the *pobA* gene of *Pseudomonas* sp. CBS3. The boldfaced arrow indicates the *pobA* region. The arrows represent the direction of sequencing from particular restriction sites. Arrows starting with squares indicate DNA fragments obtained from deletion subclones. Abbreviations for restriction enzymes: E, *Eco*RI (in polycloning site); H, *Hind*III; P, *Pst*I; S, *Sph*I; Sn, *Sna*BI; Ss, *Sst*I; XI, *Xho*I; XII, *Xho*II.

between 25°C and 45°C. 4-Hydroxybenzoate hydroxylase from *Pseudomonas* sp. CBS3 showed a narrow substrate specificity. Besides the primary substrate 4-hydroxybenzoate (100%), the substrate analogs 2-fluoro-4-hydroxybenzoate (50%), 2-chloro-4-hydroxybenzoate (40%), and 2,4-dihydroxybenzoate (8%) were the only compounds that stimulated the oxidation of NADH at a significant rate. With all substrates, oxygen consumption was tightly coupled to substrate hydroxylation as evidenced by the lack of formation of significant amounts of hydrogen peroxide.

4-Hydroxybenzoate hydroxylase from *Pseudomonas* sp. CBS3 catalyzed the oxidation of NADH as well as NADPH. As can be noted from the apparent Michaelis constants and turnover rates recorded in Table 2, the enzyme preferred NADH as the external electron donor. The activity of 4-hydroxybenzoate hydroxylase from *Pseudomonas* sp. CBS3 was inhibited in the presence of monovalent anions; the inhibition was competitive with respect to NADH. From competition experiments performed at pH 8.0 and 37°C, a K_i value of 50 mM was estimated for chloride inhibition.

The above results indicate that 4-hydroxybenzoate hydroxylase from *Pseudomonas* sp. CBS3 has many characteristics in common with the corresponding enzyme from *P. fluorescens* for which a three-dimensional structure is known (Schreuder et al., 1989; van Berkel and Müller, 1991). A main point of distinction between both enzymes is the coenzyme specificity. The preferential utilization of NADH as electron donor in case of the CBS3 enzyme is exceptional among 4-hydroxybenzoate hydroxylases of known primary structure (Entsch and van Berkel, 1995). This prompted us to to clone the gene encoding 4-hydroxybenzoate hydroxylase from *Pseudomonas* sp. CBS3.

Nucleotide sequence analysis. Fig. 2 shows a restriction map of the cloned region with the location of the *pobA* gene and the sequencing strategy. The nucleotide sequence and the derived primary structure of 4-hydroxybenzoate hydroxylase from *Pseudomonas* sp. CBS3 are presented in Fig. 3. The first 20 amino acids of the deduced protein sequence corresponded to the N-

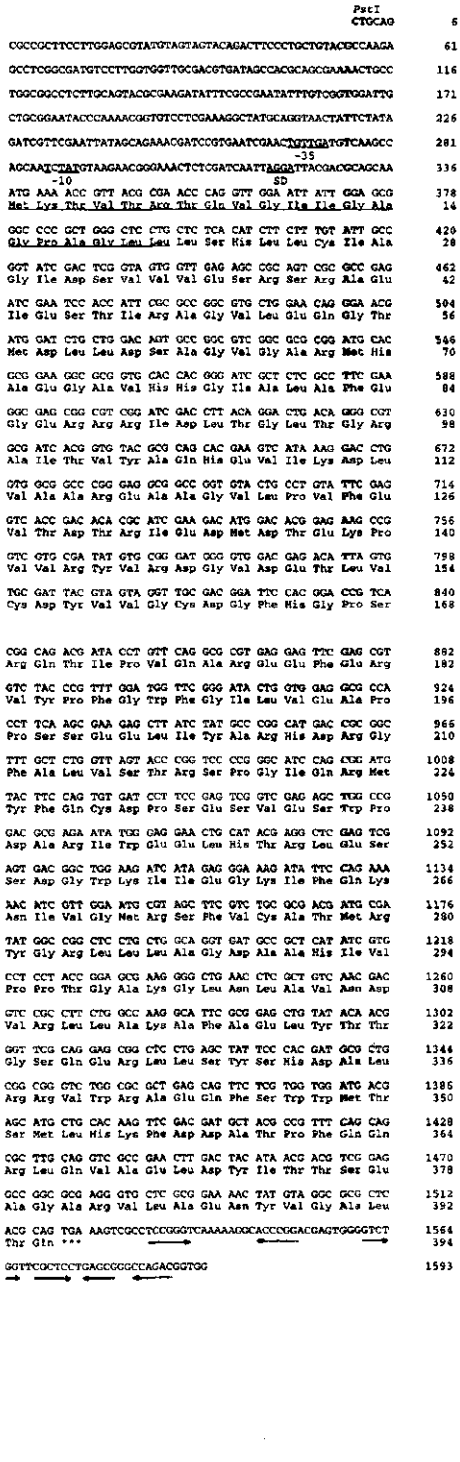

terminal sequence determined by sequence analysis of purified 4-hydroxybenzoate hydroxylase. The open reading frame predicted a 394-amino-acid protein with a calculated molecular mass of 43 632 Da. This value was consistent with that determined by SDS/PAGE for the purified enzyme.

14 bp upstream from the initiation codon was a putative Shine-Dalgarno site (Shine and Dalgarno, 1974). Further upstream, sequences homologous to the consensus sequences of *E. coli* promotors (Rosenberg and Court, 1979) were identified. Expression of *Pseudomonas* sp. CBS3 4-hydroxybenzoate hydroxylase in *E. coli* was due to its own promotor, since the enzyme was produced when the 1.6-kb fragment was inserted into pUC18 in the opposite orientation relative to the vector-encoded *lac* promotor. The termination codon of *pobA* was followed by inverted repeat sequences, which may act as transcription terminators (Rosenberg and Court, 1979). The overall G+C content of 60.5% of the *pobA* gene corresponded well to the G+C content of 60% of *Pseudomonas* sp. CBS3. As would be predicted from the high G+C content of the *pobA* gene, its codon usage was highly biased (68.4%) in favour of G or C in the wobble base, as noted with other *Pseudomonas* genes (Nakai et al., 1983; You et al., 1990).

Amino acid sequence comparison. Up to now, amino acid sequences of 4-hydroxybenzoate hydroxylase have been obtained from the *pobA* gene of six related bacterial strains (Entsch et al., 1988; van Berkel et al., 1992; DiMarco et al., 1993; Shuman and Dix, 1993; Wong et al., 1994). Based on the three-dimensional structure of 4-hydroxybenzoate hydroxylase from *P. fluorescens* (Schreuder et al., 1989) and sequence alignments it was established that these strictly NADPH-dependent enzymes share a similar three-dimensional fold and that the most variable regions lie on the surface of the protein outside the active site (Entsch and van Berkel, 1995). In agreement with this, multiple sequence alignment with the presently determined sequence of 4-hydroxybenzoate hydroxylase from *Pseudomonas* sp. CBS3 revealed about 50% of sequence identity and more than 80% sequence similarity (data not shown). The primary structure of 4-hydroxybenzoate hydroxylase from *Pseudomonas* sp. CBS3 was analyzed in further detail with reference to the sequence numbering (Weijer et al., 1982; van Berkel et al., 1992) and structural properties (Schreuder et al., 1989, 1991) of 4-hydroxybenzoate hydroxylase from *P. fluorescens*.

The amino acid sequence of 4-hydroxybenzoate hydroxylase from *Pseudomonas* sp. CBS3 showed a N-terminal insertion of four residues and did not contain a negatively charged C-terminal tail (Fig. 4). Conserved regions in the primary structure of 4-hydroxybenzoate hydroxylase from *Pseudomonas* sp. CBS3 were present in all three domains and included the $\beta\alpha\beta$-fold for binding the ADP moiety of FAD (residues 1–32, Wierenga et al., 1986), the flavin ribityl-binding motif (residues 279–289; Eggink et al., 1990), the active site loop comprising residues 290–302 and the β-strands containing the residues involved in

Fig. 3. Nucleotide sequence of the *pobA* region of *Pseudomonas* sp. CBS3 and the deduced amino acid sequence of 4-hydroxybenzoate hydroxylase. Nucleotide sequence of the 1593-bp DNA fragment containing the *pobA* gene. The open reading frame starts at base 337 and terminates at base 1521. The deduced amino acid sequence is indicated below the DNA sequence. Underlined amino acid residues are identical with those determined by Edman degradation of the purified enzyme. A potential ribosome binding site (marked SD) and an *E. coli* promotor-like sequence (marked −10 and −35) upstream of the open reading frame are indicated. The arrows designate inverted repeat sequences downstream of the termination codon (indicated by asterisks).

```
       1              11         21         31         41         51
Pf1    MK----TQVAIIGA GPSGLLLGQL LHKAGIDNVI LERQTPDYVL GRIRAGVLEQ GMVDLLREAG     60
       **    *** **** ** ****  * *  **** *   *           ******** *  ***  **
PCBS3  MKTVTRTQVGIIGA GPAGLLLSHL LCIAGIDSVV VESRSRAEIE STIRAGVLEQ GTNDLLDSAG     64

           61         71         81         91         101        111
Pf1        VDRRMARDGL VHEGVEIAFA GQRRRIDLKR LSGGKTVTVY GQTEVTRDLM EAREACGATT    120
           *  **   *  ** *   **  * ******   * *    ***  * **  **   **** *
PCBS3      VGARMHAEGA VHHGIALAFE GERRRIDLTG LTG-RAITVY AQHEVIKDLV AAREAAGVLP    123

           121        131        141        151        161        171
Pf1        VYQAAEVRLH DLQGERPYVT FERDGERLRL DCDYIAGCDG FHGISRQSIP AERLKVFERV    180
           *      *   *   * * *     ***    *  ***  **** *** *** **       ****
PCBS3      VFEVTDTRIE DMDTEKPVVR YVRDGVDETL VCDYVVGCDG FHGPSRQTIP VQAREEFERV    183

           181        191        201        211        221        231
Pf1        YPFGWLGLLA DTPPVSHELI YANHPRGFAL CSQRSATRSR YYVQVPLTEK VEDWSDERFW    240
           ***** * *    ** * *** ** * *****  * **    *  * *    *  ** * * * *
PCBS3      YPFGWFGILV EAPPSSEELI YARHDRGFAL VSTRSPGIQR MYFQCDPSES VESWPDARIW    243

           241        251        261        271        281        291
Pf1        TELKARLPAE VAEKLVTGPS LEKSIAPLRS FVVEPMQHGR LFLAGDAAHI VPPTGAKGLN    300
            **  **       *   *       *   ** **   *  ** * ******** **********
PCBS3      EELHTRLESS DGWKIIEGKI FQXMIVGMRS FVCATMRYGR LLLAGDAAHI VPPTGAKGLN    303

           301        311        321        331        341        351
Pf1        LAASDVSTLY RLLLKAYREG RGELLERYSA ICLRRIWKAE RFSWWMTSVL HRFPDTDAFS    360
           **  **  *        *  *   * *  **     *** * **  ******* * * * *   *
PCBS3      LAVNDVRLLA KAPAELYTTG SQERLLSYSH DALRRVWRAE QFSWWNTSNL HKFDDATPFQ    363

           361        371        381        391
Pf1        QRIQQTELEY YLGSEAGLAT IAENYVGLPY EEIE                                394
           ** *  ** *    ****      ******
PCBS3      QRLQVAELDY ITTSEAGARV LAENYVGALT Q                                   394
```

Fig. 4. Alignment of the amino acid sequences of 4-hydroxybenzoate hydroxylase from *P. fluorescens* and *Pseudomonas* sp. CBS3. The deduced amino acid sequence of 4-hydroxybenzoate hydroxylase from *Pseudomonas* sp. CBS3 (PCBS3) is aligned with the amino acid sequence of 4-hydroxybenzoate hydroxylase from *P. fluorescens* (Pf1, Weijer et al., 1982; van Berkel et al., 1992). The *P. fluorescens* sequence is the default sequence. Asterisks indicate identical amino acids (*).

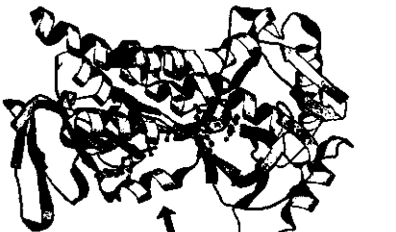

Fig. 5. Ribbon diagram of the modelled three-dimensional structure of the enzyme-substrate complex of 4-hydroxybenzoate hydroxylase from *Pseudomonas* sp. CBS3. The three-dimensional structure of 4-hydroxybenzoate hydroxylase from *Pseudomonas* sp. CBS3 was predicted by comparative model building using ProMod implemented in the Swiss-Model package (Peitsch, 1995). The crystal structure of the enzyme-substrate complex of 4-hydroxybenzoate hydroxylase from *P. fluorescens* (Schreuder et al., 1989) served as the template file. The schematic ribbon diagram was generated with MOLSCRIPT (Kraulis, 1991). FAD and 4-hydroxybenzoate are drawn with balls and sticks. Helix H2, which is supposed to be involved in NAD(P)H binding, is indicated by an arrow.

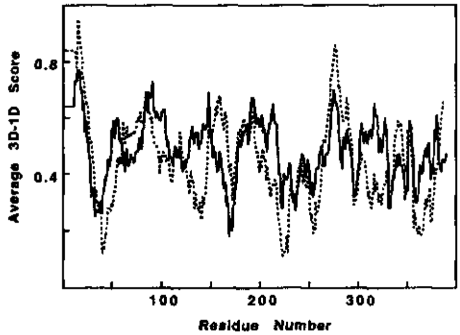

Fig. 6. Profile window plots of the protein models of 4-hydroxybenzoate hydroxylase from *P. fluorescens* and 4-hydroxybenzoate hydroxylase from *Pseudomonas* sp. CBS3. The quality of the predicted three-dimensional protein model of 4-hydroxybenzoate hydroxylase from *Pseudomonas* sp. CBS3 was assessed by comparison its 3D-1D profile score (Lüthy et al., 1992) with that of 4-hydroxybenzoate hydroxylase from *P. fluorescens*. For the calculation of the profile score, a sliding window of 21 residues was used. (A) 3D-1D profile score of 4-hydroxybenzoate hydroxylase from *P. fluorescens* (——). (B) 3D-1D profile score of 4-hydroxybenzoate hydroxylase from *Pseudomonas* sp. CBS3 (- - -).

substrate binding (Tyr201, Ser212, Arg214, and Tyr222). Other important stretches of sequence homology included the loop adjoining the *si*-face of the flavin ring (residues 43−50) and the helices involved in subunit dimerization (residues 328−386). From the conservation of active site and secondary structure elements, it is clear that the core structure of 4-hydroxybenzoate hydroxylase from *Pseudomonas* sp. CBS3 is highly identical to that of the enzyme from *P. fluorescens*. We therefore decided to construct a three-dimensional model of the *Pseudomonas* CBS3 hydroxylase, based on the structure of the *P. fluorescens* enzyme using the knowledge-based protein modelling tool ProMod (Peitsch, 1995). Fig. 5 shows a ribbon diagram of the modelled structure. The predicted fold of 4-hydroxybenzoate hydroxylase from *Pseudomonas* sp. CBS3 is almost identical to the fold of the *P. fluorescens* enzyme. The root-mean-square difference is 3.4 nm for 385 equivalent Cα atoms. The quality of the model was assessed by determining the 3D-1D profile score (Lüthy et al., 1992), which evaluates the compatibility of each residue to

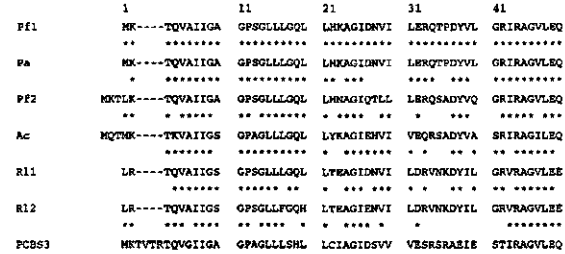

Fig. 7. Multiple sequence alignment of the N-terminal sequences of 4-hydroxybenzoate hydroxylases. The N-terminal amino acid sequence (residues 1–50) of 4-hydroxybenzoate hydroxylase from *P. fluorescens* (Pf1, Weijer et al., 1982) is aligned with the N-terminal amino acid sequences of 4-hydroxybenzoate hydroxylase from *P. aeruginosa* (Pa, Entsch et al., 1988); *P. fluorescens* isozyme (Pf2, Shuman and Dix, 1993); *A. calcoaceticus* (Ac, DiMarco et al., 1993); *R. leguminosarum* B155 (R11, Wong et al., 1994); *R. leguminosarum* MNF300 (R12, Wong et al., 1994) and *Pseudomonas* sp. CBS3 (PCBS3, this study). Identical amino acids are indicated by asterisks (*). The *P. fluorescens* (Pf1) sequence is the default sequence.

its environment independently from the crystallographic data. The profile window plots of *P. fluorescens* and *Pseudomonas* CBS3 4-hydroxybenzoate hydroxylase (Fig. 6) are very similar and the relatively high 3D-1D scores indicate that both models are likely to be correct. The lowest 3D-1D scores (< 0.2) were observed for the sequence segments 28–44 and 220–230, involved in FAD and substrate binding, respectively. The relative low score in these regions might be caused by the absence in the calculations of these ligands. In addition, the sequence segments comprising residues 128–148, 242–264, 302–330, and 355–377 have a lower score in the *Pseudomonas* CBS3 model compared to the *P. fluorescens* crystal structure. They are located near the protein surface and contain less well defined loops as indicated by relative high temperature factors (Schreuder et al., 1989). These loops belong to the most variable parts of the sequence (compare Fig. 4) and might therefore be folded slightly different in both structures. When we determined the 3D-1D score for the *P. fluorescens* monomer, we obtained a rather low score for the region 353–374 (helix H12) which is involved in dimer contacts. When we determined the profile for the *P. fluorescens* dimer, the score for this region improved significantly. Similarly, the score of the equivalent region of the *Pseudomonas* CBS3 molecule improved significantly when generating a *Pseudomonas* CBS3 dimer, using the transformation of the *P. fluorescens* molecule. These results suggest that also the dimer contacts are similar for both molecules.

Coenzyme specificity. The three-dimensional structure of 4-hydroxybenzoate hydroxylase is unusual because there is no recognizable domain for the binding of the coenzyme NADPH (Wierenga et al., 1983). Because the most striking property of 4-hydroxybenzoate hydroxylase from *Pseudomonas* sp. CBS3 is its preference for NADH over NADPH as external electron donor, it was of interest to search for structural features possibly involved in determining the coenzyme specificity. Chemical modification and site-directed mutagenesis studies on 4-hydroxybenzoate hydroxylase from *P. fluorescens* have provided some insight in the binding mode of NADPH (Eppink et al., 1995). The pyrophosphate moiety of the pyridine nucleotide cofactor most probably binds in a cleft between the FAD-binding domain and the substrate-binding domain (van Berkel and Müller, 1991; Schreuder et al., 1991). The binding mode of the 2′-phosphate group of the adenosine moiety of NADPH is far more unclear but it could involve the interaction with the side chain of Tyr38 (van Berkel et al., 1988). Tyr38 is strictly conserved in the NADPH-dependent 4-hydroxybenzoate hydroxylases (Fig. 7) and is located in a short helix near the protein surface far away from the active site (Schreuder et al., 1989). Intriguingly, the sequence of this helix (residues 35–42) deviates considerably in the primary structure of 4-hydroxybenzoate hydroxylase from *Pseudomonas* sp. CBS3 (Fig. 7).

DISCUSSION

This paper reports the biochemical properties, gene cloning, and sequence determination of 4-hydroxybenzoate hydroxylase, a flavin-dependent aromatic hydroxylase involved in the biodegradation of 4-chlorobenzoate in *Pseudomonas* sp. CBS3. Characterization of the purified enzyme clearly established that 4-hydroxybenzoate hydroxylase from *Pseudomonas* sp. CBS3 shares many properties with the corresponding enzyme from *P. fluorescens* (van Berkel and Müller, 1991). These properties included the subunit molecular mass, the quaternary structure, the pH optimum for catalysis, the substrate specificity and the inhibition by chloride ions. Remarkable differences between both enzymes concerned the temperature optimum for catalysis, the interaction with FAD and the coenzyme specificity. Whereas 4-hydroxybenzoate hydroxylase from *P. fluorescens* has a temperature optimum for catalysis around 30°C (van Berkel and Müller, 1989), the maximum turnover rate of the enzyme from *Pseudomonas* sp. CBS3 was observed at 45°C. In contrast to 4-hydroxybenzoate hydroxylase from *P. fluorescens* (Müller and van Berkel, 1982), the enzyme from *Pseudomonas* sp. CBS3 easily lost FAD. Although the reason for this is not yet clear, it should be noted that mutagenesis studies on the *P. fluorescens* enzyme have established that impaired binding of the flavin cofactor may be induced by conservative amino acid substitutions in the vicinity of the FAD-binding site (van der Bolt et al., 1994; Eppink et al., 1995).

In contrast to all 4-hydroxybenzoate hydroxylases sequenced thus far, 4-hydroxybenzoate hydroxylase from *Pseudomonas* sp. CBS3 preferred NADH as the external electron donor. Up to now, only three NAD(P)H-dependent 4-hydroxybenzoate 3-hydroxylases, which include the enzymes from *Corinebacterium cyclohexanicum* (Fujii and Kaneda, 1985), *Moraxella* sp. (Sterjiades, 1993), and *Rhodococcus erythropolis* (Suemori et al., 1993), have been purified and partially characterized. *Pseudo-*

monas 4-hydroxybenzoate 3-hydroxylases thus far were regarded as being highly specific for NADPH (van Berkel and Müller, 1991; Webb, 1992). It is clear from the present study that this view should be revised.

Cloning of the *pobA* gene encoding 4-hydroxybenzoate hydroxylase from *Pseudomonas* sp. CBS3 allowed the expression of 4-hydroxybenzoate hydroxylase activity in *E. coli* TG1, even though the gene was inserted in the opposite orientation relative to the lac promotor of pUC18. This indicates that the structural gene of 4-hydroxybenzoate hydroxylase from *Pseudomonas* sp. CBS3 was expressed by its own promotor and that no regulatory genes were present on the cloned fragment. The deduced amino acid sequence of 4-hydroxybenzoate hydroxylase from *Pseudomonas* sp. CBS3 showed about 50% sequence identity and more than 80% sequence similarity with that of the other 4-hydroxybenzoate hydroxylases sequenced thus far. This high degree of sequence conservation is in accordance with the supposed common evolutionary origin for the isofunctional enzymes of the β-ketoadipate pathway (Woese, 1987; Hartnett et al., 1990; Harayama et al., 1992).

In accordance with the highly tuned function of 4-hydroxybenzoate hydroxylase (Entsch and van Berkel, 1995), all active site residues in the novel sequence were strictly conserved. These residues included Ser212, Arg214, and Tyr222, involved in substrate binding and flavin motion (Schreuder et al., 1994; Gatti et al., 1994) and Tyr201 and Tyr385, which are involved in substrate activation and the regioselectivity of hydroxylation (Entsch et al., 1991, Eschrich et al., 1993). Another conserved structural feature involved the active site loop comprising residues 290–302. This loop has a complex twisted conformation (Schreuder et al., 1989) which may be of importance in regulating the effector specificity (van Berkel et al., 1992).

As expected from the high degree of sequence identity, structure homology modelling predicted that the 4-hydroxybenzoate hydroxylases from *Pseudomonas* sp. CBS3 and *P. fluorescens* shared superimposable globular folds. No gross deviations were detected in the 3D-1D average profiles of both enzymes indicating the conservation of secondary structural elements.

The three-dimensional structure of 4-hydroxybenzoate hydroxylase is unusual because there is no recognizable domain for the binding of the pyridine nucleotide cofactor. From stereochemical studies it is known that the nicotinamide part of the reduced pyridine nucleotide cofactor binds at the *re*-side of the flavin ring allowing rapid hydride transfer (Manstein et al., 1986). Chemical modification studies (van Berkel and Müller, 1991) and model building (van Berkel et al., 1988) have indicated that the pyrophosphate moiety of the pyridine nucleotide cofactor most probably binds in a cleft between the FAD-binding domain and the substrate-binding domain. Recent studies on mutant enzymes confirmed this idea and furthermore showed that Tyr38 plays an important role in the recognition of the adenosine 2′-phosphate part of NADPH (Eppink, M. H. M. and van Berkel, W. J. H., unpublished results). Tyr38 is situated near the protein surface in a short helix (helix H2; Schreuder et al., 1989) the sequence of which is highly conserved in the strictly NADPH-dependent 4-hydroxybenzoate hydroxylases (Fig. 7). Inspection of the present primary structural data revealed that Tyr38 is replaced by glutamic acid in the sequence of 4-hydroxybenzoate hydroxylase from *Pseudomonas* sp. CBS3. This and the strongly deviating sequence surrounding Tyr38 (Fig. 7) leads us to propose that helix H2 (residues 35–42) is involved in determining the coenzyme specificity. To test this proposal, we aim to address in more detail the role of helix H2 in NAD(P)H binding of 4-hydroxybenzoate hydroxylase from *P. fluorescens* by protein engineering. In this respect, it is important to note that structure homology modelling predicts that the secondary structure of helix H2 is retained in the enzyme from *Pseudomonas* sp. CBS3 (Fig. 5).

We thank Dr H. A. Schreuder for critically reading the manuscript and Dr B. Hauer, BASF Ludwigshafen for N-terminal sequence analysis. This work was supported by the *Bundesministerium für Forschung und Technologie* (contract no. 0319416A) and by the *Fonds der Chemischen Industrie* (Germany). Additional support was provided by the Netherlands Foundation for Chemical Research (SON) with financial aid from the Netherlands Organization for Scientific Research (NWO).

REFERENCES

Arnow, L. E. (1937) Colorimetric determination of the components of 3,4-dihydroxyphenylalanine-tyrosine mixtures, *J. Biol. Chem. 118*, 531–537.

Babbitt, P. C., Kenyon, G. L., Martin, B. M., Charest, H., Sylvestre, M., Scholten, J. D., Chang, K.-H., Liang, P.-H. & Dunaway-Mariano, D. (1992) Ancestry of 4-chlorobenzoate dehalogenase: analysis of the amino acid sequence identities among families of acyl:adenyl ligases, enoyl-CoA hydratases/isomerases, and acyl-CoA thioesterases, *Biochemistry 31*, 5594–5604.

Birnboim, H. C. & Doly, J. (1979) A rapid alkaline extraction procedure for screening recombinant plasmid DNA, *Nucleic Acids Res. 7*, 1513–1523.

Chang, K.-H., Liang, P.-H., Beck, W., Scholten, J. D. & Dunaway-Mariano, D. (1992) Isolation and characterization of the three polypeptide components of 4-chlorobenzoate dehalogenase from *Pseudomonas* sp. strain CBS-3, *Biochemistry 31*, 5605–5610.

Clewell, D. B. & Helinski, D. R. (1969) Supercoiled circular DNA-protein complex in *E. coli*: purification and induced conversion to an open circular form, *Proc. Natl Acad. Sci. USA 62*, 1159–1166.

DiMarco, A. A., Averhoff, B. A., Kim, E. E. & Ornston, L. N. (1993) Evolutionary divergence of *pobA*, the structural gene encoding *p*-hydroxybenzoate hydroxylase in an *Acinetobacter calcoaceticus* strain well suited for genetic analysis, *Gene (Amst.) 125*, 25–33.

Eggink, G., Engel, H., Vriend, G., Terpstra, P. & Witholt, B. (1990) Rubredoxin reductase of *Pseudomonas oleovorans*. Structural relationship to other flavoprotein oxidoreductases based on one NAD and two FAD fingerprints, *J. Mol. Biol. 212*, 135–142.

Elsner, A., Löffler, F., Miyashita, K., Müller, R. & Lingens, F. (1991a) Resolution of 4-chlorobenzoate dehalogenase from *Pseudomonas* sp. CBS3 into three components, *Appl. Environ. Microbiol. 57*, 324–326.

Elsner, A., Müller, R. & Lingens, F. (1991b) Separate cloning and expression analysis of two components of 4-chlorobenzoate dehalogenase from *Pseudomonas* sp. CBS3, *J. Gen. Micobiol. 137*, 477–481.

Entsch, B., Nan, Y., Weaich, K. & Scott, K. F. (1988) Sequence and organization of *pobA*, the gene coding for *p*-hydroxybenzoate hydroxylase, an inducible enzyme from *Pseudomonas aeruginosa*, *Gene (Amst.) 71*, 279–291.

Entsch, B., Palfey, B. A., Ballou, D. P. & Massey, V. (1991) Catalytic function of tyrosine residues in *para*-hydroxybenzoate hydroxylase as determined by the study of site-directed mutants, *J. Biol. Chem. 266*, 17341–17349.

Entsch, B. & van Berkel, W. J. H. (1995) Structure and mechanism of *p*-hydroxybenzoate hydroxylase, *FASEB J. 9*, 476–483.

Eppink, M. H. M., Schreuder, H. A. & van Berkel, W. J. H. (1995) Structure and function of mutant Arg44Lys of *p*-hydroxybenzoate hydroxylase, *Eur. J. Biochem. 231*, 157–165.

Eschrich, K., van der Bolt, F. J. T., de Kok, A. & van Berkel, W. J. H. (1993) Role of Tyr201 and Tyr385 in substrate activation by *p*-hydroxybenzoate hydroxylase from *Pseudomonas fluorescens*, *Eur. J. Biochem. 216*, 137–146.

Fujii, T. & Kaneda, T. (1985) Purification and properties of NADH/NADPH-dependent *p*-hydroxybenzoate hydroxylase from *Cyclobacterium cyclohexanicum*, *Eur. J. Biochem. 147*, 97–104.

Friedman, A. M., Long, S. R., Brown, S. E., Buikema, W. J. & Ausubel, F. M. (1982) Construction of a broad host range cosmid cloning

vector and its use in the genetic analysis of *Rhizobium* mutants, *Gene (Amst.) 18*, 289–296.

Gatti, D. L., Palfey, B. A., Lah, M. S., Entsch, B., Massey, V., Ballou, D. P. & Ludwig, M. L. (1994) The mobile flavin of 4-OH benzoate hydroxylase, *Science 266*, 110–114.

Gatti, D. L., Entsch, B., Ballou, D. P. & Ludwig, M. L. (1996) pH-dependent structural changes in the active-site of *p*-hydroxybenzoate hydroxylase point to the importance of proton and water movements during catalysis, *Biochemistry 35*, 567–578.

Harayama, S., Kok, M. & Neidle, E. L. (1992) Functional and evolutionary relationships among diverse oxygenases, *Annu. Rev. Microbiol. 46*, 565–601.

Hartnett, C., Neidle, E. L., Ngai, K.-L. & Ornston, L. N. (1990) DNA sequences of genes encoding *Acinetobacter calcoaceticus* protocatechuate 3,4-dioxygenase: evidence indicating shuffling of genes and of DNA sequences within genes during their evolutionary divergence, *J. Bacteriol. 172*, 956–966.

Klages, U. & Lingens, F. (1980) Degradation of 4-chlorobenzoic acid by a *Pseudomonas* species, *Zentralbl. Bakteriologie, Parasitenk., Deinfektionskr. Hyg. Abt. Orig. Reihe C 1*, 215–223.

Kraulis, P. (1991) MOLSCRIPT: a program to produce both detailed and schematic plots of protein structure, *J. Appl. Crystallogr. 24*, 946–950.

Löffler, F., Lingens, F. & Müller, R. (1995) Dehalogenation of 4-chlorobenzoate: characterisation of 4-chlorobenzoyl-coenzyme A dehalogenase from *Pseudomonas* sp. CBS3, *Biodegradation 6*, 203–212.

Lowry, O. H., Rosebrough, N. J., Farr, A. L. & Randall, R. J. (1951) Protein measurement with the folin phenol reagent, *J. Biol. Chem. 193*, 265–275.

Lüthy, R., Bowie, J. U. & Eisenberg, D. (1992) Assessment of protein models with three-dimensional profiles, *Nature 356*, 83–85.

Mandel, M. & Higa, A. (1970) Calcium dependent bacteriophage DNA infection, *J. Mol. Biol. 53*, 159–162.

Manstein, D. J., Pai, E. F., Schopfer, L. M. & Massey, V. (1986) Absolute stereochemistry of flavins in enzyme-catalyzed reactions, *Biochemistry 25*, 6807–6816.

Marmur, J. (1961) A procedure for the isolation of deoxyribonucleic acid from microorganisms, *J. Mol. Biol. 3*, 208–218.

Müller, F., Voordouw, G., van Berkel, W. J. H., Steennis, P. J., Visser, S. & van Rooijen, P. (1979) A study of *p*-hydroxybenzoate hydroxylase from *Pseudomonas fluorescens*: improved purification, relative molecular mass and amino acid composition, *Eur. J. Biochem. 101*, 235–244.

Müller, R., Thiele, J., Klages, U. & Lingens, F. (1984) Incorporation of [^{18}O]water into 4-hydroxybenzoic acid in the reaction of 4-chlorobenzoate dehalogenase from *Pseudomonas* sp. CBS3, *Biochem. Biophys. Res. Commun. 124*, 178–182.

Nakai, C., Kagamiyama, H. & Nozaki, M. (1983) Complete nucleotide sequence of the metapyrocatechase gene on the TOL plasmid of *Pseudomonas putida* mt-2, *J. Biol. Chem. 258*, 2923–2928.

Neidle, E. L., Hartnett, C., Ornston, L. N., Bairoch, A., Rekik, M. & Harayama, S. (1991) Nucleotide sequences of the *Acinetobacter calcoaceticus* ben ABC genes for benzoate 1,2-dioxygenase reveal evolutionary relationships among multicomponent oxygenases, *J. Bacteriol. 173*, 5385–5395.

Peitsch, M. C. (1995) Protein modelling by E-mail, *Biotechnology 13*, 658–660.

Rosenberg, M. & Court, D. (1979) Regulatory sequences involved in the promotion and termination of RNA transcription, *Annu. Rev. Genet. 13*, 319–353.

Sambrook, J., Fritsch E. F. & Maniatis, T. (1989) *Molecular cloning: a laboratory manual*, 2nd edn, Cold Spring Harbor Laboratory, Cold Spring Harbor NY.

Sanger, F., Nicklen, S. & Coulsen, A. R. (1977) DNA sequencing with chain-terminating inhibitors, *Proc. Natl Acad. Sci. USA 74*, 5463–5467.

Savard, P., Peloquin, L. & Sylvestre, M. (1986) Cloning of *Pseudomonas* sp. strain CBS3 genes specifying dehalogenation of 4-chlorobenzoate, *J. Bacteriol. 168*, 81–85.

Schreuder, H. A., Prick, P., Wierenga, R. K., Vriend, G., Wilson, K. S., Hol, W. G. J. & Drenth, J. (1989) Crystal structure of the *p*-hydroxybenzoate hydroxylase-substrate complex refined at 1.9 Å resolution, *J. Mol. Biol. 208*, 679–696.

Schreuder, H. A., van der Laan, J. M., Hol, W. G. J. & Drenth, J. (1991) The structure of *p*-hydroxybenzoate hydroxylase, in *Chemistry and biochemistry of flavoenzymes* (Müller, F., ed.) vol. 2, pp. 31–64, CRC Press, Boca Raton FL.

Schreuder, H. A., Mattevi, A., Obmolova, G., Kalk, K. H., Hol, W. G. J., van der Bolt, F. J. T. & van Berkel, W. J. H. (1994) Crystal structures of wild-type *p*-hydroxybenzoate hydroxylase complexed with 4-aminobenzoate, 2,4-dihydroxybenzoate and 2-hydroxy-4-aminobenzoate and mutant Tyr222Ala, complexed with 2-hydroxy-4-aminobenzoate. Evidence for a proton channel and a new binding mode of the flavin ring, *Biochemistry 33*, 10161–10170.

Shine, J. & Dalgarno, L. (1974) The 3′-terminal sequence of *Escherichia coli* 16S ribosomal RNA: complementarity to nonsense triplets and ribosome binding sites, *Proc. Natl Acad. Sci. USA 71*, 1342–1346.

Shuman, B. & Dix, T. A. (1993) Cloning, nucleotide sequence, and expression of a *p*-hydroxybenzoate hydroxylase isozyme gene from *Pseudomonas fluorescens*, *J. Biol. Chem. 268*, 17057–17062.

Slater, J. H., Weightman, A. J. & Hall, B. G. (1985) Dehalogenase genes of *Pseudomonas putida* PP3 on chromosomally located transposable elements, *Mol. Biol. Evol. 2*, 557–567.

Steennis, P. J., Cordes, M. M., Hilkens, J. G. H. & Müller, F. (1973) On the interaction of *p*-hydroxybenzoate hydroxylase from *Pseudomonas fluorescens* with halogen ions, *FEBS Lett. 36*, 177–179.

Sterjiades, R. (1993) Properties of NADH/NADPH-dependent *p*-hydroxybenzoate hydroxylase from *Moraxella* sp., *Biotechnol. Appl. Biochem. 17*, 77–90.

Suemori, A., Kurane, R. & Tomizuka, N. (1993) Purification and properties of 3 types of monohydroxybenzoate oxygenase from *Rhodococcus erythropolis*, *Biosci. Biotech. Biochem. 57*, 1487–1491.

van Berkel, W. J. H. & Müller, F. (1987) The elucidation of the microheterogeneity of highly purified *p*-hydroxybenzoate hydroxylase from *Pseudomonas fluorescens* by various biochemical techniques, *Eur. J. Biochem. 167*, 35–46.

van Berkel, W. J. H., Müller, F., Jekel, P. A., Weijer, W. J., Schreuder, H. A. & Wierenga, R. K. (1988) Chemical modification of tyrosine-38 in *p*-hydroxybenzoate hydroxylase from *Pseudomonas fluorescens* by 5′-*p*-fluorosulfonylbenzoyladenosine: a probe for the elucidation of the NADPH binding site? *Eur. J. Biochem. 176*, 449–459.

van Berkel, W. J. H. & Müller, F. (1989) The temperature and pH dependence of some properties of *p*-hydroxybenzoate hydroxylase from *Pseudomonas fluorescens*, *Eur. J. Biochem. 179*, 307–314.

van Berkel, W. J. H. & Müller, F. (1991) Flavin-dependent monooxygenases with special reference to *p*-hydroxybenzoate hydroxylase, in *Chemistry and biochemistry of flavoenzymes* (Müller, F., ed.) vol. 2, pp. 1–29, CRC Press, Boca Raton FL.

van Berkel, W. J. H., Westphal, A. H., Eschrich, K., Eppink, M. & de Kok, A. (1992) Substitution of Arg214 at the substrate-binding site of *p*-hydroxybenzoate hydroxylase from *Pseudomonas fluorescens*, *Eur. J. Biochem. 210*, 411–419.

van Berkel, W. J. H., Eppink, M. H. M., Middelhoven, W. J., Vervoort, J. & Rietjens, I. M. C. M. (1994) Catabolism of 4-hydroxybenzoate in *Candida parapsilosis* proceeds through initial oxidative decarboxylation by a FAD-dependent 4-hydroxybenzoate 1-hydroxylase, *FEMS Microbiol. Lett. 121*, 207–216.

van der Bolt, F. J. T., Drijfhout, M. C., Eppink, M. H. M., Hagen, W. R. & van Berkel, W. J. H. (1994) Selective cysteine-serine replacements in *p*-hydroxybenzoate hydroxylase from *Pseudomonas fluorescens* allow the unambiguous assignment of Cys211 as the site of modification by spin-labeled *p*-chloromercuribenzoate, *Protein Eng. 7*, 801–804.

van der Laan, J. M., Schreuder, H. A., Swarte, M. B. A., Wierenga, R. K., Kalk, K. H., Hol, W. G. J. & Drenth, J. (1989) The coenzyme analogue adenosine 5-diphosphoribose displaces FAD in the active site of *p*-hydroxybenzoate hydroxylase. An X-ray crystallographic investigation, *Biochemistry 28*, 7199–7205.

Webb, E. C. (1992) Oxidoreductases, in *Enzyme nomenclature* (Webb, E. C., ed.) pp. 133–141, Academic Press, San Diego.

Weijer, W. J., Hofsteenge, J., Vereijken, J., Jekel, P. A. & Beintema, J. J. (1982) Primary structure of *p*-hydroxybenzoate hydroxylase from *Pseudomonas fluorescens*, *Biochim. Biophys. Acta 704*, 385–388.

Wierenga, R. K., de Jong, R. J., Kalk, K. H., Hol, W. G. J. & Drenth, J. (1979) Crystal structure of *p*-hydroxybenzoate hydroxylase. *J. Mol. Biol. 131*, 55–73.

Wierenga, R. K., Drenth, J. & Schulz, G. E. (1983) Comparison of the three-dimensional protein and nucleotide structure of the FAD-binding domain of *p*-hydroxybenzoate hydroxylase with the FAD- as well as NADPH-binding domains of glutathione reductase, *J. Mol. Biol. 167*, 725–739.

Wierenga, R. K., Terpstra, P. & Hol, W. G. J. (1986) Prediction of the occurence of the ADP-binding *βαβ*-fold in proteins, using an amino acid sequence fingerprint, *J. Mol. Biol. 187*, 101–107.

Wijnands, R. A., van der Zee, J., van Leeuwen, J. W., van Berkel, W. J. H. & Müller, F. (1984) The importance of monopole-monopole and monopole-dipole interactions on the binding of NADPH and NADPH analogues to *p*-hydroxybenzoate hydroxylase from *Pseudomonas fluorescens*, *Eur. J. Biochem. 139*, 637–644.

Woese, C. R. (1987) Bacterial evolution. *Microbiol. Rev. 51*, 221–271.

Wong, C. M., Dilworth, M. J. & Glenn, A. R. (1994) Cloning and sequencing show that 4-hydroxybenzoate hydroxylase (*pobA*) is required for uptake of 4-hydroxybenzoate in *Rhizobium leguminosarum*, *Microbiology 140*, 2775–2786.

Yanisch-Perron, C., Vieira, J. & Messing, J. (1985) Improved M13 phage cloning vectors and host strains: nucleotide sequences of the M13mp18 and pUC19 vectors, *Gene (Amst.) 33*, 103–109.

You, I.-S., Ghosal, D. & Gunsalus, I. C. (1990) Nucleotide sequence analysis of the *Pseudomonas putida* PpG7 salicylate hydroxylase gene (nahG) and its flanking region, *Biochemistry 30*, 1635–1641.

CHAPTER 9

Switch of coenzyme specificity of *p*-hydroxybenzoate hydroxylase

Michel H.M. Eppink, Karin Overkamp, Herman A. Schreuder and Willem J.H. van Berkel

J. Mol. Biol. (submitted)

Switch of coenzyme specificity of *p*-hydroxybenzoate hydroxylase

Abstract

p-Hydroxybenzoate hydroxylase is the archetype of the family of NAD(P)H-dependent flavoprotein aromatic hydroxylases. These enzymes share a conserved FAD-binding domain but lack a recognizable fold for binding the pyridine nucleotide. We have switched the coenzyme specificity of strictly NADPH-dependent *p*-hydroxybenzoate hydroxylase from *Pseudomonas fluorescens* by site-directed mutagenesis. To that end, we altered the solvent exposed helix H2 region (residues 33 – 40) of the FAD-binding domain. Non-conservative selective replacements of Arg33 and Tyr38 weakened the binding of NADPH without disturbing the protein architecture. Introduction of a basic residue at position 34 increased the NADPH binding strength. Double (M2) and quadruple (M4) substitutions in the N-terminal part of helix H2 did not change the coenzyme specificity. By extending the replacements towards residues 38 and 40, M5 and M6 mutants were generated which were catalytically more efficient with NADH than with NADPH. This is the first report on the coenzyme reversion of a flavoprotein aromatic hydroxylase.

Introduction

Flavoprotein aromatic hydroxylases catalyse the insertion of one atom of molecular oxygen into the substrate, using NAD(P)H as electron donor (van Berkel and Müller, 1991):

$$ArOH + NAD(P)H + H^+ + O_2 \xrightarrow{\text{E-FAD}} Ar(OH)_2 + NAD(P)^+ + H_2O$$

These monooxygenases play an important role in the catabolism of both naturally occurring and man-made organic molecules in soil microorganisms (van Berkel *et al.*, 1997). Recently, it was found that flavoprotein aromatic hydroxylases are also widely involved in the biosynthesis of sterols, antibiotics and plant hormones (Eppink *et al.*, 1997 and references therein).

Flavoprotein aromatic hydroxylases have many catalytic properties in common and their substrate specificity is consistent with an electrophilic aromatic substitution mechanism (Massey, 1994). An important, yet poorly understood property is the control function of the aromatic substrate over flavin reduction by NAD(P)H (Palfey *et al.*, 1999). The interpretation of the effector role of the substrate is limited by the fact that so far, no structural data of enzyme-NAD(P)H complexes for this class of flavoproteins have been obtained (Enroth *et al.*, 1998). Unlike many dehydrogenases (Baker *et al.*, 1992; Lesk, 1995; Chen *et al.*, 1996; Bellamacina, 1997) and reductases (Scrutton *et al.*, 1990; Sem and Kasper, 1993; Friesen *et al.*, 1996), flavoprotein aromatic hydroxylases do not possess a recognizable NAD(P)H-binding domain (Entsch and van Berkel, 1995). Moreover, they lack a consensus sequence identifying their coenzyme specificity (Eppink *et al.*, 1997).

Insight into the mode of coenzyme recognition by flavoprotein aromatic hydroxylases mainly comes from studies on NADPH-specific *p*-hydroxybenzoate hydroxylase (PHBH) from *Pseudomonas fluorescens*. Based on the properties of PHBH variants (Eppink *et al.*, 1995, 1998a, 1998b, 1999), an interdomain binding for the pyridine nucleotide was proposed (Eppink *et al.*, 1998b). The pyrophosphate moiety of NADPH most probably binds in a cleft leading toward the active site, whereas the adenosine 2'-phosphate moiety is assumed to bind in the region around helix H2 near the protein surface (Figure 1). With the exception of NAD(P)H-dependent PHBH from *Pseudomonas* sp. CBS3, this region is highly conserved in PHBH enzymes of known sequence (Seibold *et al.*, 1996).

Fig. 1. Ribbon structure of native PHBH (see cover for full color representation). Helix H2 is depicted in white. FAD, POHB and the residues Arg33, Gln34, Tyr38 and Arg42 are indicated. The coordinates from the refined 1.9 Å structure (Schreuder *et al.*, 1989) were used to generate this figure with RIBBONS (Carson, 1991).

In this study, we have examined the structural features which determine the coenzyme specificity of PHBH from *P. fluorescens*. Guided by the amino acid sequence of PHBH from *Pseudomonas* sp. CBS3 (Seibold *et al.*, 1996) and the proposed NADPH binding mode, a mutagenesis strategy was developed to change the coenzyme specificity. To that end, single and multiple amino acid replacements were introduced in helix H2 (Table I). The characterization of the mutant proteins and the catalytic and structural consequences that occur as a result of the amino acid replacements are presented below.

Table I. Mutagenesis strategy of PHBH from *P. fluorescens*

Enzyme		Sequence
PHBH *P. fluorescens*		33 R-Q-T-P-D-Y-V-L-G-R 42
R33K/S/E	(X=K/S/E)	**X**-Q-T-P-D-Y-V-L-G-R
Q34T/R/K	(X=T/R/K)	R-**X**-T-P-D-Y-V-L-G-R
Y38K/F/E	(X=K/F/E)	R-Q-T-P-D-**X**-V-L-G-R
M2		**S**-**R**-T-P-D-Y-V-L-G-R
M4		**S**-**R**-T-**R**-**A**-Y-V-L-G-R
M5		**S**-**R**-T-**R**-**A**-**E**-V-L-G-R
M6		**S**-**R**-T-**R**-**A**-**E**-V-**E**-G-R
M10		**S**-**R**-**S**-**R**-**A**-**E**-**I**-**E**-**S**-**T**
PHBH *Pseudomonas* sp. CBS3		37 S-R-S-R-A-E-I-E-S-T 46

Results

Mutagenesis strategy, protein expression and purification. Table I presents the mutagenesis strategy. The amino acid sequence of the helix H2 region of PHBH from *P. fluorescens* was gradually changed into the corresponding sequence of PHBH from *Pseudomonas* sp. CBS3 (Seibold *et al.*, 1996). Single replacements were performed with Arg33, Gln34 and Tyr38,

whereas the number of multiple changes increases from two in mutant M2 to ten in mutant M10.

All single mutants and M2 and M4 were highly expressed. Their yield after purification (about 10% of total protein) compared favorably with that of wild-type PHBH (van Berkel *et al.*, 1992). M5 and M6 were rather poorly expressed, yielding approximately 1% of pure enzyme. Moreover, these mutants lost some FAD during purification. After replacement of ten residues in the helix H2 region (M10, Table I), we could not detect any mutant PHBH protein by antibody screening of cell extracts.

Catalytic properties. The steady-state kinetic parameters of the mutant proteins with NADPH and POHB are reported in Table II. With all mutants, no considerable changes in apparent K_m values for POHB was observed. The catalytic properties of R33K, Q34R, Q34K, Q34T, M2 and M4 were similar to the wild-type enzyme. R33S, Y38K and Y38F were poorly active with NADPH whereas R33E, Y38E, M5 and M6 exhibited impaired coenzyme binding. All single mutants and M2 and M4 catalyzed the efficient hydroxylation of POHB into 3,4-dihydroxybenzoate with virtually no formation of hydrogen peroxide. With M5 and M6, approximately 10% uncoupling of hydroxylation occurred.

The protein-flavin interaction was studied by activity measurements in the presence of varying concentrations of FAD. With the exception of M5 and M6 (apparent K_m FAD = 450 $\pm$ 50 nM), the mutants showed a similar affinity for FAD as wild-type PHBH (apparent K_m FAD = 45 $\pm$ 10 nM; Müller and van Berkel, 1982).

The binding of NADPH was further investigated by pre-steady state kinetics (Table II). To that end, the rate of anaerobic reduction of the enzyme-substrate complex was monitored at 450 nm as a function of the concentration of NADPH (Howell *et al.*, 1972; Eppink *et al.*, 1995). For all mutants, except R33E and Y38E, enzyme reduction was not rate limiting in catalysis and only slightly slower than wild-type. However, the apparent K_d NADPH varied significantly, in line with the steady-state kinetic analysis. For R33K and the M2 and M4 variants, the affinity for NADPH was similar to wild-type, whereas tight NADPH binding was observed for Q34R and Q34K. R33S, Y38K and Y38F interacted weakly with the cofactor, and R33E and Y38E had lost the affinity for NADPH.

Table II. Kinetic parameters of PHBH variants. Turnover numbers (k_{cat}) and reduction rates (k_{red}) are maximum values extrapolated to infinite concentrations of POHB and NADPH. (n.m. = not measurable). Kinetic constants have maximum error values of 10%.

	K_m		k_{cat}	k_{red}	K_d
	POHB	NADPH			NADPH
	μM	μM	s^{-1}	s^{-1}	mM
Wild-type	15	34	55	300	0.15
R33K	25	53	50	280	0.20
R33S	32	240	40	240	1.40
R33E	30	>600	> 10	> 10	> 2
Q34T	32	40	45	250	0.24
Q34R	22	24	45	240	0.08
Q34K	21	25	47	240	0.08
Y38K	33	140	52	250	0.88
Y38F	40	170	50	250	0.95
Y38E	34	>800	> 10	> 10	> 2
M2	29	35	45	245	0.25
M4	22	45	56	230	0.20
M5	45	>1000	> 5	-	-
M6	50	>1000	> 5	-	-

The Michaelis constants with NADH and POHB are reported in Table III. Like native PHBH (Eppink *et al.*, 1995), all single mutants and M2 and M4 were nearly inactive with NADH.

However, M5 and M6 clearly preferred NADH as cofactor (cf. Table II). M5 and M6 displayed similar catalytic properties, implying that the Leu40 → Glu replacement is not crucial for the switch in coenzyme specificity.

Table III. Steady-state kinetic parameters of PHBH variants with NADH. Turnover numbers are apparent maximum values extrapolated to infinite concentrations of POHB and NADH. Kinetic constants have maximum error values of 10%.

	K_m POHB	K_m NADH	k_{cat}
	μM	μM	min^{-1}
Wild-type	20	> 1000	> 10
M5	45	90	85
M6	40	90	85

Structural properties. Crystals with moderate quality diffraction properties were obtained for Q34T, Q34R and Y38E, all in complex with POHB. The mutant structures were very similar to the structure of wild-type PHBH, only minor changes at the site of mutation were observed. Superpositioning of Q34T, Q34R and Y38E onto the native enzyme gave root mean square deviations of 0.19, 0.24 and 0.21 Å, respectively for 391 equivalent Cα atoms. Replacement of Gln34 by Thr (Figure 2) breaks the hydrogen bond with Arg33 (Table IV) and abolishes the van der Waals interactions with Tyr38. As a result, a small rotation of both Arg33 and Tyr38 side chains is observed (Figure 2). The Thr34 side chain has the same orientation as Gln34 in the native structure and similar temperature factors. Similarly, the Gln34 to Arg substitution in Q34R induces only some small shifts in both Arg33 and Tyr38 side chains (Figure 3). Figure 4 shows that in Y38E, the side chain of Glu38 interacts with the NE2 of Gln34, and that the OE1 of Gln34 interacts strongly with the NH2 of Arg33 through a 90° turn of the side chain NH1/NH2 atoms of Arg33. Furthermore, the hydrogen bond interaction between Arg33 NH2 and the O2 ribose of FAD in wild-type PHBH (Schreuder *et al.*, 1989), is lost in Y38E (Table IV). No suitable crystals of the other PHBH mutants were obtained. The protein-flavin interactions in these mutants were therefore assessed by spectral analysis.

Table IV. Selected polar interactions (d < 3.2 Å) in PHBH variants

Enzyme	Atom 1	Atom 2	Distance
Wild-type	NH2 Arg33	O2* ribose FAD	2.7
	OE1 Gln34	NE Arg33	2.6
Q34T	NH2 Arg33	O2* ribose FAD	3.0
	OG1 Thr34	OE2 Glu32	3.0
Q34R	NH2 Arg33	O2* ribose FAD	2.9
Y38E	NH2 Arg33	OE1 Gln34	2.9
	NE2 Gln34	OE2 Glu38	2.7
	OE1 Glu38	NE2 Gln34	2.9
		OG1 Thr35	3.0

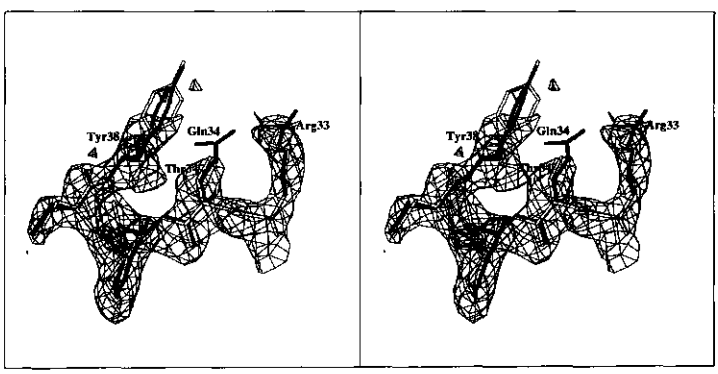

Fig. 2. Stereoview of the Q34T mutant. A $2F_o$-F_c electron density map of mutant Q34T is contoured at 2σ with Q34T in dark and the wild-type structure in open bonds.

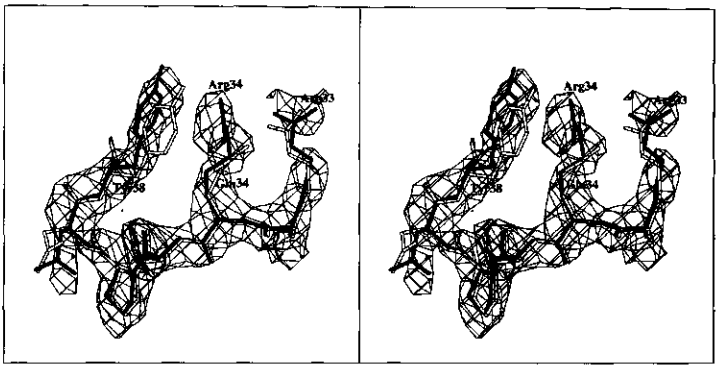

Fig. 3. Stereoview of the Q34R mutant. A $2F_o$-F_c electron density map of mutant Q34R is contoured at 2σ with Q34R in dark and the wild-type structure in open bonds.

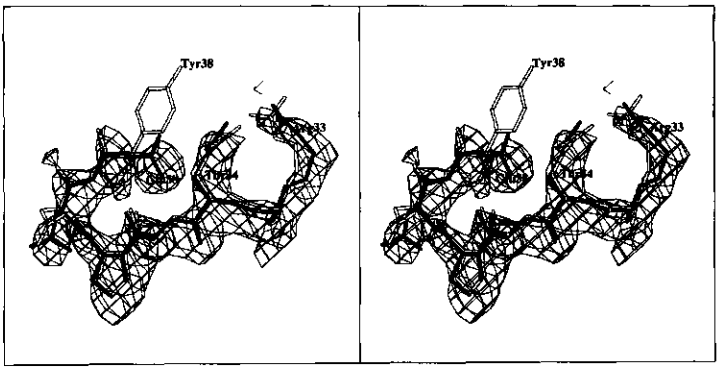

Fig. 4. Stereoview of the Y38E mutant. A $2F_o$-F_c electron density map of mutant Y38E is contoured at 2σ with Y38E in dark and the wild-type structure in open bonds.

Spectral properties. The amino acid replacements in the N-terminal part of helix H2 do not strongly influence the mode of substrate binding. This is concluded from fluorescence titration experiments in which the fluorescence emission of protein-bound FAD was measured as a function of substrate concentration. All mutants, except for M5 and M6, showed similar dissociation constants for the enzyme-substrate complex as the wild-type enzyme ($K_d = 30 \pm 10$ μM).

With M5 and M6, binding of POHB did not significantly change the fluorescence quantum yield of protein-bound FAD. A similar behaviour was reported for PHBH reconstituted with arabino-FAD (van Berkel *et al.*, 1994). Therefore, the enzyme-substrate interaction in M5 and M6 was studied by difference absorption spectroscopy. With both mutants, the affinity of the aromatic substrate (K_d = 95 ± 15 μM) is somewhat weaker than in wild-type PHBH (K_d = 50 ± 10 μM).

The shape of the substrate-induced flavin perturbation difference spectra correlates with the orientation of the flavin ring "in" or "out" of the active site (Gatti *et al.*, 1994). Except for M5 and M6, all mutants showed spectral properties indistinguishable from wild-type PHBH, indicative for the flavin "in" conformation (Figure 5A). The difference spectra of M5 (Figure 5B) and M6 (not shown) were intermediate between the changes observed for the flavin "in" and "out" conformation (Gatti *et al.*, 1994; van der Bolt *et al.*, 1996) and resembled that of mutant R42S (Eppink *et al.*, 1998a). This suggests that subtle structural changes far away from the active site can affect the dynamic behaviour of the flavin ring.

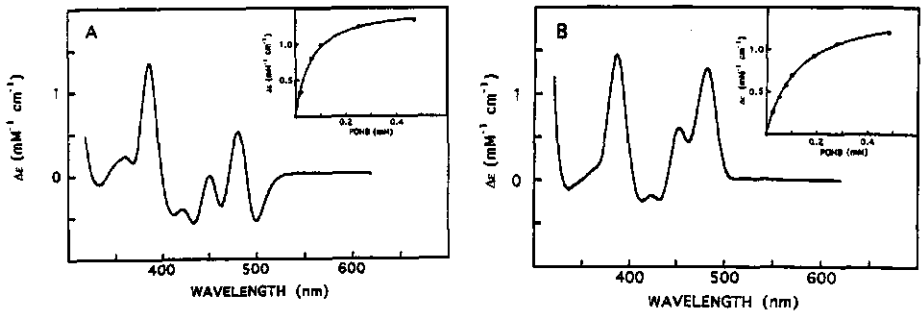

Fig. 5. Absorption perturbation difference spectra of PHBH mutants with POHB. The experiments were performed in 0.1 M Tris/sulfate pH 8.0, at 25°C. The absorbance differences are extrapolated to infinite POHB concentration. (A) mutant M4; (B) mutant M5. The inset shows the molar difference absorbance at 385 nm as a function of substrate concentration.

Discussion

PHBH is the archetype of the family of NAD(P)H-dependent flavoprotein aromatic hydroxylases. These enzymes share a large N-terminal domain for binding the FAD, but lack a well-defined domain for binding the pyridine dinucleotide (Eppink *et al.*, 1997). Recently,

we proposed that in PHBH from *P. fluorescens*, the NADPH molecule binds in an extended conformation in the interdomain cleft and that helix H2 of the FAD-binding domain is involved in determining the coenzyme specificity (Eppink *et al.*, 1998b). In this paper, the functional role of helix H2 was addressed by a sequential mutagenesis approach. First, single replacements were introduced to study the involvement of Arg33, Gln34 and Tyr38 in coenzyme recognition. Based on these results, multiple changes in helix H2 were made with the aim to change the coenzyme specificity.

The properties of the Arg33 mutants indicate that a basic residue at position 33 is important for NADPH recognition. This supports the proposal that Arg33 interacts with the 2'-phosphate moiety of NADPH (Eppink *et al.*, 1998b). Gln34 probably is less crucial for proper coenzyme binding. The structure of Q34T shows that Thr34 does not interact with Arg33 and Tyr38. Nonetheless, this mutant is catalytically as competent as the wild-type enzyme. Q34R and Q34K tightly interact with NADPH, supporting that the adenosine 2'-phosphate moiety of NADPH binds near Arg33, Tyr38 and Arg42 (Eppink *et al.*, 1998b). In Q34R, the extra introduced charge is located near the protein surface in between the side chains of Arg33 and Tyr38.

The involvement of Tyr38 in NADPH binding is confirmed by the properties of the Tyr38 mutants. Y38E does not bind NADPH, presumably due to electrostatic repulsion of the 2'-phosphate moiety of NADPH. However, the structure of Y38E shows that the side chain of Glu38 is neutralized to some extent by a hydrogen bond network with Arg33 and Gln34. This suggests that in Y38E, Arg33 contributes less to the interaction with NADPH than in wild-type enzyme. In wild-type PHBH, Arg33 is also involved in binding the 2-OH group of the adenosine ribose of FAD. However, this interaction seems not as crucial as originally suggested (Schreuder *et al.*, 1989), since R33S and R33E bind the FAD as firmly as the native enzyme.

The single amino acid replacements in helix H2 did not change the coenzyme specificity. Therefore, multiple substitutions were introduced based on the sequence of PHBH from *Pseudomonas* sp. CBS3. This enzyme, involved in the biodegradation of 4-chlorobenzoate (Müller *et al.*, 1984; Scholten *et al.*, 1991), shows 53% sequence identity with PHBH from *P. fluorescens* and is the only PHBH of known sequence which prefers NADH over NADPH as electron donor (Seibold *et al.*, 1996). When the sequence of the helix H2 region of PHBH from *P. fluorescens* was changed to the corresponding sequence of the *Pseudomonas* CBS3 enzyme (mutant M10, Table I), no protein expression was observed. The reason for this is not yet clear but it obviously relates to an improper folding of the polypeptide chain.

The properties of the double mutant M2 and the quadruple mutant M4 indicate that the amino acid residues in the N-terminal part of helix H2 are not crucial for the coenzyme

specificity. Both M2 and M4 are highly active with NADPH and not with NADH. Reversal of residues 33 and 34 does not impair FAD binding. This is in agreement with the results of the single mutants and with the fact that a similar Gln33-Arg34 arrangement is seen in PHBH from *Acinetobacter calcoaceticus* (DiMarco *et al.*, 1993). It also confirms that Glu32 rather than Arg33 is essential for the binding of the adenosine ribose moiety of FAD. Interestingly, Glu32 is conserved in the majority of flavoprotein aromatic hydroxylases (Eppink *et al.*, 1997) and in flavoprotein oxidases with a PHBH-fold (Mattevi, 1998). The Pro36Arg and Asp37Ala replacements in the quadruple mutant M4 hardly influence catalysis. This is not too surprising given the fact that Pro36 and Asp37 are located at the protein surface, somewhat remote from the putative NADPH binding site.

Extending the sequential amino acid replacements towards residue 38 established a switch in coenzyme specificity (mutant M5). Although M5 is not a very efficient enzyme, it shows for the first time that redesign of the coenzyme specificity of FAD-dependent aromatic hydroxylases is feasible. Moreover, it clearly supports our earlier proposal (Seibold et al., 1996; Eppink *et al.*, 1998b) that helix H2 of PHBH is critically involved in determining the coenzyme specificity. Unfortunately, no structural data of M5 (and M6) were obtained. The relatively weak binding and spectral properties of FAD in these mutants suggest that the multiple replacements introduce subtle conformational changes that are transmitted through long-range effects to the active site. Interestingly, a weak flavin-protein interaction was also observed in NAD(P)H-dependent PHBH from *Pseudomonas* sp. CBS3 (Seibold *et al.*, 1996). Because both Arg33 (this study) and Arg42 (Eppink *et al.*, 1998a) are involved in binding the adenosine moiety of FAD as well as the 2'-phosphate moiety of NADPH, this suggests that tight NADH binding is at the expense of the FAD binding strength and that considerable additional replacements are required to select for an optimal utilisation of NADH.

Coenzyme reversion has sofar only been described for members of the dehydrogenase/reductase families for which key specific determinants for NAD(P)H binding are known. Enzymes with the classical βαβ-fold (Rossman *et al.*, 1974; Wierenga *et al.*, 1986) for NAD(P)H binding (Scrutton *et al.*, 1990; Feeney *et al.*, 1990; Chen *et al.*, 1991; Bocanegra *et al.*, 1993; Nishiyama *et al.*, 1993; Clermont *et al.*, 1993; Bernard *et al.*, 1995; Galkin *et al.*, 1997; Rane and Calvo, 1997; Nakanishi *et al.*, 1997) and enzymes with a different but well-defined dinucleotide binding fold (Miyazaki and Oshima, 1994; Chen *et al.*, 1995; Yaoi *et al.*, 1996; Chen *et al.*, 1996; Friesen *et al.*, 1996; Shiraishi *et al.*, 1998) were succesfully changed. Crystal structures of mutant proteins with reversed coenzyme specificity (NADP → NAD) have sofar only been obtained for glutathione reductase (Mittl *et al.*, 1993, 1994) and isocitrate dehydrogenase (Hurley *et al.*, 1996).

With our studies we succeeded for the first time in the coenzyme reversion of a member of a superfamily of flavoenzymes where the exact binding mode of the cofactor is unknown. We conclude that specificity in *P. fluorescens* PHBH is conferred by hydrogen bond interaction of Tyr38 and charged interactions of Arg33 and Arg42 with the 2'-phosphate of bound NADPH. This is in keeping with the hypothesis that biological specificity is caused to some extent by hydrogen bonding but is best mediated by charged residues (Fersht *et al.*, 1985).

Materials and methods

General

Restriction endonucleases, Large fragment of DNA polymerase I (Klenow fragment), T4-DNA ligase, Taq polymerase, T4-kinase and oligonucleotides for mutagenesis were from GIBCO BRL. The QuikChange™ site-directed mutagenesis kit was obtained from Stratagene. [α-^{32}P]dATP (3000Ci/mol), sequencing primers, dNTPs, ddNTPs, oligonucleotides for mutagenesis, QAE-Sepharose fast-flow and Resource Q were purchased from Amersham Pharmacia Biotech. Calf intestinal phosphatase, glucose oxidase (grade II), NADPH, NADH, IPTG and dithiothreitol were from Boehringher. Cibacron-blue-3GA-agarose (type 3000-CL), FAD and ampicillin were from Sigma. All other chemicals were obtained from Merck and of the purest grade available.

Mutagenesis, expression and purification

The oligonucleotides used for the preparation of the PHBH mutant proteins described in this paper are listed in Table V. The single mutants R33K/S/E, Q34R/K/T, Y38K/F/E and mutant M10 were prepared according to the method of Kunkel *et al.*, (1987), essentially as described elsewhere (van Berkel *et al.*, 1992). Mutants M2 and M4 were generated with the PCR mega primer method, essentially as described elsewhere (Kamman *et al.*, 1989). The M5 and M6 mutants were constructed with the Quikchange™ site-directed mutagenesis kit, both sense and anti-sense mutagenic primers were used during mutant preparations (Stratagene, 1997). All mutations were introduced into the *E. coli* gene encoding mutant C116S (Eschrich *et al.*, 1990) and confirmed by nucleotide sequencing according to Sanger *et al.*, (1977). Because of identical catalytic properties (Eschrich *et al.*, 1990), C116S is further referred to as wild-type PHBH. Mutated PHBH genes were expressed in transformed *E. coli* TG2 grown in 5-l batches of tryptone/yeast medium containing 100 µg/ml ampicillin and 20 µg/ml IPTG at 37 °C under vigorous aeration. The mutant proteins were purified according to the procedure described for wild-type PHBH (van Berkel *et al.*, 1992).

Table V. Oligonucleotides for preparation of PHBH variants.

Oligonucleotides	Mutants
5'-CGACAACGTGATCCTCGAACGCCAGACCCCGGACTACGTGCTCGGCCGCATCCGCGCCGGCGTGCTGG-3'	Wild-type
5'-GTGATCCTCGAAAAACAGACCCCGG-3'	R33K
5'-GTGATCCTCGAAAGCCAGACCCCGG-3'	R33S
5'-GTGATCCTCGAAGAACAGACCCCGG-3'	R33E
5'-GTCATCCTCGAACGCAGGACCCCGG-3'	Q34R
5'-GTCATCCTCGAACGCAAAACCCCGG-3'	Q34K
5'-GTCATCCTCGAACGCACAACCCCGG-3'	Q34T
5'-CGCCAGACCCCGGACAAAGTGCTCGGCCGC-3'	Y38K
5'-CGCCAGACCCCGGACTTCGTGCTCGGCCGC-3'	Y38F
5'-CGCCAGACCCCGGACGAGGTGCTCGGCCGC-3'	Y38E
5'-GTGATCCTCGAACAGCGGACCCCGG-3'	R33Q/Q34R (M2)
5'-CAACGTGATCCTCGAAAGCCGGACCCGGGCCTACGTGCTCGGCCGC-3'	R33S/Q34R/P36R/D37A (M4)
5'-CGACAACGTGATCCTCGAAAGCCGGACCCGGGCCGAGGTGCTCGGCCGCATCCG-3' (sense)	R33S/Q34R/P36R/D37A/Y38E (M5)
5'-GCTGTTGCACTAGGAGCTTTCGGCCTGGGCCCGGCTCCACGAGCCGGCGTAGGC-3' (anti-sense)	R33S/Q34R/P36R/D37A/Y38E (M5)
5'-CGACAACGTGATCCTCGAAAGCCGGACCCGGGCCGAGGTGGAGGGCCGCATCCGCGCCGG-3' (sense)	R33S/Q34R/P36R/D37A/Y38E/L40E (M6)
5'-GCTGTTGCACTAGGAGCTTTCGGCCTGGGCCCGGCTCCACCTCCCGGCGTAGGCGCGGCC-3' (anti-sense)	R33S/Q34R/P36R/D37A/Y38E/L40E (M6)
5'-CGACAACGTGATCCTCGAAAGCCGGTCCCGGGCCGAGGGGGAGTCCACCATCCGCGCCGGCGTGCTGG-3'	R33S/Q34R/T35S/P36R/D37A/Y38E/ V39G/L40E/G41S/R42T (M10)

Analytical methods

Absorption (difference) spectra were recorded in 50 mM sodium phosphate buffer pH 7.0 at 25 °C on an Aminco DW-2000 spectrophotometer. Enzyme concentrations where spectrophotometrically determined using a molar absorption coefficient ε_{450} = 10.2 mM^{-1} cm^{-1} for protein bound FAD (van Berkel *et al.*, 1992). Dissociation constants of complexes between enzyme and substrate were determined fluorimetrically as described previously (Müller and van Berkel, 1982). Standard activity measurements were performed at 25 °C in air saturated 100 mM Tris/sulfate pH 8.0, containing 200 µM NAD(P)H, 200 µM POHB and 10 µM FAD. Steady-state kinetic parameters were determined as described (Eschrich *et al.*, 1993).

The efficiency of substrate hydroxylation was estimated from oxygen consumption experiments (Eschrich et al., 1993). Anaerobic enzyme reduction experiments were performed in 100 mM Tris/sulfate pH 8.0 at 25 °C using a High-Tech Scientific SF-51 stopped flow spectrophotometer (Eppink *et al.*, 1995).

Protein crystallization

Crystallization of PHBH mutants was performed in 39-41% ammonium sulfate, 0.04 mM FAD, 0.15 mM EDTA, 30 mM sodium sulfite, 1 mM POHB in 100 mM potassium phosphate (pH 7.0), essentially as described previously (Eppink *et al.*, 1998b). The crystals grew to a size of 0.3 * 0.3 * 0.3 mm^3 over a period of 3-5 days. Crystals with space group $C222_1$ of Q34T, Q34R and Y38E were obtained.

Structural data collection and refinement

X-ray diffraction data were collected at room temperature using a Siemens multiwire area detector and graphite monochromated CuKα radiation from an 18kW Siemens rotating anode generator, operating at 45 kV and 100 mA. The crystal-detector distance was 11.6 cm and the 2θ angle was 20°. Data were processed with the XDS package (Kabsch, 1988).

Guided by the structure of the wild-type enzyme-substrate complex (Schreuder *et al.*, 1989), starting electron density maps for Q34T, Q34R and Y38E were calculated, after a correction for the slightly different cell dimensions (Schreuder *et al.*, 1994). The 2*Fo*-*Fc* maps clearly showed the substitutions of Gln34 by Thr (Figure 2), Gln34 by Arg (Figure 3) and Tyr38 by Glu (Figure 4). The mutated residues were fitted in the electron-density maps with the graphics program O (Jones *et al.*, 1991). The protein model was inspected for irregularities and when necessary corrections were made. Refinement involved four cycles of map inspections followed by energy minimization and *B*-factor refinement using Xplor (Brünger, 1992). Water molecules were assigned by searching *Fo*-*Fc* maps for peaks of at least 4σ, which were between 0.20 and 0.50 nm of other atoms. Water molecules with *B*-factors higher than 70 $Å^2$ were rejected. The refined structure of Q34T has an *R* factor of 16.0 % for 16593 reflections between 8.0 and 2.4 Å and contains 239 water molecules. For Q34R an *R* factor of 14.4 % for 8809 reflections between 8.0 and 2.8 Å was obtained with 222 water molecules.

Finally, Y38E yields an *R* factor of 16.1 % for 15924 reflections between 8.0 and 2.5 Å containing 268 water molecules. For the Q34T, Q34R and Y38E structures the root mean square deviations from ideal values are respectively 0.009 - 0.010 Å for bond lengths and 1.43 - 1.58 Å for bond angles. Table VI summarizes the refinement statistics.

Table VI. X-ray diffraction data and refinement statistics of PHBH variants.

Enzyme	Q34T	Q34R	Y38E
Space group	$C222_1$	$C222_1$	$C222_1$
Cell dimensions (Å)			
A	71.7	71.8	72.3
B	146.2	146.5	146.2
C	88.7	88.6	89.1
Unique reflections	16,593	8,809	15,924
Resolution (Å)	2.4	2.8	2.5
R_{sym} (%)	6.2	7.1	5.5
Completeness (%)	89.5	91.7	92.1
Initial *R* factor (%)	24.0	25.8	25.0
Final *R* factor (%)	16.0	14.4	16.1
Water molecules	239	221	268
RMSD bond lengths (Å)	0.009	0.010	0.009
RMSD bond angles (°)	1.43	1.58	1.47
Average *B* factors (Å^2)			
Protein	25.4	25.5	25.6
Flavin ring	18.9	12.3	22.2
POHB	16.2	18.6	16.9

References

Baker,P.J., Britton,K.L., Rice,D.W., Rob,A. and Stillman,T.J. (1992) Structural consequences of sequence patterns in the fingerprint region of the nucleotide binding fold. *J. Mol. Biol.*, **228**, 662-671.

Bellamacina,C.R. (1996) The nicotinamide dinucleotide binding motif: a comparison of nucleotide binding proteins. *FASEB J.*, **10**, 1257-1269.

Bernard,N., Johnsen,K., Holbrook,J.J. and Delcour,J. (1995) D175 discriminates between NADH and NADPH in the coenzyme binding site of *Lactobacillus delbrueckii subsp.* Bulgaricus D-lactate dehydrogenase. *Biochem. Biophys. Res. Com.*, **208**, 895-900.

Bocanegra,J.A., Scrutton,N.S. and Perham,R.N. (1993) Creation of an NADP-dependent pyruvate dehydrogenase multienzyme complex by protein engineering. *Biochemistry*, **32**, 2737-2740.

Brünger,A.T. (1992) X-PLOR. *A system for crystallography and NMR, manual version 3.1*. Yale University Press, New Haven, USA.

Carson,M. (1991) Ribbons 2.0. *J. Appl. Crystallogr.*, **24**, 958-961.

Chen,Z., Lee,W.R. and Chang,S.H. (1991) Role of aspartic acid 38 in the cofactor specificity of Drosophila alcohol dehydrogenase. *Eur. J. Biochem.*, **202**, 263-267.

Chen,R., Greer,A. and Dean,A.M. (1995) A highly active decarboxylating dehydrogenase with rationally inverted coenzyme specificity. *Proc. Natl. Acad. Sci. USA*, **92**, 11666-11670.

Chen,R., Greer,A. and Dean,A.M. (1996) Redesigning secondary structure to invert coenzyme specificity in isopropylmalate dehydrogenase. *Proc. Natl. Acad. Sci. USA*, **93**, 12171-12176.

Clermont,S., Corbier,C., Mely,Y., Gerard,D., Wonacott,A. and Branlant G. (1993) Determinants of coenzyme specificity in glyceraldehyde-3-phosphate dehydrogenase: Role of the acidic residue in the fingerprint region of the nucleotide binding fold. *Biochemistry*, **32**, 10178-10184.

Dean,A.M. and Golding,G.B. (1997) Protein engineering reveals ancient adaptive replacements in isocitrate dehydrogenase. *Proc. Natl. Acad. Sci. USA*, **94**, 3104-3109.

DiMarco,A.A., Averhoff,B.A., Kim,E.E. and Ornston,L.N. (1993) Evolutionary divergence of *pobA*, the structural gene encoding *p*-hydroxybenzoate hydroxylase in an *Acinetobacter calcoaceticus* strain well-suited for genetic analysis. *Gene*, **125**, 25-33.

Enroth,C., Neujahr,H., Schneider,G. and Lindqvist,Y. (1998) The crystal structure of phenol hydroxylase in complex with FAD and phenol provides evidence for a concerted conformational change in the enzyme and its cofactor during catalysis. *Structure*, **6**, 605-617.

Entsch,B. and van Berkel,W.J.H. (1995) Structure and mechanism of *para*-hydroxybenzoate hydroxylase. *FASEB J.*, **9**, 476-483.

Eppink,M.H.M., Schreuder,H.A. and van Berkel,W.J.H. (1995) Structure and function of mutant Arg44Lys of *p*-hydroxybenzoate hydroxylase. *Eur. J. Biochem.*, **231**, 157-165.

Eppink,M.H.M., Schreuder,H.A. and van Berkel,W.J.H. (1997) Identification of a novel conserved sequence motif in flavoprotein hydroxylases with a putative dual function in FAD/NAD(P)H binding. *Protein Sci.*, **6**, 2454-2458.

Eppink,M.H.M., Schreuder,H.A. and van Berkel,W.J.H. (1998a) Lys42 and Ser42 variants of *p*-hydroxybenzoate hydroxylase from *Pseudomonas fluorescens* reveal that Arg42 is essential for NADPH binding. *Eur. J. Biochem.*, **253**, 194-201.

Eppink,M.H.M., Schreuder,H.A. and van Berkel,W.J.H. (1998b) Interdomain binding of NADPH in *p*-hydroxybenzoate hydroxylase as suggested by kinetic, crystallographic and modelling studies of His162 and Arg269 variants. *J. Biol. Chem.*, **273**, 21031-21039.

Eppink,M.H.M., Schreuder,H.A. and van Berkel,W.J.H. (1999) Phe161 and Arg166 variants of *p*-hydroxybenzoate hydroxylase. Implications for NADPH recognition and structural stability. *FEBS Lett.*, **443**, 251-255.

Eschrich,K., van Berkel,W.J.H., Westphal,A., de Kok,A., Mattevi,A., Obmolova,G., Kalk,K.H. and Hol,W.G.J. (1990) Engineering of microheterogeneity-resistant *p*-hydroxybenzoate hydroxylase from *Pseudomonas fluorescens*. *FEBS Lett.*, **277**, 197-199.

Eschrich,K., van der Bolt,F.J.T., de Kok,A. and van Berkel,W.J.H. (1993) Role of Tyr201 and Tyr385 in substrate activation by *p*-hydroxybenzoate hydroxylase from *Pseudomonas fluorescens*. *Eur. J. Biochem.*, **216**, 137-146.

Feeney,R., Clarke,A.R. and Holbrook,J.J. (1990) A single amino acid substitution in lactate dehydrogenase improves the catalytic efficiency with an alternative coenzyme. *Biochem. Biophys. Res. Com.*, **2**, 667-672.

Fersht,A.R., Shi,J-P., Knill-Jones,J., Lowe,D.M., Wilkinson,A.J., Blow,D.M., Brick,P., Carter,P., Waye,M.M.Y. and Winter,G. (1985) Hydrogen bonding and biological specificity analysed by protein engineering. *Nature*, **314**, 235-238.

Friesen,J.A., Lawrence,C.M., Stauffacher,V. and Rodwell,V.W. (1996) Structural determinants of nucleotide coenzyme specificity in the distinctive dinucleotide binding fold of HMG-CoA reductase from *Pseudomonas mevalonii*. *Biochemistry*, **35**, 11945-11950.

Galkin,A., Kulakova,L., Ohshima,T., Esaki,N. and Soda,K. (1997) Construction of a new leucine dehydrogenase with preferred specificity for $NADP^+$ by site-directed mutagenesis of the strictly NAD^+-specific enzyme. *Protein Engng.*, **10**, 687-690.

Gatti,D.L., Palvey,B.A., Lah,M.S., Entsch,B., Massey,V., Ballou,D.P. and Ludwig,M.L. (1994) The mobile flavin of 4-OH benzoate hydroxylase. *Science*, **266**, 110-114.

Howell,L.G., Spector,T. and Massey,V. (1972) Purification and properties of *p*-hydroxybenzoate hydroxylase from *Pseudomonas fluorescens*. *J. Biol. Chem.*, **247**, 4340-4350.

Hurley,J.M., Chen,R. and Dean,A.M. (1996) Determinants of cofactor specificity in isocitrate dehydrogenase: structure of an engineered $NADP^+$ -> NAD^+ specificity-reversal mutant. *Biochemistry*, **35**, 5670-5678.

Jones,T.A., Zou,J-Y., Cowan,S. and Kjeldgaard,M. (1991) Improved methods for the building of protein models in electron density maps and the location of errors in these models. *Acta Crystallogr.*, **A47**, 110-119.

Kabsch,W. (1988) Evaluation of single-crystal diffraction data from a position-sensitive detector. *J. Appl. Crystallogr.*, **21**, 916-924.

Kamman,M., Laufs,J., Schnell,J. and Gronenberg,B. (1989) Rapid insertional mutagenesis of DNA by polymerase chain reaction (PCR). *Nucleic Acids Res.*, **231**, 157-165.

Kunkel,T.A., Roberts,J.D. and Zakour,R.A. (1987) Rapid and efficient site-specific mutagenesis without phenotypic selection. *Methods Enzymol.*, **154**, 367-382.

Lesk,A.M. (1995) NAD-binding domains of dehydrogenases. *Curr. Op. Struct. Biol.*, **1**, 954-967.

Massey,V. (1994) Introduction: Flavoprotein structure and mechanism. *FASEB J.*, **9**, 473-475.

Mattevi,A. (1998) The PHBH fold: not only flavoenzymes. *Biophys. Chem.*, **70**, 217-222.

Mittl,P.R.E., Berry,A., Scrutton,N.S., Perham,R.N. and Schulz,G.E. (1993) Structural differences between wild-type NADP-dependent glutathione reductase from *Escherichia coli* and a redesigned NAD-dependent mutant. *J. Mol. Biol.*, **231**, 191-195.

Mittl,P.R.E., Berry,A., Scrutton,N.S., Perham,R.N. and Schulz,G.E. (1994) Anatomy of an engineered NAD-binding site. *Protein Sci.*, **3**, 1504-1514.

Miyazaki,K. and Oshima,T. (1994) Co-enzyme specificity of 3-isopropylmalate dehydrogenase from *Thermus thermophilus* HB8. *Protein Engng.*, **7**, 401-403.

Müller,F. and van Berkel,W.J.H. (1982) A study on *p*-hydroxybenzoate hydroxylase from *Pseudomonas fluorescens*. A convenient method of preparation and some properties of the apoenzyme. *Eur. J. Biochem.*, **128**, 21-27.

Müller,R., Thiele,J., Klages,U. and Lingens,F. (1984) Incorporation of ^{18}O water into 4-hydroxybenzoate acid in the reaction of 4-chlorobenzoate dehalogenase from *Pseudomonas* sp. CBS3. *Biochem. Biophys. Res. Commun.*, **124**, 178-182.

Nakanishi,M., Matsuura,K., Kaibe,H., Tanaka,N., Nonaka,T., Mitsui,Y. and Hara,A. (1997) Switch of coenzyme specificity of mouse lung carbonyl reductase by substitution of threonine 38 with aspartic acid. *J. Biol. Chem.*, **272**, 2218-2222.

Nishiyama,M., Birktoft,J.J. and Beppu,T. (1993) Alteration of coenzyme specificity of malate dehydrogenase from *Thermus flavus* by site-directed mutagenesis. *J. Biol. Chem.*, **7**, 4656-4660.

Palfey,B.A., Moran,G.R., Entsch,B., Ballou,D.P. and Massey,V. (1999) Substrate recognition by "Password" in *p*-hydroxybenzoate hydroxylase. *Biochemistry*, **38**, 1153-1158.

Rane,M.J. and Calvo,K.C. (1997) Reversal of the nucleotide specificity of ketol acid reductoisomerase by site-directed mutagenesis identifies the NADPH binding site. *Arch. Biochem. Biophys.*, **338**, 83-89.

Rossmann,M.G., Moras,D. and Olsen,K.W. (1974) Chemical and biological evolution of a nucleotide-binding protein. *Nature*, **250**, 194-199.

Sanger,F., Nicklen,S. and Coulson,A.R. (1977) DNA sequencing with chain-terminating inhibitors. *Proc. Natl. Acad. Sci. USA*, **74**, 5463-5467.

Scholten,J.D., Chang,K.H., Babbitt,P.C., Charest,H., Sylvestre,M. and Dunaway-Mariano,D. (1991) Novel enzymic hydrolytic dehalogenation of a chlorinated aromatic. *Science*, **253**, 182-185.

Schreuder,H.A., Prick,P.A.J., Wierenga,R.K., Vriend,G., Wilson,K.S., Hol,W.G.J. and Drenth,J. (1989) Crystal structure of the *p*-hydroxybenzoate hydroxylase-substrate complex refined at 1.9 Å resolution. *J. Mol. Biol.*, **208**, 679-696.

Schreuder,H.A., Mattevi,A., Obmolova,G., Kalk,K.H., Hol,W.G.J., van der Bolt,F.J.T. and van Berkel,W.J.H. (1994) Crystal structure of wild-type *p*-hydroxybenzoate hydroxylase complexed with 4-aminobenzoate, 2,4-dihydroxybenzoate and 2-hydroxy-4-aminobenzoate and the Tyr222Ala mutant, complexed with 2-hydroxy-4-aminobenzoate. Evidence for a proton channel and a new binding mode of the flavin ring. *Biochemistry*, **33**, 10161-10170.

Scrutton,N.S., Berry,A. and Perham,R.N. (1990) Redesign of the coenzyme specificity of a dehydrogenase by protein engineering. *Nature*, **343**, 38-43.

Seibold,B., Matthes,M., Eppink,M.H.M., Lingens,F., van Berkel,W.J.H. and Müller,R. (1996) 4-Hydroxybenzoate hydroxylase from *Pseudomonas* sp. CBS3. Purification, characterization, gene cloning, sequence analysis and assignment of structural features determining the coenzyme specificity. *Eur. J. Biochem.*, **239**, 469-478.

Sem,D.S. and Kasper,C.B. (1993) Interaction with arginine 597 of NADPH-cytochrome P-450 oxidoreductase is a primary source of the uniform binding energy used to discriminate between NADPH and NADH. *Biochemistry*, **32**, 11548-11558.

Shiraishi,N., Croy,C., Kaur,J. and Campbell,W.H. (1998) Engineering of pyridine nucleotide specificity of nitrate reductase: Mutagenesis of recombinant cytochrome *b* reductase fragment of *Neurospora crassa* NADPH: Nitrate reductase. *Arch. Biochem. Biophys.*, **358**, 104-115.

Stratagene Cloning Systems. (1997) QuikChange^{tm} Site-Directed Mutagenesis Kit, Instruction Manual.

Van Berkel,W.J.H. and Müller,F. (1991) Flavin-dependent monooxygenases with special reference to 4-hydroxybenzoate hydroxylase. In: Müller F, ed. *Chemistry and biochemistry of flavoenzymes* 2. Boca Raton, Florida: CRC Press. pp 1-29.

Van Berkel,W.J.H., Westphal,A., Eschrich,K., Eppink,M. and De Kok,A. (1992) Substitution of Arg214 at the substrate-binding site of *p*-hydroxybenzoate hydroxylase from *Pseudomonas fluorescens*. *Eur. J. Biochem.*, **210**, 411-419.

Van Berkel,W.J.H., Eppink,M.H.M. and Schreuder,H.A. (1994) Crystal structure of *p*-hydroxybenzoate hydroxylase reconstituted with the modified FAD present in alcohol oxidase from methylotrophic yeasts: evidence for an arabinoflavin. *Protein Sci.*, **3**, 2245-2253.

Van Berkel,W.J.H., Eppink,M.H.M., van der Bolt,F.J.T., Vervoort,J., Rietjens,I.M.C.M. and Schreuder,H.A. (1997) *p*-Hydroxybenzoate hydroxylase: mutants and mechanism. In: Flavins and flavoproteins XII, Calgary 1996, Ed. Stevenson,K.J., Massey,V. and Williams,C.H.,Jr, University of Calgary Press, Calgary, pp. 305-314.

Van der Bolt,F.J.T., Vervoort,J. and van Berkel,W.J.H. (1996) Flavin motion in *p*-hydroxybenzoate hydroxylase. *Eur. J. Biochem.*, **237**, 592-600.

Wierenga,R.K., Terpstra,P. and Hol,W.G.J. (1986) Prediction of the occurrence of the ADP-binding βαβ-fold in proteins, using an amino acid sequence fingerprint. *J. Mol. Biol.*, **187**, 101-107.

Yaoi,T., Miyazaki,K., Oshima,T., Komukai,Y. and Go,M. (1996) Conversion of the coenzyme specificity of isocitrate dehydrogenase by module replacement. *J. Biochem.*, **119**, 1014-1018.

CHAPTER 10

"Unactivated" *p*-hydroxybenzoate hydroxylase: Crystal structures of the free enzyme and the enzyme-benzoate complex

Michel H.M. Eppink, Willem J.H. van Berkel, Alex Tepliakov and Herman A. Schreuder

J. Mol. Biol. (in preparation)

"Unactivated" *p*-Hydroxybenzoate hydroxylase: Crystal structures of the substrate-free enzyme and the enzyme-benzoate complex.

Abstract

Substrate binding in the flavoprotein *p*-hydroxybenzoate hydroxylase (PHBH) strongly stimulates enzyme reduction by NADPH. To obtain more insight in the effector specificity of the substrate, the crystal structures of substrate-free PHBH and in complex with benzoate were solved.

This is the first report of a crystal structure from substrate-free PHBH and in a crystal form, space group $P2_12_12_1$, which has not been described earlier. The $P2_12_12_1$ crystals of the substrate-free enzyme diffracted to 2.5 Å under cryo conditions and the structure was refined to an R factor of 20.7 %. No significant structural changes were observed between substrate-free enzyme in the $P2_12_12_1$ crystal form and the enzyme-substrate complex in the extensively studied space group $C222_1$. The observed differences were quite small and localized in the active site cleft and in a flexible loop region involved in crystal contacts. The isoalloxazine ring of FAD is flexible in the substrate-free enzyme and located intermediate between the "in" and "out" conformation.

$C222_1$ crystals of PHBH in complex with benzoate diffracted to high resolution (2.0 Å) with an R factor of 16.7% after refinement. The structure of the enzyme-benzoate complex is virtually identical to that of the enzyme-substrate complex, with the flavin ring occupying the inner orientation in the active site. The absence of the 4-hydroxy moiety of the substrate allows Tyr201 and Tyr385 in the active site to contact His72 at the protein surface via a bridge of two water molecules.

In agreement with earlier suggestions, we conclude that efficient flavin reduction by NADPH is facilitated by substrate deprotonation as controlled by the proton relay network between His72 and Pro293.

Introduction

p-Hydroxybenzoate hydroxylase (PHBH) (EC 1.14.13.2) is the model enzyme of the family of flavoprotein aromatic hydroxylases. These enzymes catalyze the insertion of one atom of molecular oxygen into the substrate using NAD(P)H as electron donor (van Berkel, 1991). The catalytic cycle of PHBH consists of two half-reactions (Massey, 1994). During the reductive part of the reaction, the substrate 4-hydroxybenzoate (POHB) acts as an effector, highly stimulating the rate of flavin reduction by NADPH. In the oxidative half-reaction, the aromatic substrate is converted to 3,4-dihydroxybenzoate via the formation of a transiently stable flavin C4a-hydroperoxide oxygenating species (Entsch and van Berkel, 1995).

Although many details of the catalytic cycle are known, it is unclear how the enzyme controls the reactivity of the flavin during the various reaction steps (Entsch and van Berkel, 1995). One of the unsolved items concerns the effector role of the aromatic substrate. Early spectroscopic and electron microscopic studies of PHBH from various sources suggested large protein conformational changes upon substrate binding (Yano, 1969a; Hesp, 1969; Schepman, 1976). However, preliminary crystallographic analysis of the substrate-free enzyme (Wierenga, 1979; van der Laan, 1986) indicated that no gross structural changes occur. Recently, crystallographic studies demonstrated two flavin conformations for PHBH. It was suggested that flavin movement is essential for the exchange of substrate and product during catalysis (Schreuder, 1994; Gatti, 1994) and for the recognition of NADPH (van Berkel, 1994; Palfey, 1997). Crystal structures of PHBH complexed with 2,4-dihydroxybenzoate or 2-hydroxy-4-aminobenzoate showed that the 2-hydroxy substituent of the substrate analogs induce the flavin ring to adopt the "open" conformation out of the active site (Table 1). However, no correlation exists between the position of the flavin ring in the crystal structure and the rate of enzyme reduction by NADPH. Kinetic studies have shown that efficient reduction is only accomplished in the presence of POHB derivatives (Spector, 1972; Husain, 1980). Moreover, studies from site-directed mutants suggested that rapid reduction is facilitated by deprotonation of the substrate phenol (Entsch, 1991; Eschrich, 1993; Palfey, 1999).

For a better understanding of the effector role of the substrate, we have solved the crystal structure of substrate-free PHBH and of PHBH in complex with the non-substrate effector benzoate.

A new crystal form of the substrate-free enzyme was obtained, but no significant conformational changes were observed. In the absence of aromatic ligands, the flavin ring is much more flexible and adopts a position, intermediate between the "in" and "out"

conformation. The novel structural data are discussed with respect to recent results from site-directed mutagenesis.

Table 1. Some characteristics of PHBH with substrate analogs.

Substrate analog	k_{red}	k_{cat}	Flavin conformer
	s^{-1}	s^{-1}	
4-hydroxybenzoate	300[a]	55[a]	in[e]
3,4-dihydroxybenzoate	4[b]	4[b]	in[f]
2,4-dihydroxybenzoate	1.1[c]	0.7[c]	out[g]
4-aminobenzoate	0.09[d]	0.09[d]	in[g]
2-hydroxy-4-aminobenzoate	0.003[a]	0.003[a]	out[g]

[a] van Berkel et al., 1992; [b] Eschrich et al., 1993; [c] van der Bolt et al., 1996; [d] Gatti et al., 1996; [e] Schreuder et al., 1989; [f]Schreuder et al., 1988; [g] Schreuder et al., 1994.

Experimental Procedures

Enzyme preparations. Recombinant PHBH was purified as described (van Berkel, 1992). The enzyme was stored as an ammonium sulfate precipitate at 4 °C.

Analytical methods. PHBH activity was routinely assayed in 100 mM Tris/sulfate, pH 8.0, containing 0.5 mM EDTA, 200 μM NADPH, 200 μM POHB and 10 μM FAD (Müller & van Berkel, 1982).

Crystallization. Crystals of substrate-free enzyme and in complex with benzoate were obtained using the hanging drop method. The protein solution contained 10-15 mg/ml enzyme in 100 mM potassium phosphate buffer (pH 7.0). The reservoir solution contained 25% PEG4000, 0.04 mM FAD, 0.30 mM EDTA, 30 mM sodium sulfite and 0.1 M potassium phosphate buffer (pH 7.0). Drops of 2 μl protein solution, 2 μl reservoir solution and 1 μl 10 mM benzoate were allowed to equilibrate at 4°C against 1 ml of

reservoir solution. Crystals of the enzyme-benzoate complex with dimensions of 0.3 x 0.3 x 0.1 mm^3 and space group $C222_1$ grew within 5 days. For crystallization of substrate-free PHBH, 1 µl 25 mM 2'-AMP was added instead of benzoate. Crystals with dimensions of 0.3 x 0.2 x 0.15 mm^3 and space group $P2_12_12_1$ were obtained within 15 days. $P2_12_12_1$ is a new symmetry group for PHBH, with two molecules in the asymmetric unit and cell dimensions of a=76.1, b=92.1, c=138.4 Å.

Data Collection. Crystallographic data of the enzyme-benzoate complex were collected at 4°C using a multiwire area detector (Siemens, Analytical Instruments, Inc., Madison, WI) mounted on a Siemens rotating anode generator, operating at 45 kV and 100 mA, equipped with a graphite monochromator. Data were processed with the XDS package (Kabsch, 1988). Data collections of the substrate-free enzyme were performed at cryo-temperature (110K), because at room temperature the crystals were radiation sensitive. The substrate-free enzyme data were obtained on beam-line X11 of the EMBL Outstation in Hamburg using a MAR image plate detector and 1.08 Å radiation. Intensities were integrated using DENZO and scaled with SCALEPACK (Otwinowski, 1993). Data collection statistics are given in Table 2. The diffraction of PHBH with benzoate extends to high resolution (2.0 Å), whereas the substrate-free enzyme crystals diffracted to a resolution of 2.5 Å.

Refinement. The structure of enzyme-benzoate was refined starting from the coordinates of the enzyme-substrate complex after a correction for the slightly different cell dimensions. Refinement was started with manual inspection of unweighted $2F_o$-F_c and F_o-F_c maps based on the corrected starting model of the enzyme-substrate complex (Schreuder, 1989). The structure of the enzyme-benzoate complex clearly showed the absence of the 4-hydroxy group in the substrate analog and some small changes in the active site. Refinement was carried out by four rounds of map inspections and rebuilding using O (Jones, 1991) with subsequent energy minimization and temperature factor refinement using XPLOR (Brünger, 1992). For the enzyme-benzoate complex, overall anisotropic B-factors were applied to the dataset, with the following B-factors: B11 = -8.3218 $Å^2$; B22 = 6.1993 $Å^2$; B33 = 2.1225 $Å^2$.

The substrate-free enzyme crystallized in a new crystal form ($P2_12_12_1$) with two monomers in the asymmetric unit. The structure was solved by molecular replacement using the AMoRe package (Navaza, 1994) and the enzyme-substrate complex as a search model. The structure was refined with the XPLOR package (Brünger, 1992) using two different protocols, (i) application of strict NCS on one monomer and (ii) the use of NCS restraints on two monomers. The reflections were scaled by refining overall anisotropic B-factors, resulting in the following B-factors: B11 = -2.9690 $Å^2$; B22 = -0.9389 $Å^2$; B33

= 3.9080 Å^2. After each round of strict NCS refinement, two monomers were regenerated and refined without NCS and subsequently superimposed to obtain an improved rotation matrix and translation vector. After 10 cycles of NCS refinement and optimization of NCS, the R-factor with strict NCS was 23.1 % (R_{free} = 31.6 %) and without NCS a value of 20.0 % (R_{free} = 32.8 %) was reached. Finally, the positions of the atoms were restrained (NCS restraints) with an effective energy term of 300 kcal/(mol Å^2) resulting in an R-factor of 20.7 % (R_{free} = 31.6 %). Due to the local symmetry we measured 29,316 unique reflections. Without NCS we would reach with this number of reflections a resolution of 2.0 Å. Hence, by applying strict NCS at 2.5 Å, we obtain the same observation to parameter ratio as at 2.0 Å without NCS.

Table 2. Data collection and refinement statistics of free PHBH and in complex with benzoate.

	enzyme-benzoate complex	substrate-free enzyme
cell dimensions (Å)		
a	72.1	76.1
b	146.5	92.1
c	88.76	138.4
space group	$C222_1$	$P2_12_12_1$
unique reflections	27,754	29,316
resolution (Å)	2.0	2.5
R_{sym} (%)	5.5	4.9
completeness (%)	94.5	96.0
Initial R-factor	28.0	40.0
Final R-factor	16.8	20.7
R_{free}	-	31.6
water molecules	336	217
rms bond lengths (Å)	0.010	0.011
rms bond angles (deg)	1.46	1.57
average *B* factors (Å^2)		
protein	23.9	25.5
flavin ring	20.1	39.5
substrate (analog)	17.8	-

Results

Structural studies

Structure verification. The crystal structure of the enzyme-substrate complex of PHBH at 1.9 Å (Schreuder, 1989) was used as a start for refining the different crystal structures. The stereochemistry of the refined structures is very good, with root mean square deviations of 0.010-0.011 Å for bond lengths, 1.5-1.6° for the bond angles, and R-factors of 16.8-20.7%. The Ramachandran plots of substrate-free enzyme (Fig.1) and in complex with benzoate (not shown) have similar ϕ and ψ angles as compared to the enzyme-substrate complex (Schreuder, 1989). Superpositioning of the structures onto the enzyme-substrate complex revealed no changes in the overall folding in any of the structures. The rms deviations for all 391 equivalent C_α atoms varied from 0.19 Å for the enzyme-benzoate complex to 0.74 Å for the substrate-free enzyme. Also the average temperature factors listed in Table 2 do not differ significantly between the different crystal structures, indicating that cryocooling did not influence the temperature factors. For the substrate-free enzyme, the B-factors for the flavin ring were significantly higher than for the enzyme-substrate complex, probably because the position of flavin ring is no longer restricted by the presence of the aromatic substrate(analog).

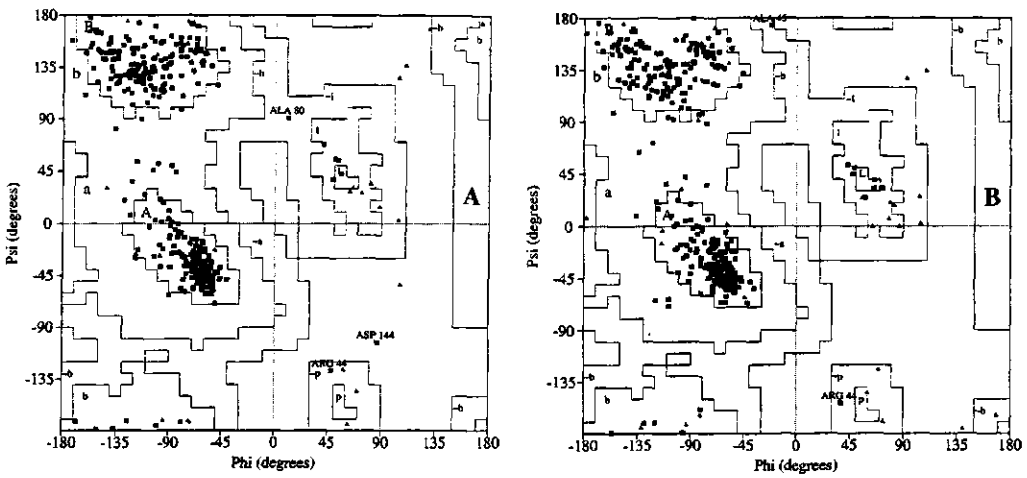

Fig 1. Ramachandran plots: A) enzyme-substrate complex with spacegroup $C222_1$; B) substrate-free PHBH with spacegroup $P2_12_12_1$.

Substrate-free PHBH. The crystal structure of the substrate-free enzyme was refined at 2.5 Å using NCS, because of the presence of two monomers in the asymmetric unit in space group $P2_12_12_1$. The structural changes with respect to the enzyme-substrate complex are limited to the C-terminus and in the active site region. For the first time the three flexible residues Glu392, Ile 393 and Glu394 of the C-terminus could be build into the electron density maps. Furthermore, no water molecules were visible in the substrate binding pocket of the enzyme, probably due to disorder of the waters or the limited resolution (Fig.2a). From the active site residues Arg214 changed position (Fig.2b). The Arg214 side chain, which binds the carboxylate moiety of the substrate (Table 3a), becomes highly disordered with B-values of up to 90 $Å^2$. In the enzyme-substrate complex the Arg214 side chain is tightly fixed by the substrate, with side chain B-values below 20 $Å^2$ (Schreuder, 1989; van Berkel, 1992). From another essential active site residue, Tyr222, a shift in the aromatic side chain is observed (Fig.2b) together with an significant increase in temperature factor from 12.0 $Å^2$ to 28.0 $Å^2$ in relation to the enzyme-substrate complex. Mutagenesis studies of Tyr222 revealed that this residue is indeed important for substrate binding (Gatti, 1994; van der Bolt, 1996). The other active site residues, such as Tyr201, Ser212, Pro293 and Tyr385 have similar or very marginally shifted positions (Fig.2b) and B-factors comparable to wild-type enzyme. The absence of the substrate increases the flexibility of the isoalloxazine ring and the flavin ring shifts 11° (Table 5) towards the protein surface. This movement of the isoalloxazine ring breaks both interactions between O2 FAD with N Leu299 and of N3 FAD with O Val47 (Table 3b), suggesting that these interactions do not contribute much to the binding energy. A similar flavin movement has been observed with PHBH and mutant enzymes in the presence of substrate or substrate analog(s) (Schreuder, 1994; Gatti, 1994; van Berkel, 1994; van Berkel, 1997). There it was argued that flavin mobility is necessary for substrate entrance, product release and efficient reduction by NADPH.

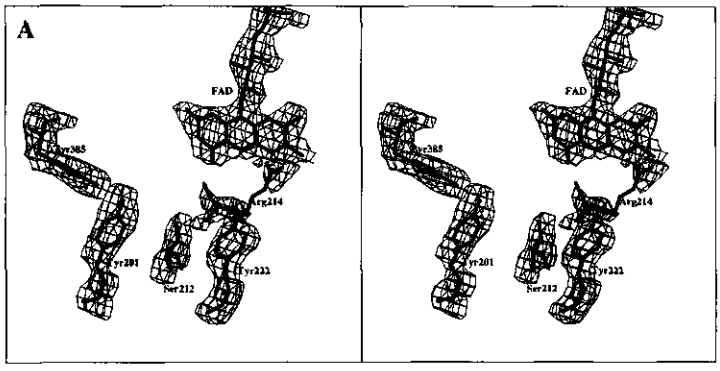

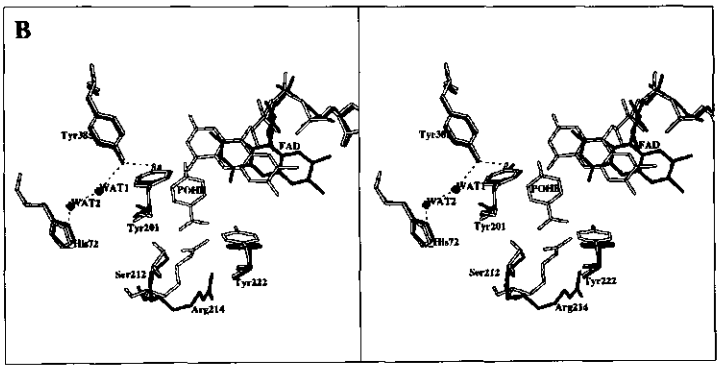

Fig 2. Structure of substrate-free PHBH. A) $2F_O$-F_C map, contoured at 2σ, of the active site region with the residues Tyr201, Ser212, Arg214, Tyr222, Tyr385 and the flavin ring in grey bonds. B) Superposition of the structures of the enzyme-substrate complex (open bonds), and substrate-free enzyme (grey bonds). The flavin ring in substrate-free enzyme occupies the "out" position. Both dots are WAT1 (Wat819) and WAT2 (Wat871). WAT1 is also present in the enzyme-substrate complex, whereas WAT2 is only present in substrate-free enzyme. 4-hydroxybenzoate (POHB).

Table 3a. Atomic contacts (d<3.2Å) between PHBH and substrate(analog).

Substrate atom	[a]enzyme-substrate complex	enzyme-benzoate complex
O4	(2.6) OH Tyr201	
	(2.9) O Pro293	
	(3.0) O Thr294	
O1*	(2.8) OG Ser212	(2.7) OG Ser212
	(2.8) NH2 Arg214	(2.9) NH2 Arg214
O2*	(2.6) OH Tyr222	(2.6) OH Tyr222
	(3.1) NH2 Arg214	(3.0) NH2 Arg214

[a]enzyme-substrate complex (Schreuder, 1989).

Table 3b. Atomic contacts (d<3.2Å) between PHBH and the flavin ring of FAD in the different complexes.

FAD atom	protein	[a]enzyme-benzoate complex	enzyme-benzoate complex	substrate-free enzyme
N1	N Leu299	3.1	3.1	
	O Wat216		3.1	
O2	N Leu299	3.0	2.9	3.0
	N Asn300	3.1	3.1	
	ND2 Asn300	3.1	3.0	
N3	O Val47	2.9	3.0	
O4	N Gly46	3.1	3.0	
	N Val47	3.1		

[a]enzyme-substrate complex (Schreuder, 1989).

Benzoate Complex. The 2.0 Å crystal structure of the enzyme-benzoate complex indicated only a few but clear differences with the 4-hydroxybenzoate complex (Fig.3a). The absence of the hydroxy group at the 4-position of the substrate analog is the most obvious change and as a consequence, the hydrogen bonds between the substrate analog and the residues Tyr201, Pro293 and Thr294 (Table 3a) are lost. In spite of this, the position of the benzoate, the flavin and the active site residues do not change with respect to the structure of the enzyme-substrate complex (Fig.3a). The B-factors for benzoate and the active site residues are as low as with the enzyme-substrate complex indicating that the benzoate is tightly fixed. Another interesting feature, also observed in complexes with 4-aminobenzoate analogs (Schreuder, 1994; Gatti, 1996) and substrate-free enzyme, is the presence of an extra water molecule (WAT2) next to Tyr385 (Fig.3b; Table 4). As a result, a hydrogen bonding network is created which extends from Tyr201 and Tyr385 via WAT2 and WAT1 towards His72 at the protein surface (Schreuder, 1994; Gatti, 1996). This WAT2 is firmly held in position since its temperature factor of 18 $Å^2$ for the BZT complex and 28 $Å^2$ for substrate-free enzyme, is as low as the average B factors of the protein.

Table 4. H-bond distances involved in the hydrogen-bonding network around Tyr201 and Tyr385 in different crystal structures of PHBH. Enzyme-substrate complex (PHBH); enzyme-4-aminobenzoate complex (PAB); enzyme-benzoate complex (BZT); substrate-free enzyme (HOLO).

Length of hydrogen bond distance (Å) for the different complexes				
Hydrogen bond	[a]PHBH	[b]PAB	BZT	HOLO
O4/N4-OH Tyr201	2.7	3.1	-	-
OH Tyr201-OH Tyr385	2.8	2.9	2.9	3.2
OH Tyr385-WAT2	-	2.8	2.9	3.0
WAT2-WAT1	-	3.0	2.8	2.7
WAT1-ND1 His72	2.5	2.8	2.7	2.7

[a]enzyme-substrate complex (Schreuder, 1989)

[b]enzyme-4-aminobenzoate complex (Schreuder, 1994)

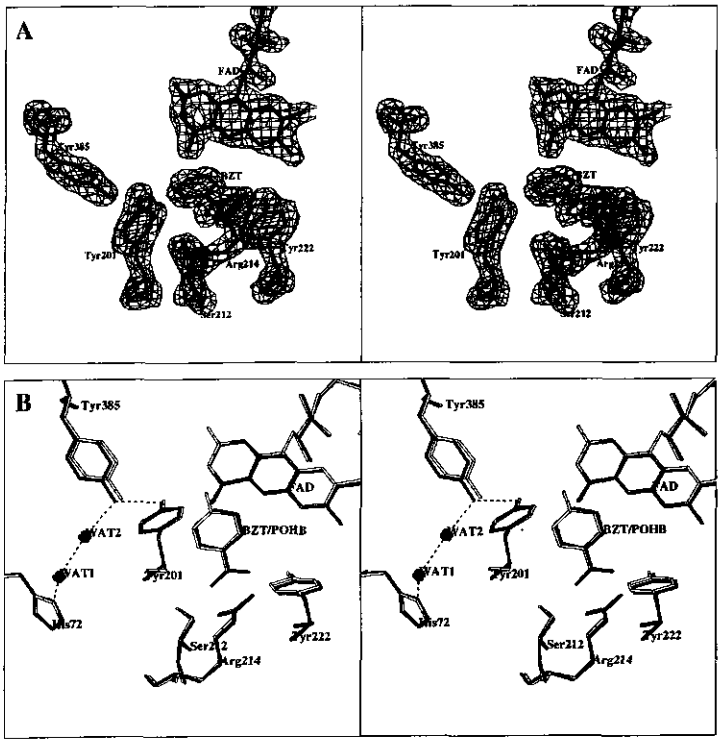

Fig 3: Structure of PHBH in complex with benzoate. A) $2F_O$-F_C omit map, contoured at 2σ, of the active site region with the same residues as in free enzyme (cf. Fig.2). B)

Superposition of the structures of the enzyme-substrate complex (open bonds) and the enzyme-benzoate complex (grey bonds). Like in free enzyme, WAT1 (Wat126) and WAT2 (Wat237) are present. Benzoate (BZT); 4-hydroxybenzoate (POHB).

Dimer interaction and crystal packing analysis. Substrate binding influences the packing of the enzyme, because substrate-free $C222_1$ crystals are very small and crack easily in ammonium sulfate, whereas in the presence of PEG4000 and 2'-AMP larger and more rigid $P2_12_12_1$ crystals are formed. Nonetheless, it should be noted here that no electron density was found for the NADPH analog 2'-AMP, it acted only as a stabilizer during crystal formation. Earlier studies have shown that in the presence of substrate PHBH is more thermotolerant (van Berkel, 1989), most likely because the bound substrate reduces the flexibility of the protein by "crosslinking" the FAD binding and substrate binding domains. Superpositioning of the homodimer of the enzyme-substrate complex (Scheuder, 1989) in spacegroup $C222_1$ onto the substrate-free enzyme in spacegroup $P2_12_12_1$ shows small shifts in some parts of the protein structure. The residues involved in dimer interaction are highly similar in both the enzyme-substrate complex and in substrate-free enzyme. Regions not involved in dimer contacts and situated near the protein surface have their backbone positions slightly shifted by 1-2 Å. The most important change is a 4 Å shift in the flexible loop region between the β-sheets C3 and C4 (residues 142-146) of the FAD-binding domain (Fig.4). This loop region is involved in crystal contacts in both spacegroups. In summary, the present crystal structures show that the changes in the protein structure due to the presence or absence of substrate must be very small.

Fig 4: Superpositioning of substrate-free PHBH with spacegroup $P2_12_12_1$ onto the enzyme-substrate complex with spacegroup $C222_1$. Ribbon diagram of substrate-free

enzyme (light) with FAD (in dark), and the enzyme-substrate complex (dark) with FAD (in light) and substrate (in dark). The loop region between β-sheets C3 and C4 important for crystal contacts is white colored in the substrate-free enzyme.

Flavin ring conformations. From previous crystal structures of PHBH, it is known that the flavin ring can adopt two different conformations, "in" or "out" the active site (Schreuder, 1994; Gatti, 1994; van Berkel, 1994). By superimposing these crystal structures onto the newly determined crystal structures we observe for substrate-free enzyme an intermediate position of the flavin ring in between the "in" and "out" conformation (Fig.5). In order to quantify this, the angle between the N5 (reference protein) - C3 ribose - N5 (sample protein) atoms of FAD was calculated with the enzyme-substrate complex as reference protein (Table 5). The C3 ribose of FAD was choosen, because this is the first FAD atom which is not significantly shifted in position when the flavin moves from "in" to "out" and located in plane with the N5 of FAD. Table 5 shows that the angle increases when the flavin ring shifts towards the "out" conformation. For substrate-free enzyme (Table 5), an intermediate conformation is observed, suggesting that in the absence of substrate the highly flexible flavin ring adopts an intermediate position.

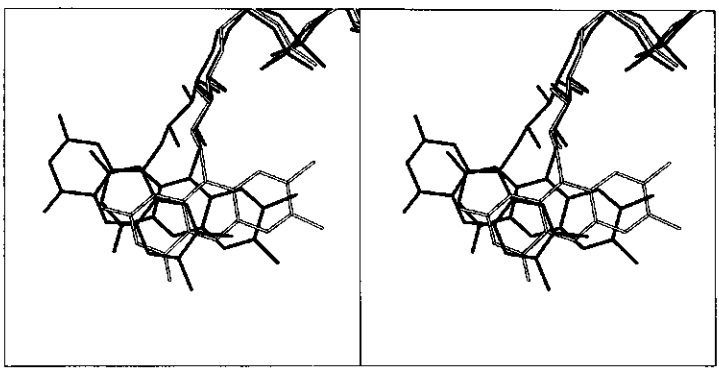

Fig 5: Superpositioning of the flavin conformers in PHBH. The isoalloxazine ring of FAD is positioned in three different conformations: A) "in" (black bonds) for the PHBH/substrate complex, B) "out" (white bonds) for the PHBH/2,4-dihydroxybenzoate complex, C) "intermediate" (grey bonds) for substrate-free PHBH.

Table 5. Positional differences of the flavin ring in various crystal structures of PHBH. Angle between N5 (reference)–C3 ribose–N5 (sample) atoms of FAD. Reference is enzyme-substrate complex.

Crystal Structure	N5(reference)-C3 ribose-N5(sample) (deg)
PHBH/4-hydroxybenzoate[a]	-
PHBH/3,4-dihydroxybenzoate[b]	0.4
PHBH/4-aminobenzoate[c]	0.8
PHBH/2-hydroxy-4-aminobenzoate[c]	16.8
PHBH/2,4-dihydroxybenzoate[c]	17.1
PHBH (substrate-free)	11.0
PHBH/4-hydroxybenzoate (+ aFAD) [d]	15.5
Tyr222Ala/2-hydroxy-4-aminobenzoate[c]	16.9
Tyr222Phe/4-hydroxybenzoate[e]	16.8

[a]Schreuder et al., 1989; [b]Schreuder et al., 1988; [c]Schreuder et al., 1994; [d]Van Berkel et al., 1994; [e]Gatti et al., 1994.

Discussion

In this paper, a detailed analysis of the crystal structures of PHBH without substrate and in complex with the non-substrate effector benzoate is presented. Preliminary low resolution data of substrate-free PHBH with and without chloride ions were presented by Wierenga et al. (1979) and van der Laan et al. (1986). By using PEG4000 as a precipitant, we obtained crystals of substrate-free enzyme in spacegroup $P2_12_12_1$, a spacegroup which has not been described before for PHBH. This allowed us to collect diffraction data at low temperature to a resolution of 2.5 Å.

During early studies of PHBH from several *Pseudomonas* species it was noted that substrate binding greatly stimulates the rate of reduction of protein-bound FAD by NADPH (Hosokawa, 1966; Yano, 1969b; Howell, 1970; Spector, 1972). At that time it was suggested that substrate binding induces a large protein conformational change. This

conclusion was based mainly on differences in absorption, fluorescence and circular dichroism properties (Yano, 1969a; Hesp, 1969). Moreover, different crystal forms of PHBH were obtained, in the absence and presence of substrate (Hosokawa, 1966; Yano, 1969a; Schepman, 1976; van der Laan; 1986). Here we found that the crystal structure of substrate-free enzyme, in a different space group, is almost identical to the structure of the enzyme-substrate complex, in full agreement with preliminary studies of van der Laan et al. (1986). The perturbations in spectral properties upon binding of aromatic ligands (van Berkel, 1989) must therefore be ascribed to local changes in the active site. Large protein conformational changes are not necessary from a catalytic point of view, since it has become clear that the isoalloxazine ring is mobile. This mobility allows the substrate to enter the active site and the product to leave (Schreuder, 1994; Gatti, 1994). In addition, flavin mobility is necessary for efficient reduction in the presence of substrate (van Berkel, 1994; Palfey, 1997,1999; Eppink, 1998). The recently determined crystal structure of the related phenol hydroxylase from *Trichosporon cutaneum* shows a similar displacement of the flavin ring, together with a loop movement, presumably with an identical function as in PHBH (Enroth, 1998).

Since there seems to be no protein conformational change responsible for the effector role in PHBH, how could the substrate stimulate the rate of reduction by five orders of magnitude? When comparing the crystal structures of the substrate-free enzyme and the enzyme-substrate complex, the most important changes are an increased flexibility and shift of the flavin ring towards the protein surface in substrate-free enzyme. A possible explanation could be that the increased flexibility of the flavin disturbs the optimal alignment between the isoalloxazine and nicotinamide rings.

However, there must be another important effect that influences the effector role of the substrate, since the substrate analogs 4-aminobenzoate, 2-hydroxy-4-aminobenzoate (Schreuder, 1994) and benzoate (this study) keep the flavin ring "in" while hardly stimulating the reduction rate. Interestingly, none of these benzoate derivatives bears a hydroxyl moiety (substituent) at the 4-position and in all crystal structures of PHBH with poor effectors an extra water molecule (WAT2) is present next to Tyr385 (Schreuder, 1994; Lah, 1994; Gatti, 1996). It has been suggested that this extra water molecule is transiently available in the enzyme-substrate complex and necessary for (de)protonation of the 4-hydroxy group of the substrate by forming a proton channel between the active site residues Tyr201 and Tyr385 via the water molecules WAT2 and WAT1 and His72 at the surface of the protein (Schreuder, 1994; Gatti, 1994). After transfer of a proton from the substrate phenol via this "proton wire", the hydrogen bond direction changes and WAT2 is no longer stabilized and lost. It might be that disruption of this "proton wire" somehow influences the hydride transfer between NADPH and the flavin ring by causing

subtle changes in or near the active site. Kinetic studies of mutant His72Asn showed that deprotonation of substrate is required for a rapid flavin reduction by NADPH (Palfey, 1999), and indicated that the flavin ring must move to the "out" conformation in order to react (Palfey, 1999). In line with this, the failure of the active site mutants Tyr201Phe and Tyr385Phe to stabilize the phenolate form of the substrate could explain the slow reduction of both mutants (Entsch, 1991; Eschrich, 1993). Palfey et al. (1999) concluded that with nonionizable ligands or proton-transfer mutants the phenolate and phenolic forms of the substrate are unable to equilibrate rapidly. However, caution should be taken with these conclusions, because rapid reduction studies of the slowly reducing Tyr385Phe mutant were performed at high (non-physiological) pH and mutant Tyr201Phe was omitted from the experiments (Palfey, 1999).

Substrates with a 4-hydroxy group make hydrogen bonds with the side chain of Tyr201 and with the backbone oxygen of Pro293 (Table 3a). Pro293 belongs to the conserved active site loop at the *re*-side of the flavin ring (Eppink, 1997). Since the nicotinamide ring binds at the *re*-side (Manstein, 1986), one can envision that a change in hydrogen bonding interactions in this region might cause an non-optimal alignment of nicotinamide and isoalloxazine ring, thereby preventing efficient hydride transfer. In this respect it is interesting to note that in the free enzyme, the side chain of Pro293 bends 20° over its Cβ and Cγ atoms, and that in the enzyme-substrate complex at pH 9.5 (Gatti, 1996) the peptide backbone comprising residues 293 to 296 adopts two conformations. These findings support an earlier proposal (Entsch, 1991; Eschrich, 1993) that substrate deprotonation plays some role in NADPH recognition. However, a clear correlation between the rate of reduction, flavin movement and internal proton transport remains to be elucidated.

References

Brünger AT. 1992. X-plor version 3.1 A system for the X-ray crystallography and NMR. Yale University press, New Haven, Connecticut.

Enroth C, Neujahr H, Schneider G, Lindqvist Y, 1998. The crystal structure of phenol hydroxylase in complex with FAD and phenol provides evidence for a concerted conformational change in the enzyme and its cofactor during catalysis. Structure. 6:605-617.

Entsch B, Ballou DP. 1989. Purification, properties, and oxygen reactivity of *p*-hydroxybenzoate hydroxylase from *Pseudomonas aeruginosa*. Biochim. Biophys. Acta. 999:313-322.

Entsch B, van Berkel WJH. 1995. Structure and mechanism of para-hydroxybenzoate hydroxylase. FASEB J. 9:476-483.

Eppink MHM, Schreuder HA, van Berkel WJH. 1997. Identification of a novel conserved sequence motif in flavoprotein hydroxylases with a putative dual function in FAD/NAD(P)H binding. Prot. Sci. 6:2454-2458.

Eppink MHM, Schreuder HA, van Berkel WJH. 1998. Interdomain binding of NADPH in *p*-hydroxybenzoate hydroxylase as suggested by kinetic, crystallographic and modeling studies of histidine 162 and arginine 269 variants. J.Biol.Chem. 273:21031-21039.

Eschrich K, van der Bolt FJT, de Kok A, van Berkel WJH. 1996. Role of Tyr201 and Tyr385 in substrate activation by *p*-hydroxybenzoate hydroxylase from *Pseudomonas fluorescens*. Eur. J. Biochem. 216:137-146.

Gatti DL, Palfey BA, Lah MS, Entsch B, Massey V, Ballou DP, Ludwig ML. 1994. The mobile flavin of 4-OH benzoate hydroxylase. Science. 266:110-114.

Gatti DL, Entsch B, Ballou DP, Ludwig ML. 1996. pH-dependent structural changes in the active site of p-hydroxybenzoate hydroxylase point to the importance of proton and water movements during catalysis. Biochemistry. 35:567-578.

Hesp B, Calvin M, Hosokawa K. 1969. Studies on *p*-hydroxybenzoate hydroxylase from *pseudomonas putida*. J.Biol.Chem. 244:5644-5655.

Hosokawa K, Stanier RY. 1966. Crystallization and properties of *p*-hydroxybenzoate hydroxylase from *pseudomonas putida*. J.Biol.Chem. 241:2453-2460.

Howell LG, Massey V. 1970. A non-substrate effector of *p*-hydroxybenzoate hydroxylase. Biochem. Biophys. Res. Com. 40:887-893.

Husain M, Entsch B, Ballou DP, Massey V, Chapman P. 1980. Fluoride elimination from substrates in hydroxylation reactions catalyzed by *p*-hydroxybenzoate hydroxylase. J. Biol. Chem. 255:4189-4197.

Jones TA, Zou J-Y, Cowan S, Kjeldgaard M. 1991. Improved methods for the building of protein models in electron density maps and the location of errors in these models. Acta.Cryst. A47:110-119.

Kabsch W. 1988. Evaluation of single-crystal diffraction data from a position-sensitive detector. J. Appl. Crystallogr. 21:916-924.

Lah MS, Palfey BA, Schreuder HA, Ludwig ML. 1994. Crystal structures of mutant Pseudomonas aeruginosa p-hydroxybenzoate hydroxylase: The Tyr201Phe, Tyr385Phe and Asn300Asp variants. Biochemistry. 33:1555-1564.

Manstein JM, Pai EF, Schopfer LM, Massey V. 1986. Absolute stereochemistry of flavins in enzyme-catalyzed reactions. Biochemistry. 25:6807-6816.

Massey V 1994. Activation of molecular oxygen by flavins and flavoproteins. J. Biol. Chem. 269:22459-22462.

Müller F, van Berkel WJH. 1982. A study on *p*-hydroxybenzoate hydroxylase from *Pseudomonas fluorescens*. A convenient method of preparation and some properties of the apoenzyme. Eur.J.Biochem. 128:21-27.

Navaza J. 1994. AMoRe - an automated package for molecular replacement. Acta Cryst. A 50, 157-163.

Otwinowski Z. 1993. Data collection and processing. In *proceedings of the CCP4 study weekend.* (Sawyer, L. Issacs, N. & Bailey, S. eds) pp 56-62, SERC, Daresbury Laboratory, UK.

Palfey BA, Ballou DP, Massey V. 1997. Flavin conformational changes in the catalytic cycle of *p*-hydroxybenzoate hydroxylase substituted with 6-azido- and 6-aminoflavin adenine dinucleotide. Biochemistry. 36:15713-15723.

Palfey BA, Moran GR, Entsch B, Ballou DP, Massey V. 1999. Substrate recognition by "Password" in *p*-hydroxybenzoate hydroxylase. Biochemistry. 38:1153-1158.

Schepman AMH, Schutter WG, van Bruggen EFJ. 1976. Electron microscopic studies on microcrystals of parahydroxybenzoate hydroxylase from *Pseudomonas fluorescens*. FEBS Lett. 65:84-86.

Schreuder HA, van der Laan JM, Hol WGJ, Drenth J. 1988. Crystal structure of p-hydroxybenzoate hydroxylase complexed with its reaction product 3,4-dihydroxybenzoate. J.Mol.Biol. 199:637-648.

Schreuder HA, Prick PAJ, Wierenga RK, Vriend G, Wilson KS, Hol WGJ, Drenth J. 1989. Crystal structure of the p-hydroxybenzoate hydroxylase-substrate complex refined at 1.9 Å resolution. J. Mol. Biol. 208:679-696.

Schreuder HA, Mattevi A, Obmolova G, Kalk KH, Hol WGJ, van der Bolt FJT, van Berkel WJH. 1994. Crystal structures of wild-type p-hydroxybenzoate hydroxylase complexed with 4-aminobenzoate, 2,4-dihydroxybenzoate and 2-hydroxy-4-aminobenzoate and the Tyr222Ala mutant, complexed with 2-hydroxy-4-aminobenzoate. Evidence for a proton channel and a new binding mode of the flavin ring. Biochemistry. 33:10161-10170.

Spector T, Massey V. 1972. Studies on the effector specificity of *p*-hydroxybenzoate hydroxylase from *Pseudomonas fluorescens*. J. Biol. Chem. 247:4679-4687.

van Berkel WJH, Müller F. 1989. The temperature and pH dependence of some properties of p-hydroxybenzoate hydroxylase from Pseudomonas fluorescens. Eur. J. Biochem. 179:307-314.

van Berkel WJH, Müller F. 1991. Flavin-dependent monooxygenases with special reference to p-hydroxybenzoate hydroxylase, in Chemistry and biochemistry of flavoenzymes (Müller, F., ed.) vol. 2, pp. 1-29, CRC Press. Boca Raton.

van Berkel WJH, Westphal AH, Eschrich K, Eppink MHM, de Kok A. 1992. Substitution of Arg214 at the substrate-binding site of p-hydroxybenzoate hydroxylase from Pseudomonas fluorescens. Eur. J. Biochem. 210:411-419.

van Berkel WJH, Eppink MHM, Schreuder HA. 1994. Crystal structure of *p*-hydroxybenzoate hydroxylase reconstituted with the modified FAD present in alcohol oxidase from methylotrophic yeasts: Evidence for an arabinoflavin. Protein Sci. 3:2245-2253.

van Berkel WJH, Eppink MHM, van der Bolt FJT, Vervoort J, Rietjens IMCM, Schreuder HA. 1997. *P*-Hydroxybenzoate hydroxylase: mutants and mechanism, in *Flavins and flavoproteins* XII (Stevenson, K., Massey, V. and Williams, Ch., eds) pp. 305-314, University Press, Calgary.

van der Bolt FJT, Vervoort J, van Berkel WJH. 1996. Flavin motion in p-hydroxybenzoate hydroxylase. Substrate and effector specificity of the Tyr222Ala mutant. Eur. J. Biochem. 237:592-600.

van der Laan JM. 1986. Ph.D thesis, University of Groningen.

Wierenga RK. 1979. Ph.D thesis, University of Groningen.

Yano, K, Higashi, N, Arima, K. 1969a. *p*-Hydroxybenzoate hydroxylase: conformational changes in crystals of holoenzyme vs holoenzyme-substrate complex. Biochem.Biophys.Res.Com. 34:1-7.

Yano K, Higashi N, Nakamura S, Arima K. 1969b. The reaction mechanism of *p*-hydroxybenzoate hydroxylase and a role of the substrate as an effector. Biochem. Biophys. Res. Com. 34:277-282.

CHAPTER 11

Summary

Biochemistry is the science that studies the chemistry of life. This 'biological' chemistry includes growth, differentiation, movement, conductivity, immunity, transport and storage. During these processes proteins play an important role. The building blocks of proteins are amino acids, of which twenty are known. With these building blocks at hand it is possible to construct numerous proteins with many specific functions. A protein is not an elongated chain of amino acid residues but a compact very well defined three-dimensional structure. Two basic substructures are known in a protein, a cylindrical α-helix and an elongated β-strand (Fig.1a). A number of these α-helices and/or β-strands connected by loop regions form a protein domain (Fig.1b) and a protein is built up of one or more domains (Fig.1c). Furthermore, proteins can contain certain motifs (folds), structural conserved patterns. A large group of proteins with similar function and/or structure are called a protein family.

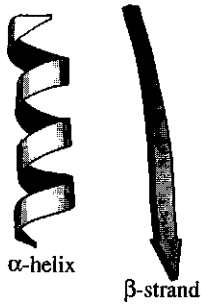

Fig.1a: α-helix + β-strand

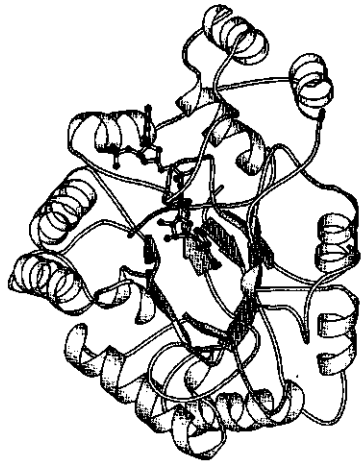

Fig.1b: protein domain

Fig.1c: protein

A special group of proteins, called enzymes or biocatalysts, are able to increase the rate of a chemical reaction by lowering the activation energy of that reaction. Enzymes are highly specific, because they influence the reactivity of the substrate in such a way that the substrate

is quickly and efficiently converted into a product. Moreover, flexible/dynamic movements in enzymes may play an important role during catalysis, because enzymes are not always rigid bodies. To control the reaction, enzymes often need cofactors. Some examples are the already mentioned dinucleotides NAD(P)H and FAD, that play a role in electron transfer (redox) reactions. Generally speaking, these cofactors bind very specific to a protein. A well-known binding motif for NAD(P)H and FAD in different enzyme families is the Rossmann fold (Chapter 1), discovered by Michael Rossmann in 1974.
The NAD(P)H cofactor binds to the enzyme, electron transfer takes place and finally, the oxidized cofactor is released. In some proteins, the mode of NADPH binding is unknown. One example is *p*-hydroxybenzoate hydroxylase (PHBH), a flavoprotein monooxygenase that belongs to the family of FAD-dependent aromatic hydroxylases.

FAD-dependent Aromatic Hydroxylases

FAD-dependent aromatic hydroxylases play a role in the biodegradation of aromatic compounds. In nature, these compounds occur in plant polymers (lignin) as well as in proteins, steroïds and terpenes. During this century, the natural pool of aromatic compounds has been extended with products of industrial origin. Many of these synthetic compounds (pesticides, herbicides, fungicides and detergents) place a heavy burden on the environment and accumulate in soil and sludge. Microbial FAD-dependent aromatic hydroxylases catalyze the conversion of natural and synthetic aromatic substrates into products that can be further degraded to carbon dioxide and water. Recently, it was found that these enzymes are also involved in the biosynthesis of steroïds, plant hormones and antibiotics. PHBH is the archetype (prototype) of the family of FAD-dependent aromatic hydroxylases. In Wageningen, research on PHBH and related enzymes is embedded in the Wageningen Graduate School of Environmental Chemistry & Toxicology.

p-Hydroxybenzoate Hydroxylase

p-Hydroxybenzoate hydroxylase is isolated from the soil bacterium *Pseudomonas fluorescens*. This microbe can grow on 4-hydroxybenzoate (POHB) and other aromatic compounds as sole carbon source. PHBH catalyzes the conversion of POHB into 3,4-dihydroxybenzoate (DOHB) in the presence of NADPH and molecular oxygen (Fig.2). DOHB is a common intermediate in the aerobic degradation of plant material. After ring cleavage of DOHB and further degradation, the final products acetyl coenzyme A and succinate are fed into the citric acid cycle to provide energy for the cell.

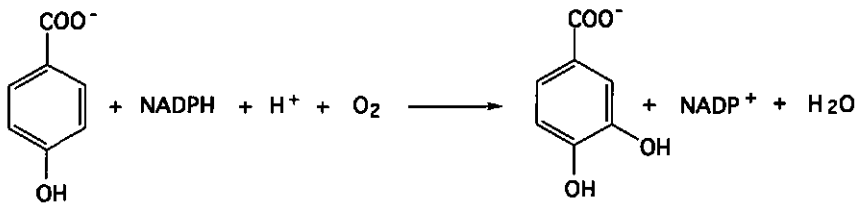

Fig.2 Overall reaction of PHBH

p-Hydroxybenzoate hydroxylase has been subject to detailed kinetic and structural studies. The three-dimensional structure of PHBH is built up of three domains (Chapter 1). The first domain is the FAD-binding domain with the specific Rossmann fold for binding the ADP part of FAD. The second domain is the substrate-binding domain and the third domain (interface domain) is important for the interaction with another PHBH subunit, because PHBH exists as a dimer.

The structure of the enzyme-substrate complex is known in atomic detail. Recently, it was found that the flavin ring is able to move between an "open" and "closed" conformation. This flavin mobility is important for substrate binding and product release. However, unknown is the NADPH-binding site and where the reaction between NADPH and FAD takes place. Related questions are:

- Which amino acids play a role in cofactor binding?
- Is there a particular sequence motif for cofactor binding?
- Which amino acids are responsible for the coenzyme specificity and involved in binding of the 2'-phosphate moiety of NADPH?

Another very important question concerns the effector role of the substrate. Upon binding of the aromatic substrate the flow of electrons from NADPH to FAD is 10^5 times enhanced. However, the molecular principles of this control are poorly understood. In this thesis we have tried to shed more light on the coenzyme recognition by PHBH.

Flavin ring mobility

In **Chapter 2** the FAD in PHBH is substituted by a modified FAD, normally present in alcohol oxidase from methylotrophic yeasts. The crystal structure of *p*-hydroxybenzoate hydroxylase with this flavin analog not only represents the first crystal structure of an enzyme reconstituted with a modified flavin, but also provides direct evidence for the presence of an arabityl sugar chain in the modified form of FAD. The reconstituted enzyme-substrate complex shows that the flavin ring attains the "open" conformation. In the native enzyme-substrate complex the flavin ring is located in the "closed" conformation. The rate of flavin reduction by NADPH is much more rapid as compared to the native enzyme-substrate complex, suggesting that the mobility of the flavin ring is essential for the efficient reduction of the enzyme/substrate complex.

Amino acids involved in NADPH binding

To investigate the mode of NADPH binding, several amino acid residues were replaced by site-directed mutagenesis. The amino acids were selected on the basis of earlier results from chemical modification, crystallographic and modeling studies. **Chapters 3, 4, 6** and **8** describe the properties of single mutants. It is concluded that Arg33, Gln34, Tyr38, Arg42, Arg44, His162 and Arg269 are involved in NADPH binding. Figure 3 shows the location of these amino acid residues in the PHBH structure.

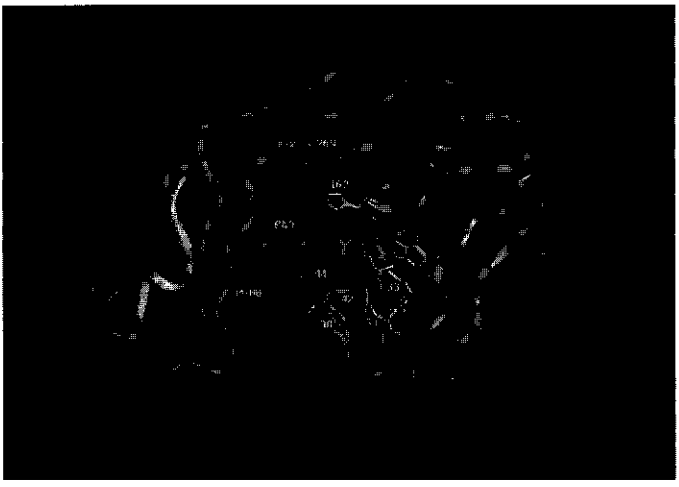

Fig.3: PHBH with the important residues for NADPH binding

Structural motif for NADPH binding

PHBH contains two conserved sequence motifs, both involved in FAD binding. **Chapter 5** describes a new unique sequence motif for the family of FAD-dependent aromatic hydroxylases, putatively involved in both FAD and NAD(P)H binding. From the recently determined crystal structure of phenol hydroxylase it is deduced that this sequence motif is also structurally conserved. **Chapter 6** and **7** show that only His162 of this novel motif is directly important for the binding of NADPH.

Coenzyme specificity

Chapter 8 describes the cloning, purification and characterization of PHBH from *Pseudomonas* species CBS3. This is the first PHBH enzyme with known sequence that is active with NADH. Based on sequence analysis and homology modelling it is proposed that the helix H2 region is important for the binding of the 2'-phosphate moiety of NADPH. In **Chapter 9**, the coenzyme specificity of PHBH from *Pseudomonas fluorescens* was addressed in further detail. Multiple replacements in helix H2 showed that Arg33 and Tyr38 are crucially involved in determining the coenzyme specificity. For the first time, a PHBH enzyme was constructed, which is more efficient with NADH.

Effector specificity

Substrate binding is essential for a rapid reduction of FAD. This allows the subsequent attack of oxygen and the formation of the flavinhydroperoxide hydroxylating species. The question arises whether the stimulating effect of substrate binding on flavin reduction is caused by a large conformational change or merely due to subtle rearrangements in the active site. **Chapter 10** describes the crystal structure of the substrate-free enzyme. This study shows that no large conformational changes take place upon substrate (analog) binding. The stimulating role of POHB is probably caused by several subtle effects. Stabilisation of the phenolate form of the substrate results in distribution of the electronic charges in the active site. These charge distributions influence the dynamic equilibrium between the "open" and "closed" conformation of FAD in such a way that the nicotinamide ring of NADPH and the isoalloxazine ring of FAD become optimally oriented for efficient reduction.

Samenvatting

Biochemie is de wetenschap die zich bezighoudt met de chemie van het leven. Hieronder verstaat men de verschillende processen zoals groei, differentiatie, geleiding, beweging, immuniteit, transport en opslag die zich afspelen in een levend wezen. Eiwitten spelen hierbij een belangrijke rol. De bouwstenen van eiwitten zijn aminozuren waarvan er in totaal twintig zijn. Door deze aminozuren in allerlei combinaties aaneen te rijgen kunnen zeer veel verschillende eiwitten worden gemaakt. Elk eiwit heeft vaak zijn eigen specifieke taak. Een eiwit is niet een langgerekte keten, maar is vaak opgevouwen tot een zeer goed gedefinieerde drie-dimensionale structuur. In deze eiwitstructuur komen twee substructuren voor, een cylindervormige α-helix en een meer vlakke β-strand (Fig.1a). Een aantal van deze α-helices en/of β-sheets tesamen, verbonden via loop structuren, vormen een domein (Fig.1b), en meestal bestaat het eiwit uit meerdere domeinen (Fig.1c). Veelal kunnen eiwitten ook één of meerdere structurele motieven (folds) bevatten. Dit zijn geconserveerde vouwingspatronen die in verschillende eiwitten voorkomen en vaak een vergelijkbare functie hebben. Wanneer er sprake is van een grote groep eiwitten met een zelfde soort functie en/of structuur, dan spreken we van een eiwitfamilie.

Fig.1a: α-helix + β-strand

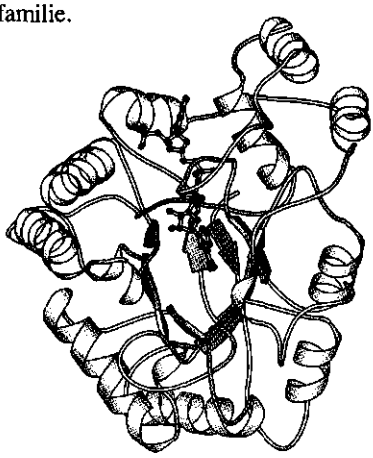

Fig.1b: protein domain

Fig.1c: protein

Een speciale klasse van eiwitten zijn de enzymen. Dit zijn biokatalysatoren, eiwitten die chemische reacties kunnen versnellen. Enzymen zijn over het algemeen zeer specifiek, en hebben het vermogen om de reaktiviteit van het substraat (de stof die veranderd moet

worden) zodanig te beïnvloeden dat het substraat snel en efficient omgezet kan worden tot een bepaald produkt. Flexibele/dynamische bewegingen in enzymen kunnen hierbij een grote rol spelen, daar enzymen niet altijd rigide structuren zijn. Vaak hebben enzymen hulpstoffen (cofactoren) nodig om de reaktie goed te laten verlopen. Voorbeelden van deze hulpstoffen zijn de in de inleiding genoemde dinucleotiden NAD(P)H en FAD die vaak een rol spelen bij reacties waarbij electronen worden overgedragen (redox reacties). Deze cofactoren binden niet willekeurig aan het eiwit maar vaak heel specifiek. Een zeer bekend en veel voorkomend motief dat in verschillende enzymfamilies bij de binding van zowel FAD als NAD(P)H betrokken is, is de Rossmann fold (Hoofdstuk 1); genoemd naar zijn ontdekker Michael Rossmann in 1974.

NAD(P)H is een co-enzym, een stof die bij een enzym slechts even op bezoek komt om z'n werk te doen. NAD(P)H bindt vaak via een Rossmann fold, maar in een aantal gevallen is de manier van binding niet bekend. Dit komt o.a. doordat het NADPH bij deze enzymen een bliksembezoek aflegt. Een voorbeeld hiervan is het in dit proefschrift beschreven *p*-hydroxybenzoaat hydroxylase (PHBH), een enzym dat behoort tot de familie van FAD-afhankelijke aromatische hydroxylasen.

FAD-afhankelijke Aromatische Hydroxylasen

FAD-afhankelijke aromatische hydroxylasen zijn enzymen die betrokken zijn bij de afbraak van aromatische verbindingen. Deze verbindingen komen in de natuur voor in plant polymeren (lignine) alsook in eiwitten, steroïden en terpenen. Verder zijn er de laatste tientallen jaren veel synthethische aromatische verbindingen in bodem en water terechtgekomen, o.a. via bestrijdingsmiddelen en afwasmiddelen. Deze synthetische (gehalogeneerde) verbindingen belasten in hoge mate het milieu. FAD-afhankelijk aromatische hydroxylasen zijn in staat om zowel natuurlijke als synthetische aromatische substraten om te zetten in een produkt dat verder kan worden verwerkt in een specifieke afbraakroute tot koolstofdioxide en water. Daarnaast zijn er ook FAD-afhankelijke aromatische hydroxylasen bekend die betrokken zijn bij de biosynthese van steroïden, plant hormonen en antibiotica.

Omdat PHBH model staat voor vele FAD-afhankelijke aromatische hydroxylasen, is het in dit proefschrift beschreven werk uitgevoerd binnen de Wageningse onderzoeksschool Milieuchemie & Toxicologie.

p-Hydroxybenzoaat Hydroxylase

p-Hydroxybenzoaat hydroxylase (PHBH) is een enzym, geïsoleerd uit de bodembacterie *Pseudomonas fluorescens*. Deze bacterie is in staat om 4-hydroxybenzoaat (POHB) en andere aromaten te gebruiken als enige koolstofbron. PHBH katalyseert de omzetting van POHB in 3,4-dihydroxybenzoaat (DOHB) in aanwezigheid van NADPH en zuurstof (Fig.2). DOHB is een belangrijk intermediair in de aerobe afbraak van aromatisch plantenmateriaal. Via het openbreken van de aromatische ring van DOHB ontstaan uiteindelijk acetylcoënzym A en succinaat die in de citroenzuurcyclus gebruikt worden voor de essentiële energievoorziening van de cel.

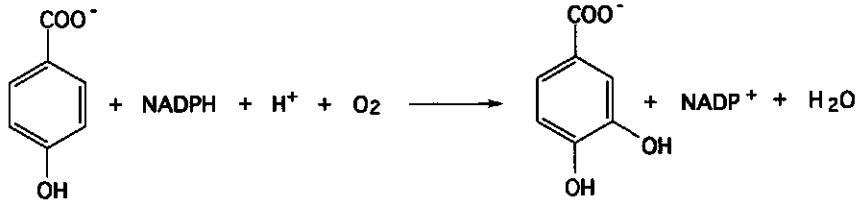

Fig.2 De PHBH reactie

p-Hydroxybenzoaat hydroxylase is uitvoerig bestudeerd qua functie en structuur. De drie-dimensionale structuur van PHBH is opgebouwd uit 3 domeinen (Hoofdstuk 1). Het eerste domein is het FAD-bindend domein met de specifieke Rossmann fold voor de binding van FAD. Het tweede domein is het substraat-bindend domein dat zorgt voor de specificiteit van het enzym. Tenslotte is er nog een domein (interface domein) dat van belang is voor de interactie met een tweede PHBH enzym molecuul, omdat PHBH als dimeer voorkomt.

De structuur van het enzym-substraat complex is bekend, en verder is ook gevonden dat de flavine ring in het eiwit kan bewegen tussen een "open" en "gesloten" conformatie. Deze mobiliteit van de flavine ring is niet alleen van belang voor de binding van het substraat maar

ook voor het vertrekken van het produkt. Onbekend is echter hoe NADPH bindt en waar de reaktie van NADPH met FAD plaatsvindt. Vragen hieraan gerelateerd zijn o.a.:

- Welke aminozuren spelen een rol bij de binding van de cofactor?
- Is er een structureel motief voor cofactor binding?
- Welke aminozuren zijn verantwoordelijk voor de co-enzymspecificiteit en betrokken bij de binding van de 2'-fosfaatgroep van NADPH?

Een ander belangrijk aspect in relatie tot de NADPH binding betreft de effector rol van het substraat. In aanwezigheid van het substraat wordt de electronenoverdracht van NADPH naar FAD een factor 10^5 versneld, echter niet duidelijk is hoe dit precies gebeurt. Het vermoeden bestaat dat de mobiliteit van de flavinering een belangrijke rol speelt in dit proces. In dit proefschrift is getracht meer inzicht in deze vraagstukken te verkrijgen.

Mobiliteit flavinering

In **hoofdstuk 2** is het FAD in PHBH vervangen door een FAD analoog (arabino-FAD) dat normaal gesproken voorkomt in het enzym alcohol oxidase uit gist. Gevonden werd dat in de kristalstructuur van het gereconstitueerde enzym-substraat complex de flavine ring zich in de "open" conformatie bevindt. In het natieve enzym-substraat complex bevindt de flavine zich in de "gesloten" positie. Omdat de electronen overdracht van NADPH naar het arabino-FAD sneller verloopt dan in het natieve enzym-substraat complex suggereert dit dat de mobiliteit van de flavinering van belang is voor een efficiënte reductie van het enzym-substraat complex.

Aminozuren betrokken bij NADPH binding

Om het bindingsgebied van NADPH in het eiwit te localiseren zijn verschillende aminozuren vervangen via plaatsgerichte mutagenese. Op basis van eerdere chemische modificatie, X-ray kristallografische en modeling studies zijn daartoe bepaalde aminozuren geselecteerd. In **hoofdstuk 3, 4, 6** en **8** worden de gevolgen van een serie enkelvoudige mutaties beschreven. De structurele en functionele eigenschappen van de mutant enzymen geven aan dat Arg33, Tyr38, Arg42, Arg44, His162 en Arg269 betrokken zijn bij de NADPH binding. Figuur 3 laat zien waar deze aminozuren zijn gelokaliseerd.

Fig.3: PHBH met de belangrijke aminozuren voor NADPH binding

Structureel motief NADPH binding

PHBH bevat twee geconserveerde sequentiemotieven die betrokken zijn bij de FAD binding, maar over de verwantschap van NADPH binding in dit soort enzymen is niets bekend. Omdat er de laatste jaren veel nieuwe genen zijn ontdekt, werd besloten een zoektocht te verrichten in de verschillende eiwitsequentie databanken. **Hoofdstuk 5** laat zien dat PHBH tot een nieuwe superfamilie van flavoproteinen behoort. Bovendien werd een nieuw uniek sequentiemotief voor FAD-afhankelijke aromatische hydroxylasen gevonden dat waarschijnlijk zowel een functie vervult in FAD als in NAD(P)H binding. Uit de recentelijk opgehelderde kristalstructuur van fenol hydroxylase blijkt dat dit sequentiemotief structureel bewaard is gebleven. Verder is in **hoofdstuk 6** en **7** aangetoond dat alleen His162 van dit motief direct betrokken is bij de binding van NADPH.

Co-enzym-specificiteit

In **hoofdstuk 8** wordt de klonering, zuivering en karakterisering beschreven van PHBH uit *Pseudomonas species* CBS3. Dit is het eerste PHBH enzym met bekende sequentie dat ook

actief is met NADH. Op basis van sequentie vergelijkingen en het bouwen van een eiwit homologie model blijkt dat het gebied rond helix H2 belangrijk is voor de binding van de 2'-fosfaat groep in NADPH. Deze gegevens zijn in **hoofdstuk 9** gebruikt om de co-enzym-specificiteit van PHBH uit *Pseudomonas fluorescens* te veranderen. Uit deze studies kan geconcludeerd worden dat Arg33 en Tyr38 het meest belangrijk zijn voor de co-enzym-specificiteit.

Effector-specificiteit

Substraat binding is essentieel voor een snelle reductie van het enzym waardoor reaktie met zuurstof mogelijk wordt. De vraag is of de stimulerende rol van het substraat veroorzaakt wordt door grote conformationele veranderingen of alleen door subtiele veranderingen in het actieve centrum.

In **hoofdstuk 10** is de kristalstructuur van het enzym zonder substraat opgehelderd. Deze studie laat zien dat er geen grote conformatieveranderingen plaatsvinden bij substraat binding. De stimulerende werking van het substraat wordt waarschijnlijk veroorzaakt door een combinatie van een aantal subtiele effecten. Stabilisering van de phenolaat vorm van het substraat resulteert in ladingsverschuivingen in het actieve centrum. Hierdoor wordt het evenwicht tussen de "open" en "gesloten" vorm van het FAD zodanig beïnvloed dat de nicotinamide ring van het NADPH en de isoalloxazine ring van het FAD optimaal worden gepositioneerd voor efficiënte electronenoverdracht.

Curriculum vitae

Michel Hendrikus Maria Eppink werd geboren op 21 juli 1964 te Denekamp. In 1980 behaalde hij het diploma MAVO (R.K. San Salvator Mavo te Denekamp). In datzelfde jaar begon hij aan de MBO opleiding voor Klinische Chemie/Hematologie aan de School voor Laboratoriumpersoneel te Hengelo. De stage werd uitgevoerd op het Klinisch Chemisch Laboratorium van het Streekziekenhuis te Oldenzaal (Dr. P. Dingjan). Vervolgens werd in 1983 begonnen met de HLO-opleiding voor Klinische Chemie/Hematologie/Biochemie aan de Hogeschool voor Techniek en Gezondheidszorg te Hengelo. De stage werd uitgevoerd op het Klinisch Chemisch Laboratorium van het Ziekenhuis Ziekenzorg te Enschede (Drs. P. Smit), en de afstudeeropdracht werd gevolgd bij de vakgroep Biochemie van de Landbouwhogeschool te Wageningen (Dr. A.J.W.G. Visser, Dhr. J.S. Santema). Van juli 1987 tot september 1988 werd de militaire dienstplicht vervuld als medisch analist op de Korporaal van Oudheusden kazerne bij Hilversum en de Luitenant Kolonel Tonnet kazerne in 't Harde. Daarna heeft hij van november 1988 tot juni 1989 als medisch analist gewerkt in het Ziekenhuis Velp te Velp (Dr. W.G.M. van den Broek, Drs. F.L.A. Willekens) en het Sint Anna Ziekenhuis te Oss (Dr. A.G.M. Gribnau, Dr. F.P.A.M.N. Peters). Per 1 juli 1989 is hij in dienst getreden als biochemisch analist bij de vakgroep Biochemie van de Landbouwuniversiteit te Wageningen (Prof. Dr. C. Veeger, Dr. W.J.H. van Berkel). In 1990 werd naast zijn werkzaamheden in Wageningen begonnen met de studie Biologie (in deeltijd) aan de Rijksuniversiteit te Utrecht. Een 10-maands afstudeervak werd gevolgd bij de vakgroep Biochemie van de Landbouwuniversiteit te Wageningen (Prof. Dr. W.P.M. Hoekstra, Dr. W.J.H. van Berkel). Verder werd de cursus Stralingshygiëne (deskundigheidsniveau 3) gevolgd bij het Interfacultair Reactor Instituut van de Technische Universiteit te Delft (Dr. C.E. Rasmussen). In 1993 studeerde hij af als Bioloog.

In 1994 werd als biochemisch onderzoeker (in vast dienstverband) gestart met het hier beschreven promotie-onderzoek. Dit onderzoek werd uitgevoerd naast de reguliere onderwijs- en beheers-taken. Samen met Dr. W.J.H. van Berkel werden ook diverse samenwerkingsverbanden onderhouden in binnen- en buitenland. Van 1996 tot 1998 werd jaarlijks een cursus verzorgd in eiwit homologie modelling tijdens de FEBS-EFS Advanced Course "Chemistry of Metals in Biological Systems" aan de Universiteit van Louvain La Neuve te België (Prof. Dr. R.R. Crichton, Prof. Dr. C. Veeger). Vanaf 1998 is meegewerkt aan het opzetten van een nieuw multidisciplinair werkcollege: " An Integrated Course in Bioinformation Technology (BIT)".

Per 1 juni 1999 begint hij als Trainee bij de afdeling R&D Biotechnologie van Diosynth B.V. (Akzo Nobel) in Oss.

List of publications

WJH van Berkel, AH Westphal, K Eschrich, **MHM Eppink** & A de Kok (1992) Substitution of Arg214 at the substrate-binding site of *p*-hydroxybenzoate hydroxylase from *Pseudomonas fluorescens*. *Eur J Biochem* 210: 411-419.

WJH van Berkel, **MHM Eppink**, WJ Middelhoven, J Vervoort & IMCM Rietjens (1994) Catabolism of 4-hydroxybenzoate in *Candida parapsilosis* proceeds through initial oxidative decarboxylation by a FAD-dependent 4-hydroxybenzoate 1-hydroxylase. *FEMS Microbiol Lett* 121: 207-216.

FJT van der Bolt, MC Drijfhout, **MHM Eppink**, WR Hagen & WJH van Berkel (1994) Selective cysteine -> serine replacements in *p*-hydroxybenzoate hydroxylase from *Pseudomonas fluorescens* allow the unambiguous assignment of Cys211 as the site of modification by spin-labeled *p*-chloromercuribenzoate. *Protein Engng* 7: 801-804.

WJH van Berkel, FJT van der Bolt, **MHM Eppink**, A de Kok, IMCM Rietjens, C Veeger & J Vervoort (1994) Substrate and effector specificity of two active-site mutants of *p*-hydroxybenzoate hydroxylase from *Pseudomonas fluorescens*. In: Flavins and flavoproteins XI, Nagoya 1993, Ed. K. Yagi, Walter de Gruyter, Berlin, pp. 231-234.

WJH van Berkel, **MHM Eppink** & HA Schreuder (1994) Crystal structure of *p*-hydroxybenzoate hydroxylase reconstituted with the modified FAD present in alcohol oxidase from methylotrophic yeasts: Evidence for an arabinoflavin. *Protein Sci* 3: 2245-2253.

MHM Eppink, HA Schreuder & WJH van Berkel (1995) Structure and function of mutant Arg44Lys of 4-hydroxybenzoate hydroxylase: implications for NADPH binding. *Eur J Biochem* 231: 157-165.

B Seibold, M Matthes, **MHM Eppink**, F Lingens, WJH van Berkel & R Müller (1996) 4-Hydroxybenzoate hydroxylase from *Pseudomonas* sp. CBS3. Purification, characterization, gene cloning, sequence analysis and assignment of structural features determining the coenzyme specificity. *Eur J Biochem* 239: 469-478.

WJH van Berkel, **MHM Eppink**, FJT van der Bolt, J Vervoort, IMCM Rietjens & HA Schreuder (1997) *p*-Hydroxybenzoate hydroxylase: mutants and mechanism. In: Flavins and

flavoproteins XII, Calgary 1996, Ed. KJ Stevenson, V Massey & CH Williams, Jr. University of Calgary Press, Calgary, pp. 305-314.

WJH van Berkel, E Cammaert, **MHM Eppink** & J Vervoort (1997) Purification and properties of phenol hydroxylase from the ascomycetous yeast *Candida parapsilosis*. In: Flavins and flavoproteins XII, Calgary 1996, Ed. KJ Stevenson, V Massey & CH Williams, Jr. University of Calgary Press, Calgary, pp. 341-344.

WJH van Berkel, K de Ruiter, **MHM Eppink** & J Vervoort (1997) Substrate specificity of 4-hydroxybenzoate 1-hydroxylase from *Candida parapsilosis*. In: Flavins and flavoproteins XII, Calgary 1996, Ed. KJ Stevenson, V Massey & CH Williams, Jr. University of Calgary Press, Calgary, pp. 399-402.

MHM Eppink, DA Jacobs and WJH van Berkel (1997) Involvement of His162 in NADPH binding of *p*-hydroxybenzoate hydroxylase. In: Flavins and flavoproteins XII, Calgary 1996, Ed. KJ Stevenson, V Massey & CH Williams, Jr. University of Calgary Press, Calgary, pp. 315-318.

MHM Eppink, HA Schreuder & WJH van Berkel (1997) Identification of a novel conserved sequence motif in flavoprotein hydroxylases with a putative dual function in FAD/NAD(P)H binding. *Protein Sci* 6: 2454-2458.

M van Iersel, **MHM Eppink**, WJH van Berkel, FM Rombouts & J Abee (1997) Purification and characterization of a novel NADP-dependent branched-chain alcohol dehydrogenase from *Saccharomyces cerevisiae*. *Appl Environ Microbiol* 63:4079-4082.

MHM Eppink, HA Schreuder & WJH van Berkel (1997) Interdomain binding of NADPH in *p*-hydroxybenzoate hydroxylase from *Pseudomonas fluorescens*. *Prot Sci 6 suppl. 1*:3104.

MHM Eppink, SA Boeren, J Vervoort & WJH van Berkel (1997) Purification and properties of 4-hydroxybenzoate 1-hydroxylase (decarboxylating), a novel flavin adenine dinucleotide-dependent monooxygenase from *Candida parapsilosis* CBS604. *J Bacteriol* 179:6680-6687.

MHM Eppink, HA Schreuder & WJH van Berkel (1998) Lys42 and Ser 42 variants of *p*-hydroxybenzoate hydroxylase from *Pseudomonas fluorescens* reveal that Arg42 is essential for NADPH binding. *Eur J Biochem* 253: 194-201.

MHM Eppink, HA Schreuder & WJH van Berkel (1998) Interdomain binding of NADPH in *p*-hydroxybenzoate hydroxylase as suggested by kinetic, crystallographic and modelling studies of histidine 162 and arginine 269 variants. *J Biol Chem* 273: 21031-21039.

MHM Eppink, C Bunthof, HA Schreuder & WJH van Berkel (1999) Phe^{161} and Arg^{166} variants of *p*-hydroxybenzoate hydroxylase. Implications for NADPH recognition and structural stability. *FEBS Lett* 443:251-255.

WJH van Berkel, JA Benen, **MHM Eppink** & MW Fraaije (1999) Flavoprotein kinetics. *Methods of Mol Biol* (in press).

MJ van der Werf, C van der Ven, F Barbirato, **MHM Eppink**, JAM de Bont & WJH van Berkel (1999) Stereoselective carveol dehydrogenase from *Rhodococcus erythropolis* DCL14. *J Biol Chem* (in press).

MHM Eppink, KM Overkamp, HA Schreuder & WJH van Berkel (1999) Switch of coenzyme specificity of *p*-hydroxybenzoate hydroxylase. *J Mol Biol* (submitted).

JHW Leusen, C Meischl, **MHM Eppink**, PM Hilarius, M de Boer, RS Weening, A Åhlin, L Sanders, D Goldblatt, H Skopczynska, E Bernatowska-Matuszkiewicz, J Palmblad, AJ Verhoeven, WJH van Berkel & D Roos (1999) Four novel mutations in the gene encoding gp91-*phox* of human NADPH oxidase: consequences for oxidase assembly. *Blood* (submitted).

M Hink, R Griep, A van Hoek, **MHM Eppink**, A Schots & AJWG Visser (1999) Structural dynamics of green fluorescent protein fused with a single chain Fv protein. *Nat Struct Biol* (submitted).

MHM Eppink, WJH van Berkel, A Tepliakov & HA Schreuder (1999) "Unactivated" *p*-hydroxybenzoate hydroxylase: Crystal structures of the free enzyme and the enzyme-benzoate complex. *J Mol Biol* (in preparation).

MHM Eppink, E Cammaart, J Vervoort, D van Wassenaar, WJ Middelhoven & WJH van Berkel (1999) Purification and properties of hydroquinone hydroxylase, a flavin adenine dinucleotide-dependent monooxygenase involved in the catabolism of 4-hydroxybenzoate in *Candida parapsilosis* CBS604. *J Bacteriol* (in preparation).